DEMONSTRATION OF THE USE OF COST-EFFECTIVE TOOLS TO ANALYZE CORE, LOG, AND PRODUCTION DATA TO DEVELOP A RESERVOIR MODEL FOR MINNEOLA FIELD, CLARK COUNTY, KANSAS, AND TO EVALUATE ITS PERFORMANCE UNDER WATERFLOOD

by

Saibal Bhattacharya
Paul Gerlach

Kansas Geological Survey
Open-fIle Report 99-34

Disclaimer

The Kansas Geological Survey does not guarantee this document to be free from errors or inaccuracies and disclaims any responsibility or liability for interpretations based on data used in the production of this document or decisions based thereon. This report is intended to make results of research available at the earliest possible date, but is not intended to constitute final or formal publication.

TITLE: Demonstration of the use of cost-effective tools to analyze core, log, and production data to develop a reservoir model for Minneola Field, Clark County, Kansas, and to evaluate its performance under waterflood.

Cooperative Agreement No.:	C73590016-35
Contractor Name and Address:	The University of Kansas Center for Research Inc.
Date of Report:	Nov 22, 1999
Award Date:	February 16, 1999
Cost of Project:	$ 27,937
Principal Authors:	Saibal Bhattacharya Paul Gerlach
Project Manager:	F. David Martin, Manager, Strategic Technologies Resources, LLC
Reporting Period:	Report 1

Minneola Unitization Study

Introduction

The Minneola Unit is located in Clark County, Kansas, and is part of the Norcan East Field which is approximately one mile north and two miles west of Minneola, Kansas. The other fields located in the general vicinity are Norcan and Fager fields. Initial development started in this area with the drilling of Norton #1-8 in Section 8 of 30s-25w. This well was completed in September 1980 and upon testing it flowed 157 bopd and 120 mcfd. Murfin Drilling Co. began active drilling in this area since 1983. Effective July 1993, Murfin Drilling purchased all of Swift Energy's (successor to Ladd Petroleum) interest in the general area.

Figure 1 is a map showing the locations of wells in the general area that includes the Minneola unit. The figure also shows the boundary of the Minneola unit along with the well locations, well names, and corresponding unit numbers. The producing horizon in the field is the Morrow sandstone. The reservoir drive mechanism is solution gas drive. The initial oil production varied from 38 to 164 bopd with many of the wells producing associated gas. DST analyses show that wells completed in early half of 1983 averaged an initial reservoir pressure of 1555 psi while those completed in 1985 averaged 817 psi. Production from a solution gas drive reservoir without any pressure support resulted in a rapid decline of reservoir pressure. By June 1993, the production from the Minneola unit had dropped to 26 bopd after a cumulative production of 555304 barrels of oil and 1087 MMcf of associated gas. By 1993, the wells in the unitized area were approaching economic limits under primary production.

In 1994, for the purposes of secondary recovery, 13 tracts, all operated by Murfin Drilling Co., were unitized to initiate a water-flooding program. The area unitized covers about 1040 acres and includes the W/2 of the NE/4, and the S/2 of section 3; the S/2 of section 4; and the N/2 of section 10; all in 30s-25w, Clark County, Kansas. Included in the unitized area are 12 producing wells and 2 water injection wells. The Patton #1-3 (unit # 3-1) and Goeller #1-4 (unit #7-1) were converted into injection wells.

The objective of this study is to evaluate the performance of waterflooding in the Minneola Unit. As a part of this exercise, a geologic model has been constructed from the petrophysical logs. Available DST data were analyzed to determine the initial reservoir pressures and effective permeabilities. Data from the petrophysical logs were used to construct Super-Pickett plots to calculate average pay thickness, porosity and initial saturations. Laboratory measurements on core plug were used to generate permeability versus porosity correlation. This correlation was used to develop a permeability map, using log-derived porosity, for the unitized area. The available production data, since waterflooding, were analyzed at the unit level and also at the well level to understand the performance of the waterflooding.

Geologic Mapping

Most of the wells in the unitized area and its surrounding have petrophysical logs, and they were used to construct a geologic model. Figures 2 and 3 are subsea structure maps of the Atokan group and Mississippian system. Figure 4 displays the variation in thickness of the Atokan formation. Lithogic cross-sections enabled the identification of three sand bodies within the Morrow.

Figures 5, 6 and 7 are the isopachs of sand #1, sand #2, and sand #3. Initial mapping indicated that shale layers separated these sands. The above figures also show the sand intervals present in each of the wells. The isopach maps (Figures 5 and 6) show that sand #1 and sand #2 extend, into section 2 of 30s-25w, beyond the boundaries of the water-flooding unit. Figure 5 shows that sand #1 covers part of south-western corner of section 2 while Figure 6 shows sand #2 to extend into the same region of section 2. The zero isopach lines for sand #2 form a narrow neck at the south-western corner of section 2, and for the purposes of this study it was assumed that the border of sand #2 was located where the zero isopach lines were closest to each other. Because of the extension of the sand bodies beyond the boundaries of the unit, wells such as Rooney B #1-2, Hall #2-2, Hall #1-2, Hall B #1-2, all located in the south western part of section 2, were included in this study and this expanded study area will be termed as "unit plus Hall". Of these wells, only Hall #1-2 is a producer and its production was included in the volumetric study.

Petrophysical Analysis

Petrophysical analysis was undertaken using Super-Pickett crossplots were constructed for each well, in the unit and surrounding area. The Super-Pickett plots are included in Appendix A. The Super-Pickett crossplot is a spreadsheet based technique for log analysis. It plots the log-derived porosity against the deep resistivity on a log-log axis. Using Archie's equation it generates the saturation contours on the plot. It also overlays the BVW (bulk-volume-water) contours on the plot. For sandstones, permeability contours can be displayed on the crossplot by using equations such as the Timur's correlation. The graphic capabilities of the spreadsheet environment allow pattern recognition of trends and clusters. These patterns when evaluated in light of the knowledge about sedimentary facies, grain and crystal size, capillary pressures, fluid saturations, pore geometries, and other factors result in modeling of the "petrofacies" in the reservoir. Details about the Super-Pickett plot and its applications can be found in References 1 and 2. The plots attached with this report are in black and white and this makes pattern recognition difficult. The colored versions of these plots are available at the KGS website (http://www.kgs.ukans.edu/DPA/Reports/Minneola/).

.

Table 1 summarizes the results of the petrophysical analysis and tabulates the average porosity, water saturation (calculated using Rw = 0.04 ohm-m), and BVW for each of the sands. In some cases, water free production was recorded during the initial testing and this identified the BVW_i (i.e. the immobile bound water). The average BVW increases from sand #1 to sand #3 indicating that the fraction of the pore volume that is occupied

by water is the maximum in sand #3. BVW_i could be obtained in only a few cases, so doubts remain about their representativeness. However, the average values in sand #1 and sand #2 are very similar while those of sand #3 are significantly higher. Such difference in the BVW_i values indicates that the pore size distribution in sand #3 contains a greater number of smaller pores as compared to the other two sands. Thus, the water saturation (S_w) cut-off for water-free production from sand #3 is higher than that of sands #1 and #2. Figure 8 is a plot of BVW versus water saturation for the three sands.

Rhomma-Umma plots were used to carry out lithology analyses in wells where the PE log was available. The Rhomma-Umma plots are included along with the Super-Pickett plots of the respective wells in Appendix A. Lithology analysis on sand #2 (in four wells) and sand #3 (in three wells) indicated the composition to be dominated by quartz with minor dolomite. Data from only one well could provide an analysis for sand #1 and it too was found to be predominantly quartz with minor dolomite.

Core data analysis

Results of laboratory analyses on whole cores were available for 4 wells in and around the unitized area. The wells for which core data was analyzed are: Widner #1-17 (NW NE of Section 17 in 30s-25w), Patton #1-3 (inside the unitized area, N/2 SW SE of Section 3 in 30s-25w), Statton #2-12 (NW NW NW of Section 12 in 30s-25w), and Fager #1-16 (NW NW NW of Section 16 in 30s-25w). Helium porosity and horizontal permeability measurements were available for 34 whole core samples taken from the Morrow sands in the above four wells. The log of the permeability was plotted (Figure 9) against the porosity to develop a permeability-porosity correlation. The equation of the best fitting linear trend through the plotted points is also shown in Figure 9.

Maximum horizontal permeability and permeability in the direction perpendicular to the maximum horizontal permeability was available for eighteen core plugs from two wells: Patton #1-3 and Widner #1-17. This data is plotted in Figure 10 along with the equation of the best fitting linear trend.

Petrophysical Mapping

The permeability-porosity correlation obtained from Figure 9 was used to obtain average permeability for the sands at each well from the corresponding average porosity value (from Super-Pickett plot analysis). Transmissibility maps of the three sands in the unitized area are displayed in Figures 11, 12, and 13. These maps contour the permeability-thickness of the individual sands and also show the location of the wells. A comparison of Figure 12 and 13 reveals that most of the injected water from injector #7-1 will tend to enter sand #2. In case of injector #3-1, the situation is reversed. Both sand #2 and sand #3 have finite transmissibilities near injector #3-1. However, the transmissibility of sand #3 at injector #3-1 is about three and half times that of sands #2. Thus, in absence of bottom hole flow measurements of the injected fluids, it is reasonable to assume that most of the injected water in well #3-1 is entering sand #3.

The storativity distributions in the three sands are plotted in Figures 14, 15 and 16. It is apparent from Figures 15 and 16, that the storativity of sand #3 around injector #3-1 is about 3 times that of sand #2. This difference in storativity will cause the major portion of the injected water at this injection well to flow into sand #3. Also, the storativity of sand #3 around the injector #7-1 is insignificant to that of sand #2 and this will divert most of the injected water into sand #2.

Storativity and transmissibility maps show that almost all the injected water at well #7-1 will tend to flood sand #2 and while at well #3-1 the injected water enters sand #3 in preference to sand #2. Neither of the two injection-wells is open in sand #1 and thus wells producing out of sand #1 will remain out of the reach of water flood barring any hydraulic communication that may exist between these sands in the inter-well areas.

Figures 17, 18, and 19 show the oil saturation-feet distribution in the three sands. The oil saturations were used in the volumetric calculations to obtain the original oil in place.

DST Analysis

DST data was available for 6 wells in the unitized area. Wells that produced liquid during the DST were analyzed with the help of standard Horner plots. Gas wells were analyzed by two methods, i.e., by the SPE Monograph method suggested by Mathews and Russel (Reference 3) and by either of the high pressure gas test analysis or the low pressure gas test analysis method (Reference 4). The high pressure gas test analysis was employed when the pressures in the Horner straight line portion exceeded 1500 psi while the low pressure test was used when these pressures were less than 1500 psi. For gas wells with shut-in pressures were close to 1500 psi, both the high and low pressure methods were used. The results of the DST analysis are summarized in Table 2. The DST build-up plots and calculations are included in Appendix B.

Table 2 shows the intervals of the sands that are present in each of the wells along with the intervals that were tested by DST and are open for production. It also includes the completion date and the initial reservoir pressure (P_i, psi) calculated from the DST. The decline of the reservoir pressure with time is plotted in Figure 20 and it shows a rapid decline of reservoir pressure from 1600 psi to 800 psi in a period of just more than two years. By the beginning of 1995, the fluid levels above the bottom-hole pump ranged from less than 50 ft to a maximum of 200 ft across the unit. Such a rapid fall in the reservoir pressure is characteristic of a solution-gas drive reservoir with no pressure support.

The average effective permeability as calculated by one or more of the relevant methods of DST-analysis stated before, is shown in Table 2. Table 3 compares the permeability, of each of the sands, derived from the porosity-permeability correlation (Figure 9) with that calculated from the DST. The DST interval in every case is bigger than the sand thickness in the well. During permeability calculations, the effective pay thickness of the reservoir was taken to be the total vertical thickness of effective-porosity present within the DST interval. Only the sand units (#1, #2, and #3) were considered to contain

effective-porosity. This significant difference between permeability calculated from DST and that obtained from the correlation, developed on core data, indicates that either a high degree of flow-heterogeneity exists around the wells or that the limitations inherent to DST measurements are coming into display. If the cause behind this difference in permeability values is indeed the flow-heterogeneity then a more detailed characterization needs to be carried out within each of the identified sand bodies.

Production Data Analysis

Unitization of the Minneola field was completed in August '94 and water flooding started in December '94. Plots were constructed for each well to trace the monthly production of oil and water at them along with the volume of water injected per month from the nearest injector. These production/injection profiles are presented in Appendix C. Analyses of these production/injection profiles were carried out to determine the influence of permeability distribution and connectivity between the sands on the performance of the waterflood.

As mentioned earlier, storativity and the transmissibility maps indicate that most of the water injected at well #7-1 is invading sand #2. Figure 1 shows that the wells located near injector #7-1 include #9-1, #8-1, and #6-1. Table 4 lists the producing sands in each of the wells and it shows that wells #9-1 and #8-1 are both open in sand #2, while well #6-1 is open in both sand #2 and #3. Well #10-1B is almost equidistant from both the injectors and its perforation interval is not available. However, production records show that it has been kept closed through out the water-flooding period and thus this well was not analyzed in this study.

The production/injection profile for well #9-1 (Figure C1) demonstrates the restriction of the fluid movement in areas of low permeability (obtained from DST) around well #9-1. This results in the dying out of the oil production after the immediate area around the well has been drained. By the time this well is reopened at later date, oil recharges the sand around the well and the well produces for a while again. Production during the second opening of the well exceeds that of the first possibly because some of the injected water at well #7-1 build an oil bank in the direction of this well. The low permeability around the well may also have prevented a breakthrough of injected water. The high permeability around well #8-1 and its proximity to the injector #3-1 resulted in early break through (Figure C2) of injected water. Rapid short-circuit of the injected water may be due to high permeability streaks, and in such a case most of the secondary oil reserves remain unswept in the reservoir. The response to the water flooding becomes apparent in well #6-1 at a later date, than well #8-1, because of its greater distance from the injector and also perhaps due to the lower permeability of sand #2. Only a small oil bank is recovered prior to water breakthrough.

The wells around this injector #3-1 include #3-2, #2-2, #4-1, #5-2, #11-4, #12-2, #13-1, and #1-1. A comparison (Table 4) of the sand interval/s present at the wells and the perforated interval/s in the same well reveals that wells #3-3, #2-2, #4-1, #11-4, and #1-1 produce from sand #2, while wells #5-2 and #13-1 produce from sand #1, and that the

perforations in well #12-2 extend through sand #2 on to the top of sand #3. In the vicinity of injector #3-1, both storativity and transmissibility of sand #3 are more than three times those of sand #2. The result is that most of the water is injected into sand #3 in preference to sand #2. However, as none of the wells around this injector is perforated in sand #3, any flood response in these wells will be attributable to hydraulic communication between the sands #2 and #3 in the inter-well region.

Figure C4 shows that well #3-2 had been kept shut for all but 4 months during the waterflood and the reasons are not known. This profile shows some oil production but due to the very short period of flow it is difficult to interpret the performance of this well. Well #2-2 shows a very good response (Figure C5) to the waterflood with no observed water cut. Though this well is perforated in sand #2 only, its oil production closely traces the injection volumes at well #3-1. As most of the injected water is expected to travel into sand #3 from well #3-1, it appears that the flood response in well #2-2 is due to hydraulic communication between sand #2 and #3. The high permeability of sand #2 around well #2-2 must have also helped to maintain performance. Oil and water production curves (Figure C6) of well #4-1 show a response between June to July '97, with the production of a small oil bank being followed by water breakthrough. This well is also completed only in sand #2, and thus hydraulic communication between the sands, good permeability of sand #2 around the well, and its proximity to the injection well may be the factors that attribute to water breakthrough. The first response to the waterflood occurs in well #11-4 between July to August '97 (Figure C7). This well is open only in sand #2 and behaves in manner similar to well #4-1, with water breakthrough following the production of a small oil bank. Such a behavior suggests hydraulic communication between sand #2 and #3 in the region between the injector and the producer. The permeability value in sand #2 for this well is modest (49.2 md) and is lower than that of well #4-1 (88 md). Thus while well #4-1 showed insignificant oil production after water breakthrough, well #11-4 shows continuing oil production even after breakthrough. Performance profile of well #1-1 is traced in Figure C8. Here the response to the flood appears as early as between June and July '95 and suggests communication between the sands #2 and #3. The erratic behavior of the water production suggests that significant reservoir heterogeneity exist between well #1-1 and the nearest injector. Wells #5-2 (Figure C9) and #13-1 (Figure C10) have remained open for short intermittent periods during the course of the waterflood and thus it is difficult to interpret their performance. Also, both of these wells are open in sand #1 and thus may not feel the effects of waterflooding in sand #3. Well #12-2 is perforated in sand #2 primarily with the bottom-most perforation touching the top of sand #3. In spite of low permeabilities both in sand #2 and #3 at the well, water breakthrough occurs as early as Jan '96. However, these low permeabilities might also have resulted in some oil production along with water during the life of the flood.

Production data analysis reveals that response to the water flood is present in most of the wells in the unit plus Hall area. However, reservoir heterogeneity in the form of high permeability streaks appear to short circuit the injected water to the producing well leaving behind significant unswept secondary reserves.

Volumetric Calculations

Volumetric calculations for OOIP (original-oil-in-place) were carried out on each of the sands on a grid-cell by grid-cell basis. Geographix mapping package was used to grid and map sand attributes such as net pay, porosity, and S_w. Each of the sand bodies was gridded with cells sized 165 feet by 165 feet. Standard gridding algorithm inside the mapping package was used to populate the grid cells with attribute values. Grid values were migrated to a spreadsheet environment to facilitate grid-to-grid operations. Figure 9 shows that the permeability value tends to zero as the porosity value gets smaller and smaller. A permeability cut-off of 0.5 md was assumed to be unproducible for Minneola Unit, and thus an effective-porosity grid was generated for each sand by zeroing off grid cells with porosity values less than 4.69%. The OOIP in each grid cell, in each sand body, was calculated by the formula below:

$$OOIP = (165^2 * h * \Phi e * (1-S_w))/5.615$$

The OOIP is calculated by this equation is in reservoir barrels (RB), and the other parameters are defined as follows: Φe = effective porosity (fraction), h = pay height, ft, and S_w = water saturation (fraction).

Table 5 summarizes the volumetric calculations and tabulates the pore volume (PV) and OOIP of each of the sands in RBs. The total OOIP of the three sands in the unit plus Hall area is 2.78 MMRB. Laboratory measured data regarding the oil formation volume factor (B_o) was not available.

In solution gas driven reservoirs, gas saturation increases in the reservoir with a lowering of reservoir pressure due to production. Relative flow of gas increases in the reservoir at higher gas saturations, and this results in a continuous rise in the produced gas-oil-ratio (GOR). The peak GOR is at times several times greater than the original solution GOR. Above bubble point pressures, the reservoir rock and remaining fluids expand to fill the void created by the produced fluids. Both rock and reservoir fluids have low compressibility and so a large decrease in pressure is necessary to allow the rock and remaining fluids to expand enough to replace the relatively small amount of oil produced. The result is that above bubble point the pressure decreases rapidly. The producing GOR, recorded at the surface, shows a constant trend till reservoir pressure is at bubble point and thereafter it increases rapidly.

Lease production data was used to plot the GOR profile with time. One of the leases, namely Fager, was found to display constant GOR (Figure 21), around 500 scf/bbl, during the early periods of its production life. This lease contains a single producing well and it was brought online during the initial development of the field, i.e., in January '84. The constancy of the GOR value indicates that the reservoir pressure around the well was above the bubble point pressure. Due to unavailability of any laboratory-measured GOR value, the solution GOR for the unit plus Hall area was assumed to be 500 scf/STB.

The solution GOR was used to calculate the B_o for the oil. Available well records revealed produced gas analysis where the average specific gravity of the gas was found to be 0.73 (air=1.0). The average reservoir temperature is 116°F and the API gravity of oil is 46. Standard correlations (reference 5) were used to calculate B_o, and it was found to be 1.25 RB/STB. The bubble point pressure was calculated by standard correlations (reference 5) to be around 1370 psia. Initial reservoir pressure, calculated from DST analysis, was around 1600 psi and given the rapid decline in reservoir pressure (Figure 20), it appears that a gas cap must have formed in the reservoir during the later half of 1983.

The cumulative production from the unit plus Hall area before the onset of the water flood was 0.64 MMSTB of oil and 1760 MMscf of gas. This results in a primary recovery efficiency of 29%, assuming that the representative solution GOR for the reservoir is 500 scf/STB. Generally the recovery efficiency of solution-gas driven reservoirs varies between 15 to 20% of the OOIP, with occasional values varying between 5 to 30% (reference 6, page 37-2). The API study on crude oil recovery efficiency (reference 7, page 5) tabulates average primary recovery efficiency between 15 to 31% (of OOIP) for solution-gas driven sandstone reservoirs.

Production records indicate that after the onset of the waterflood there was no significant gas production from any of the wells. Also by the early part of 1995, the operating fluid levels in the wells was no more than 150 ft, suggesting that the reservoir pressure to be no greater than 100 psi. Thus the remaining oil in the reservoir can be assumed to be gas free by the start of the waterflood. The cumulative oil produced from the unit plus Hall area during the waterflood amounts to 40.8 MSTB and this translates to a secondary recovery efficiency of 3% of the reserves remaining after the primary stage. Thus, a significant amount of the recoverable reserves remain to be recovered in the unit plus Hall area.

Figure 22 shows the production and injection history in the unit plus Hall area during the waterflooding stage. It is apparent from this figure that the volume of water production closely traces that of the total fluid production. Also, the difference between the volumes of total fluid produced and that of water injected diminish with time. This indicates that an increasing amount of the injected water is short-circuiting to the producing wells. Another important observation is that an average production of 378 STB of oil was obtained in the unit plus Hall area during the four months when there was no water injection. Figure 23 summarizes the voidage and fill-up that has taken place due to the water injection. It shows that the volume occupied by free gas in the reservoir is near 400,000 bbls. Thus the total amount of water injected, so far, has not been able to fill-up the voidage created by the fluid production.

The fluid component with the maximum energy in a reservoir is gas, and in case of the unit plus Hall area most of the gas has evolved out of the oil and has been produced. The gas left behind in the reservoir is low-pressure unproducible free gas. Thus at this stage in the reservoir's life, it is ineffective to pressurize the reservoir by water injection as there is not enough gas left behind to pressurize. So the focus of the water injection should not

be to achieve fill-up. The effective mechanism to recover the remaining oil will be to design a water flood that will create and push banks of oil towards the producing wells. Given the size, distribution, and heterogeneity of the sands it appears that two injector wells, namely #3-1 and #7-1, are insufficient to sweep the remaining reserves in an efficient manner. A successful waterflood in this field should take into account different factors including: a) water should be injected in a manner such that each of the three sands are flooded, and b) producing wells should be selected such that their perforations can produce the oil bank built by the nearby injectors. Analyses of the current production-profiles show evidence of connectivity between the sands and of the presence of high permeability streaks within the sands. Detailed characterization studies are required to refine the reservoir model, which can serve as the base for a strategy to effectively sweep the remaining reserves.

Conclusions

a) Reservoir consists of three sands as opposed to what was originally considered to be a single layer reservoir.
b) Petrophysical studies show that the fraction of the pore volume occupied by water increases from sand #1 to sand #3. From the limited data that is available, it appears that the cut-off value of water saturation for water-free production is higher in sand #3 as compared to the other two sands.
c) Responses to water flooding have occurred in most wells.
d) Injection water breakthroughs to the producing wells indicating reservoir heterogeneity.
e) Production response to water flooding indicates that sand #2 and sand #3 are in communication around the injector #3-1.
f) Primary recovery has been 29% of OOIP.
g) Secondary recovery from water flood has been very poor, i.e.; about 3% of reserves remaining at the onset of the flood, and thus significant recoverable reserves remain.

Future Studies

a) Identify the connectivity between the sands and also the permeability distributions within the sands.
b) Gather reservoir pressure and PVT data to carry out a material balance study to cross check the reservoir volumetrics.
c) Simulate the field performance under solution gas drive and under the current water flood.
d) Design an effective strategy to recover residual oil that has been bypassed by the waterflood in place.

References

1. Doveton, J.H., W.L. Guy, W.L. Watney, G.C. Bohling, S. Ullah, and D. Adkins-Heljeson, 1996, Log Analysis of petrofacies and flow-units with microcomputer spreadsheet software: 1995 American Association of Petroleum Geologist Mid-Continent Meeting.

2. Bhattacharya, S., W.L. Watney, J.H. Doveton, W.L. Guy, and Geoff Bohling, 1999, From geomodels to engineering models – opportunities for spreadsheet computing: 19th Annual B.F. Perkins Research Conference, Gulf Coast Section Society of Economic Paleontologists and Mineralogists Foundation, December 1999.

3. Mathews, C.S., and D.G. Russell, 1967, Pressure buildup and flow tests in wells: SPE Monograph Volume 1, Henry L. Doherty Series.

4. Reid, H.W., Modern concepts in drillstem testing: Hugh W. Reid & Associates Ltd, Calgary, Canada.

5. McCain, W.D., The properties of petroleum fluids: 2nd Edition, PennWell Books, 1990, Tulsa, Oaklahoma.

6. SPE, Petroleum engineering handbook: 3rd printing, 1992, Richardson, Texas

7. API Bulletin D14, Statistical analysis of crude oil recovery and recovery efficiency: April 1994.

Table 1

Well name	API	SD#1	Phi	Sw	BVW -sd #1	BVWi - sd#1	SD#2	Phi	Sw	BVW -sd #2	BVWi - sd#2	SD#3	Phi	Sw	BVW - sd #3	BVWi -sd#3
Fager # 2-3	15-025-20671	5266-68	0.054	1	0.054		5275-85	0.231	0.212	0.049						
Patton # 2-3	15-025-20685						5293-00	0.221	0.26	0.057		5301-04	0.205	0.36	0.074	
Hindman # 1 (# 1-3)	15-025-20635						5307-13	0.207	0.23	0.048	0.069					
Harris # 1-3	15-025-20616	5312-13	0.112	0.52	0.058		5320-24	0.175	0.37	0.065		5325-32	0.222	0.47	0.104	
Harris # 2-3	15-025-20708	5290-94	0.203	0.344	0.070	0.065										
Patton # 2-3	15-025-20859	5286-89	0.21	0.304	0.064		5291-96	0.154	0.39	0.060						
Patton # 1	15-025-20594	5307-09	0.072	0.64	0.046		5318-24	0.164	0.55	0.090						
Patton # 1-3	15-025-20668						5322-25	0.131	0.58	0.076		5328-34	0.194	0.545	0.106	0.105
Fager # 1-3	15-025-20696															
Goeller # 1-4	15-025-20615						5314-18	0.166	0.34	0.056		5325-26	0.025	1	0.025	
Goeller # 1-4	15-025-20858						5316-22	0.189	0.44	0.083	0.085					
Norton # 1-4	15-025-20890															
Norton # E-1	15-025-20837						5340-44	0.156	0.7	0.109						
Tedford # 4-10	15-025-20720	5298-99	0.197	0.262	0.052	0.0475	5305-12	0.189	0.23	0.043						
Tedford # 1-10	15-025-20621	5278-83	0.155	0.46	0.071	0.075										
Tedford # 2-10	15-025-20669						5316-20	0.151	0.9	0.136		5323-25	0.137	0.73	0.100	
Tedford # 1	15-025-20416	5274-75	0.078	0.5	0.039		5285-89	0.149	0.494	0.074						
Tedford # B1-10	15-025-20905						5300-07	0.204	0.49	0.100						
Tedford # 2-10	15-025-20686											5331-35	0.184	0.7	0.129	
Tedford # 3-10	15-025-20788						5283-85	0.185	0.493	0.091		5290-93	0.215	0.795	0.171	
Hall #2-2	15-025-20838						5303-05	0.13	0.633	0.082						
Hall B #1-2	15-025-20919	5278-81	0.191	0.333	0.064		5283-85	0.128	0.53	0.068						
Latzke #1	15-025-20611						5305-08	0.235	0.665	0.156	.13 (avg #3)	5310-19	0.224	0.565	0.127	.13 (avg #2)
Norton B#1	15-025-20672						5303-05	0.13	0.4	0.052						
Alley #1-9	15-025-20911						5293-95	0.191	0.46	0.088						
Rooney B#1-2	15-025-20917	5280-83	0.19	0.46	0.087		5287-89	0.187	0.64	0.120						
Hall #1-2	15-025-20785	5307-10	0.097	0.57	0.055		5316-24	0.173	0.44	0.076	0.082					
Min			***0.054***	***0.262***	***0.039***			***0.128***	***0.212***	***0.043***			***0.025***	***0.36***	***0.025***	
Max			***0.21***	***1***	***0.0874***			***0.235***	***0.9***	***0.156***			***0.224***	***1***	***0.170925***	
Average			***0.142***	***0.490***	***0.060***			***0.175***	***0.475***	***0.081***			***0.176***	***0.646***	***0.104***	

Table 2

Well/Unit name	IP	Sd #1, ft	Sd #2, ft	Sd #3, ft	Test Int., ft	Prod. Int, ft	Completion	Pi, psi	FSIP, psi	Rec/Flowed	SPE K md	High Pr. K, md	Low Pr. K, md
Patton # 2-3 (3-2)	IP - N/A (O&G well in Morrow)		5293-00	5301-04	5283-5315	5294-5300	May-83	1510.5	1503.5	1048 mcfd	10.4	8.9	7.7
Goeller # 1-4 (8-1)	90 bopd, 98 mcfd		5316-22		5300-5335	5315-5321.5	Jan-85	800	790	465' GO, 485' GSMCO & 163 mcfd	9.1		6.3
Norton # 1-4 (9-1)	66 bopd, 145 bwpd		5289-94		5292-5316	5288-93	Apr-85	886	854	30' HOGCM, 120' OCM & 610' MCO	4.1		2.6
Tedford # 4-10 (11-4)	164 bopd, 65 mcfpd	5298-99	5305-12		5294-5330	5304-5314	Sep-83	1518	1501	10 BO, 22.9 mcfd	0.4	0.3	0.4
Tedford # 1-10 (13-1)	512 mcfpd	5278-83			5272-5302	5278-5282	Jan-83	1637	1630.2	120' O&GCM, 60' OG&WCM 1458 mcfd	96	56	
Tedford # B1-10 (10-1B)	IP & Int - N/A. Oil well		5300-07		5296-5319	N/A	Jul-85	766	763	170' GMCO, 40.9 mcfd	2.9		1.2

Table 3

Well/Unit name	Sd #1, ft	K-Phi cor. Sd#1, K md	Sd #2, ft	K-Phi cor. Sd#2 K, md	Sd #3, ft	K-Phi cor. Sd#3 K,md	Test Int., ft	Avg. DST K, md	Prod. Int, ft
Patton # 2-3 (3-2)			5293-00	138.5	5301-04	82.6	5283-5315	9	5294-5300
Goeller # 1-4 (8-1)			5316-22	49.2			5300-5335	7.7	5315-5321.5
Norton # 1-4 (9-1)			5289-94				5292-5316	3.4	5288-93
Tedford # 4-10 (11-4)	5298-99	63.8	5305-12	49.2			5294-5330	0.4	5304-5314
Tedford # 1-10 (13-1)	5278-83	16.4					5272-5302	76	5278-5282
Tedford # B1-10 (10-1B)			5300-07	80			5296-5319	2.1	N/A

Table 4

Well name	Unit name	SD#1	SD#2	SD#3	Prod. Int	Prod. Sd#
Fager # 2-3	2-2	5266-68	5275-85		5274-5286	2
Patton # 2-3	3-2		5293-00	5301-04	5294-5300	2
Hindman # 1 (# 1-3)	4-1		5307-13		5306-5315	2
Harris # 1-3	6-1	5312-13	5320-24	5325-32	5320-5332	2 & 3
Harris # 2-3	5-2	5290-94			5290-5294	1
Patton # 2-3	1-2	5286-89	5291-96		D&A	D&A
Patton # 1	1-1	5307-09	5318-24		5318-5324	2
Patton # 1-3	**3-1**		5322-25	5328-34	Injector	Injector
Goeller # 1-4	**7-1**		5314-18	5325-26	Injector	Injector
Goeller # 1-4	8-1		5316-22		5315-5321.5	2
Norton # 1-4	9-1		5289-94		5288-93	2
Norton # E-1	9-1E		5340-44		Wtr. Supply	Wtr. Supply
Tedford # 4-10	11-4	5298-99	5305-12		5304-5314	2
Tedford # 1-10	13-1	5278-83			5278-5282	1
Tedford # 2-10	12-2		5316-20	5323-25	5316-5323	1 & touch 2
Tedford # 1	10-1	5274-75	5285-89		5284-88	2
Tedford # B1-10	10-1B		5300-07		N/A	N/A
Tedford # 2-10	11-2			5331-35	D&A	D&A
Tedford # 3-10	13-3		5283-85	5290-93	D&A	D&A

Table 5					
Reservoir Volumetrics:					
				Reservior PV, BBLS	
OOIP sand 1	476588	RB		sand 1	875,630
OOIP sand 2	2042543	RB		sand 2	3,568,060
OOIP sand 3	260791	RB		sand 3	603,345
TOTAL OOIP (Unit + Hall)	**2779922**	**RB**		**TOTAL PV**	**5,047,035**
Bo = 0.972+0.000147*(Rs*(Rog/Roo)^0.5+1.25*T)^1.175				Unit Cum (12/94), STB	564733
Rs (soln. GOR)	500	scf/STB		Unit Cum (12/94), Mcf	1428132
Rog (gas sp. Gravity)	0.73				
API (oil gravity)	46.00	degree		Hall Cum (12/93), STB	77731
Roo (oil sp. Gravity)	0.80			Hall Cum (1/94-12/94) STB	1390
T (res temp in F)	116.00	F		Hall Cum(12/93) Mcf	330292
				Hall Cum (1/94 to 8/94) Mcf	2132
Boi:	1.25				
	1.25	**RB / STB**		**Cum Oil (Unit+Hall, 12/94), STB**	**643854**
	OOIP STB				
				Cum Gas (Unit+Hall, 12/94), Mcf	**1760556**
OOIP sand 1	381,270	STB	381270.4		
OOIP sand 2	1,634,034	STB		**Primary RF =**	**0.29**
OOIP sand 3	208,633	STB			
TOTAL OOIP (Unit+Hall)	**2,223,938**	**STB**		ROIP (@ Dec-94), bbls =	1,580,084
				Since Dec-94, Bo = 1	
Approx Gas prod. (Unit+Hall) till date	1,760,556	Mcf		Cum Oil (Unit + Hall, 1/95-8/99), STB	40797
Field Soln GOR	791.6	scf/STB			
				Secondary RF (of ROIP) =	**0.03**
Bubble point pressure (psia), Pb = 18.2(CNpb-1.4)					
CNpb = ((Rs/Rog)^.83)*10^(.00091*T-.0125*API)					
CNpb =	76.59				
Pb, psi =	**1,368**				

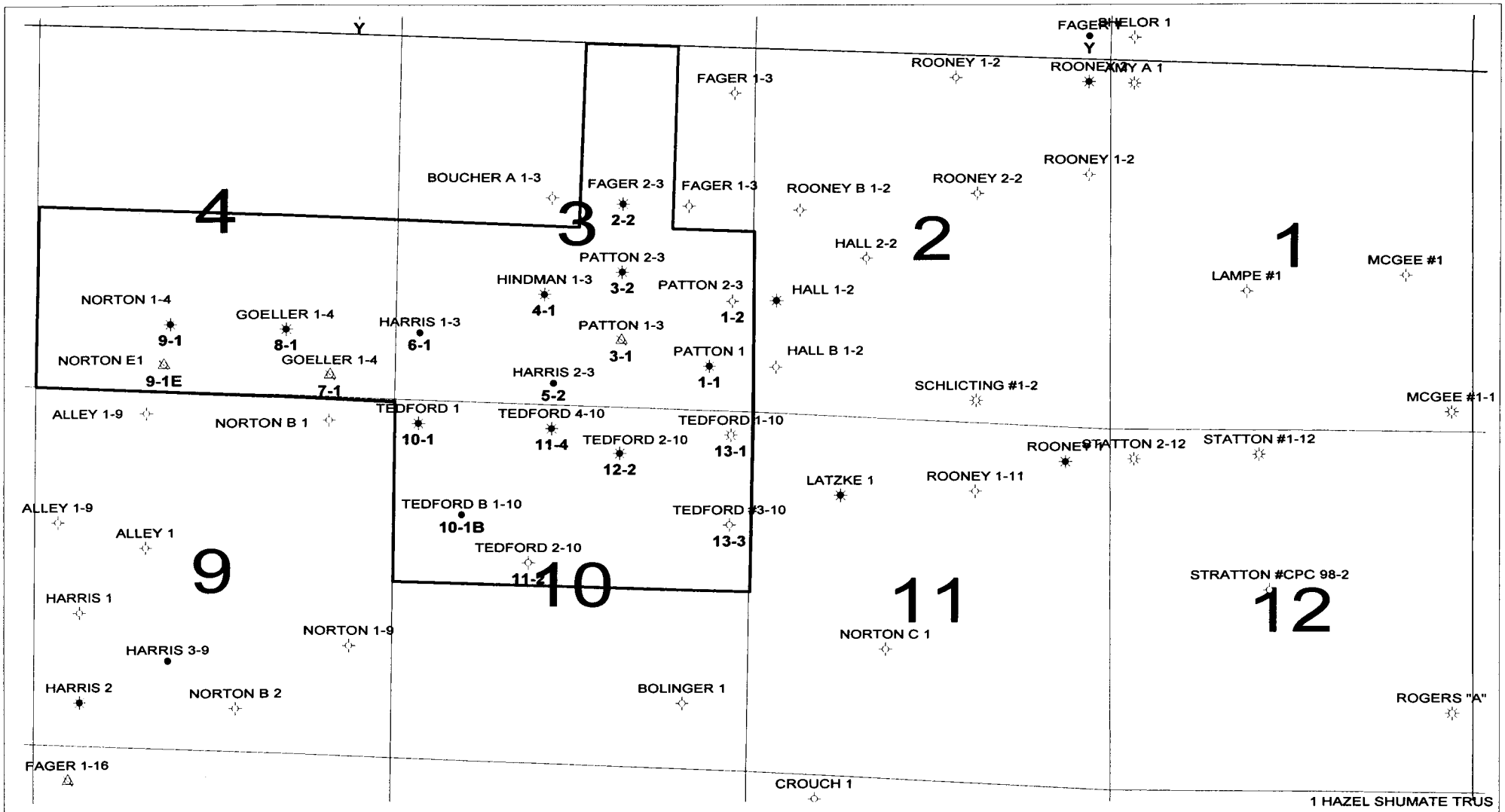

KANSAS GEOLOGICAL SURVEY

MINNEOLA FIELD SIMULATION
Figure 1
Unit Well Name & Lease Name X-REF

paul gerlach		02/03/19100
	Scale 1:25847.31	

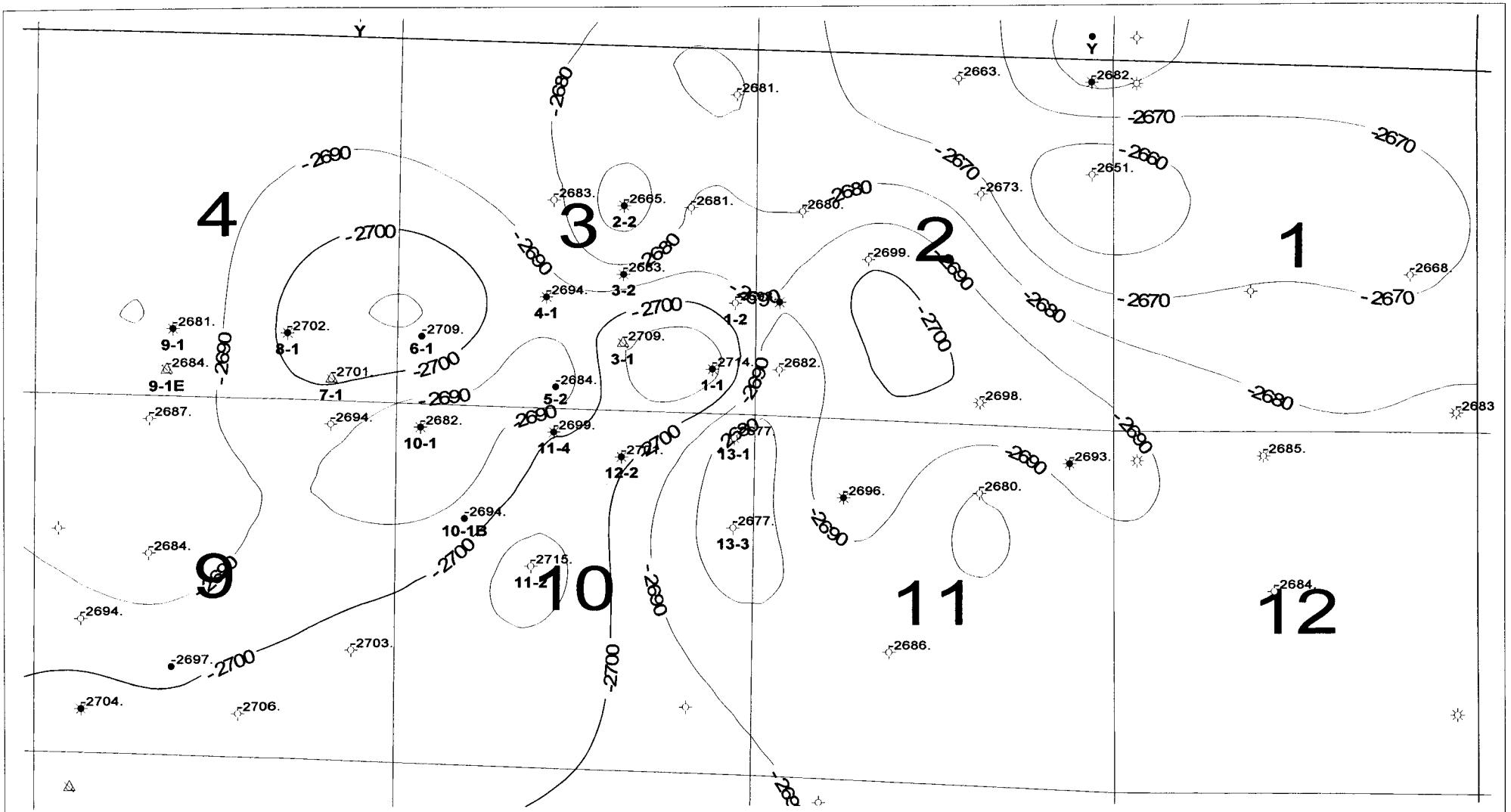

KANSAS GEOLOGICAL SURVEY		
MINNEOLA FIELD SIMULATION Figure 2 Atokan Subsea		
paul gerlach		02/03/19100
	Scale 1:25847.31	

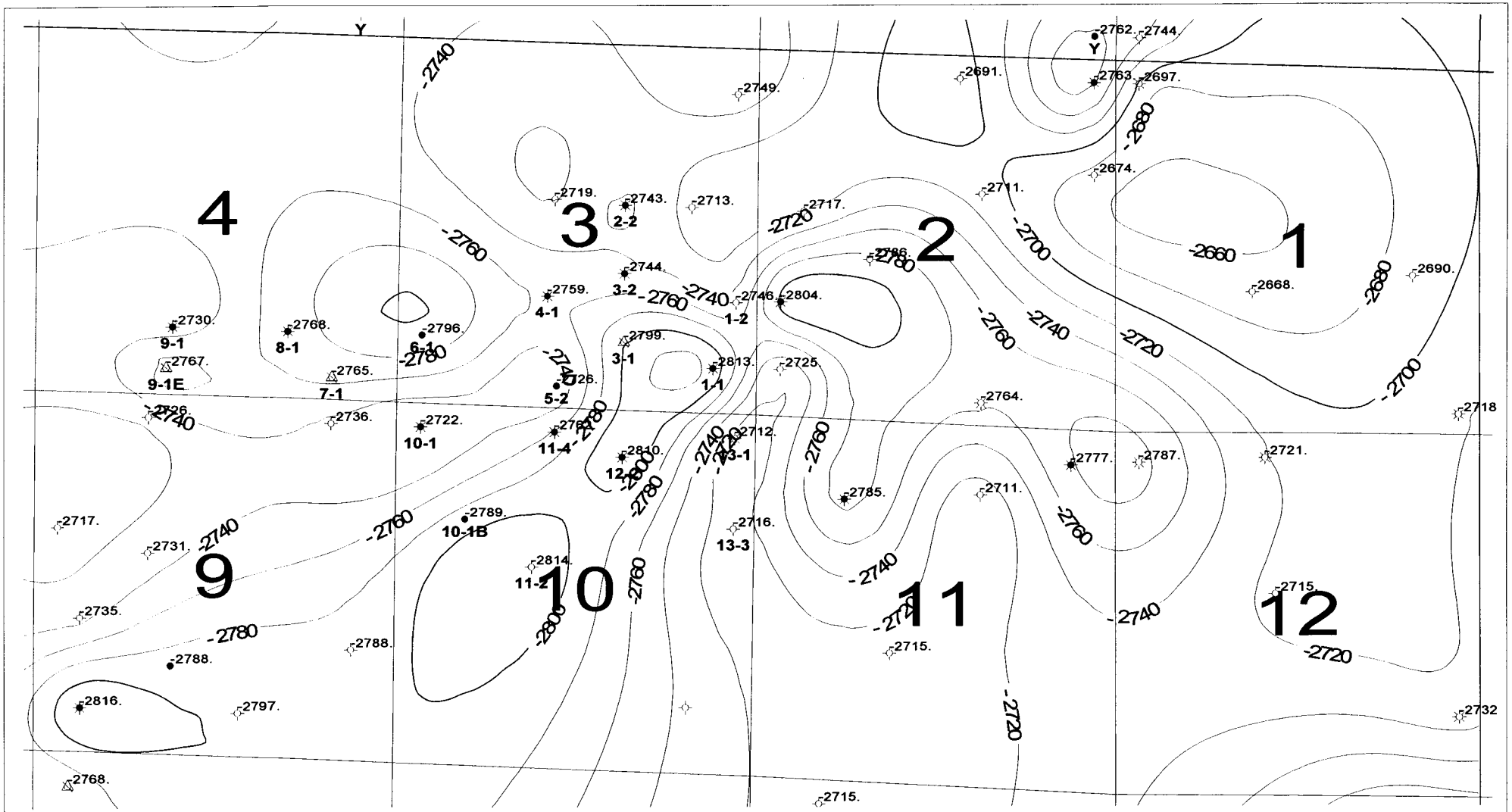

KANSAS GEOLOGICAL SURVEY

MINNEOLA FIELD SIMULATION
Figure 3
Mississippian Subsea

paul gerlach		02/03/19100
	Scale 1:25847.31	

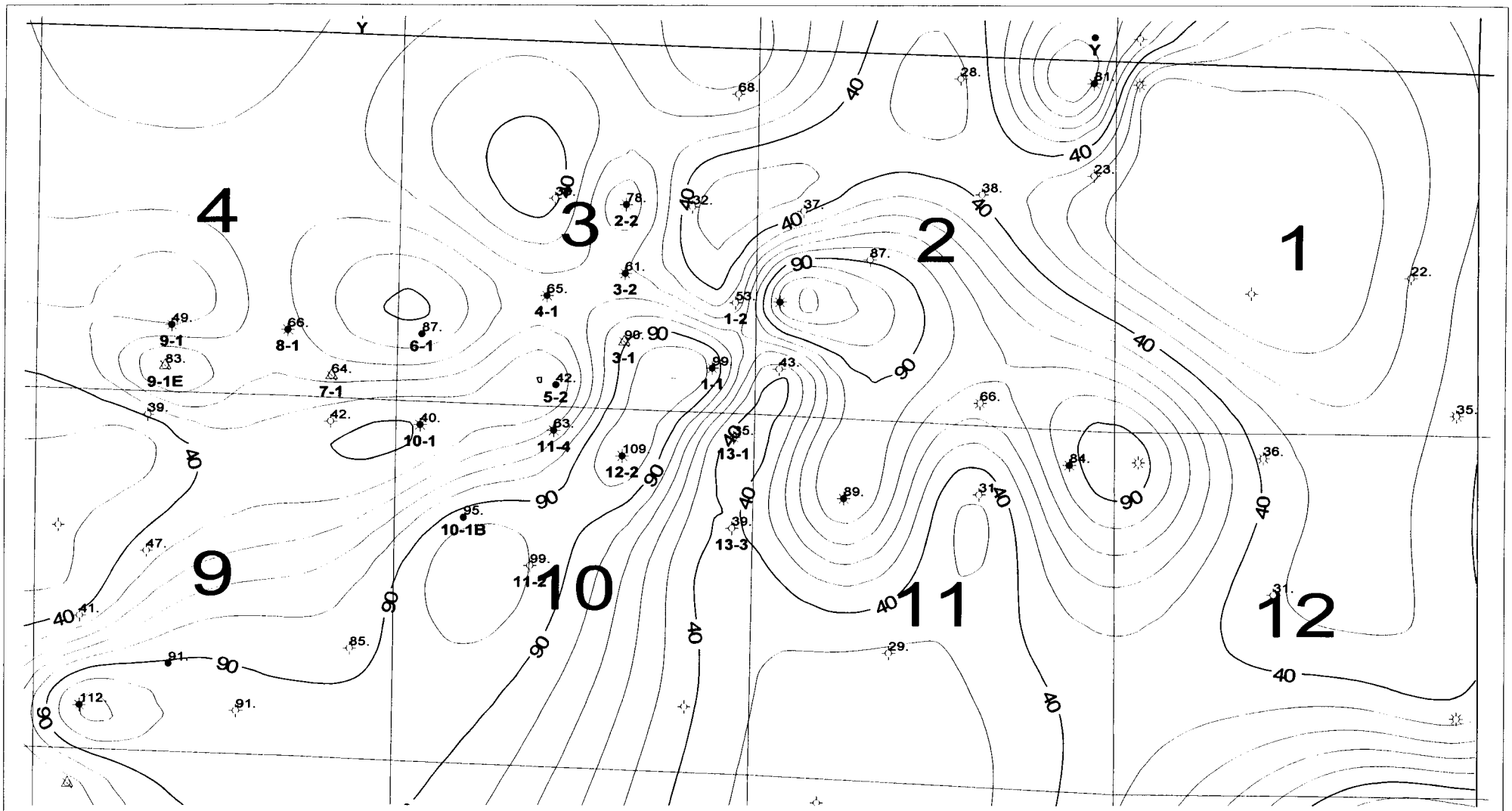

KANSAS GEOLOGICAL SURVEY		
MINNEOLA FIELD SIMULATION Figure 4 Atokan Isopach		
paul gerlach		02/03/19100
	Scale 1:25847.31	

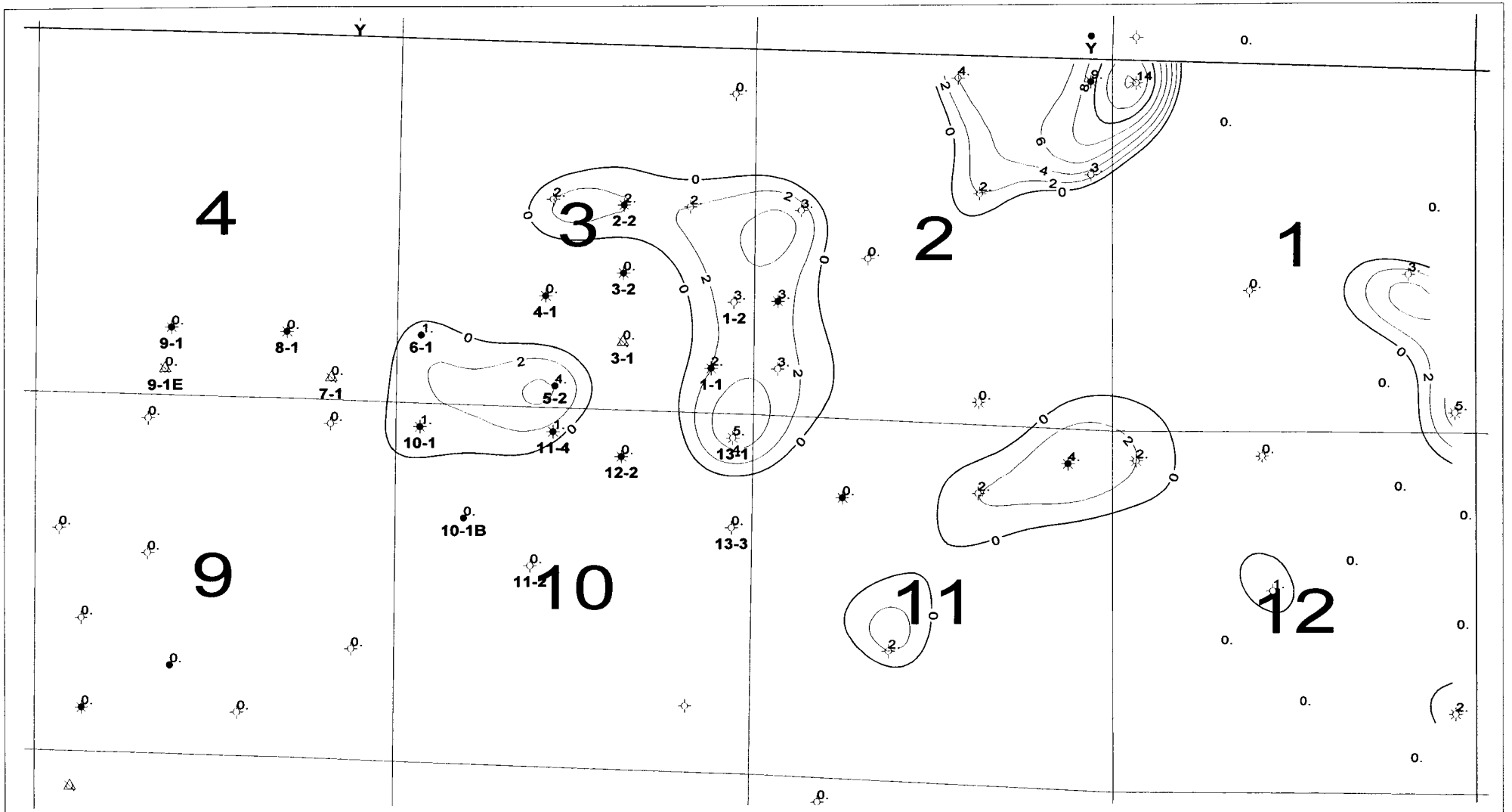

KANSAS GEOLOGICAL SURVEY		
MINNEOLA FIELD SIMULATION Figure 5 Sand #1 Isopach		
paul gerlach		02/03/19100
	Scale 1:25847.31	

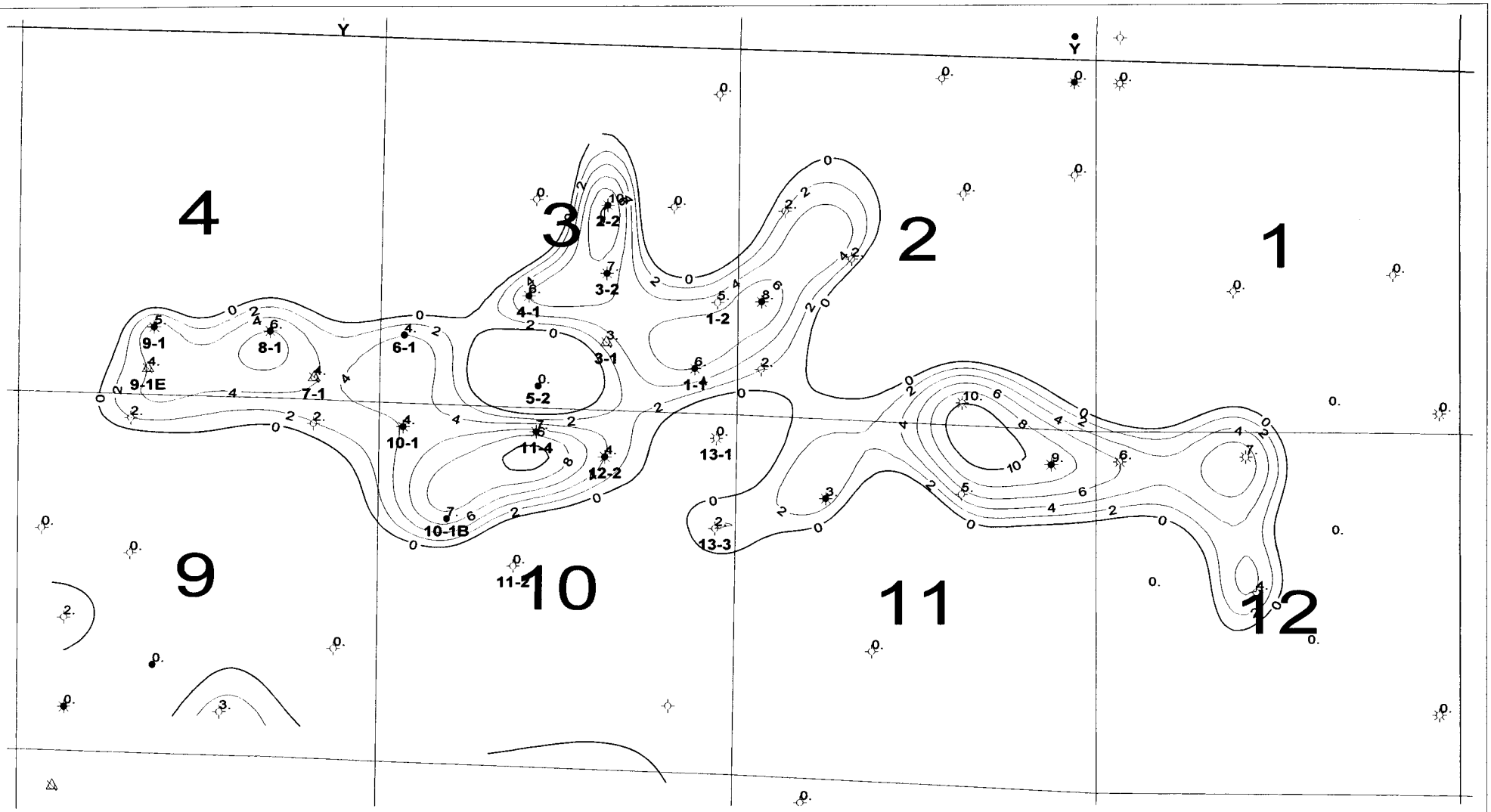

KANSAS GEOLOGICAL SURVEY		
MINNEOLA FIELD SIMULATION Figure 6 Sand #2 Isopach		
paul gerlach		02/03/19100
	Scale 1:25847.31	

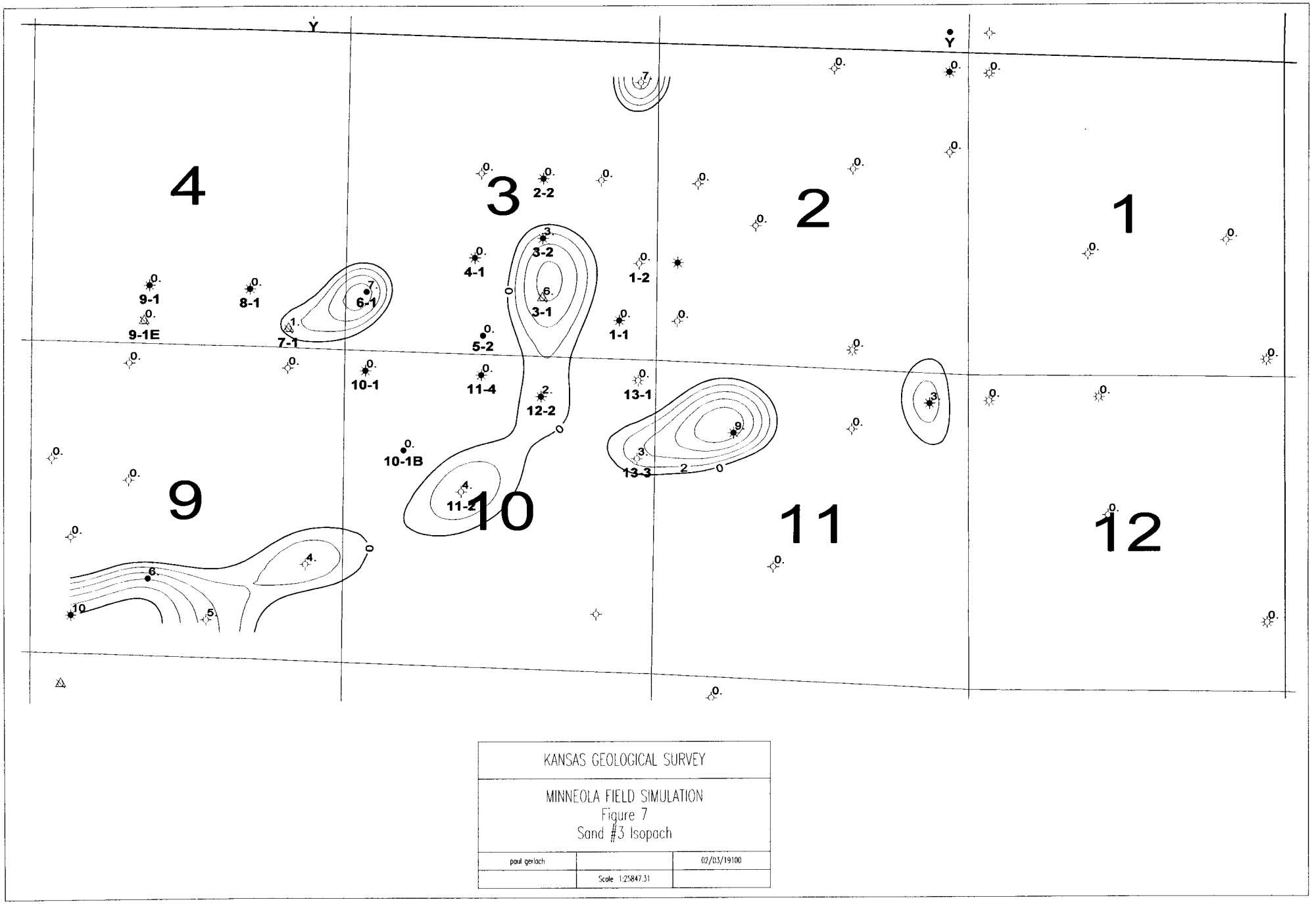

KANSAS GEOLOGICAL SURVEY		
MINNEOLA FIELD SIMULATION Figure 7 Sand #3 Isopach		
paul gerlach		02/03/19100
	Scale 1:25847.31	

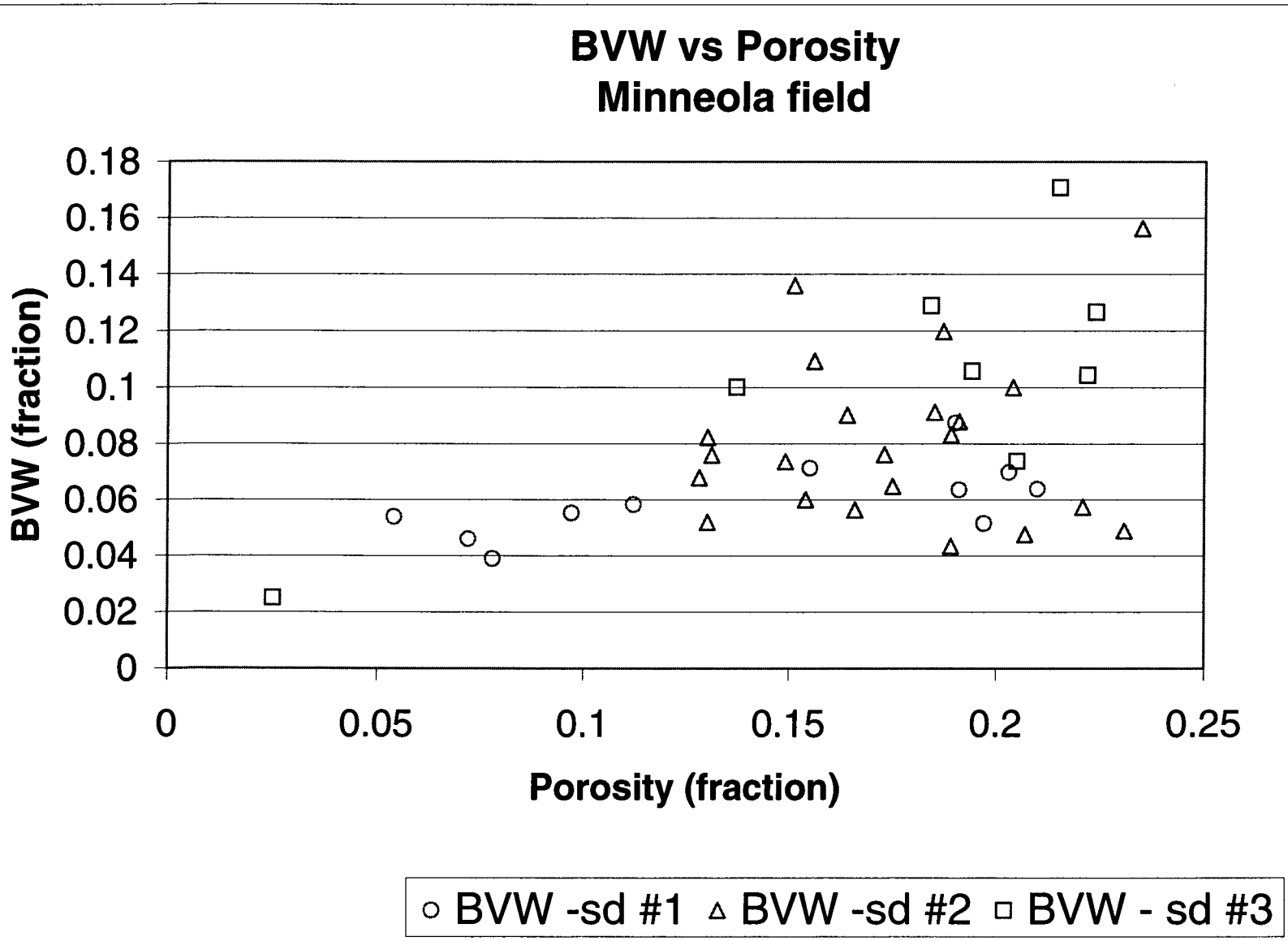
BVW vs Porosity
Minneola field
BVW (fraction)
0.18
0.16
0.14
0.12
0.1
0.08
0.06
0.04
0.02
0
0
0.05
0.1
0.15
0.2
0.25
Porosity (fraction)
BVW -sd #1
BVW -sd #2
BVW - sd #3

Figure 8

At log K = 0, K = **1 md**. Porosity = **6.8**
At log K = -0.30103, K = **0.5 md**. P 4.69

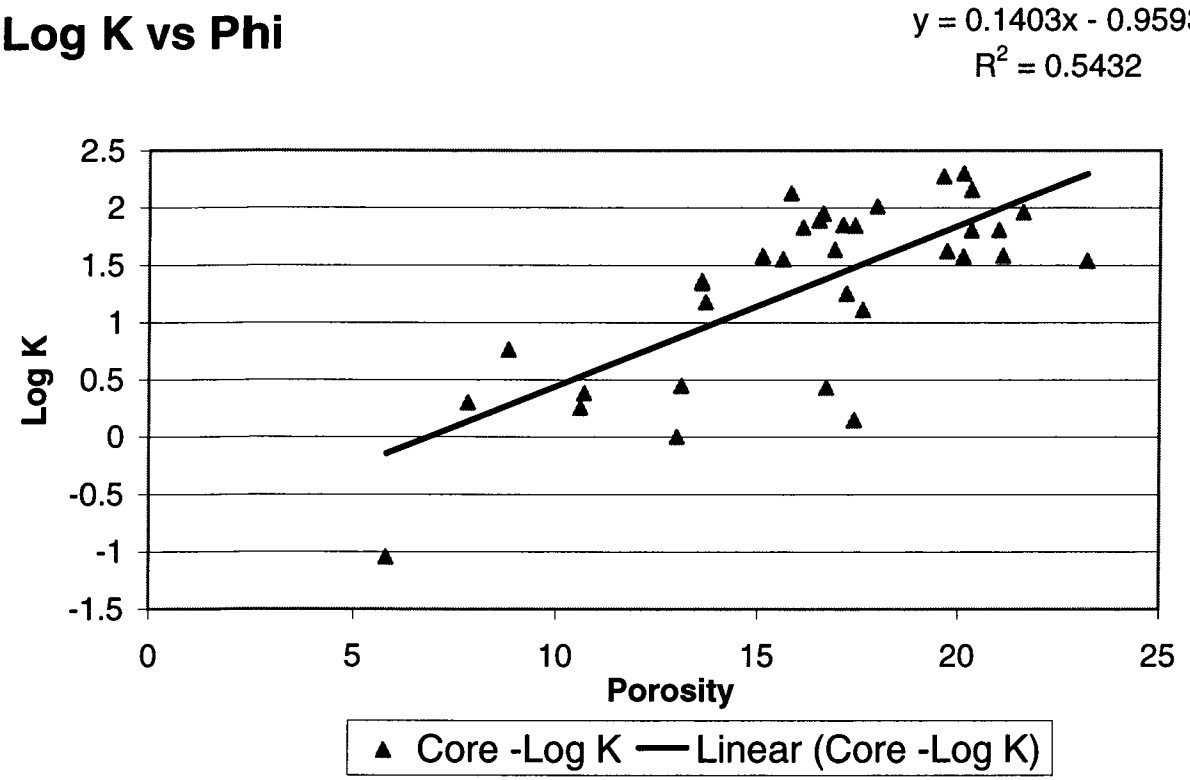

Figure 9

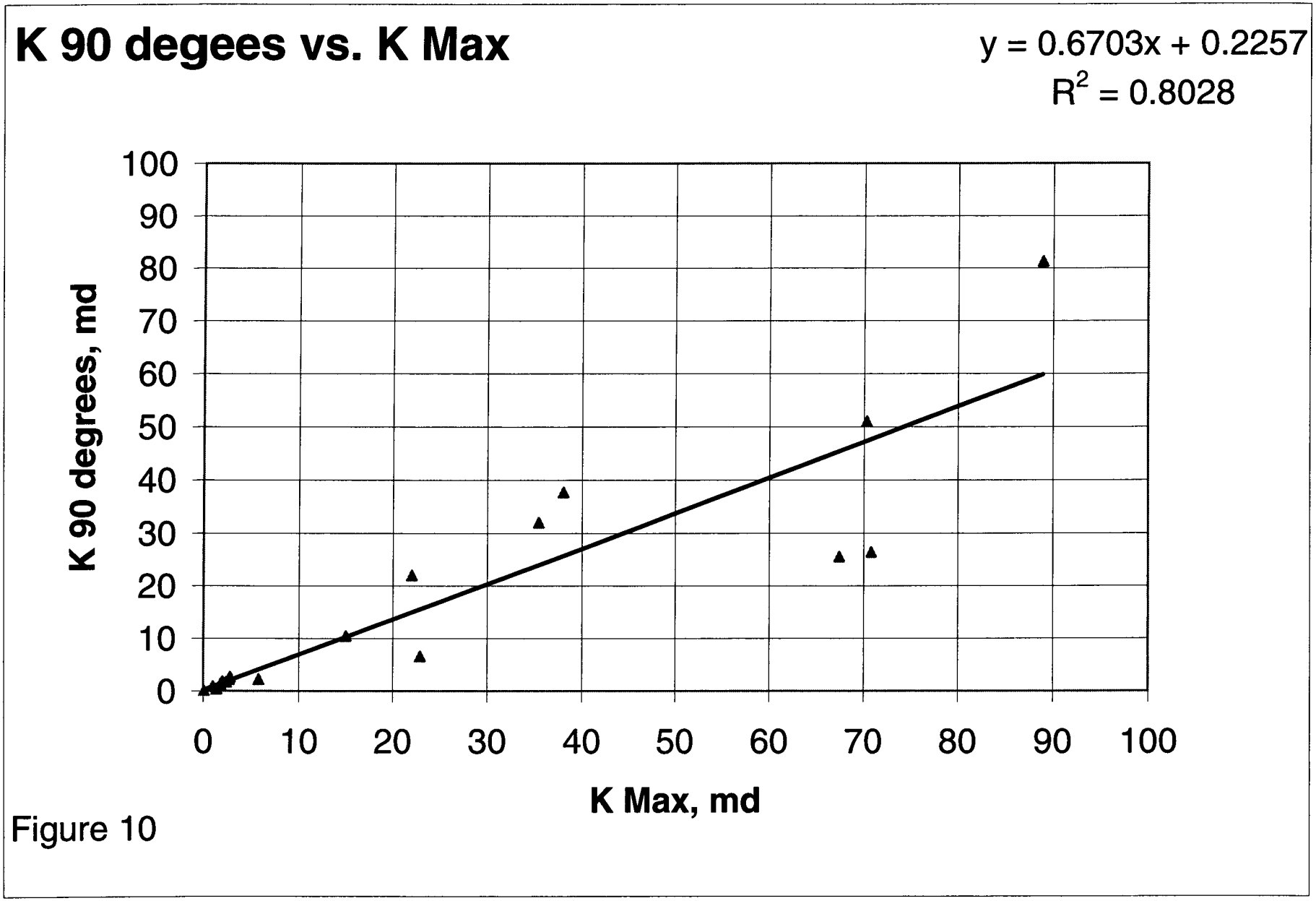
K 90 degees vs. K Max
y = 0.6703x + 0.2257
R2 = 0.8028
K 90 degrees, md
K Max, md
0
10
20
30
40
50
60
70
80
90
100

Figure 10

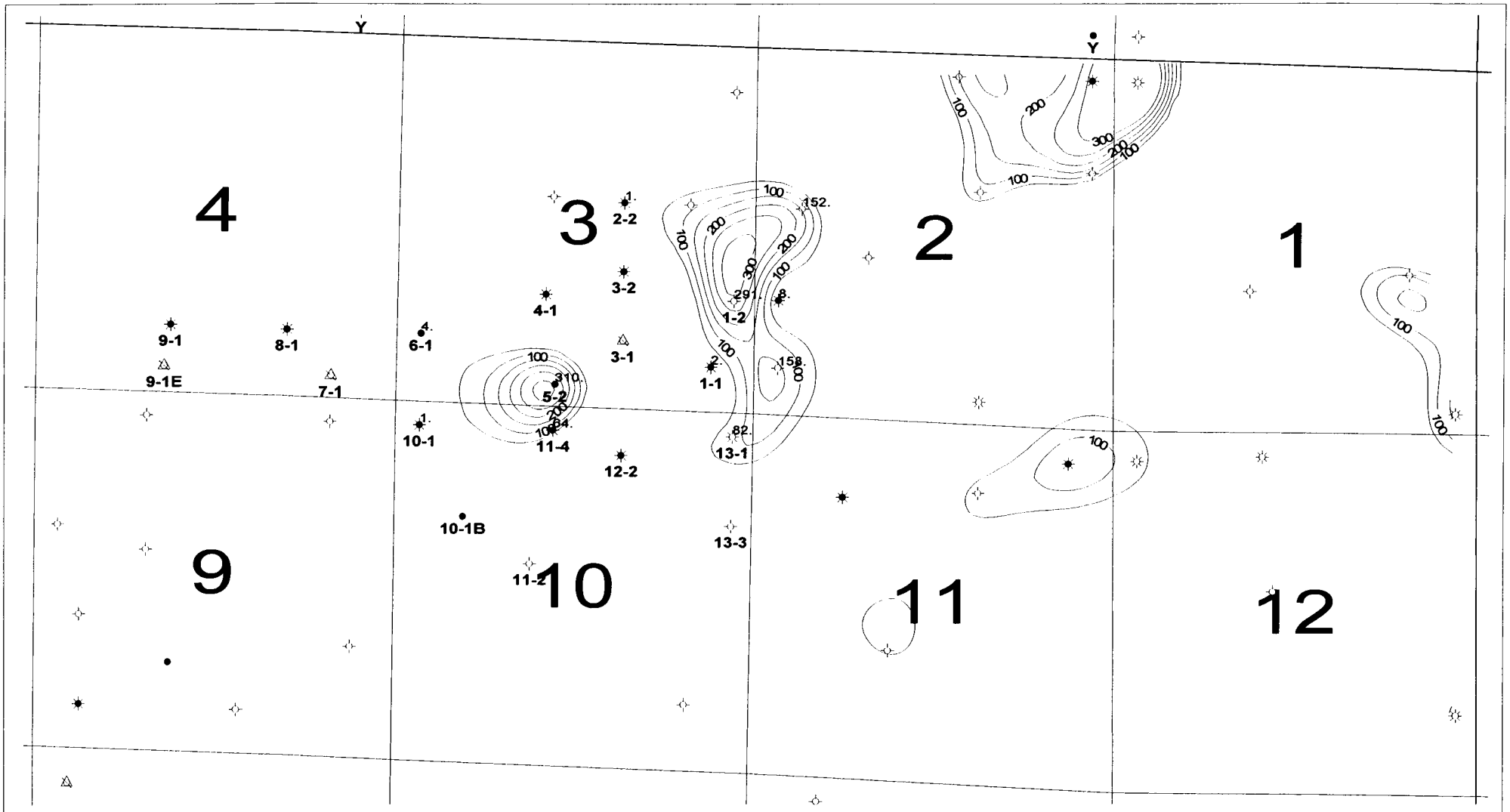

KANSAS GEOLOGICAL SURVEY		
MINNEOLA FIELD SIMULATION Figure 11 Sand #1 Transmissibility (KhFt.)		
paul gerlach		02/03/19100
	Scale 1:25847.31	

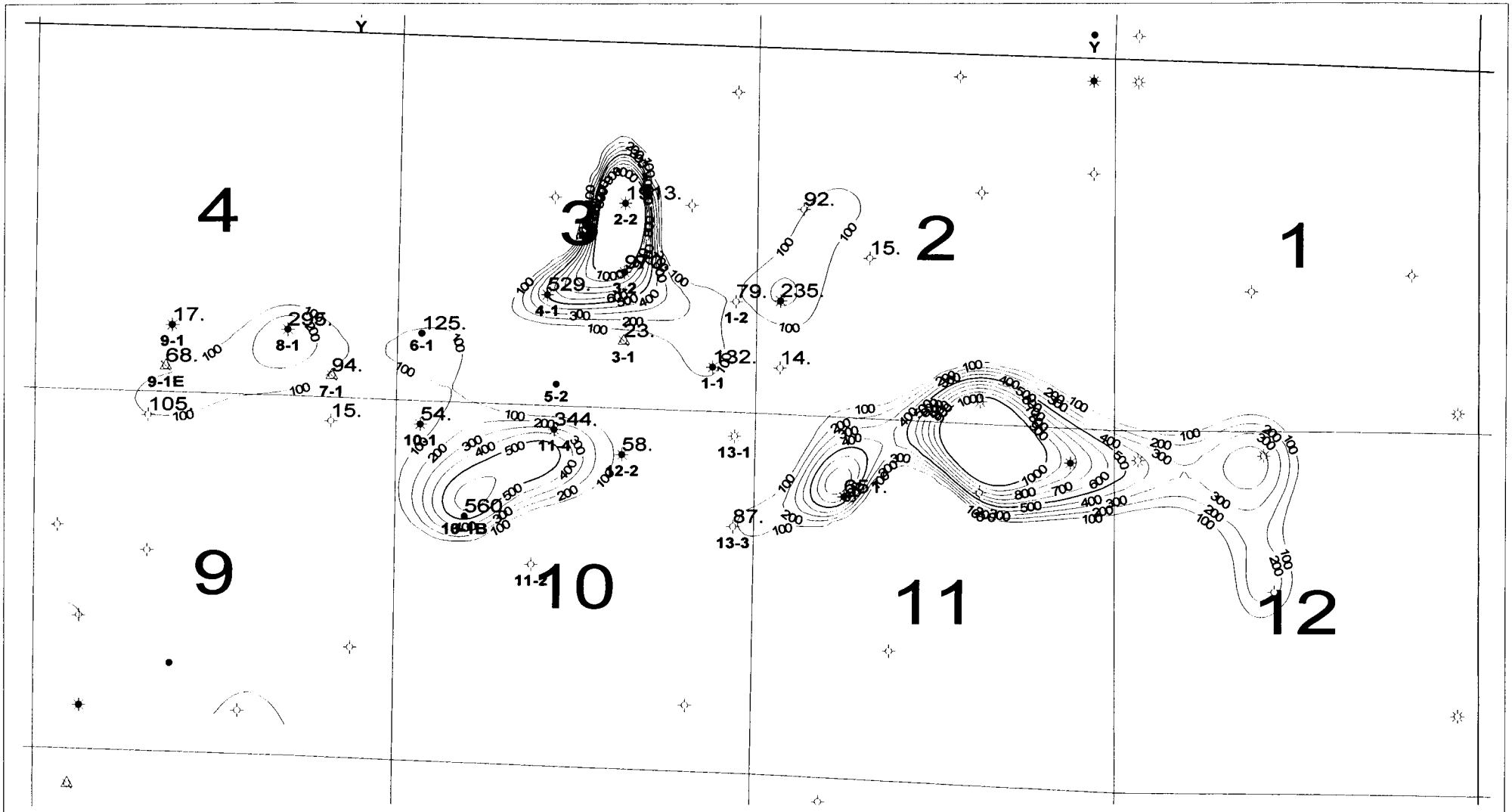

KANSAS GEOLOGICAL SURVEY		
MINNEOLA FIELD SIMULATION Figure 12 Sand #2 Transmissibility (KhFt.)		
paul gerloch		02/03/19100
	Scale 1:25847.31	

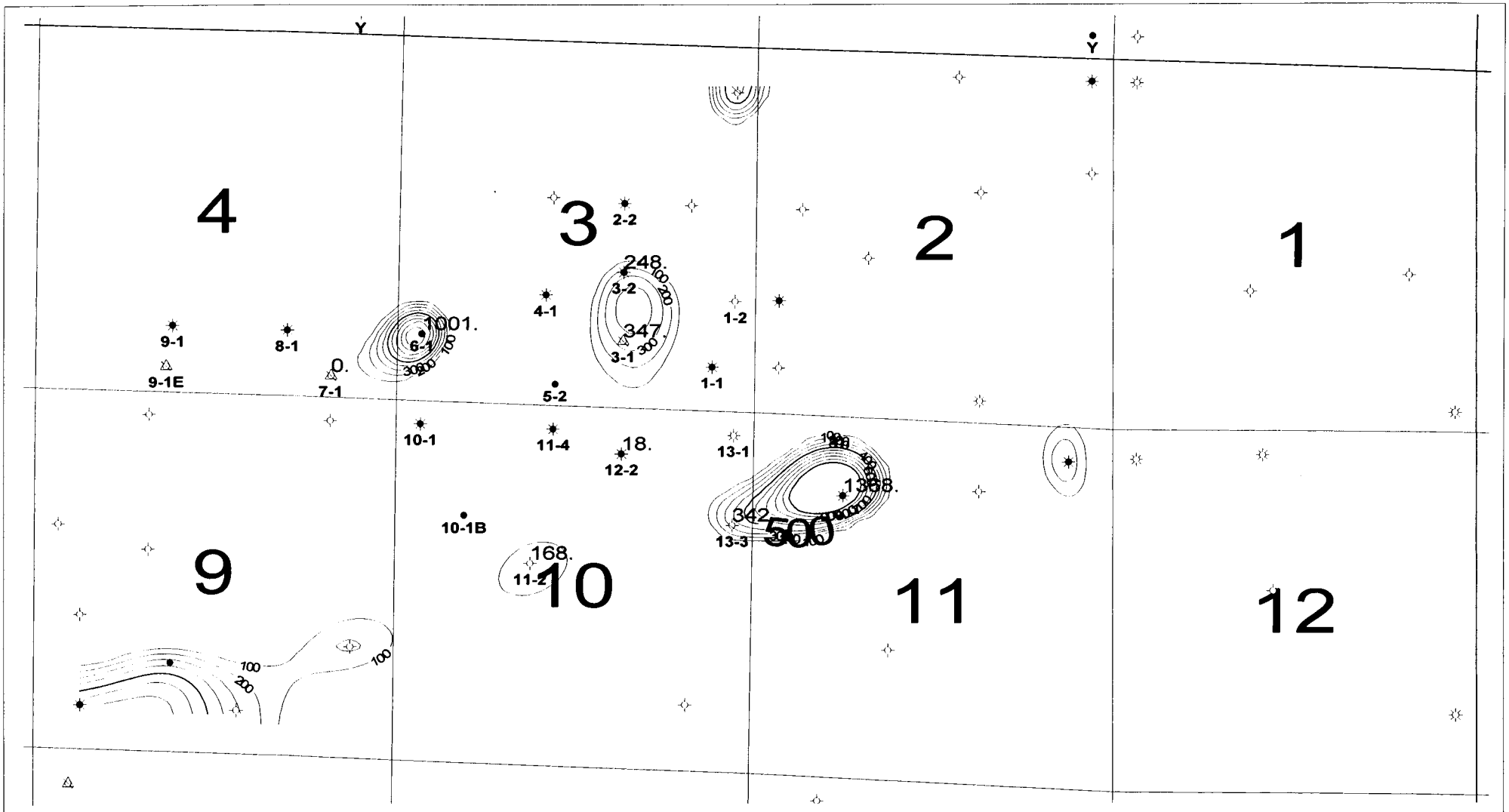

KANSAS GEOLOGICAL SURVEY		
MINNEOLA FIELD SIMULATION Figure 13 Sand #3 Transmissibility (KhFt.)		
paul gerloch		02/03/19100
	Scale 1:25847.31	

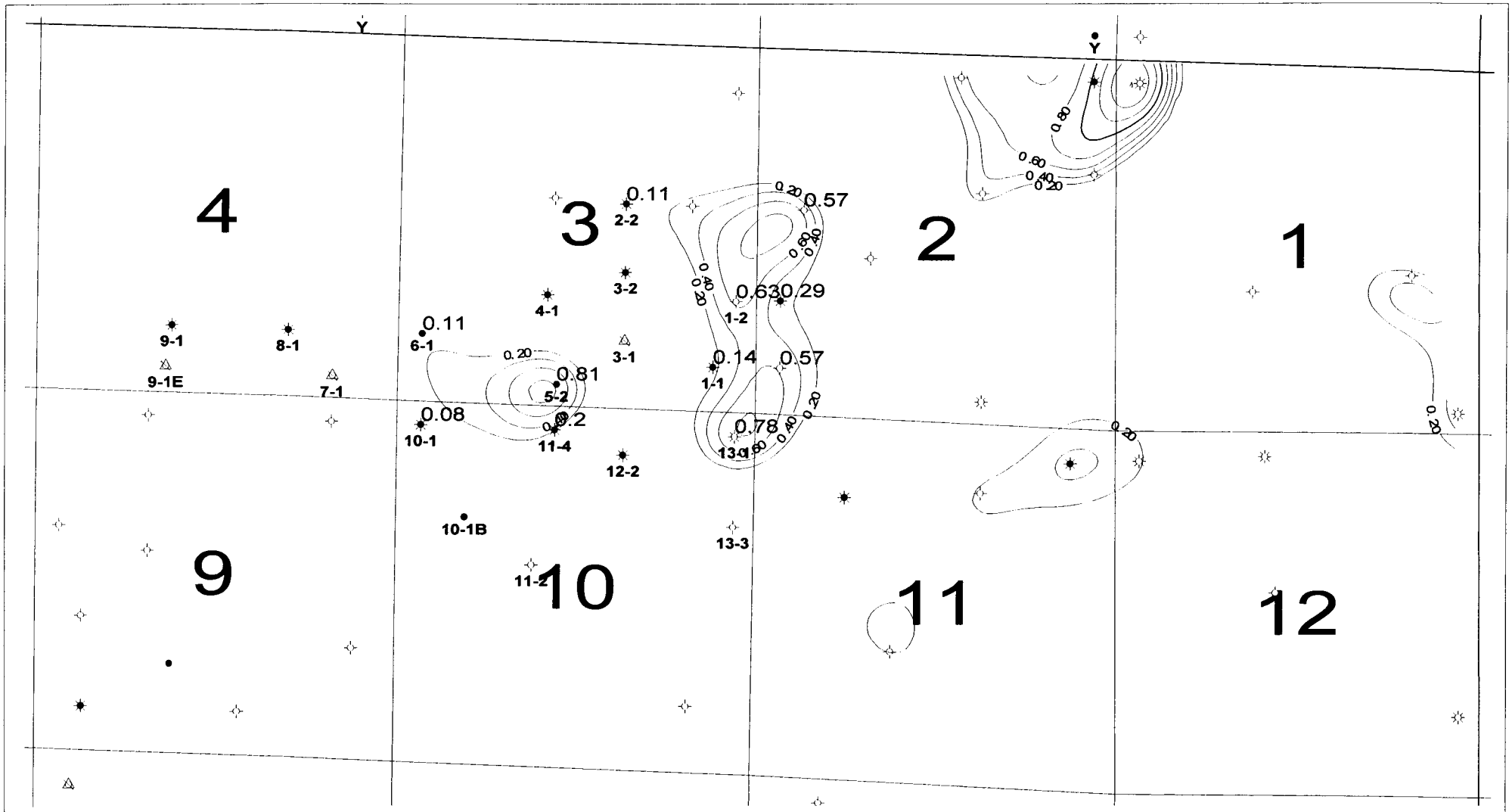

KANSAS GEOLOGICAL SURVEY		
MINNEOLA FIELD SIMULATION Figure 14 Sand #1 Storativity (PhiFt.)		
paul gerlach		02/03/19100
	Scale 1:25847.31	

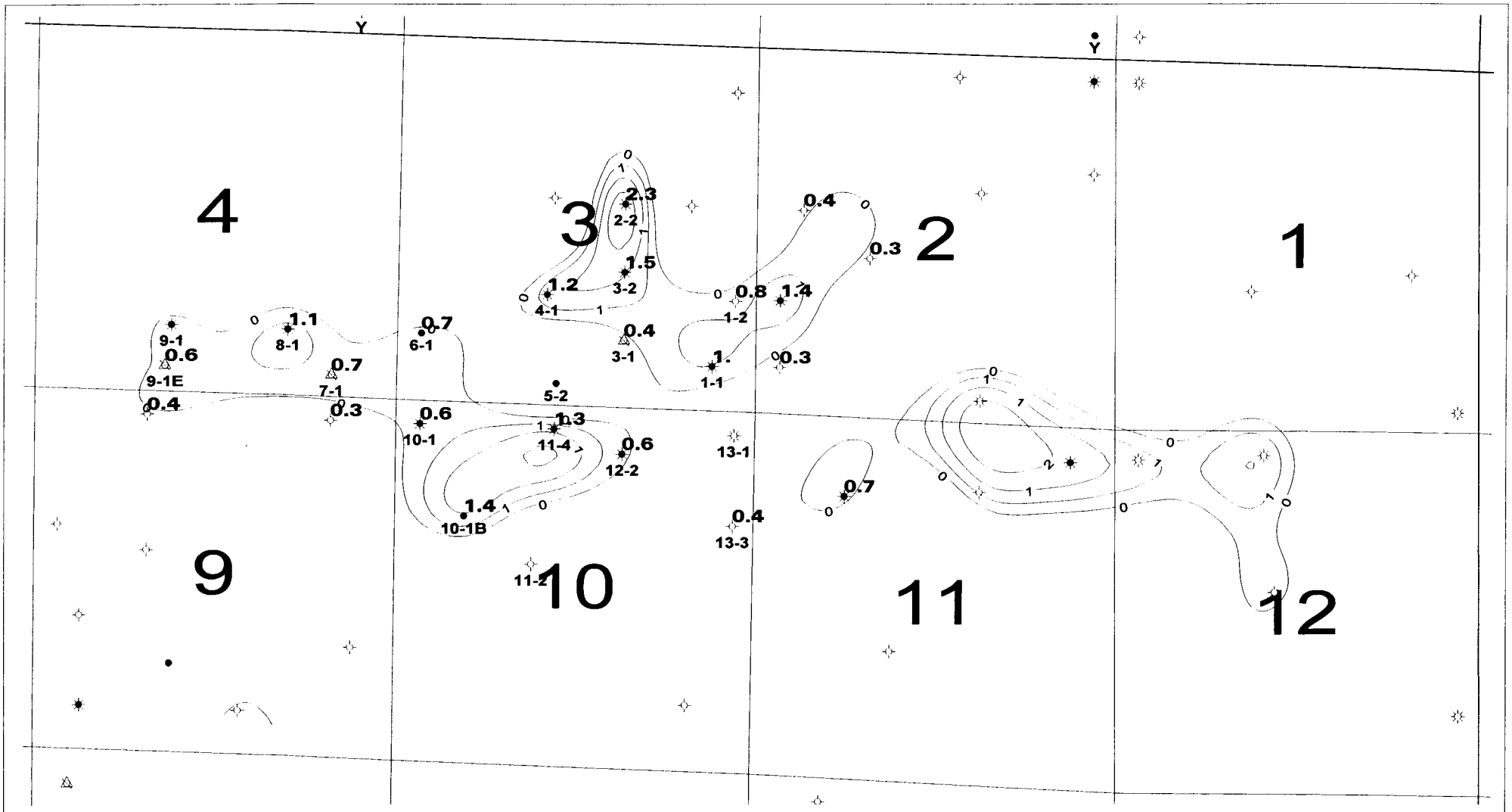

KANSAS GEOLOGICAL SURVEY		
MINNEOLA FIELD SIMULATION Figure 15 Sand #2 Storativity (PhiFt.)		
paul gerlach		02/03/19100
	Scale 1:25847.31	

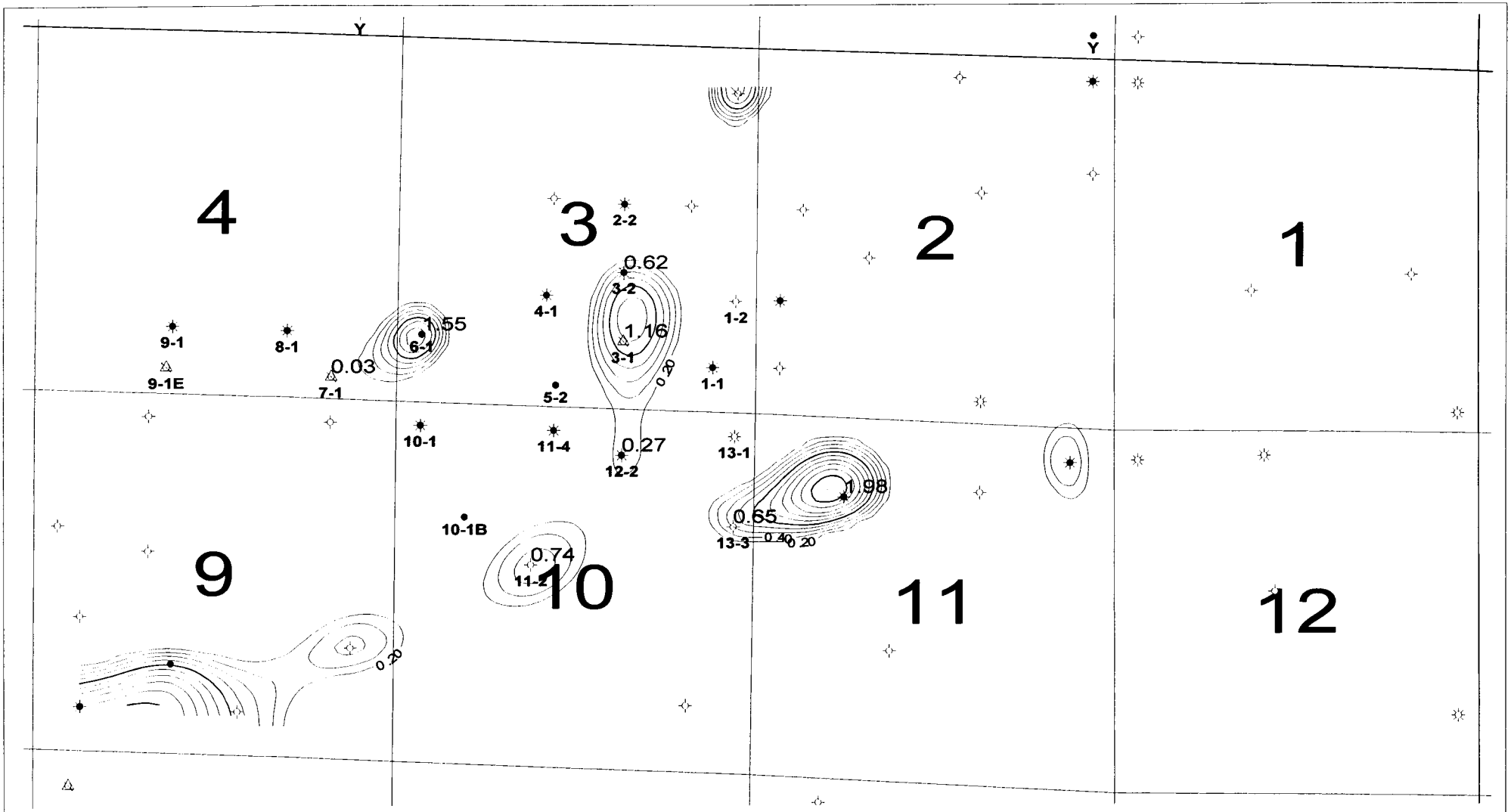

KANSAS GEOLOGICAL SURVEY		
MINNEOLA FIELD SIMULATION Figure 16 Sand #3 Storativity (PhiFt.)		
paul gerlach		02/03/19100
	Scale 1:25847.31	

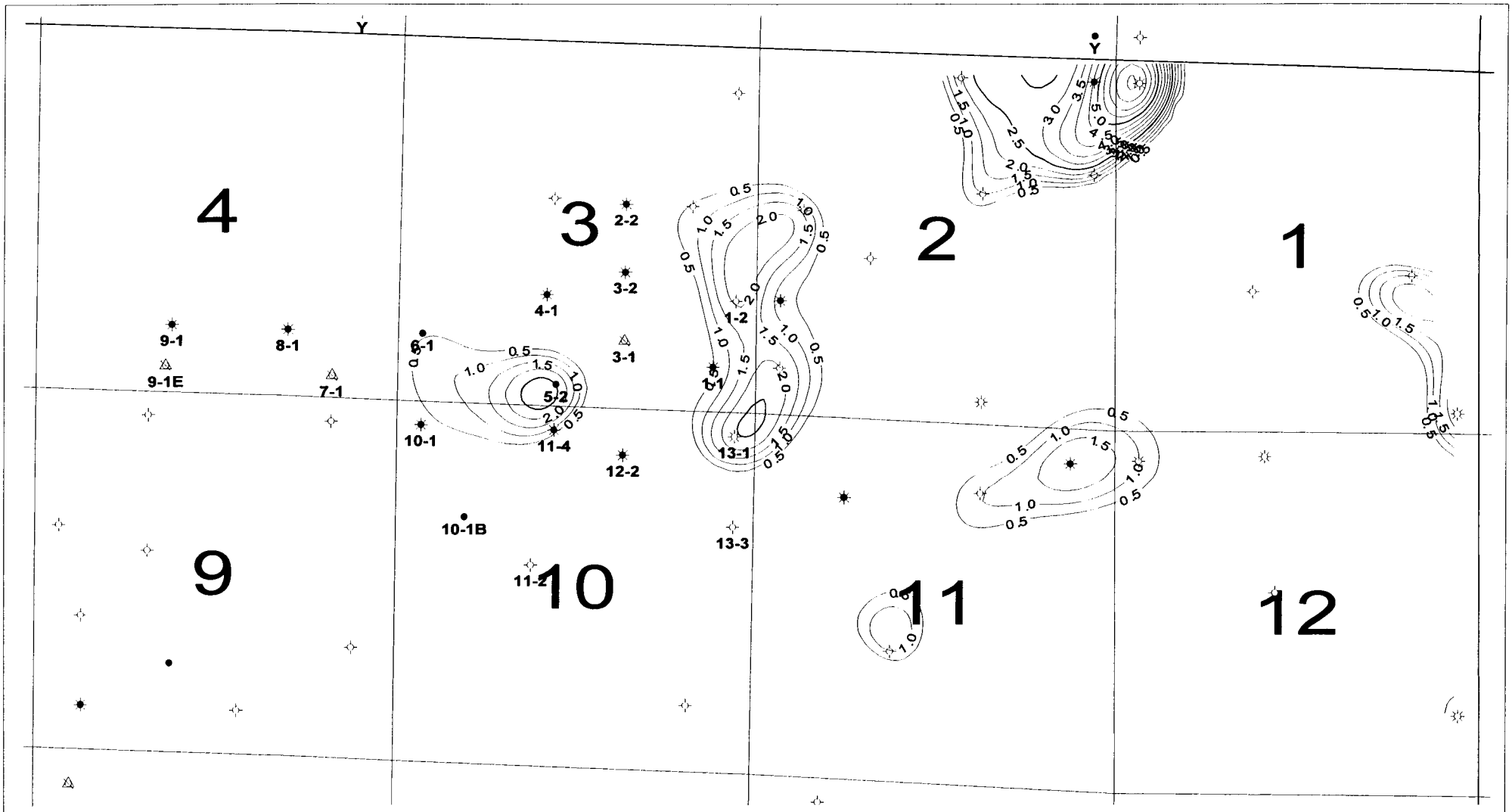

KANSAS GEOLOGICAL SURVEY		
MINNEOLA FIELD SIMULATION Figure 17 Sand #1 Saturation-Feet (SoFt)		
paul gerlach		02/03/19100
	Scale 1:25847.31	

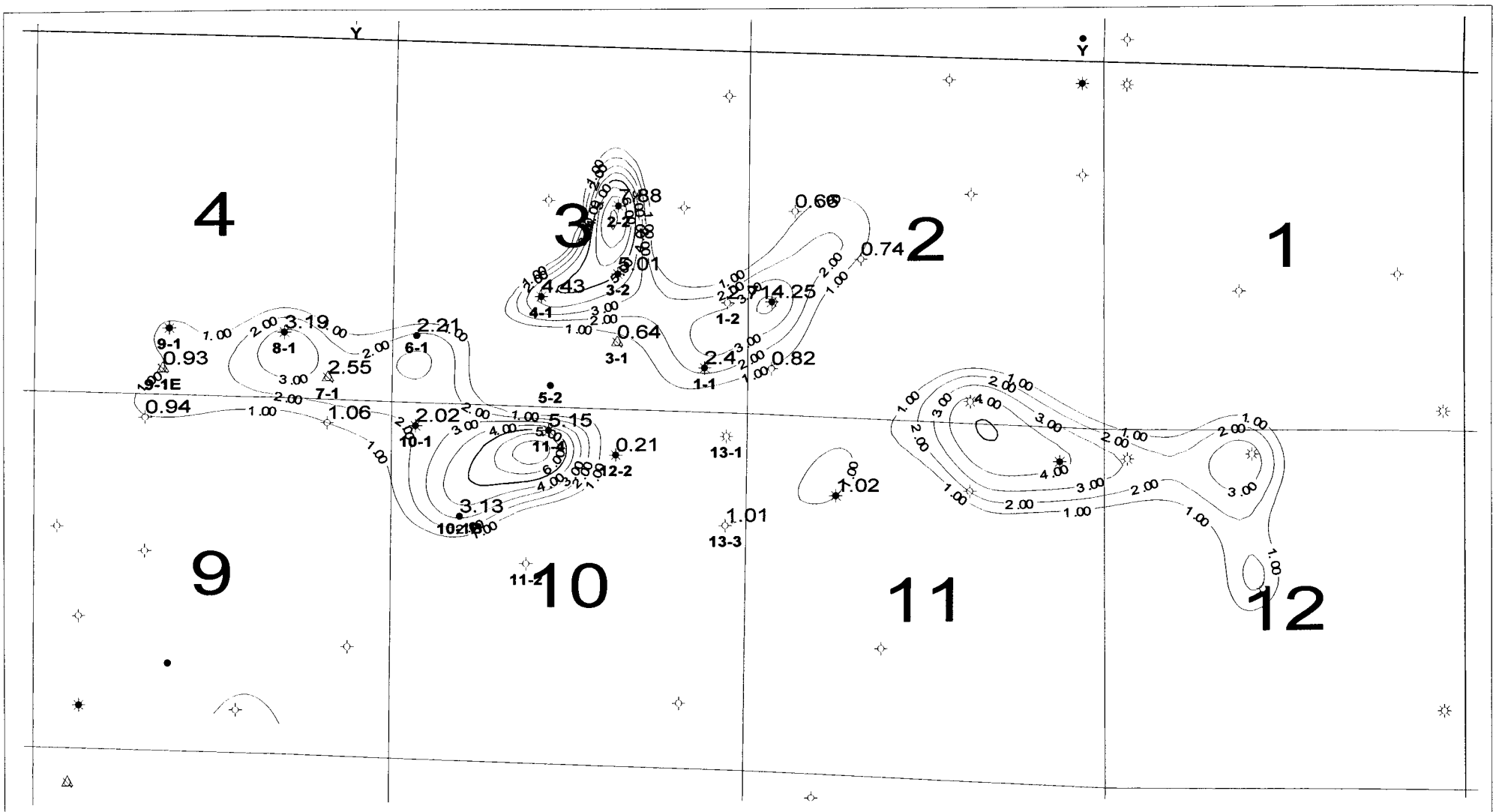

KANSAS GEOLOGICAL SURVEY		
MINNEOLA FIELD SIMULATION Figure 18 Sand #2 Saturation-Feet (SoFt)		
paul gerlach		02/03/19100
	Scale 1:25847.31	

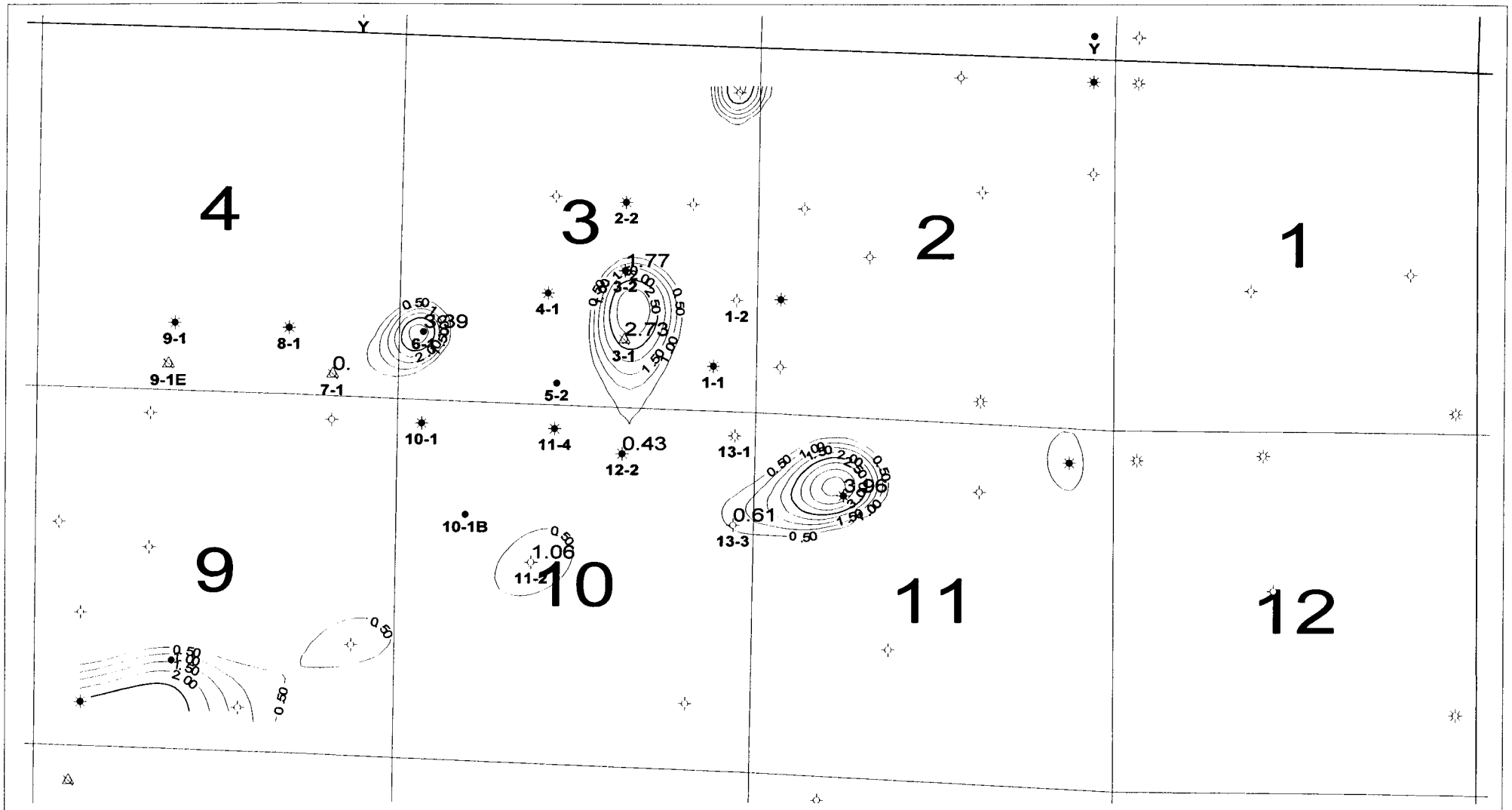

KANSAS GEOLOGICAL SURVEY		
MINNEOLA FIELD SIMULATION Figure 19 Sand #3 Saturation-Feet (SoFt)		
paul gerlach		02/03/19100
	Scale 1:25847.31	

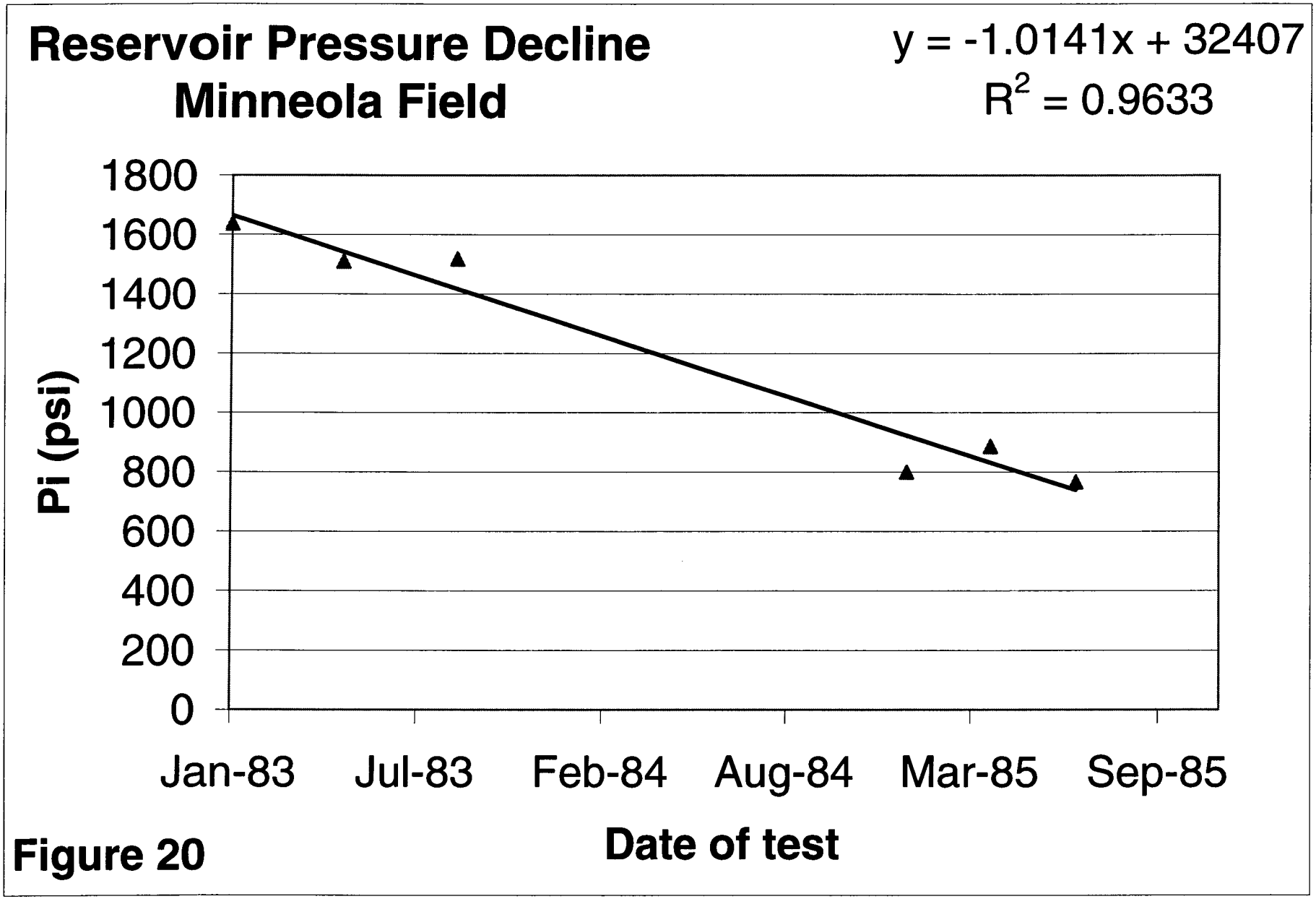
Reservoir Pressure Decline
Minneola Field
y = -1.0141x + 32407
R2 = 0.9633
Pi (psi)
1800
1600
1400
1200
1000
800
600
400
200
0
Jan-83
Jul-83
Feb-84
Aug-84
Mar-85
Sep-85
Date of test

Figure 20

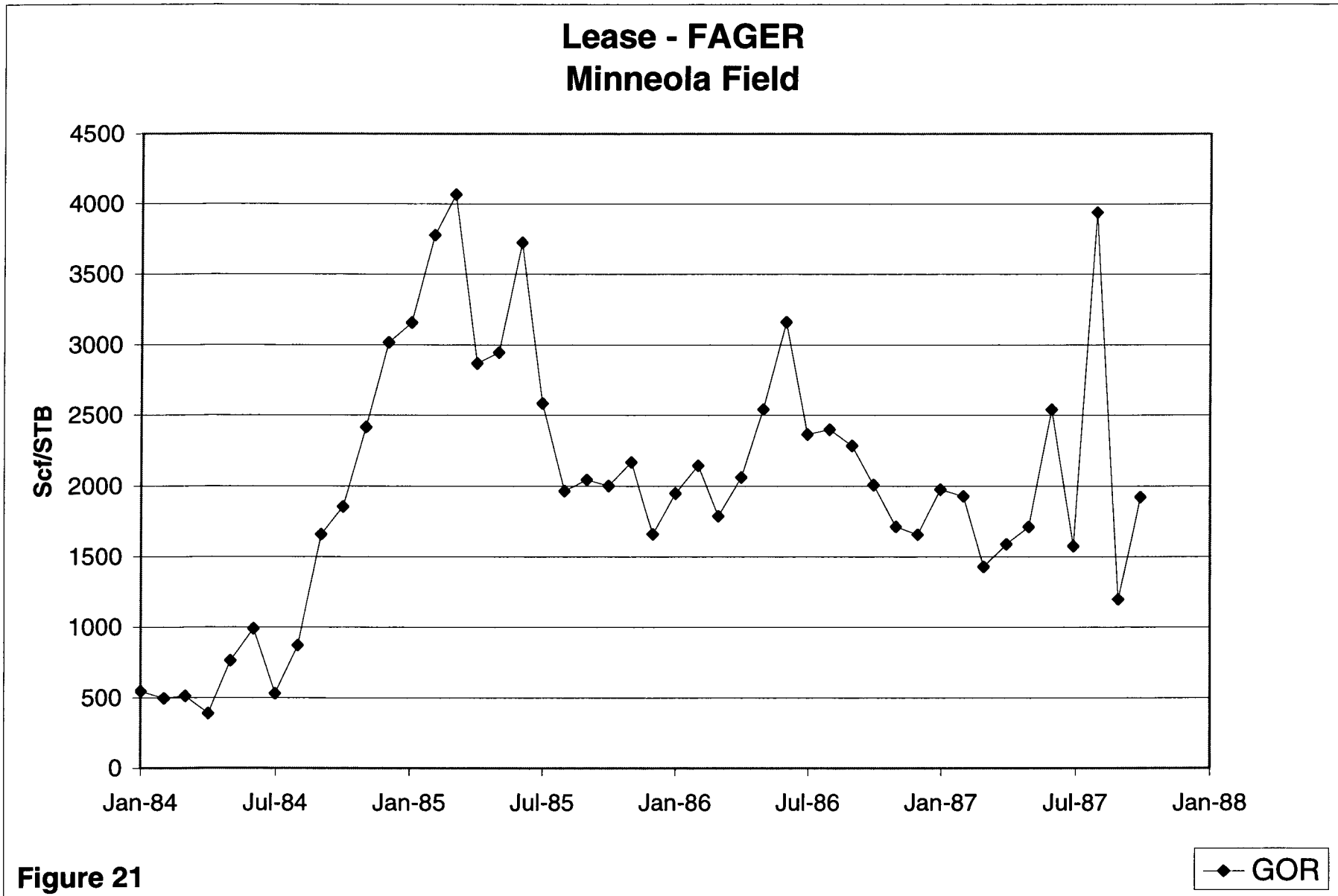
Lease - FAGER
Minneola Field
Scf/STB
4500
4000
3500
3000
2500
2000
1500
1000
500
0
Jan-84
Jul-84
Jan-85
Jul-85
Jan-86
Jul-86
Jan-87
Jul-87
Jan-88
GOR

Figure 21

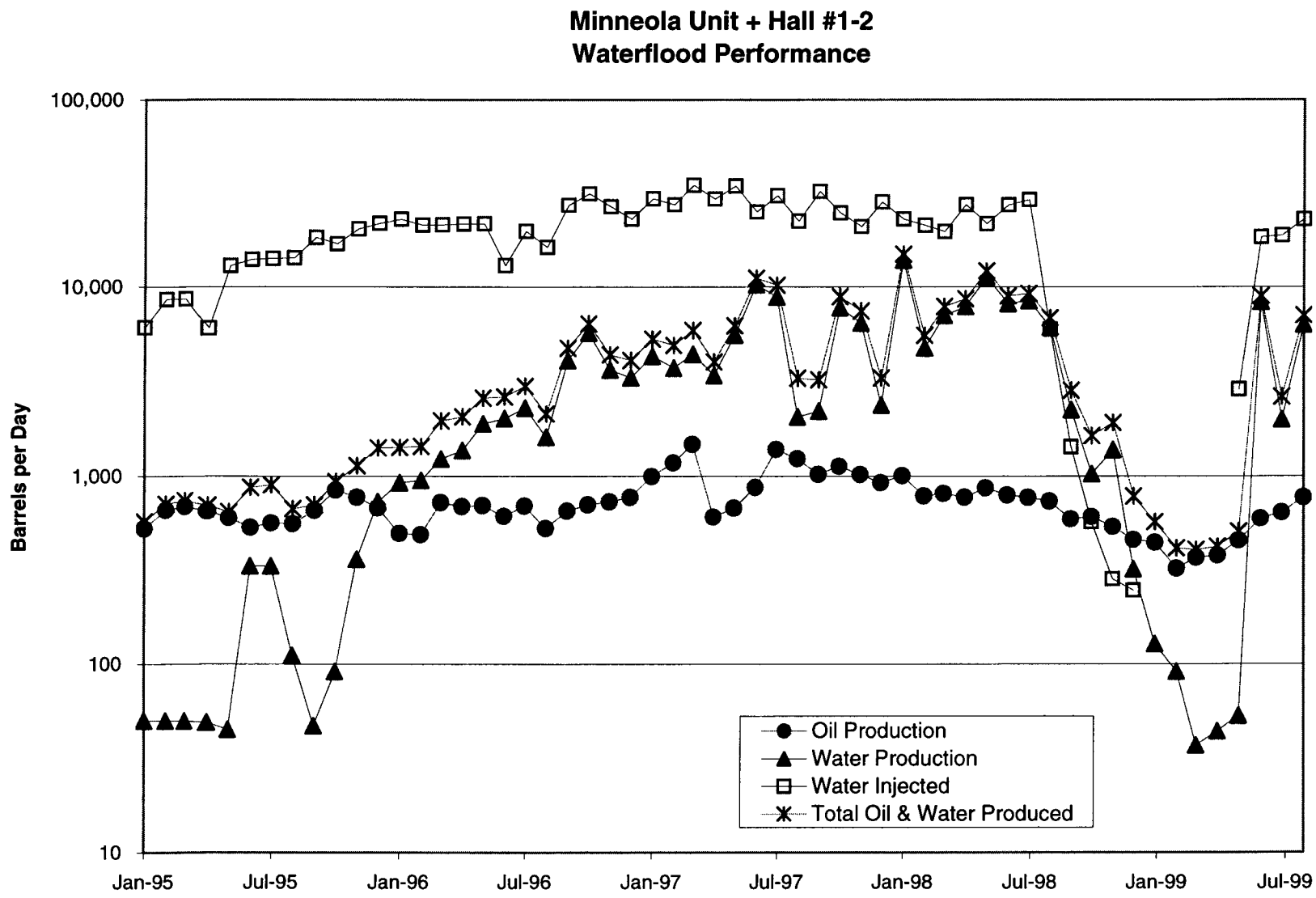
Minneola Unit + Hall #1-2
Waterflood Performance
100,000
10,000
1,000
100
10
Barrels per Day
Jan-95
Jul-95
Jan-96
Jul-96
Jan-97
Jul-97
Jan-98
Jul-98
Jan-99
Jul-99
Oil Production
Water Production
Water Injected
Total Oil & Water Produced

Figure 22

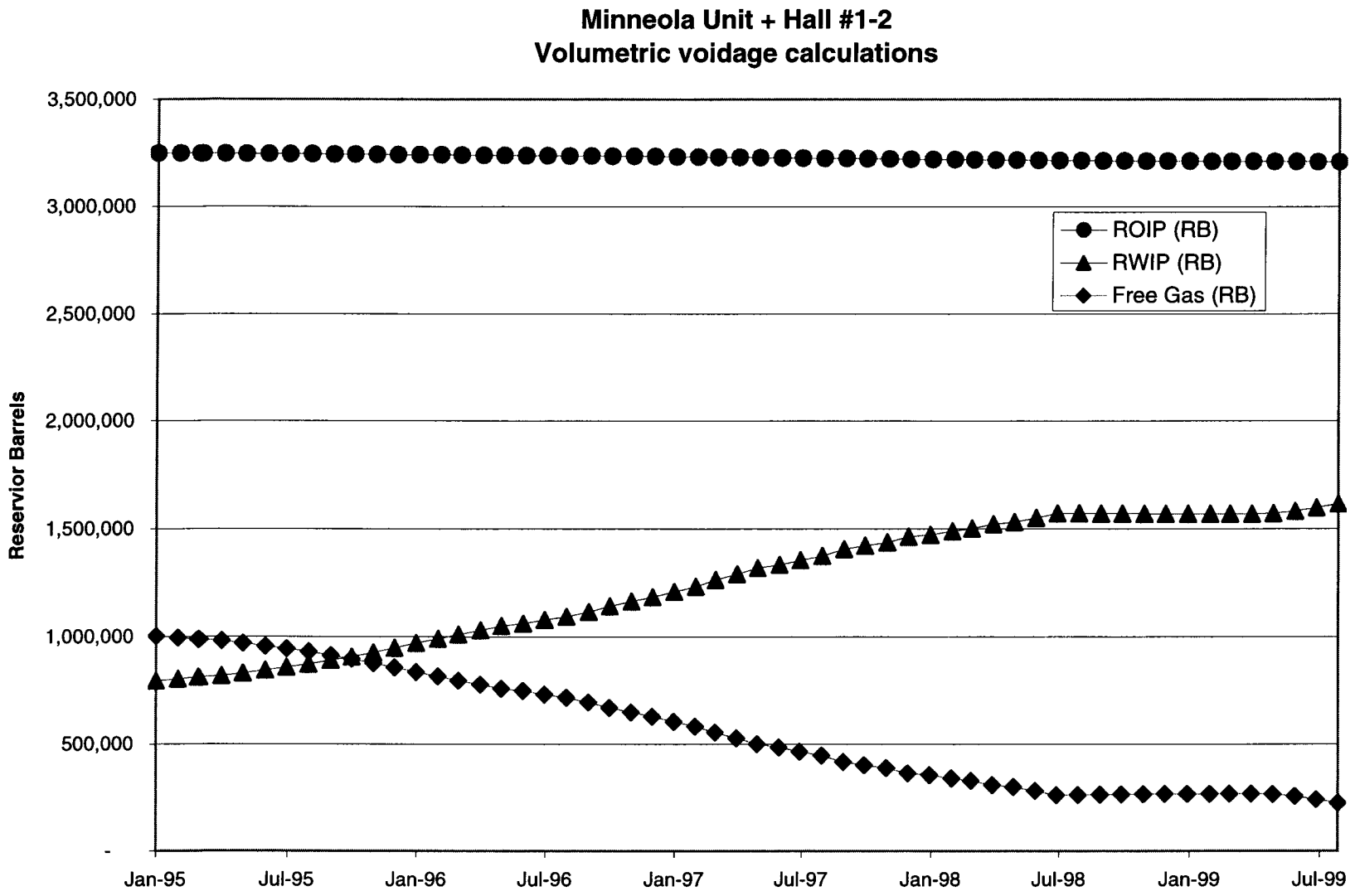
Minneola Unit + Hall #1-2
Volumetric voidage calculations
Reservior Barrels
3,500,000
3,000,000
2,500,000
2,000,000
1,500,000
1,000,000
500,000
-
Jan-95
Jul-95
Jan-96
Jul-96
Jan-97
Jul-97
Jan-98
Jul-98
Jan-99
Jul-99
ROIP (RB)
RWIP (RB)
Free Gas (RB)

Figure 23

Appendix - A

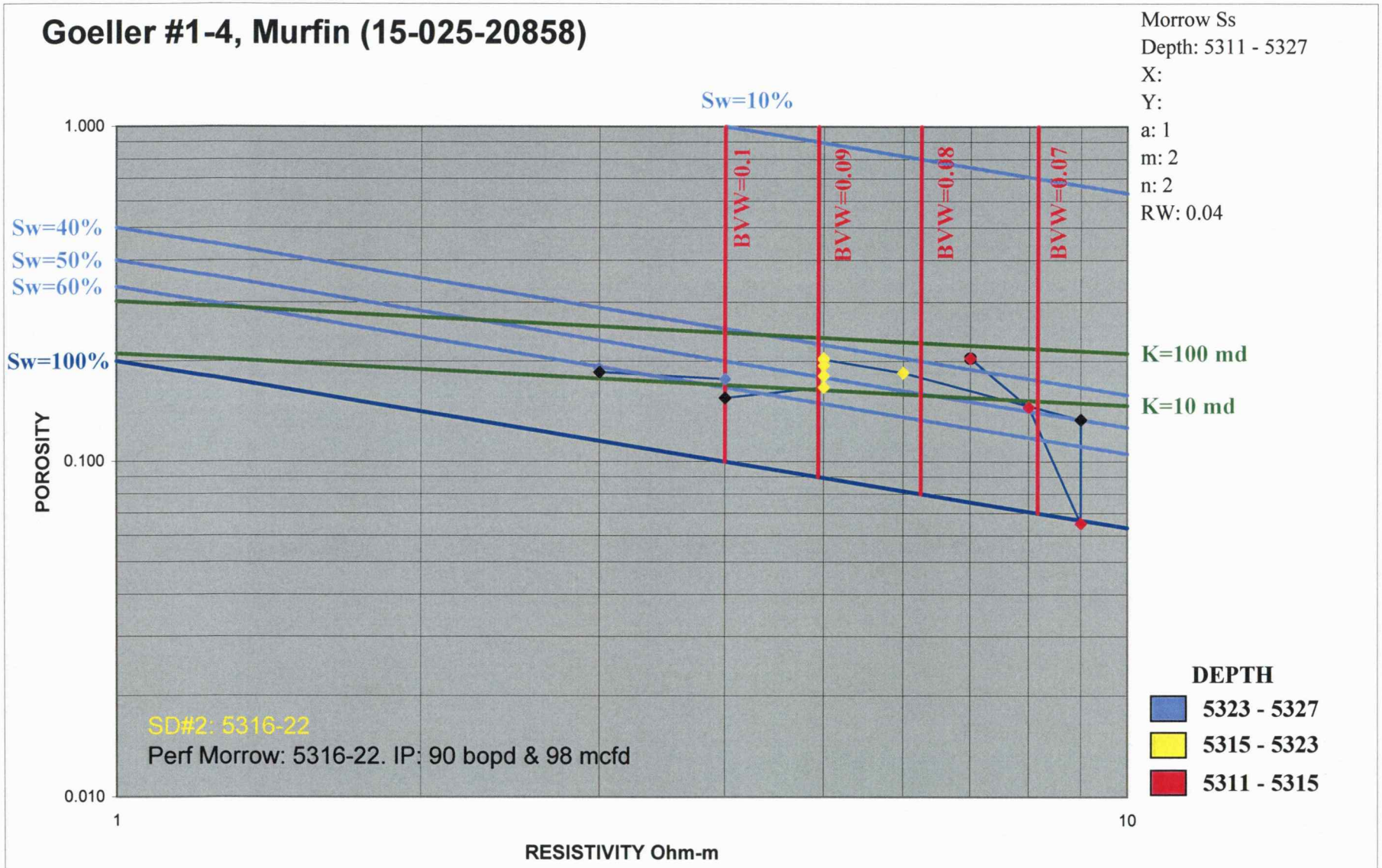
Goeller #1-4, Murfin (15-025-20858)
Morrow Ss
Depth: 5311 - 5327
X:
Y:
a: 1
m: 2
n: 2
RW: 0.04
Sw=10%
Sw=40%
Sw=50%
Sw=60%
Sw=100%
BVW=0.1
BVW=0.09
BVW=0.08
BVW=0.07
K=100 md
K=10 md
1.000
0.100
0.010
POROSITY
SD#2: 5316-22
Perf Morrow: 5316-22. IP: 90 bopd & 98 mcfd
DEPTH
5323 - 5327
5315 - 5323
5311 - 5315
1
10
RESISTIVITY Ohm-m

Figure A-1a

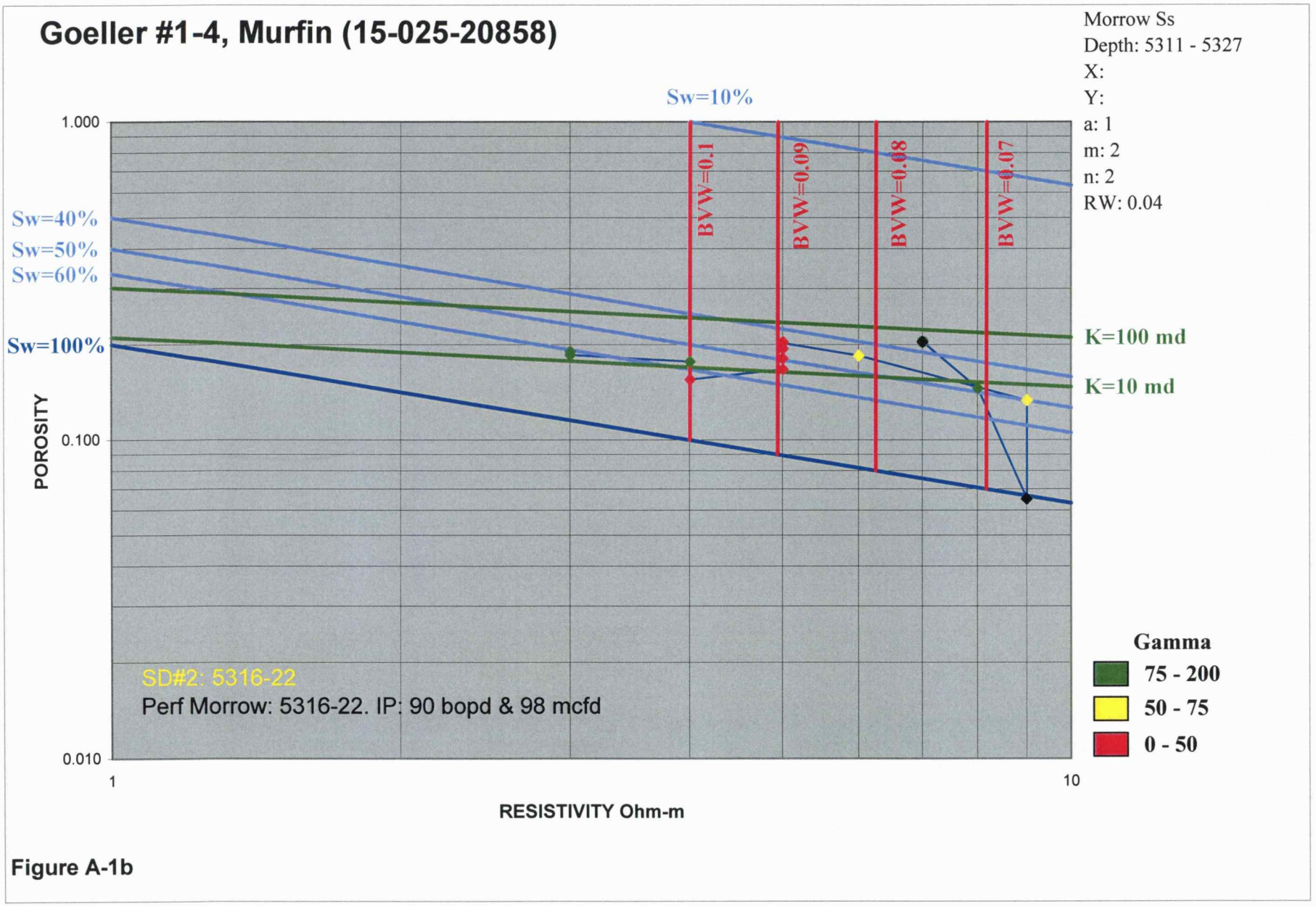
Goeller #1-4, Murfin (15-025-20858)
Morrow Ss
Depth: 5311 - 5327
X:
Y:
a: 1
m: 2
n: 2
RW: 0.04
Sw=10%
Sw=40%
Sw=50%
Sw=60%
Sw=100%
BVW=0.1
BVW=0.09
BVW=0.08
BVW=0.07
K=100 md
K=10 md
1.000
0.100
0.010
POROSITY
1
10
RESISTIVITY Ohm-m
SD#2: 5316-22
Perf Morrow: 5316-22. IP: 90 bopd & 98 mcfd
Gamma
75 - 200
50 - 75
0 - 50

Figure A-1b

Patton #2-3 Murfin (15-025-20685)

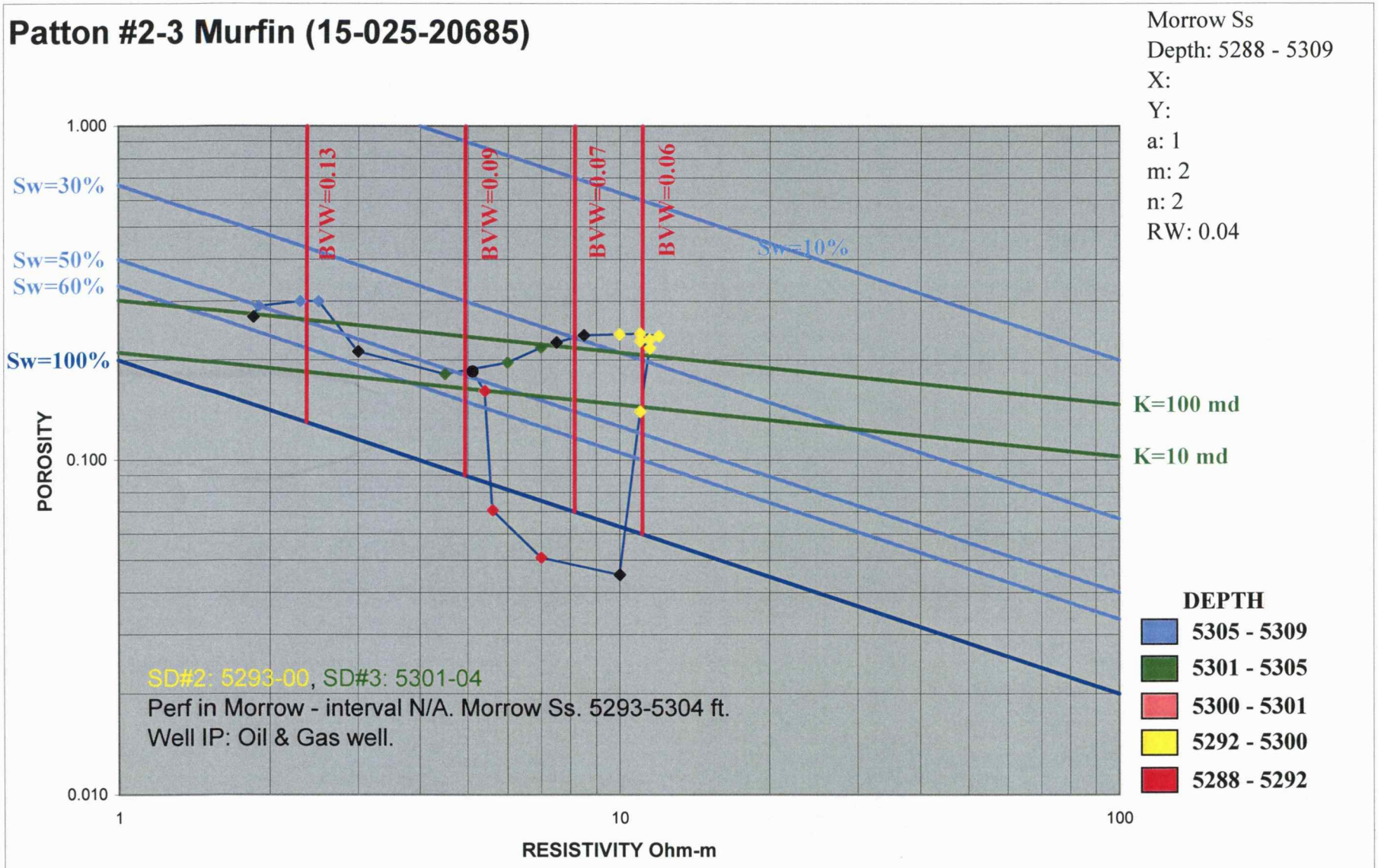

Figure A 2a

Patton #2-3 Murfin (15-025-20685)

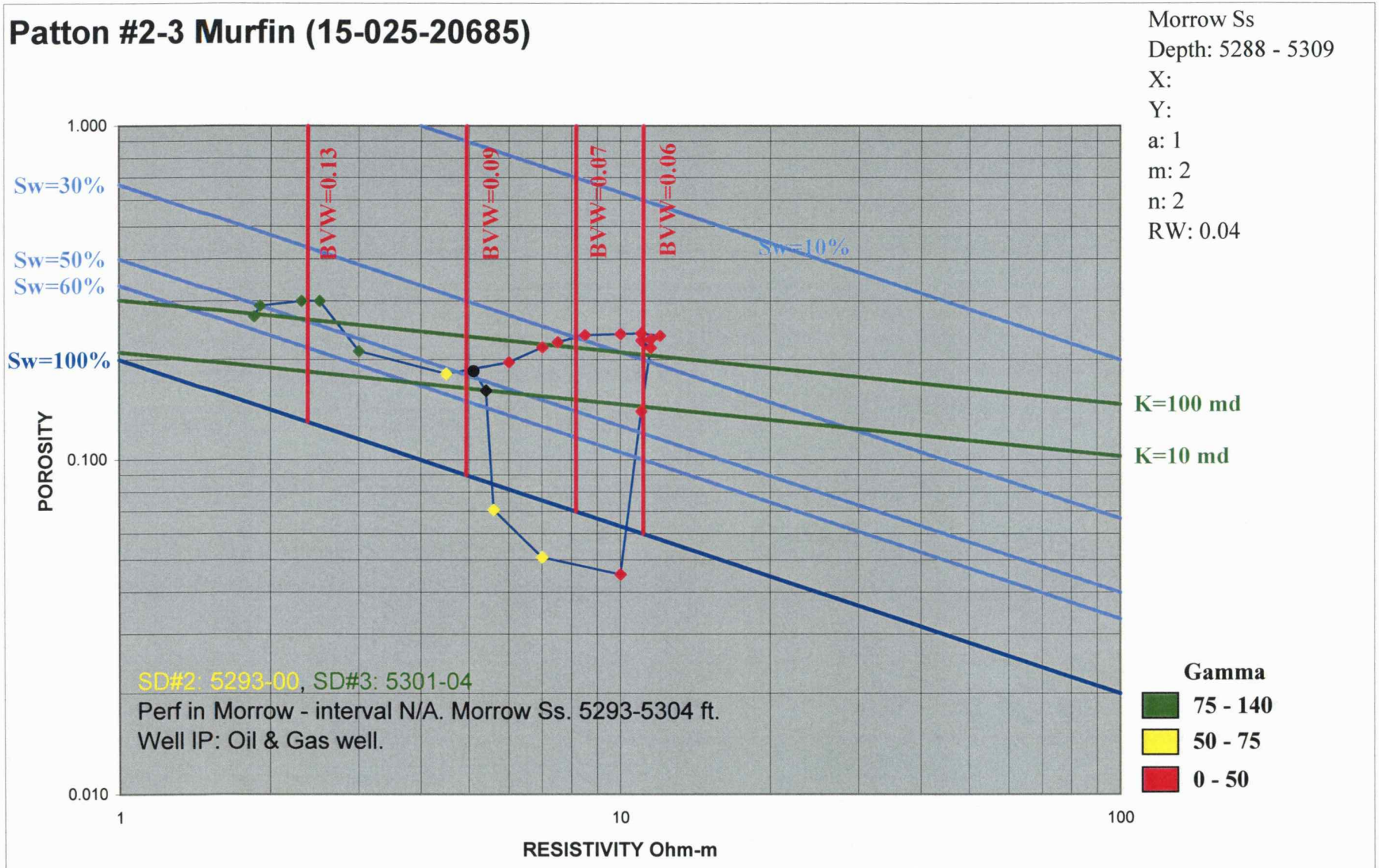

Figure A 2b

Rooney B #1-2 (15-025-20917)

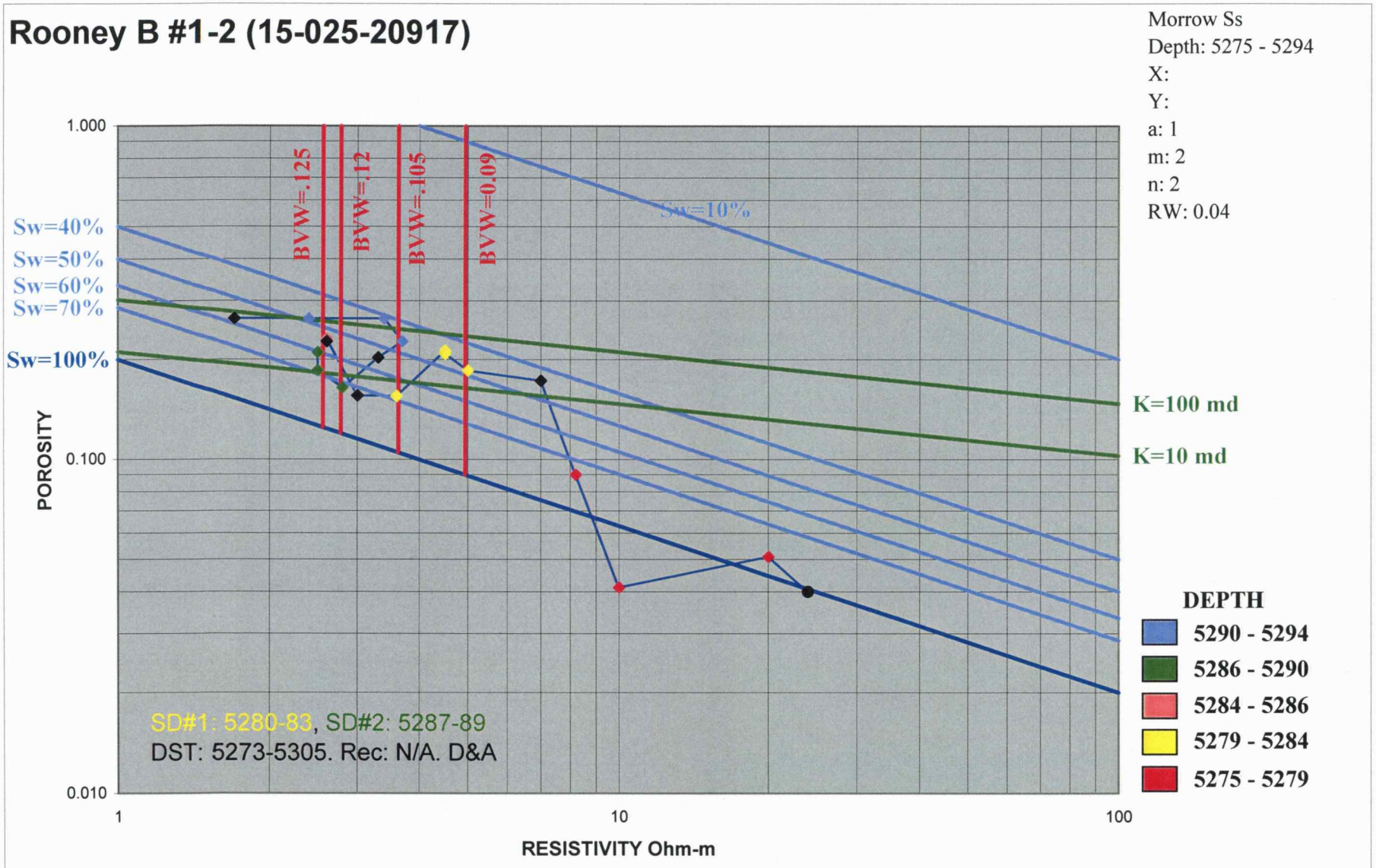

Figure A 3a

Rooney B #1-2 (15-025-20917)

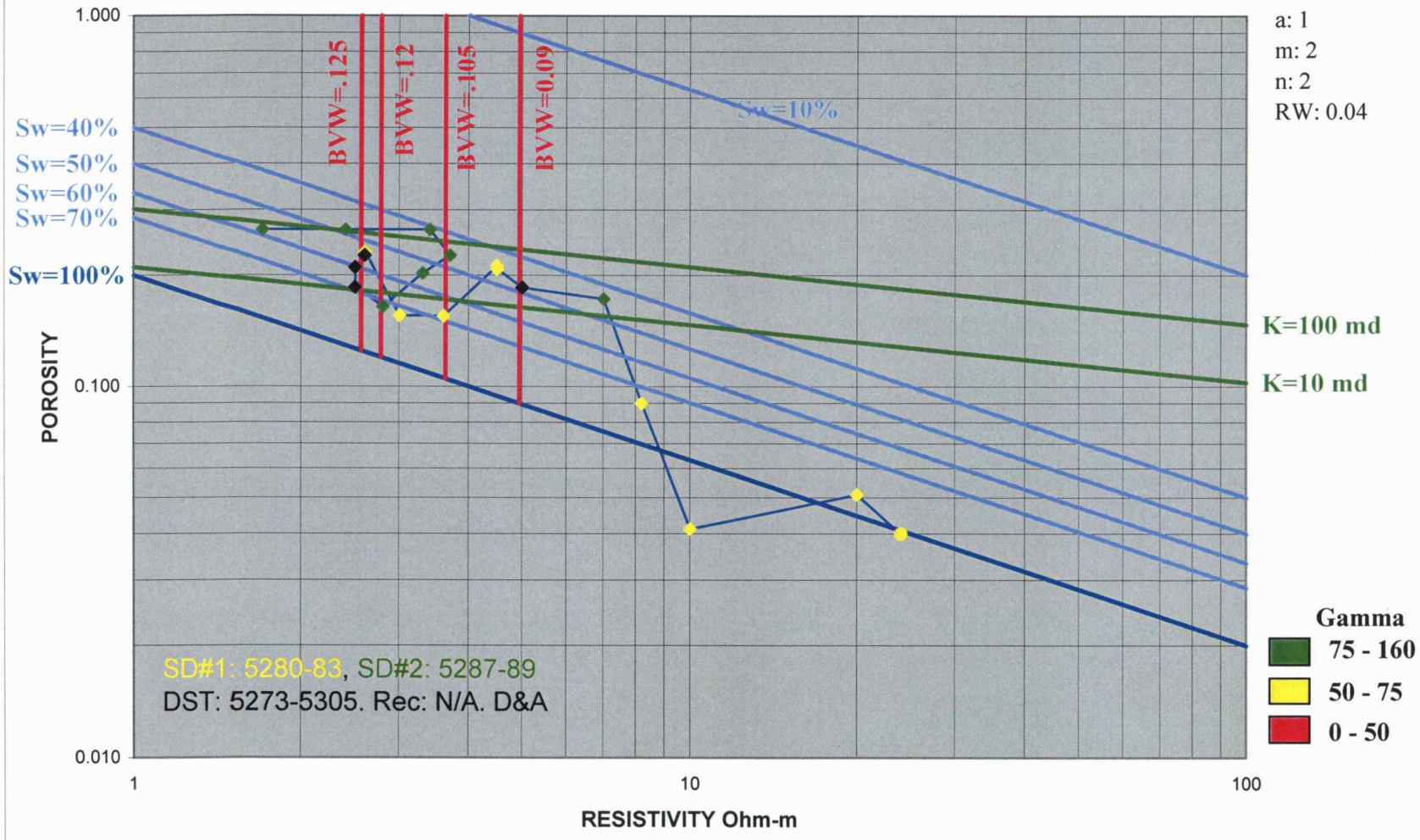

Figure A 3b

Hall #1-2 (15-025-20785)

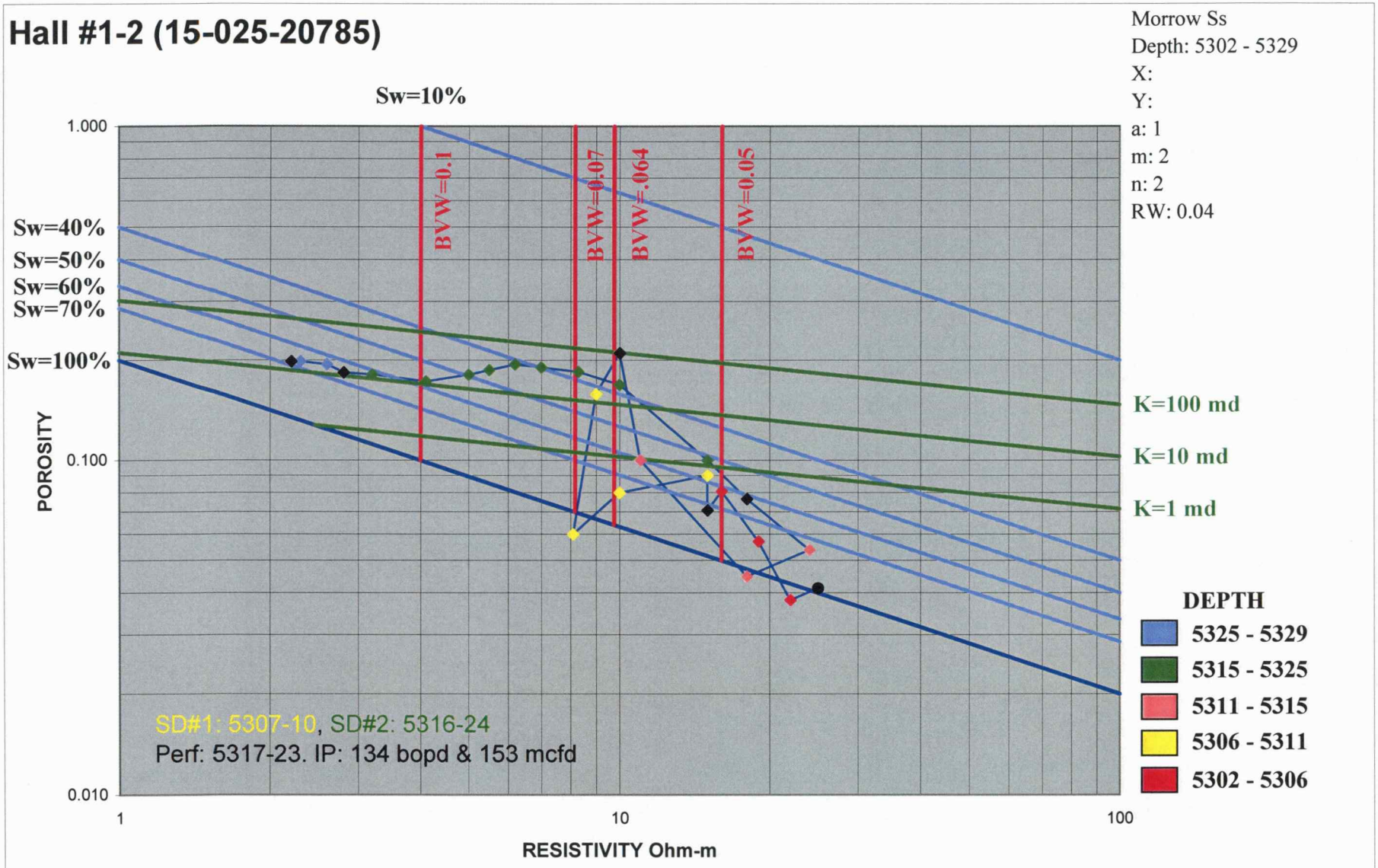

Figure A 4a

Hall #1-2 (15-025-20785)

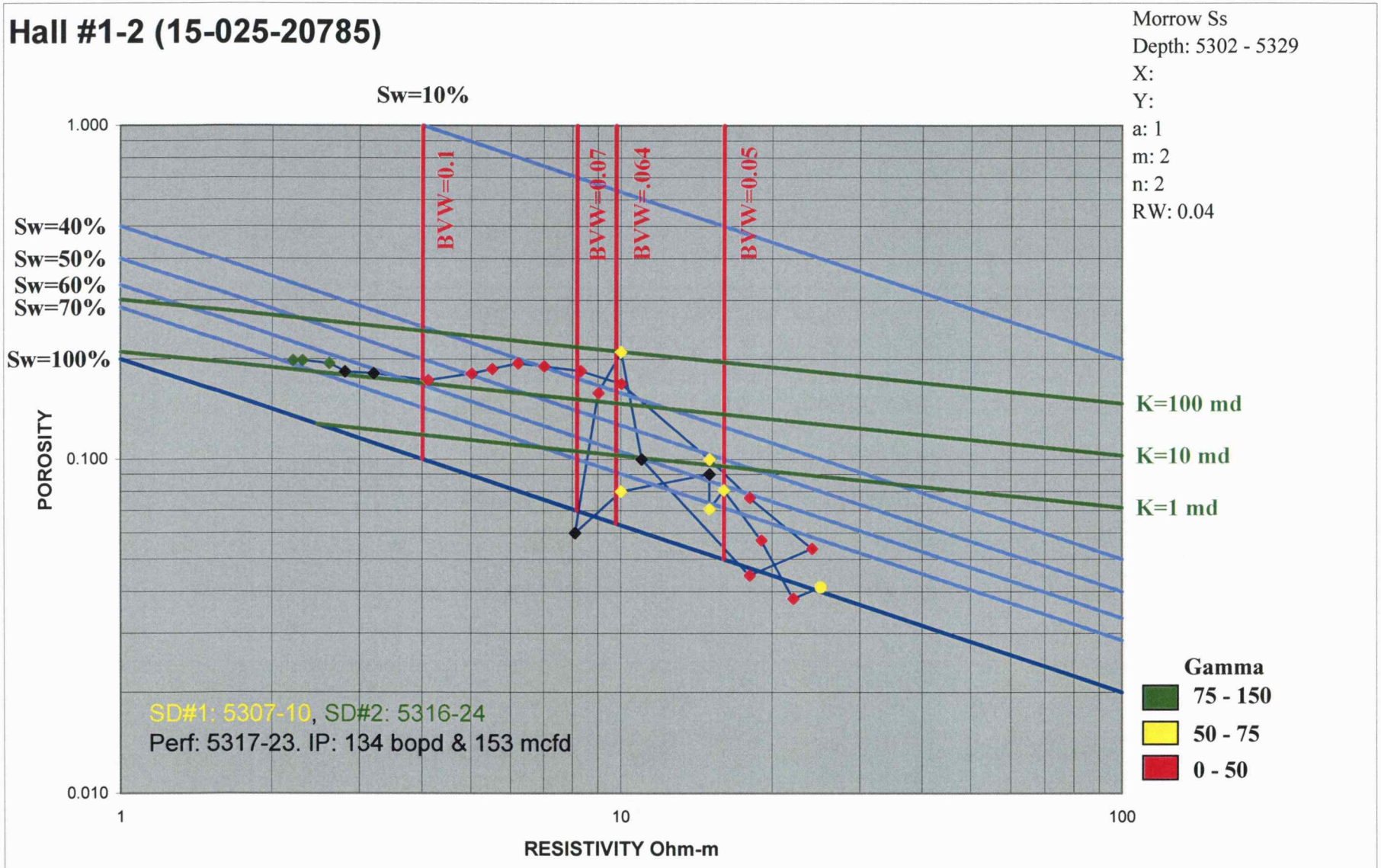

Figure A 4b

Alley #1-9 (15-025-20911)

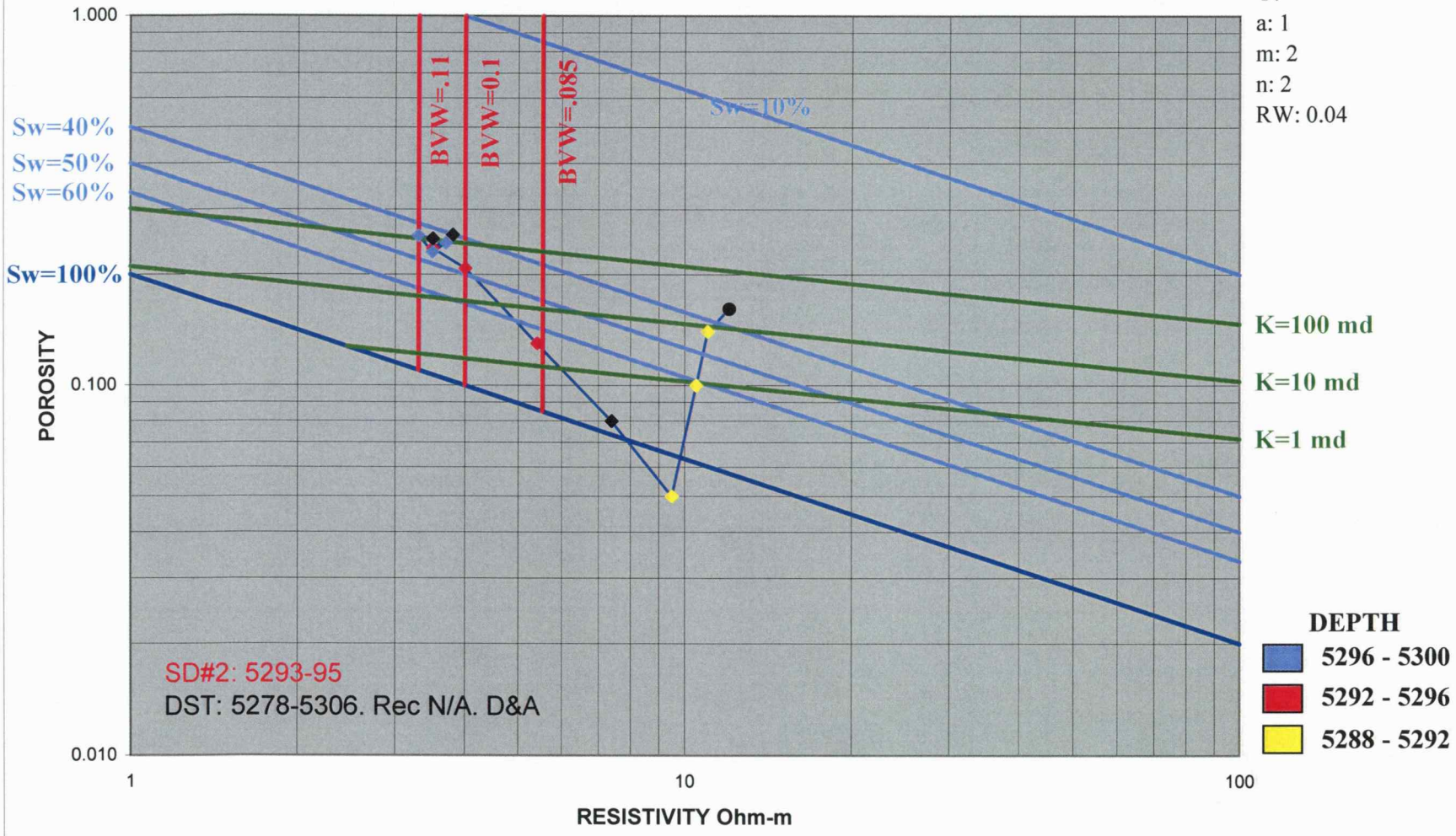

Figure A 5a

Alley #1-9 (15-025-20911)

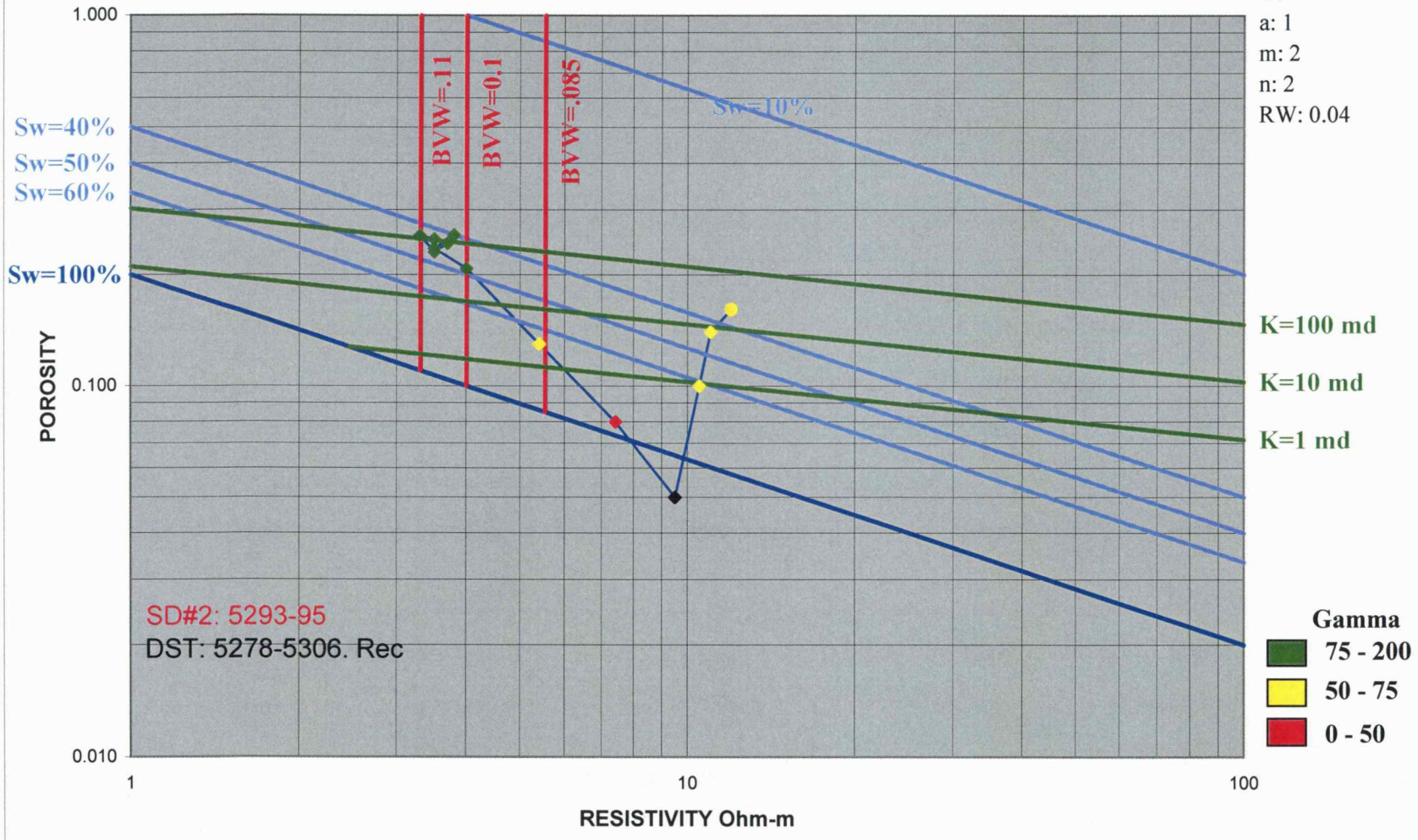

Figure A 5b

Norton B #1 (15-025-20672)

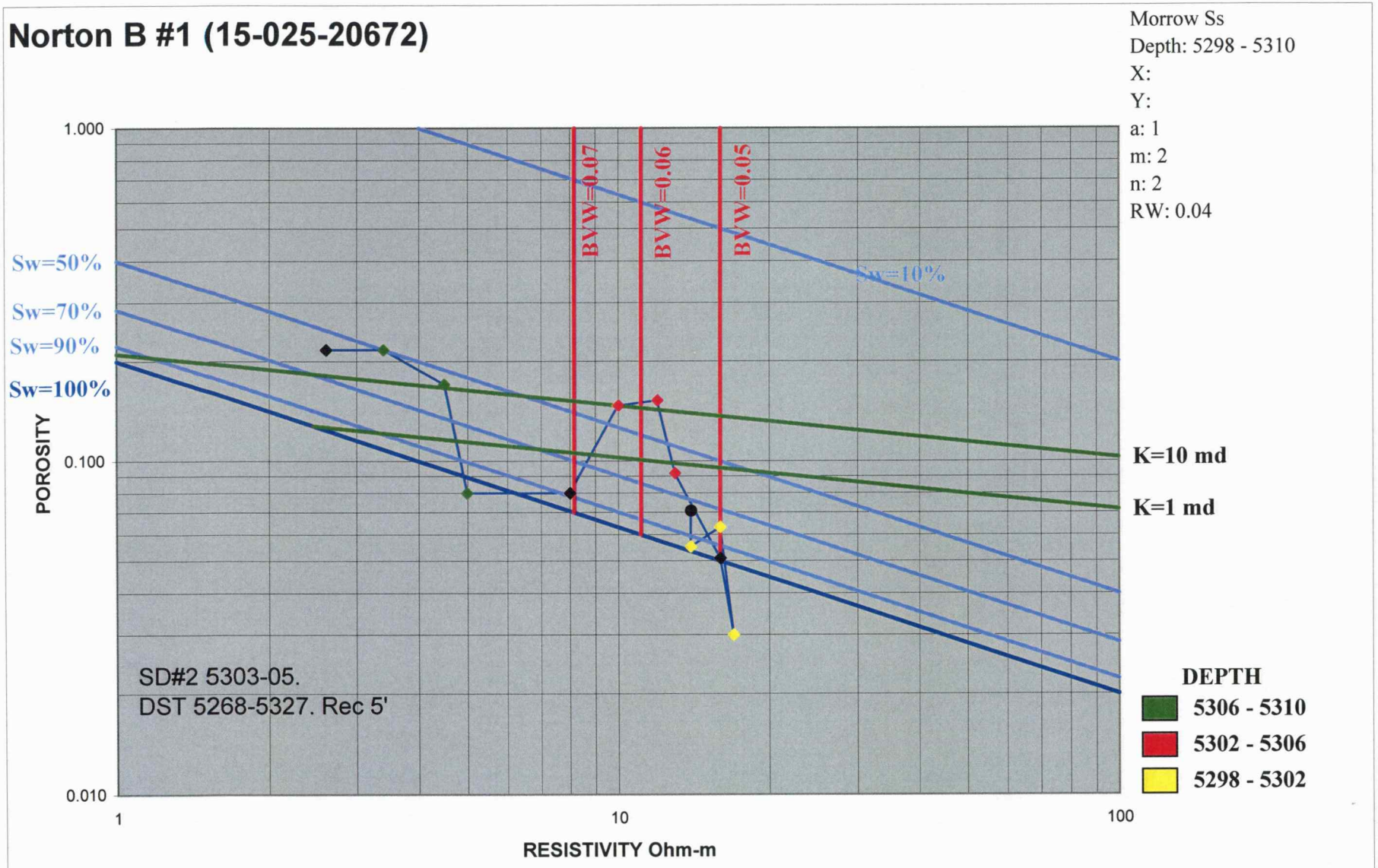

Figure A 6a

Norton B #1 (15-025-20672)

Figure A 6b

Latzke #1 (15-025-20611)

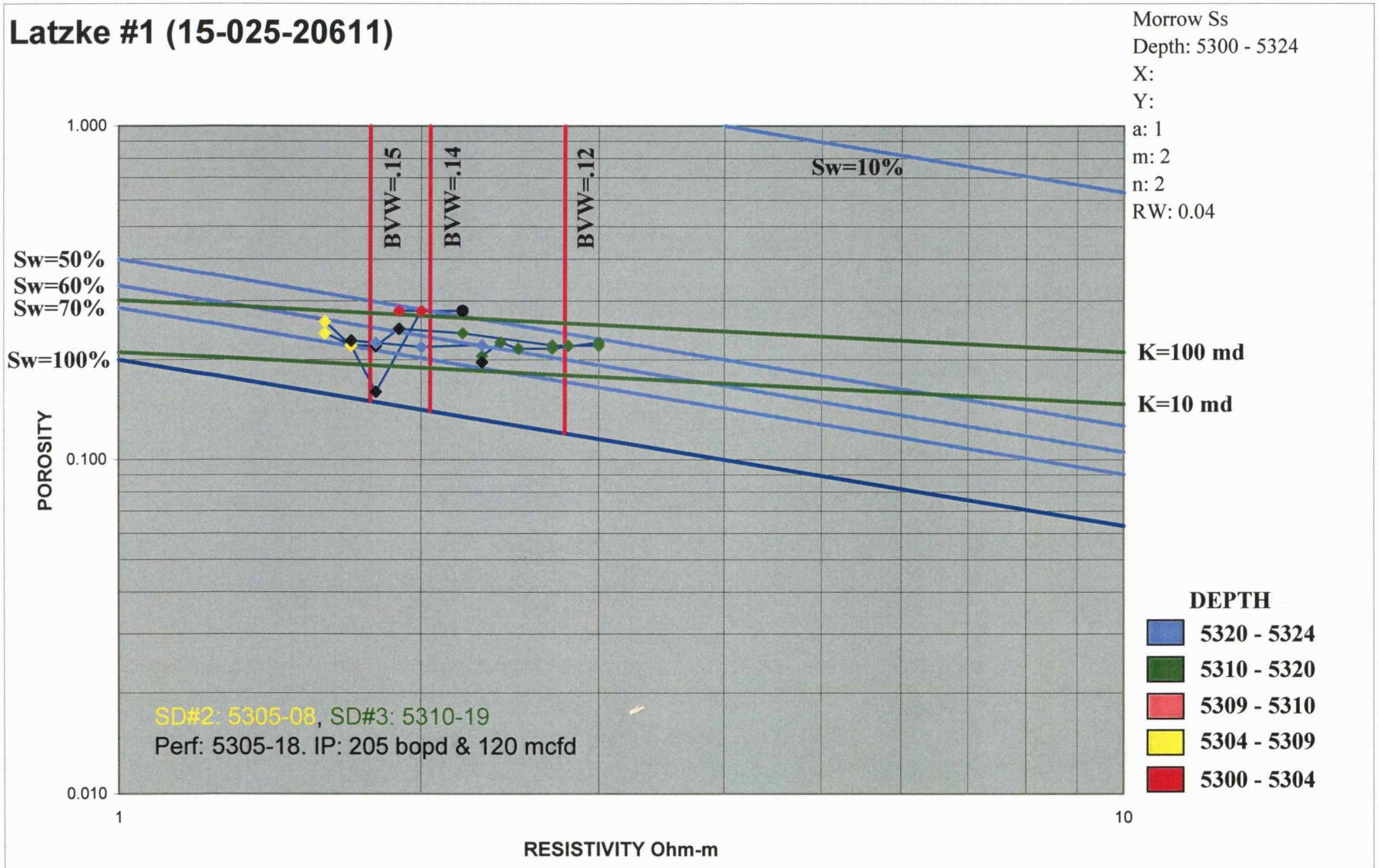

Figure A 7a

Latzke #1 (15-025-20611)

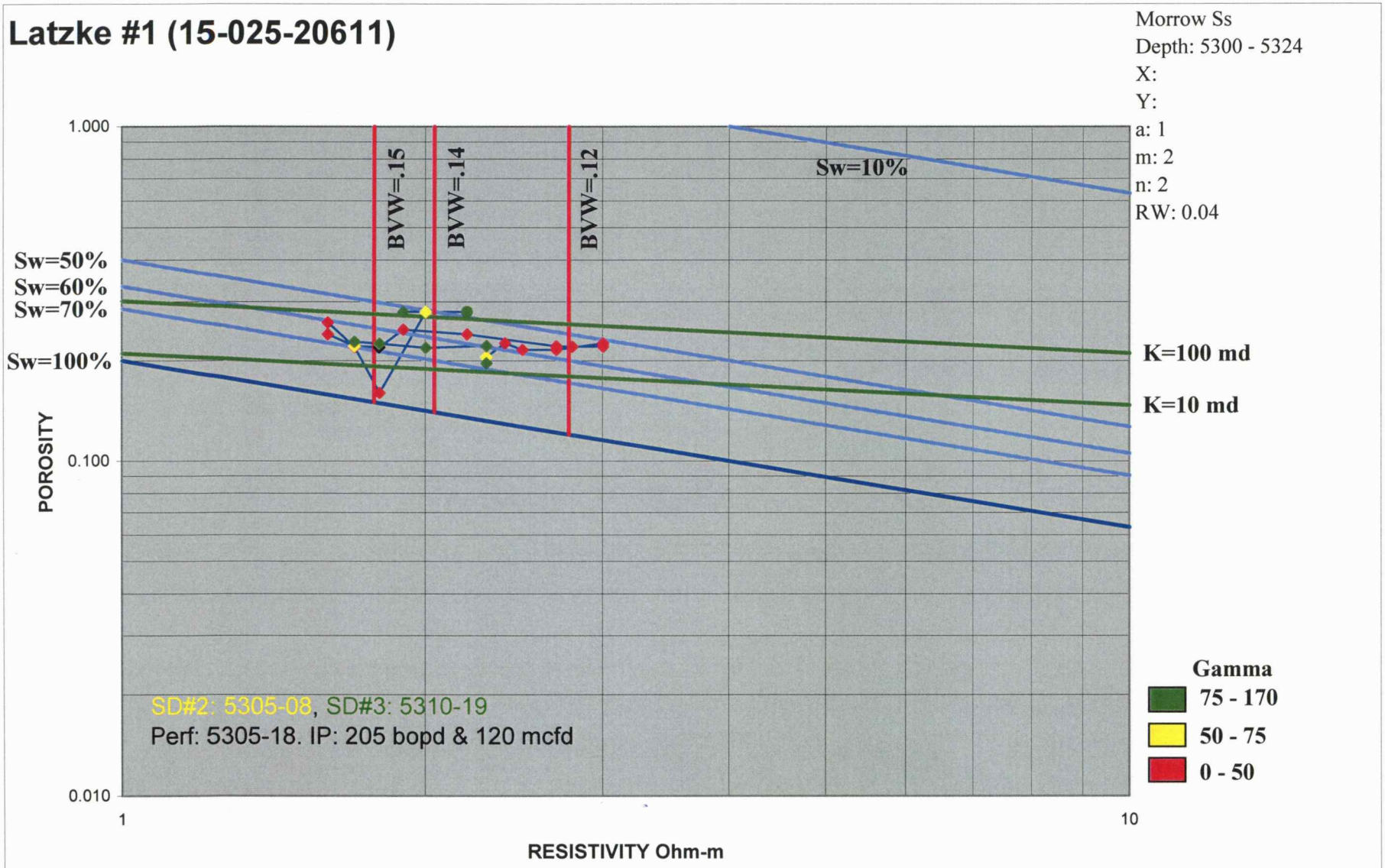

Figure A 7b

Hall B #1-2 (15-025-20919)

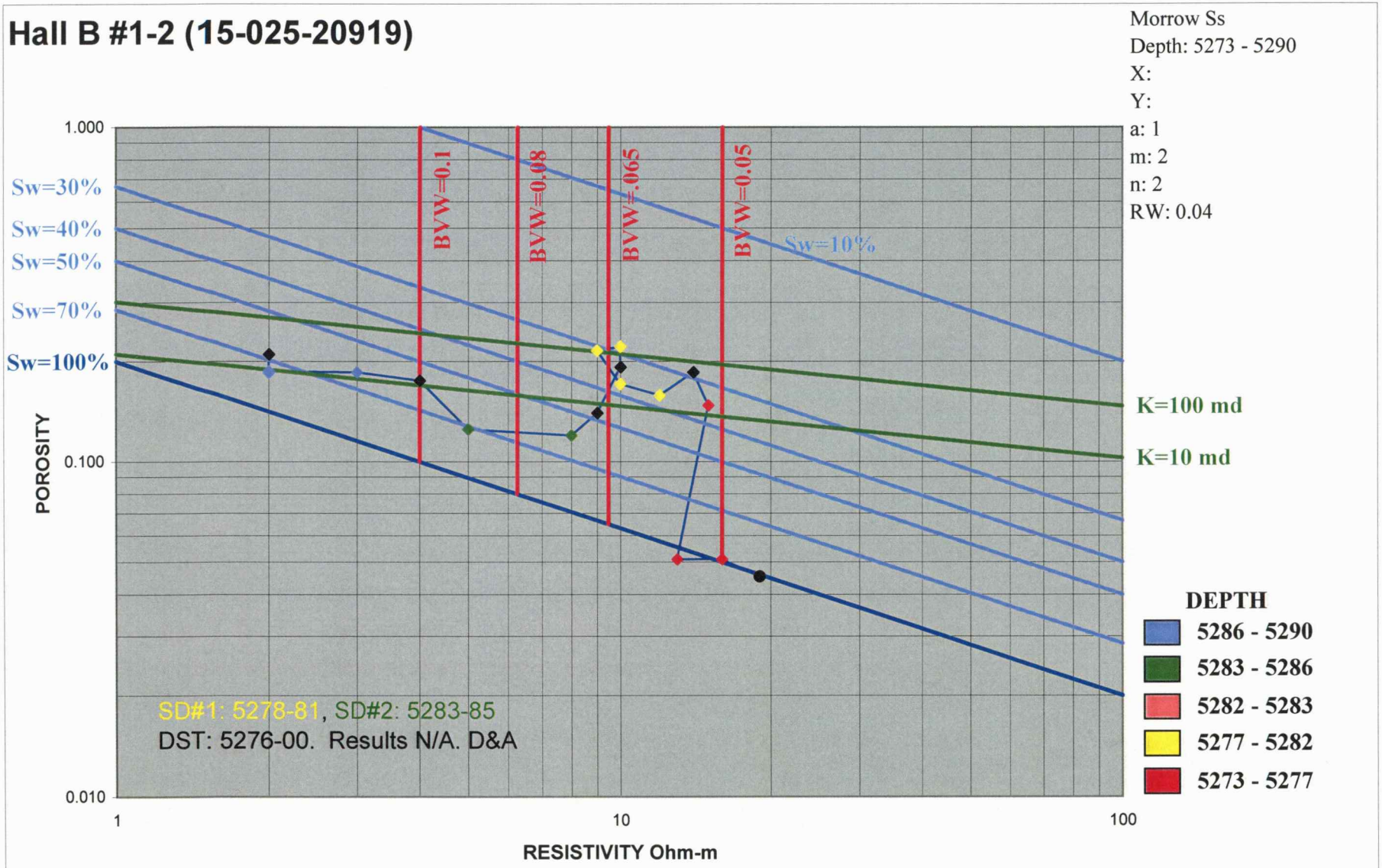

Figure A 8a

Hall B #1-2 (15-025-20919)

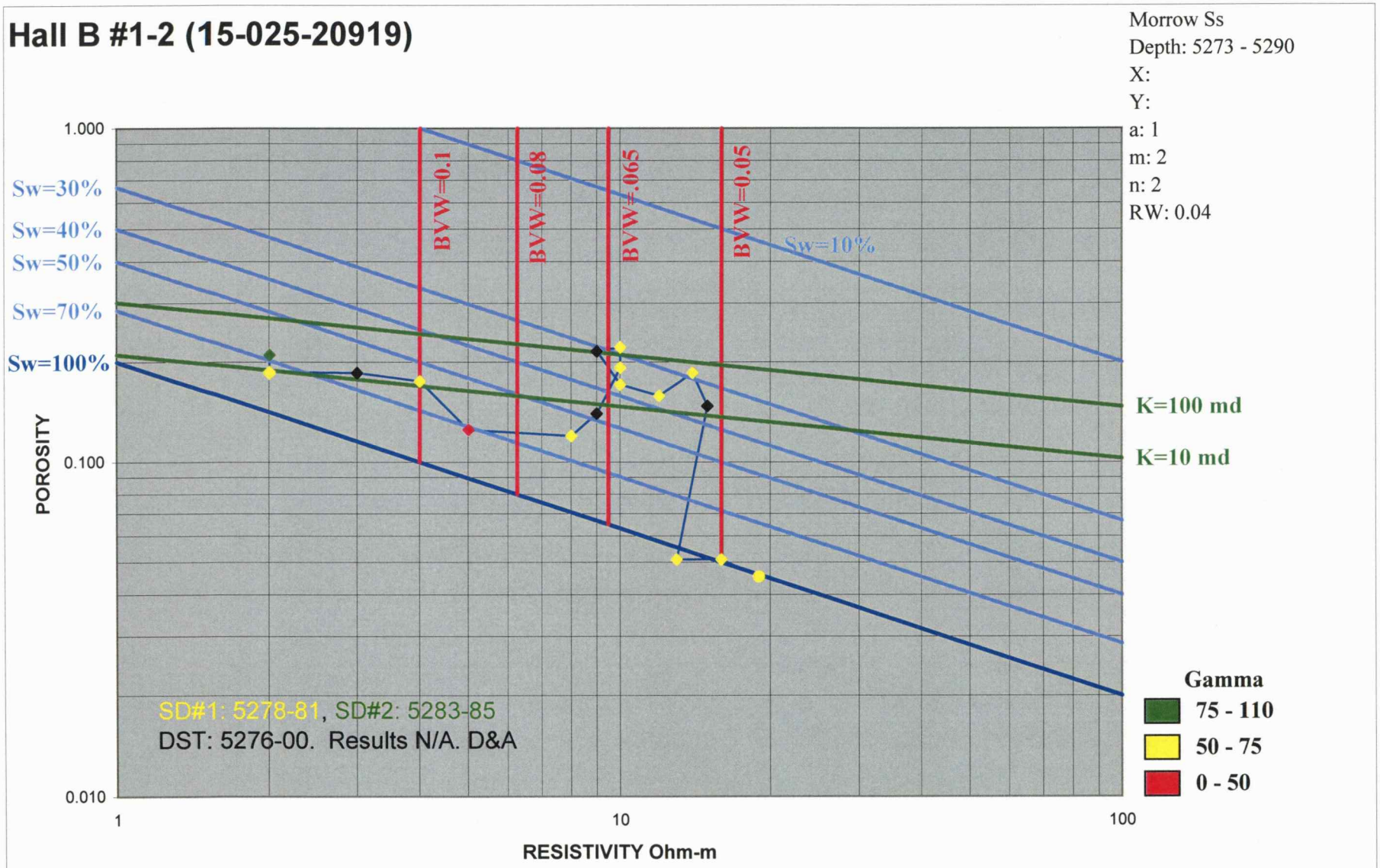

Figure A 8b

Hall #2-2 (15-025-20838)

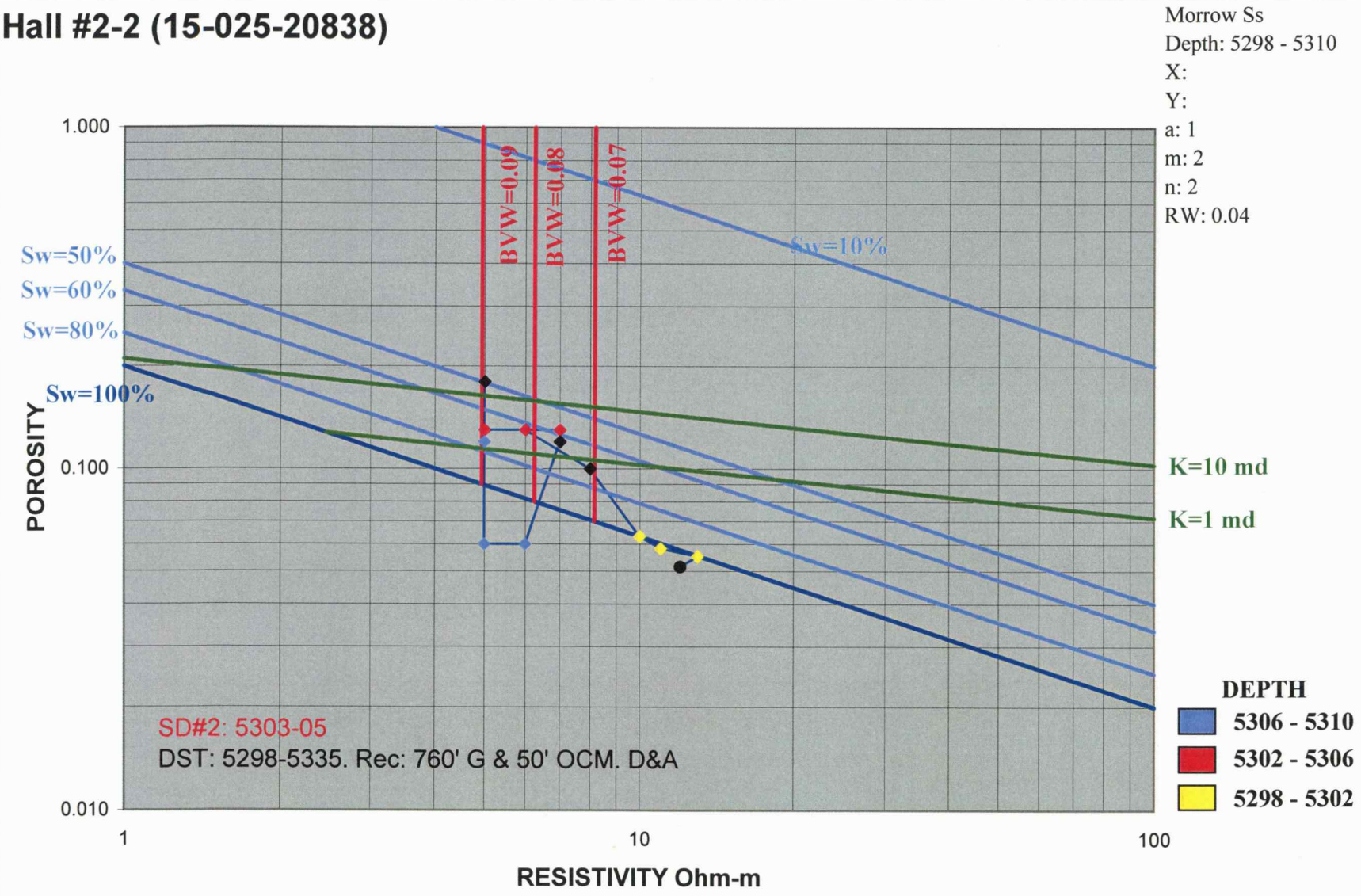

Figure A 9a

Hall #2-2 (15-025-20838)

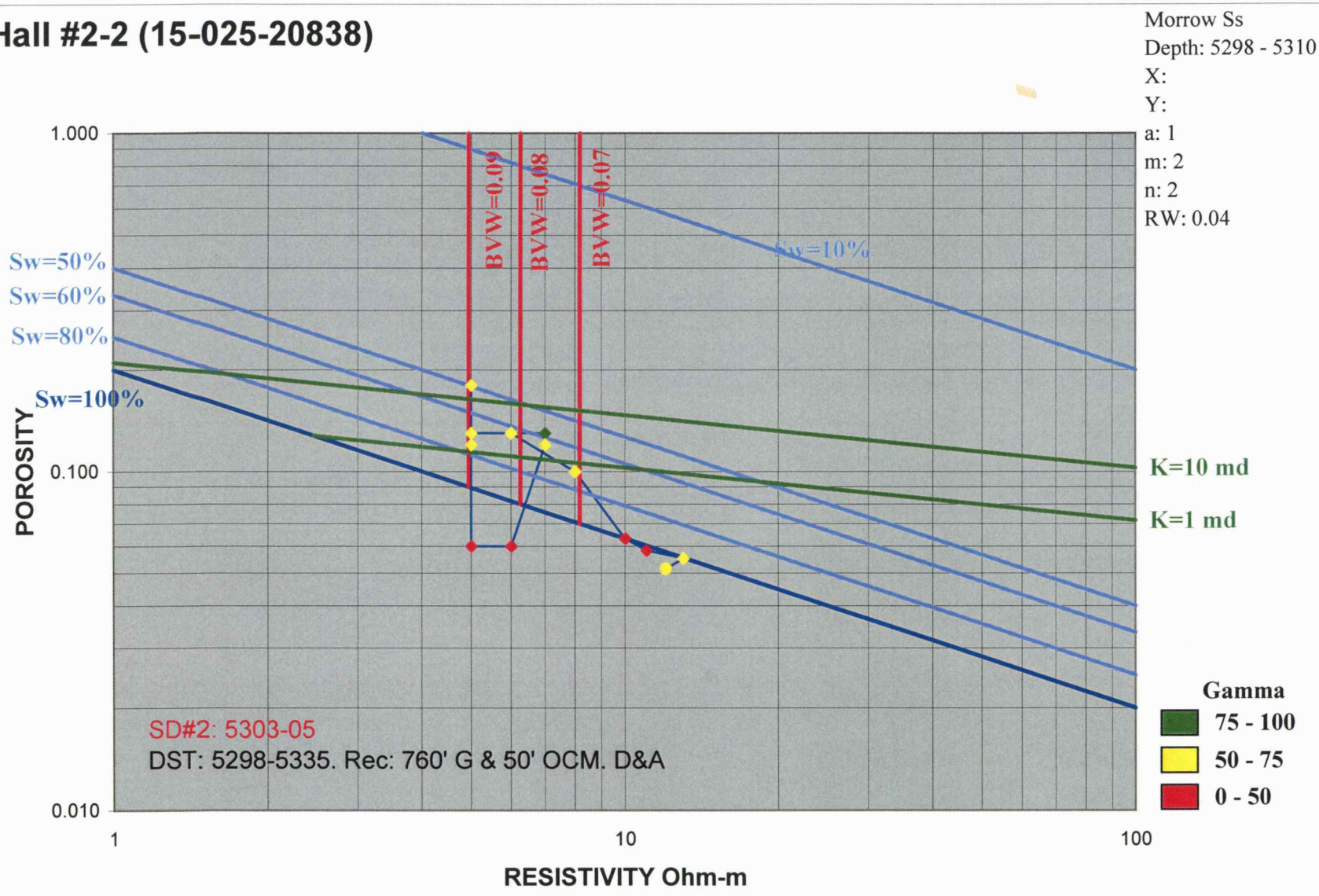

Figure A 9b

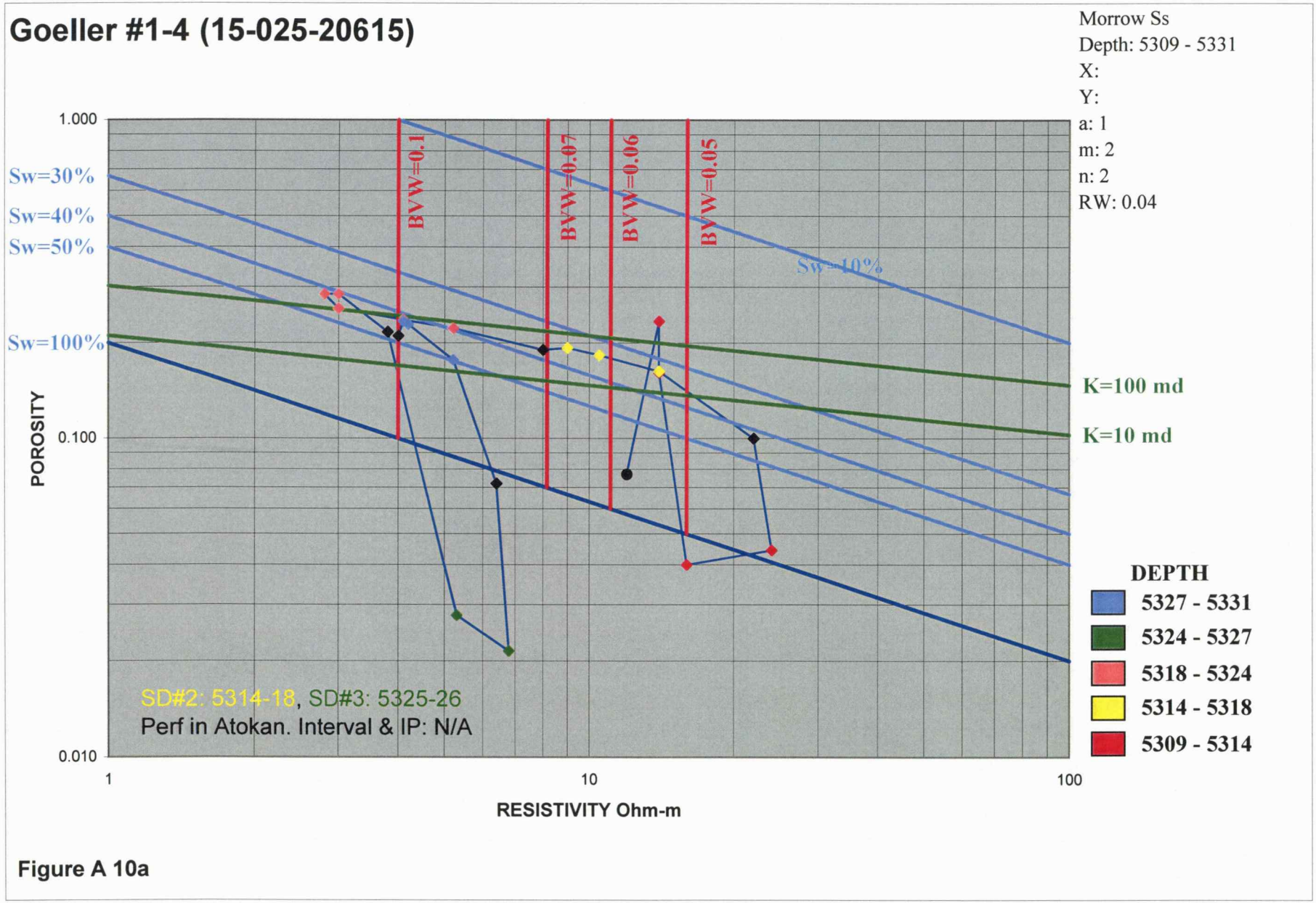
Goeller #1-4 (15-025-20615)
Morrow Ss
Depth: 5309 - 5331
X:
Y:
a: 1
m: 2
n: 2
RW: 0.04
1.000
0.100
0.010
POROSITY
Sw=30%
Sw=40%
Sw=50%
Sw=100%
Sw=10%
BVW=0.1
BVW=0.07
BVW=0.06
BVW=0.05
K=100 md
K=10 md
SD#2: 5314-18, SD#3: 5325-26
Perf in Atokan. Interval & IP: N/A
DEPTH
5327 - 5331
5324 - 5327
5318 - 5324
5314 - 5318
5309 - 5314
1
10
100
RESISTIVITY Ohm-m

Figure A 10a

Goeller #1-4 (15-025-20615)

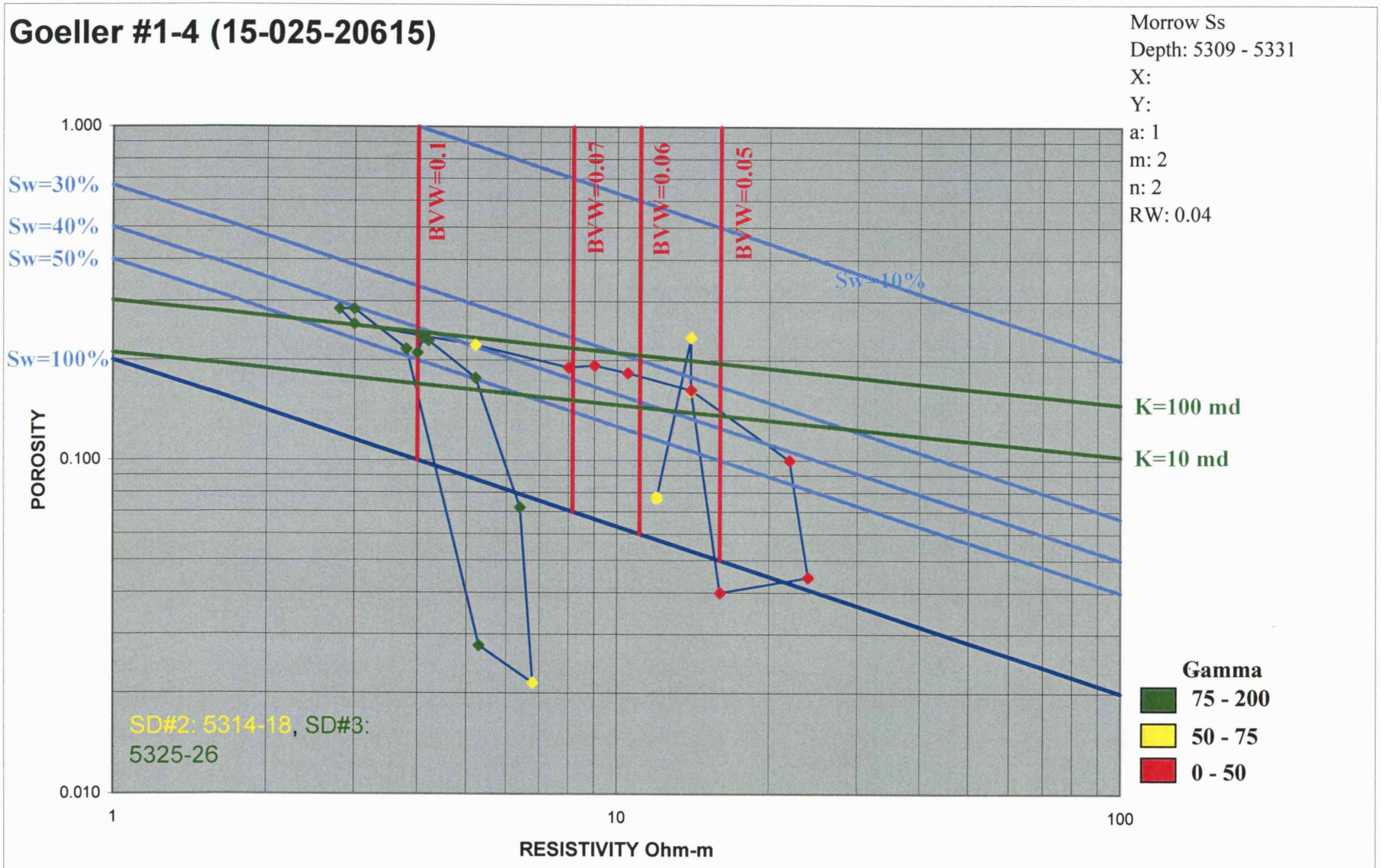

Figure A 10b

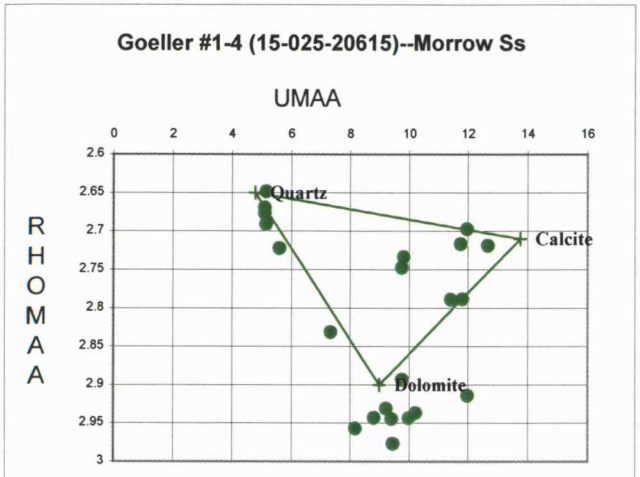

Figure A 10c

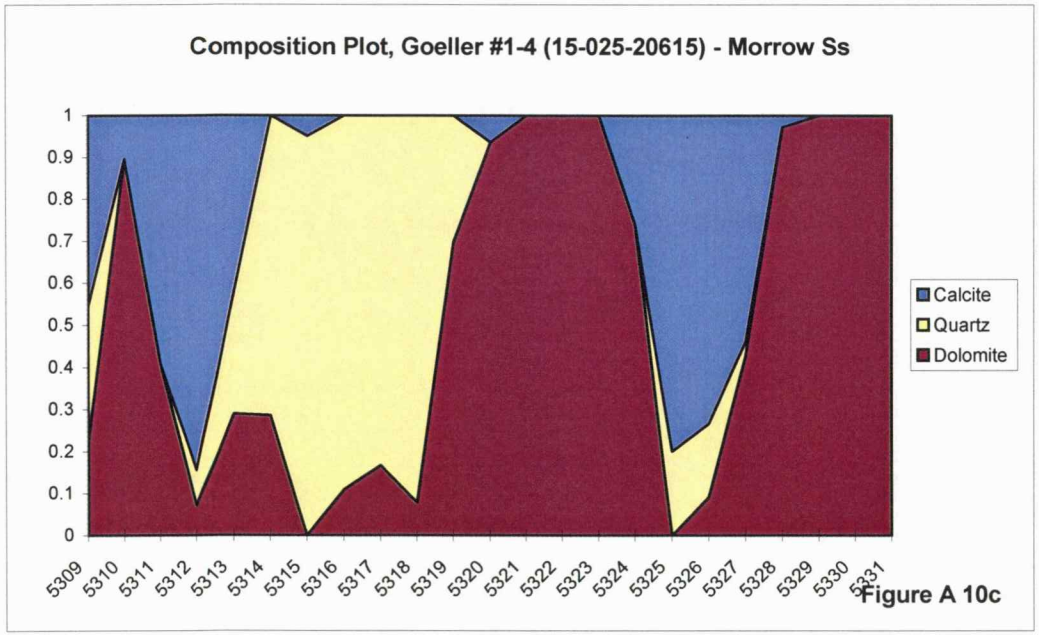

Figure A 10c

E F Harris #1-3 (15-025-20616)

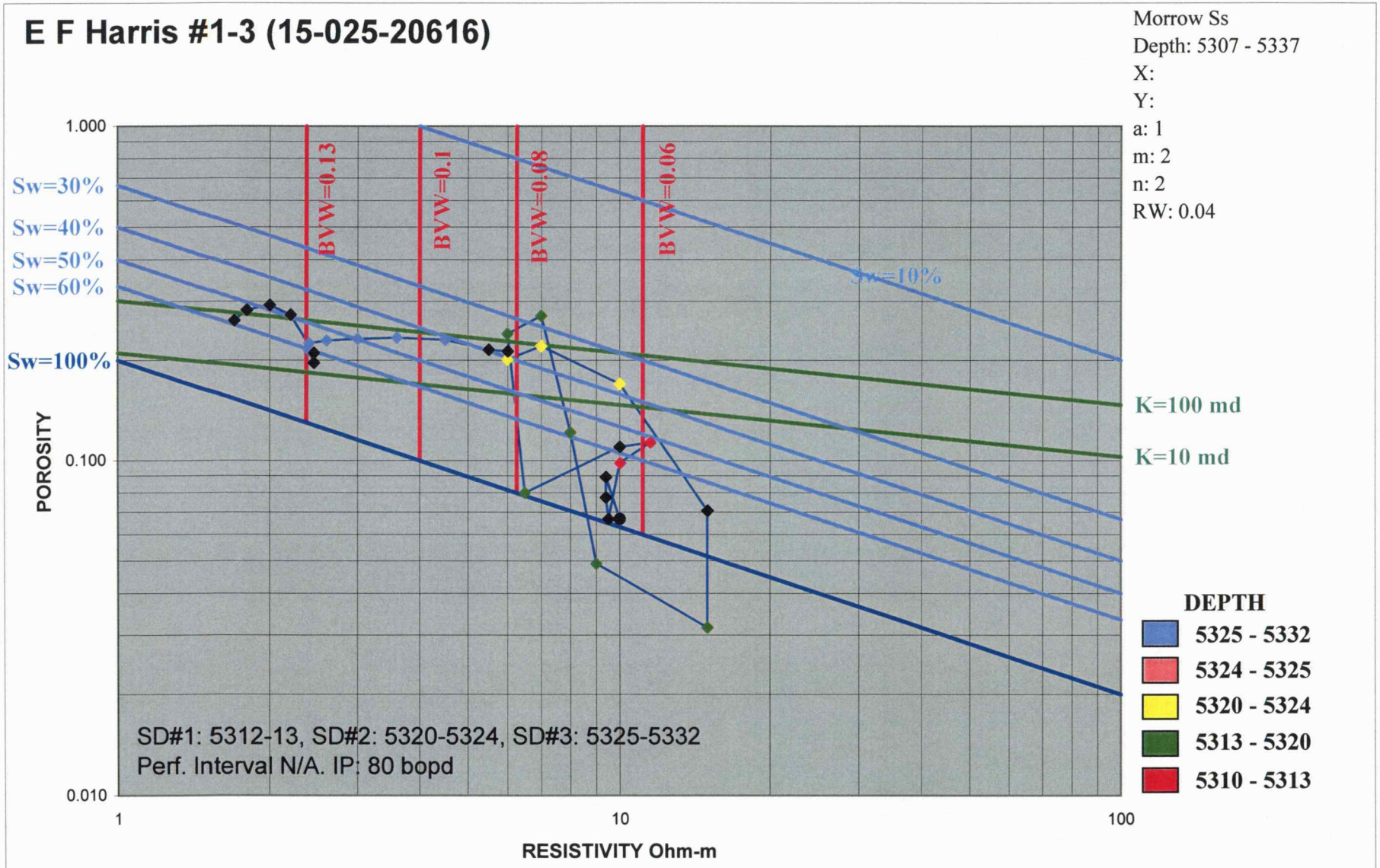

Figure A 11a

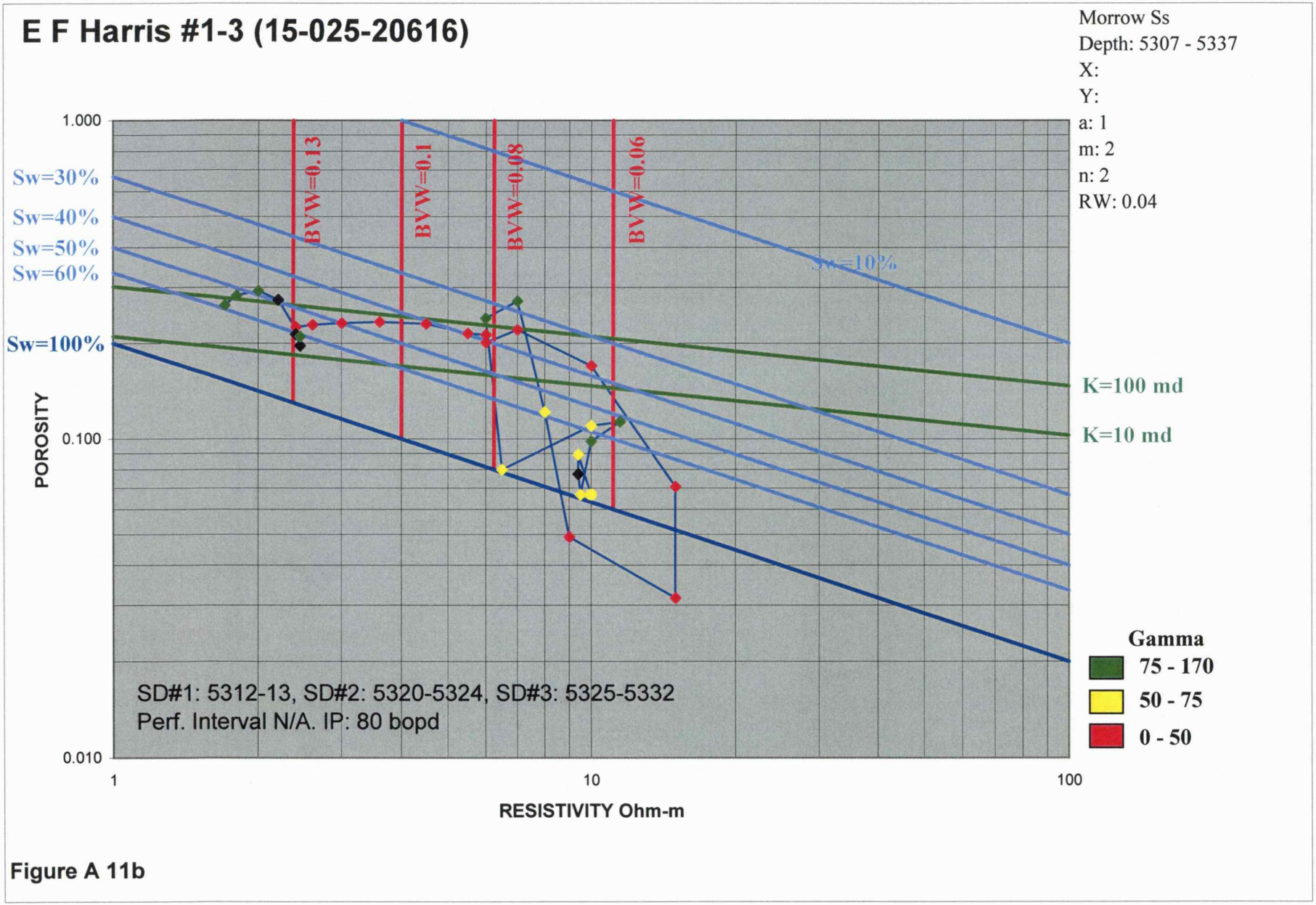
E F Harris #1-3 (15-025-20616)
Morrow Ss
Depth: 5307 - 5337
X:
Y:
a: 1
m: 2
n: 2
RW: 0.04
1.000
0.100
0.010
POROSITY
Sw=30%
Sw=40%
Sw=50%
Sw=60%
Sw=100%
Sw=10%
BVW=0.13
BVW=0.1
BVW=0.08
BVW=0.06
K=100 md
K=10 md
Gamma
75 - 170
50 - 75
0 - 50
SD#1: 5312-13, SD#2: 5320-5324, SD#3: 5325-5332
Perf. Interval N/A. IP: 80 bopd
1
10
100
RESISTIVITY Ohm-m

Figure A 11b

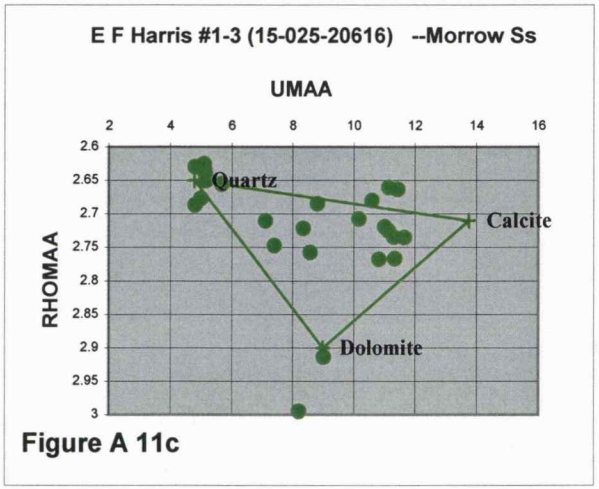

Figure A 11c

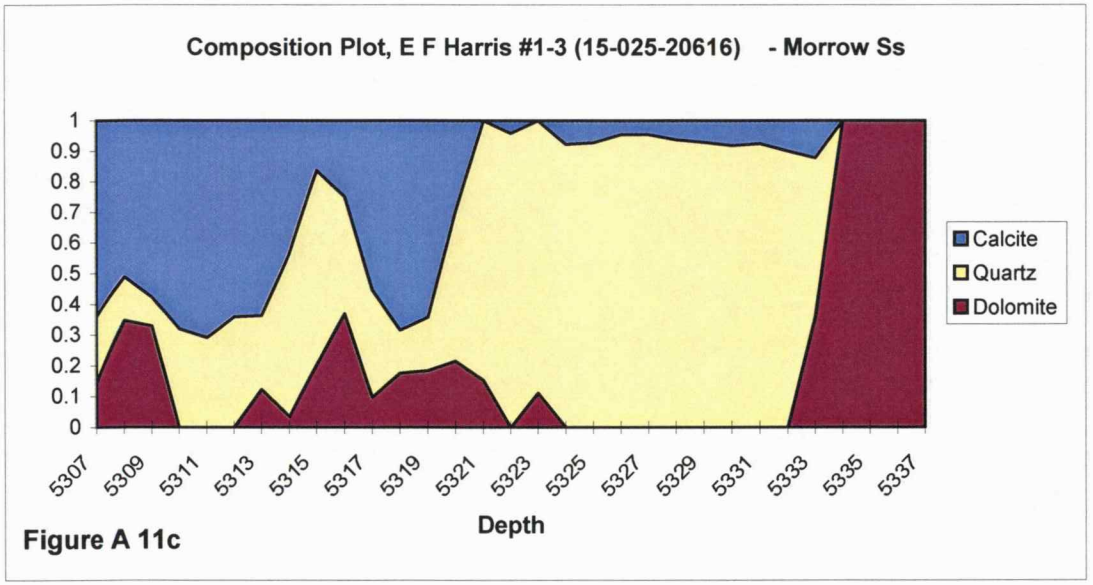

Figure A 11c

Fager #2-3 (15-025-20671)

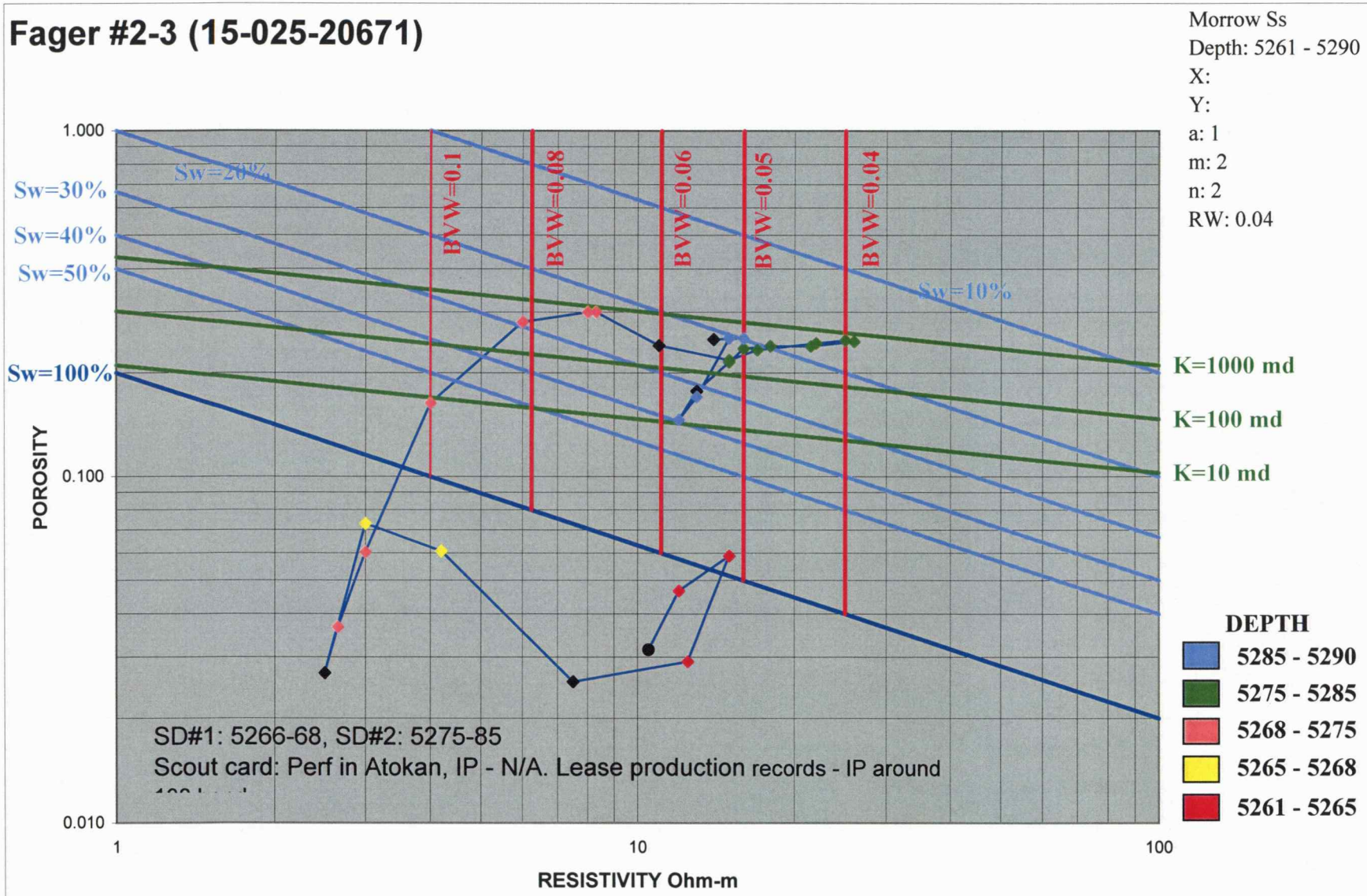

Figure A 12a

Fager #2-3 (15-025-20671)

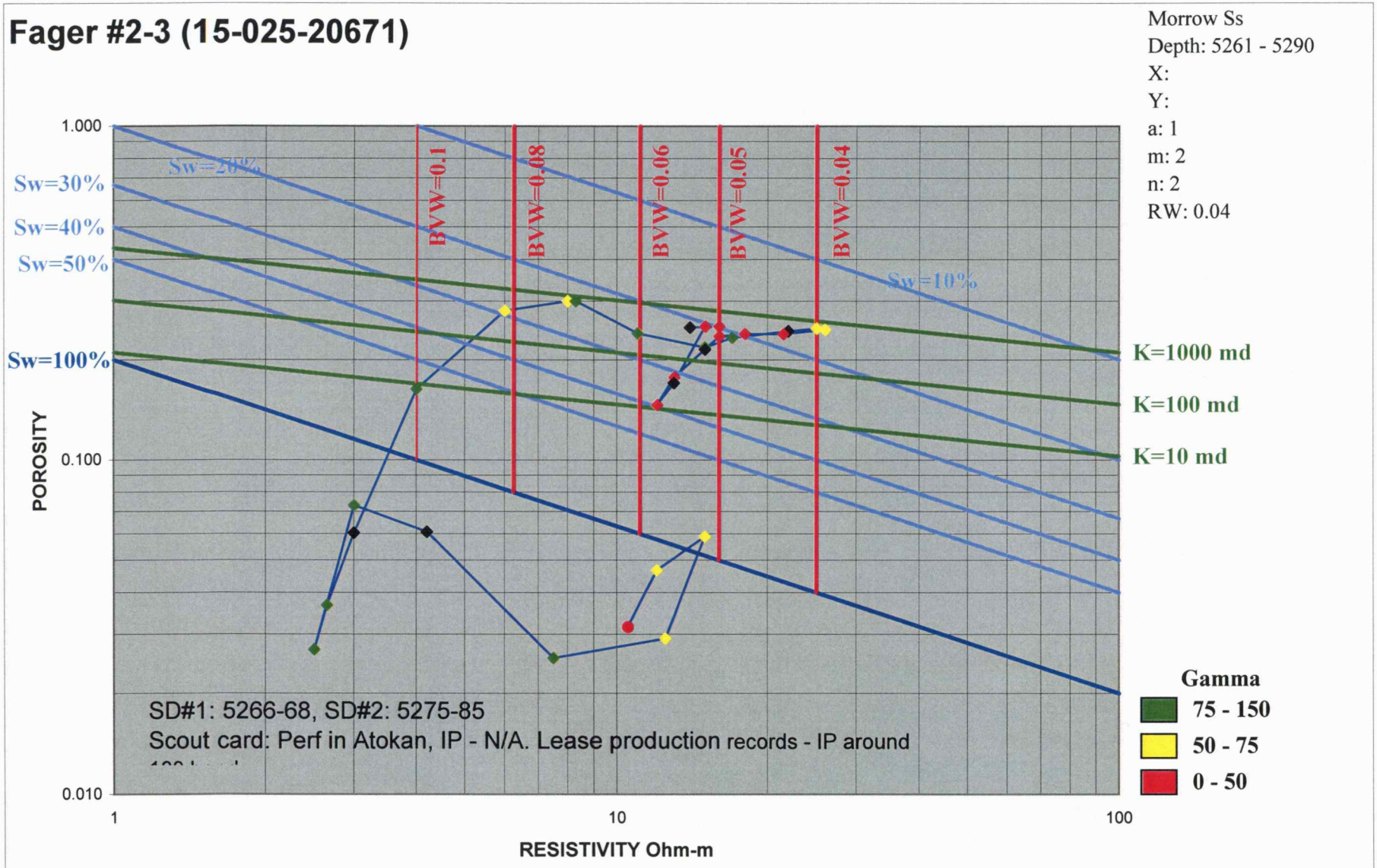

Figure A 12b

Harris # 2-3 (15-025-20708)

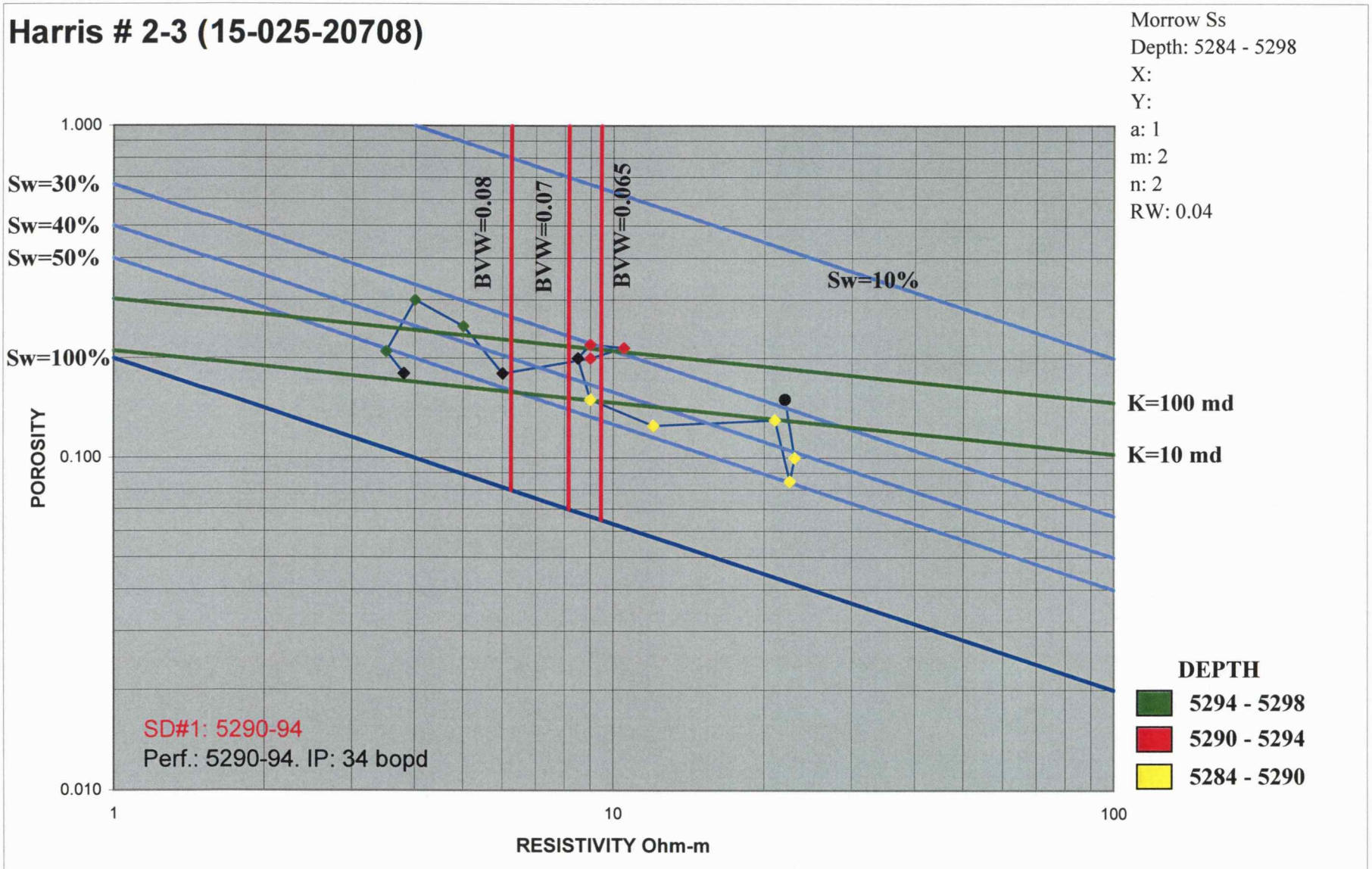

Figure A 13a

Harris # 2-3 (15-025-20708)

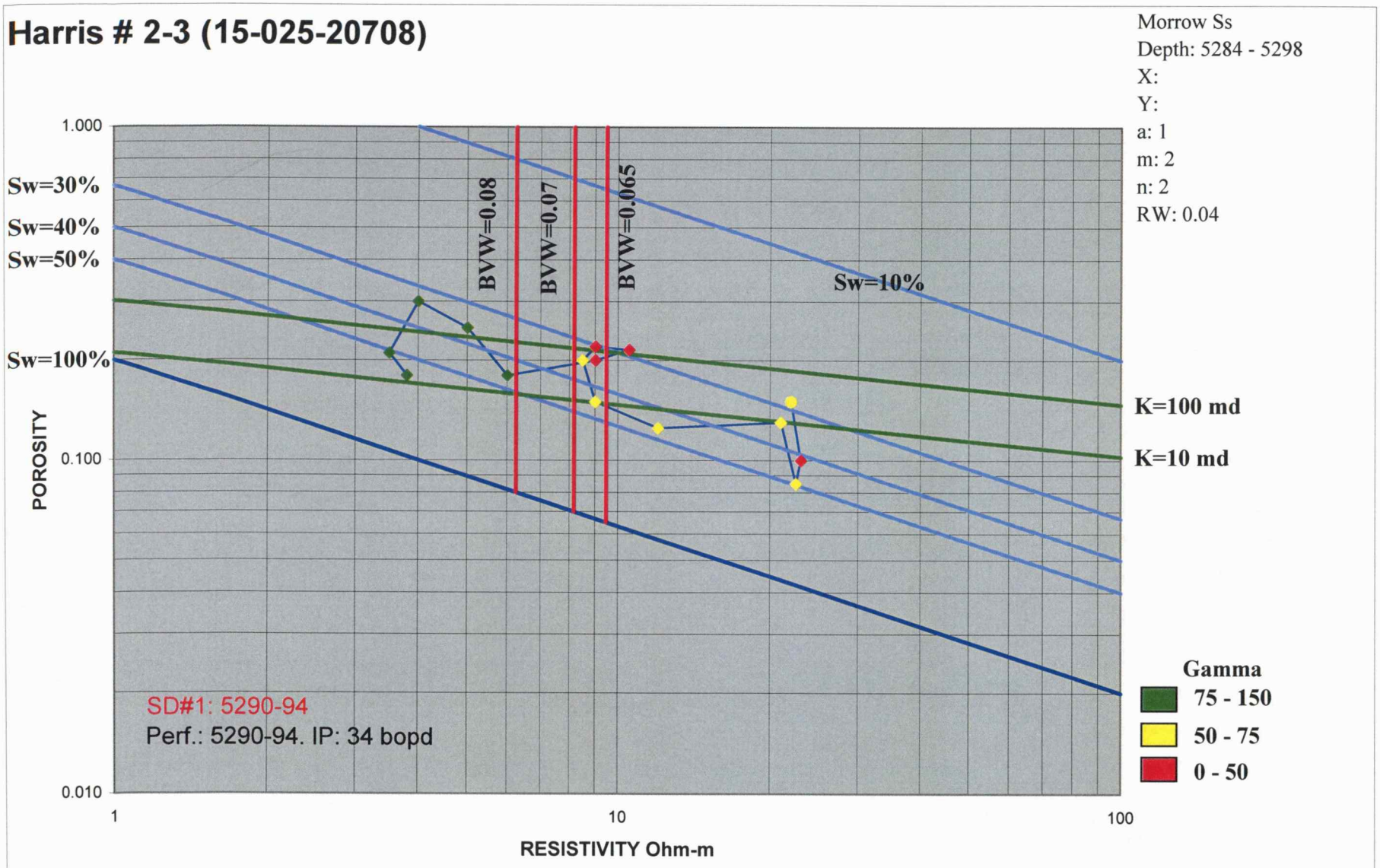

Figure A 13b

Hindman #1-3 (15-025-20635)

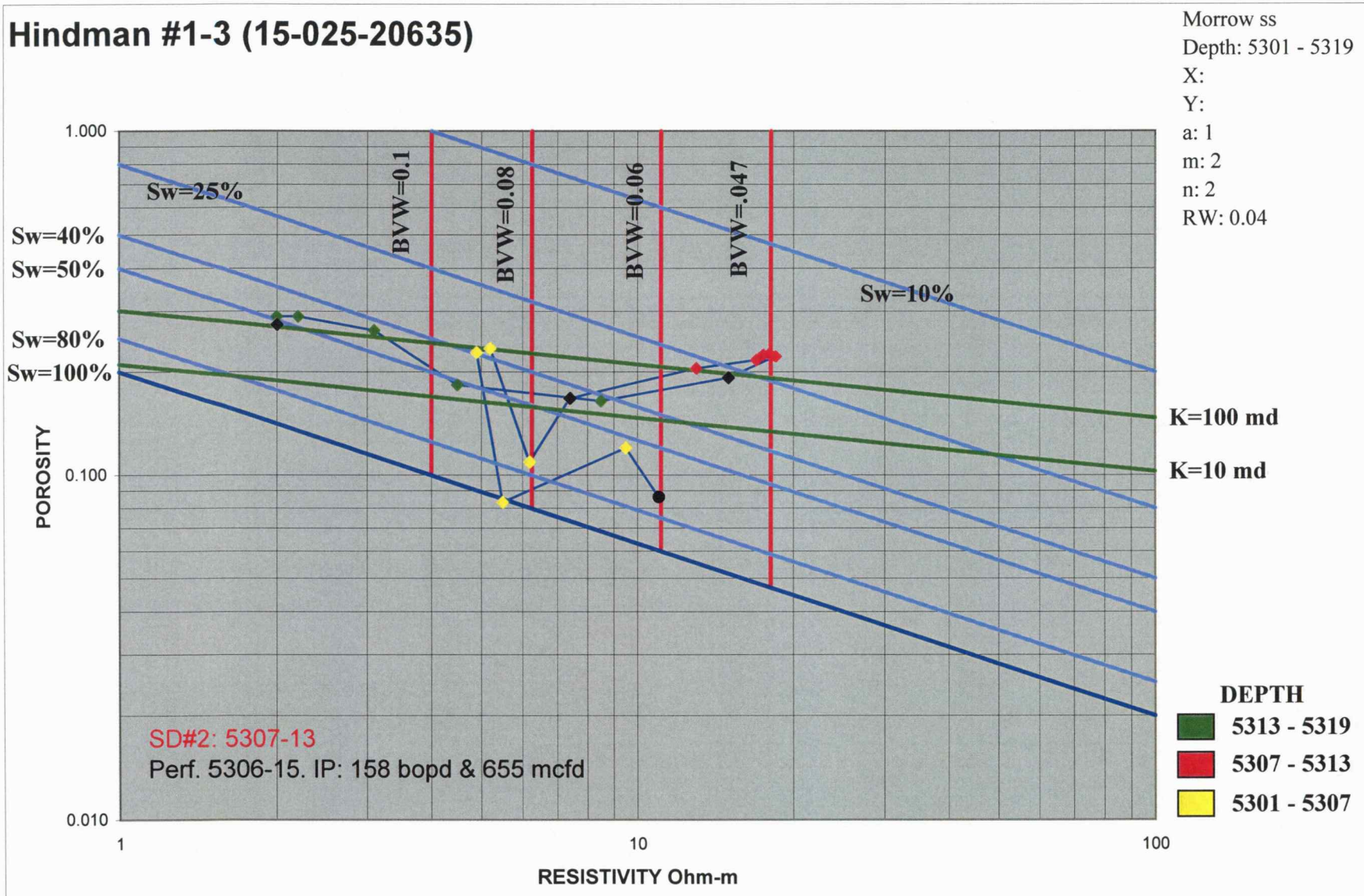

Figure A 14a

Hindman #1-3 (15-025-20635)

Figure A 14b

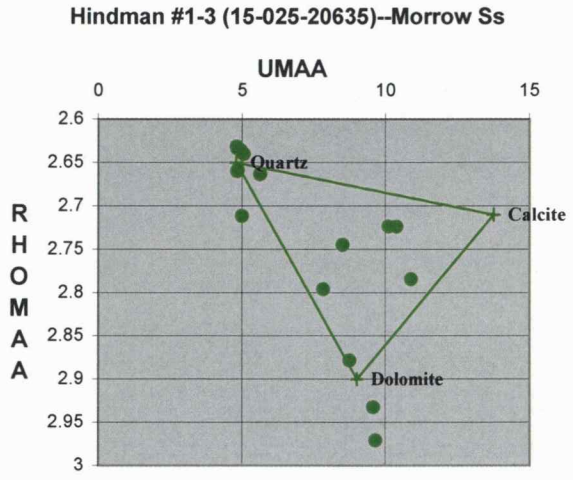

Figure A 14c

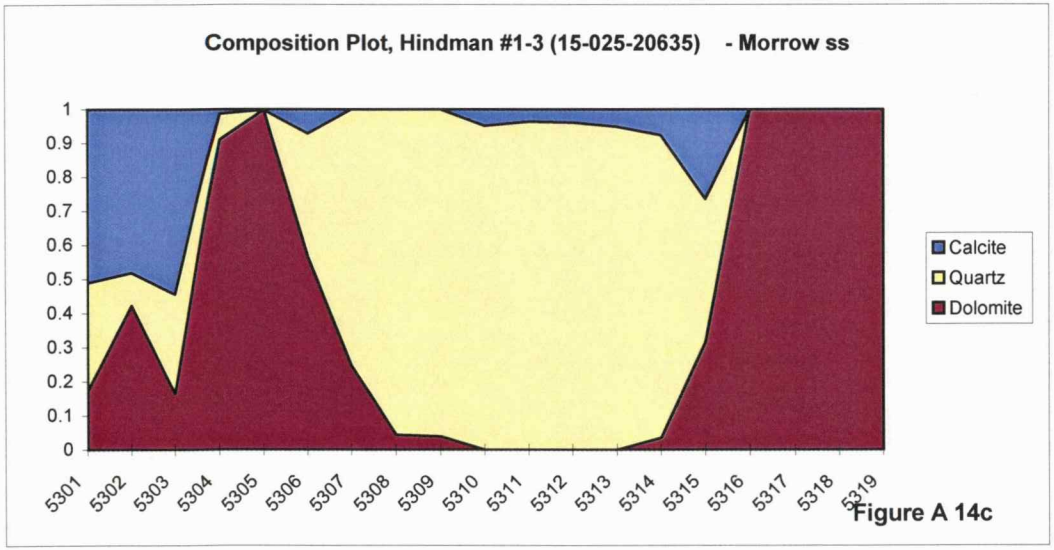

Figure A 14c

Patton #1 (15-025-20594)

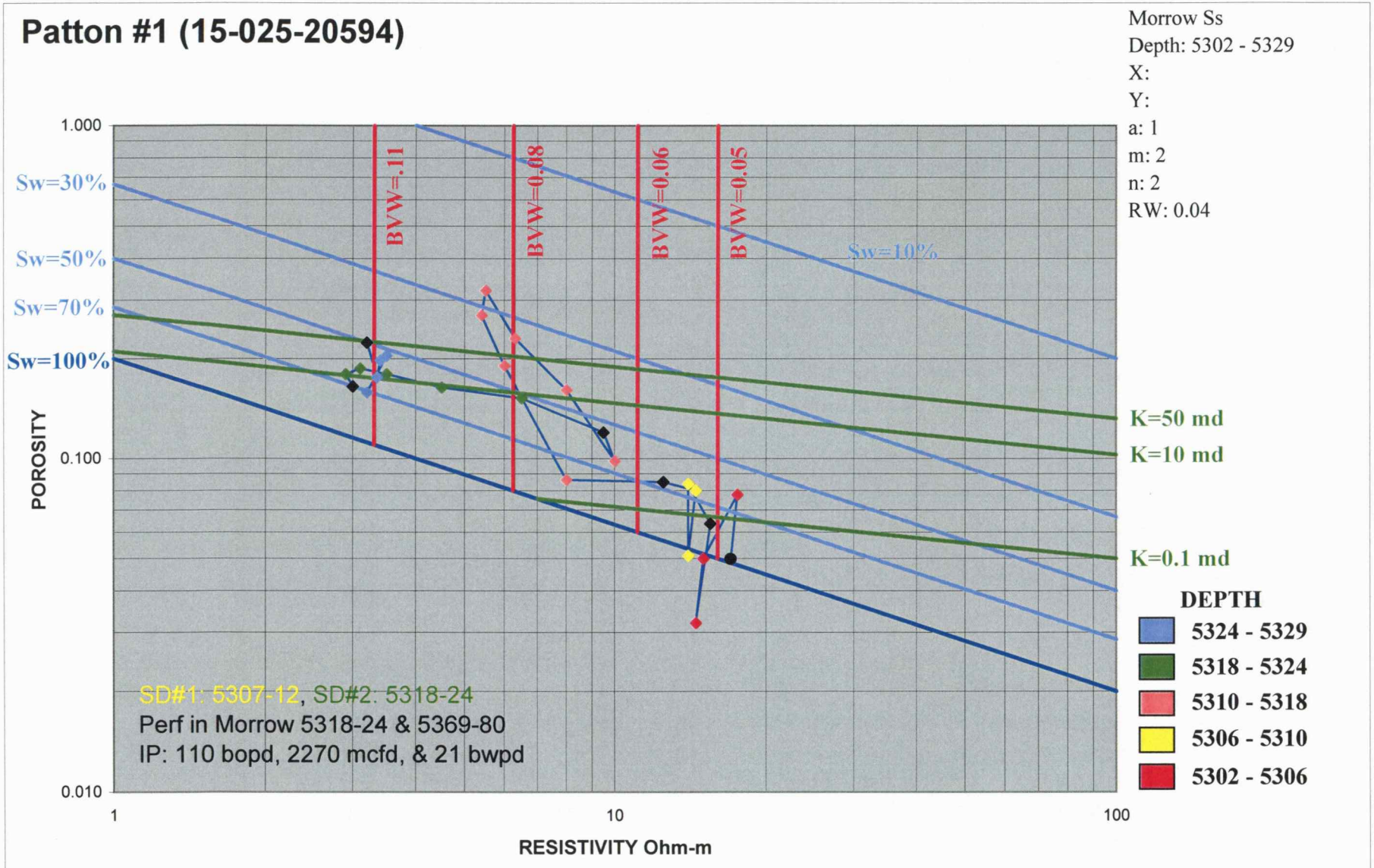

Figure A 15a

Patton #1 (15-025-20594)

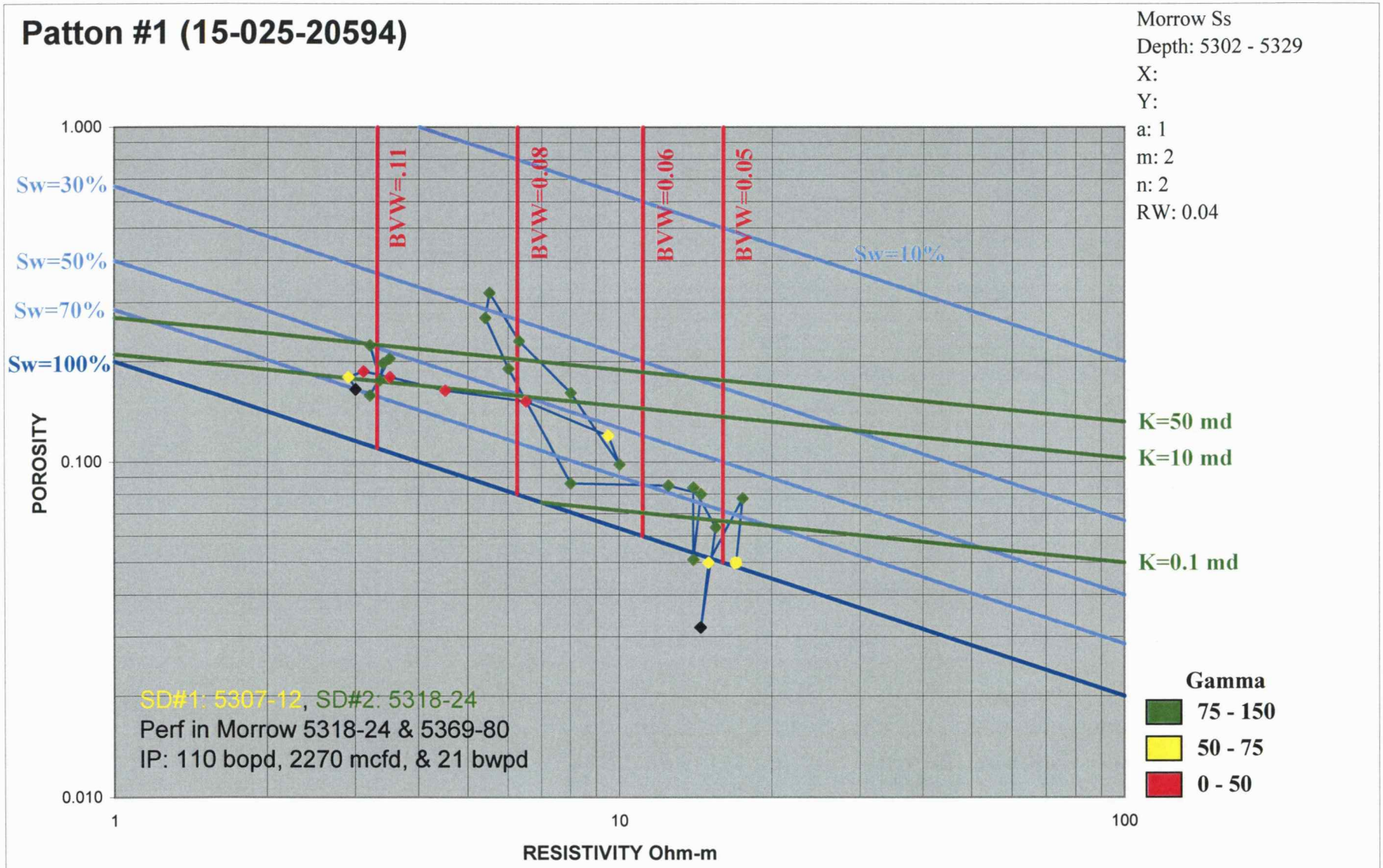

Figure A 15b

Patton #1-3 (15-025-20668)

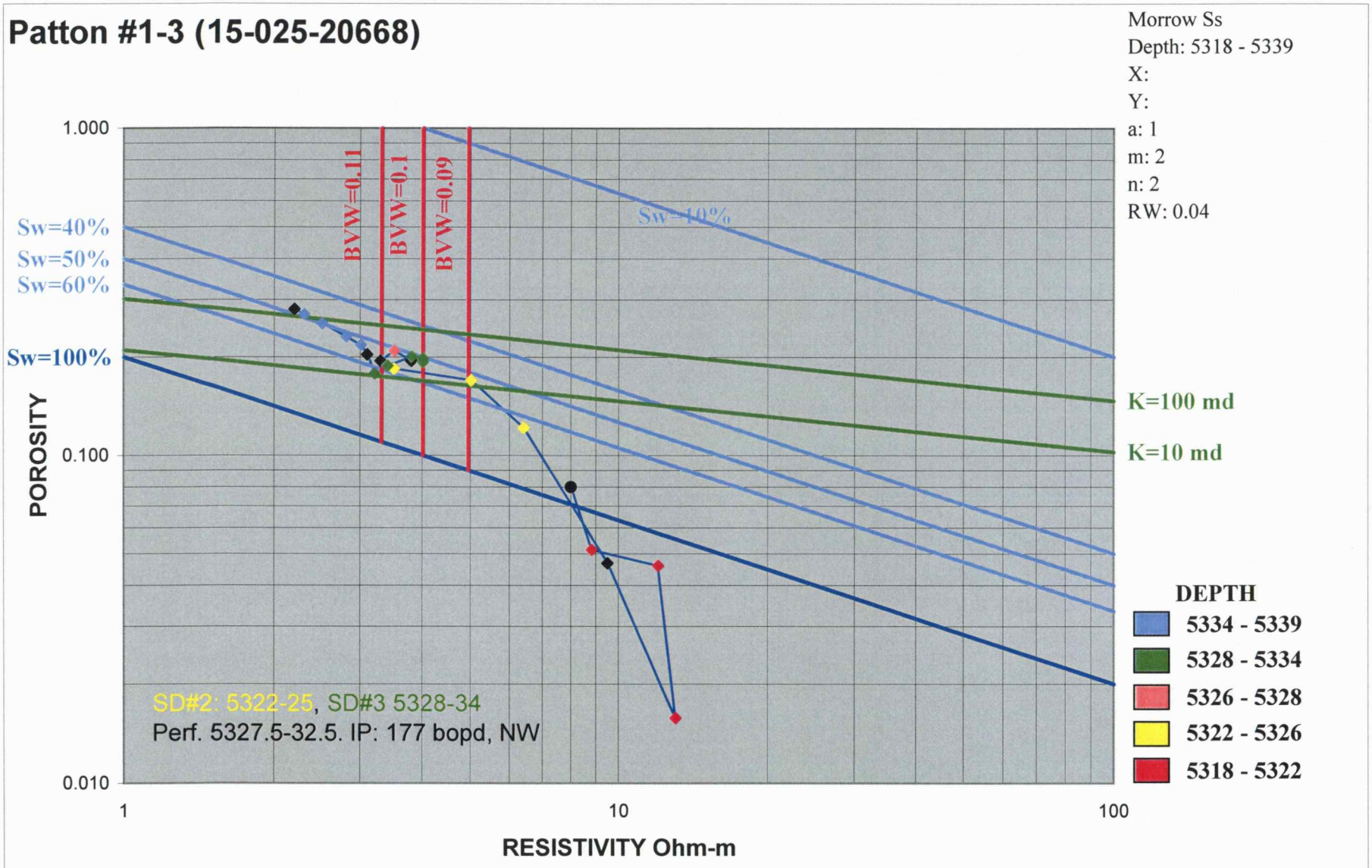

Figure A 16a

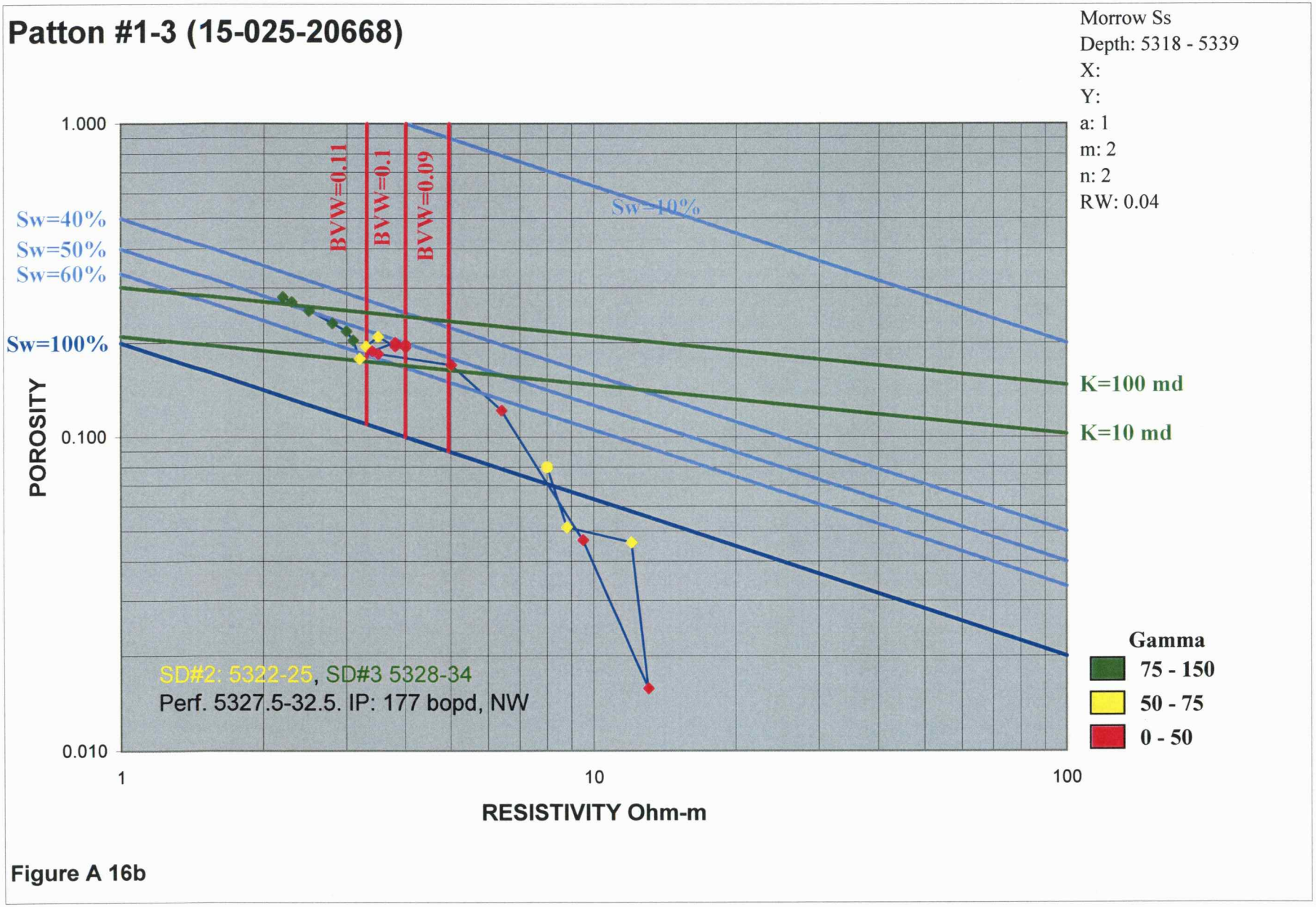
Patton #1-3 (15-025-20668)
Morrow Ss
Depth: 5318 - 5339
X:
Y:
a: 1
m: 2
n: 2
RW: 0.04
1.000
0.100
0.010
POROSITY
Sw=40%
Sw=50%
Sw=60%
Sw=100%
Sw=10%
BVW=0.11
BVW=0.1
BVW=0.09
K=100 md
K=10 md
SD#2: 5322-25, SD#3 5328-34
Perf. 5327.5-32.5. IP: 177 bopd, NW
Gamma
75 - 150
50 - 75
0 - 50
1
10
100
RESISTIVITY Ohm-m

Figure A 16b

Depth

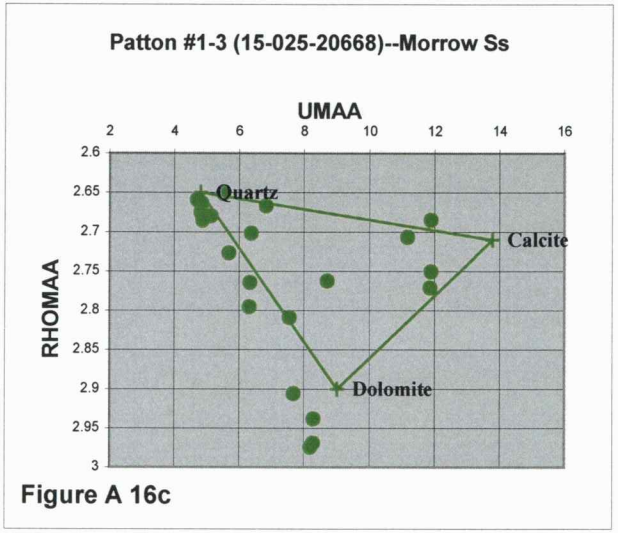

Figure A 16c

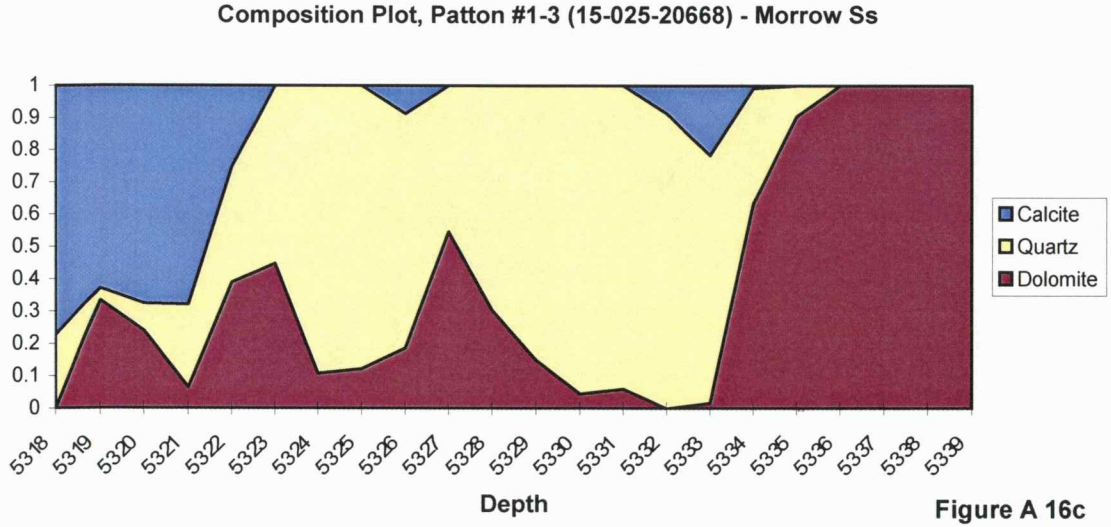

Figure A 16c

Patton #2-3-Ladd (15-025-20859)

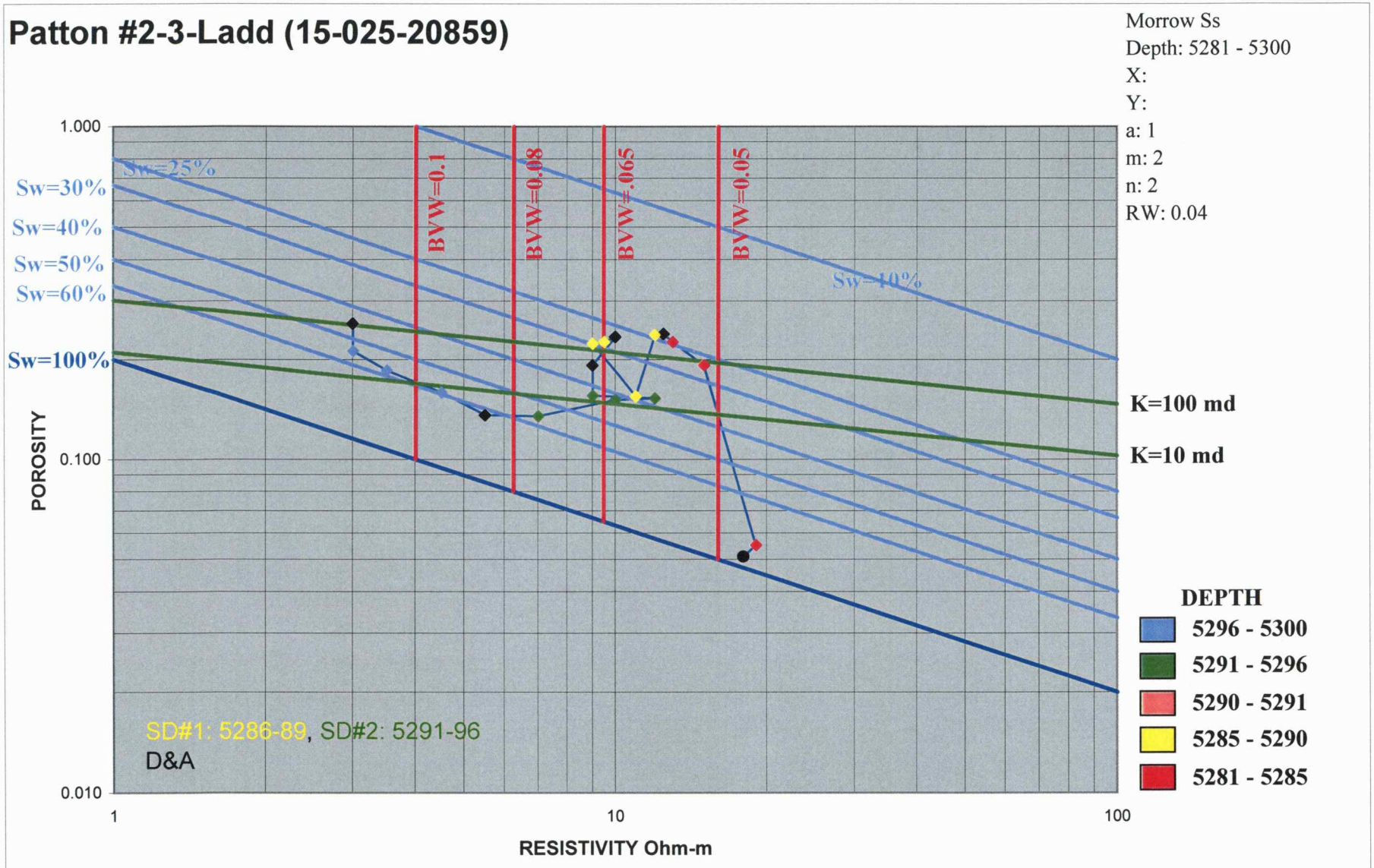

Figure A 17a

Patton #2-3-Ladd (15-025-20859)

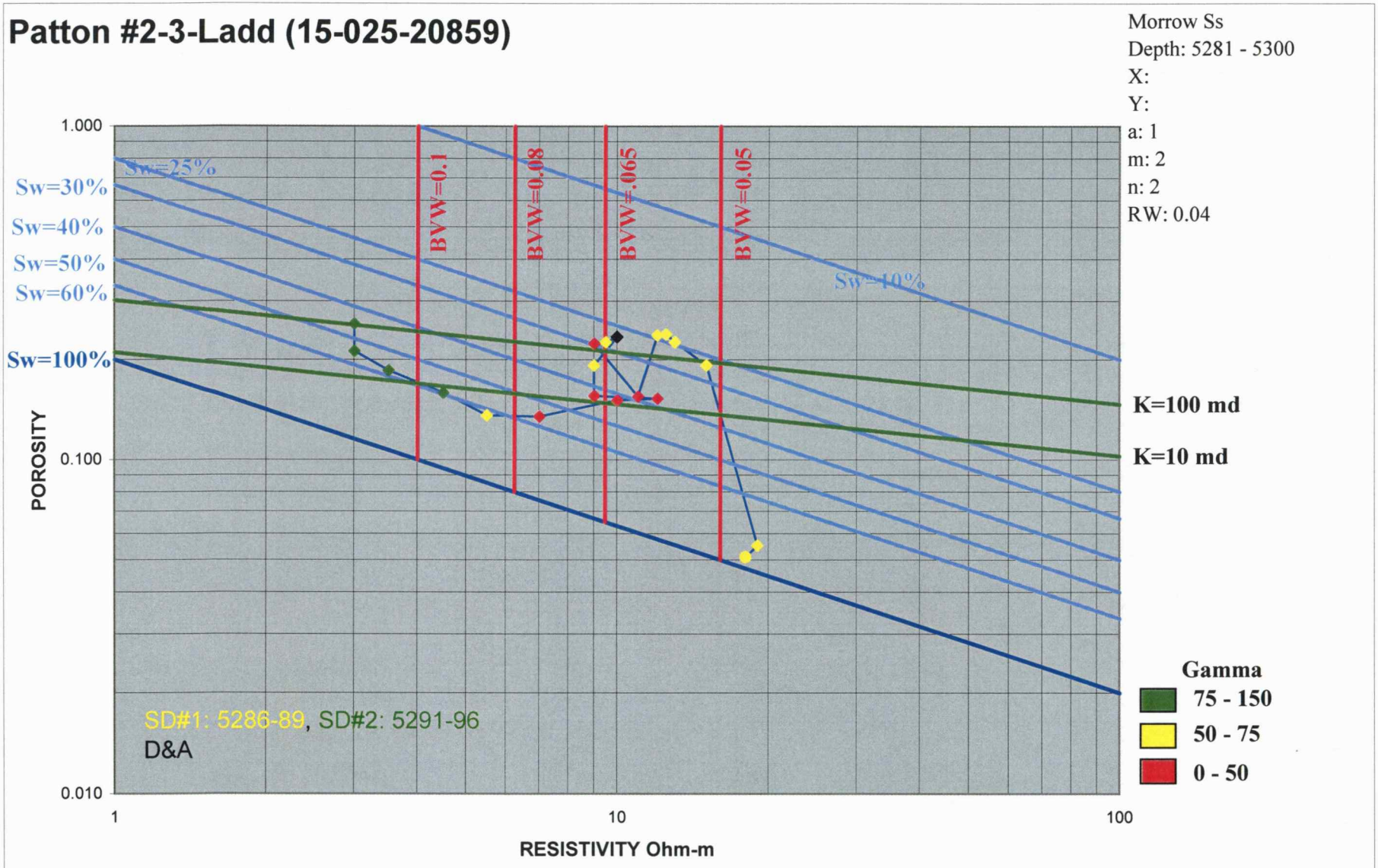

Figure A 17b

Tedford # 1 (15-025-20416)

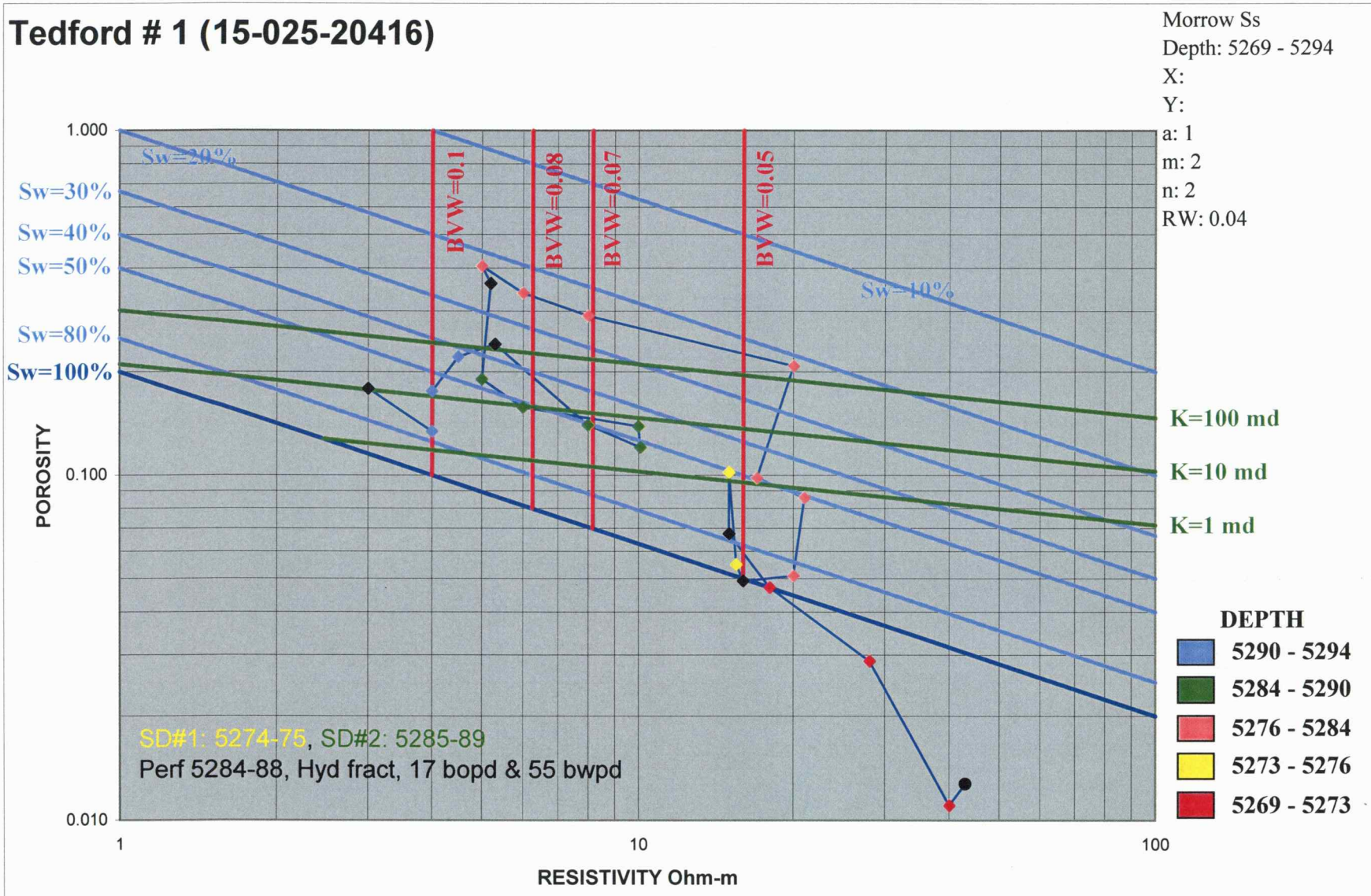

Figure A 18a

Tedford # 1 (15-025-20416)

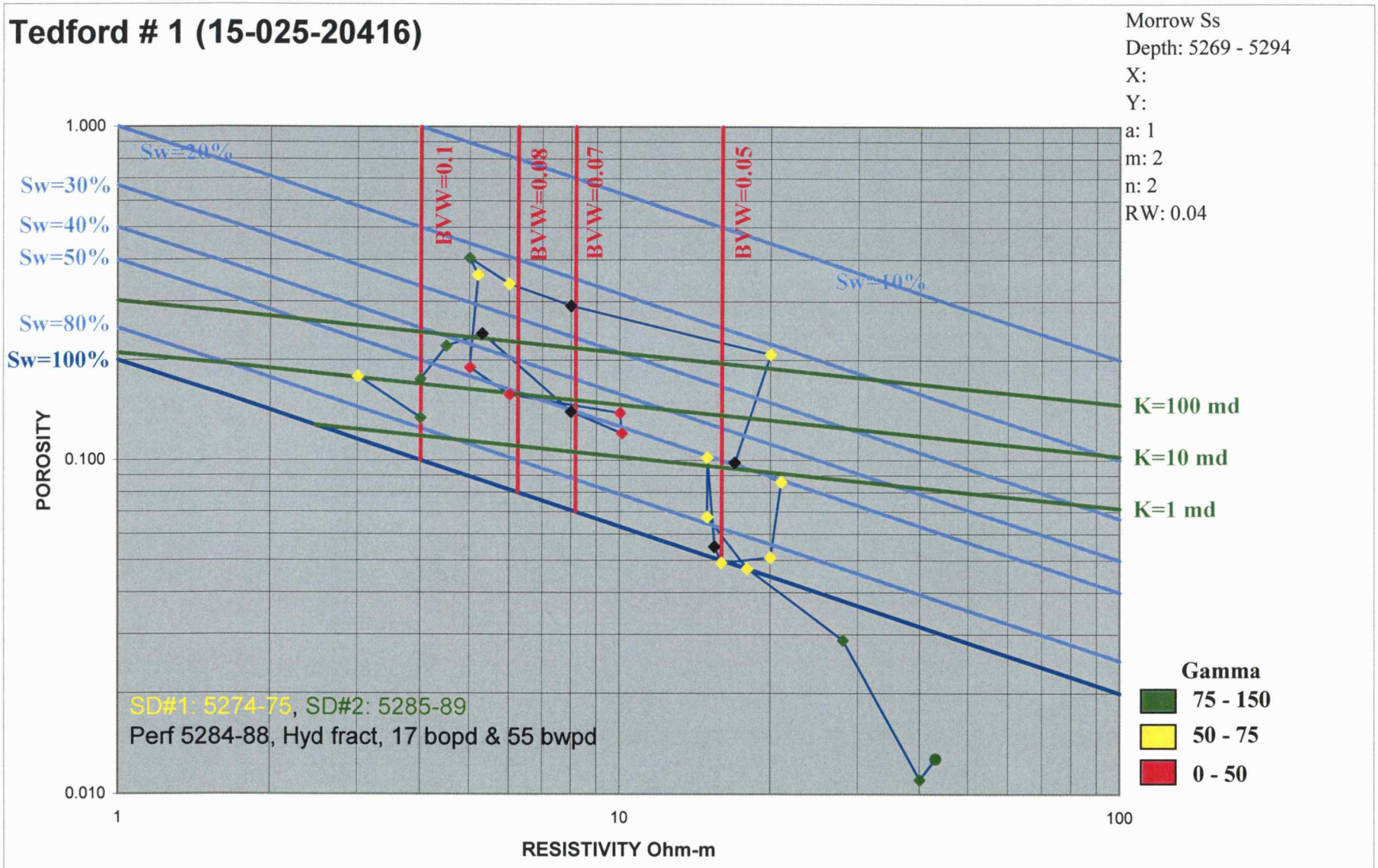

Figure A 18b

Tedford # 1-10 (15-025-20621)

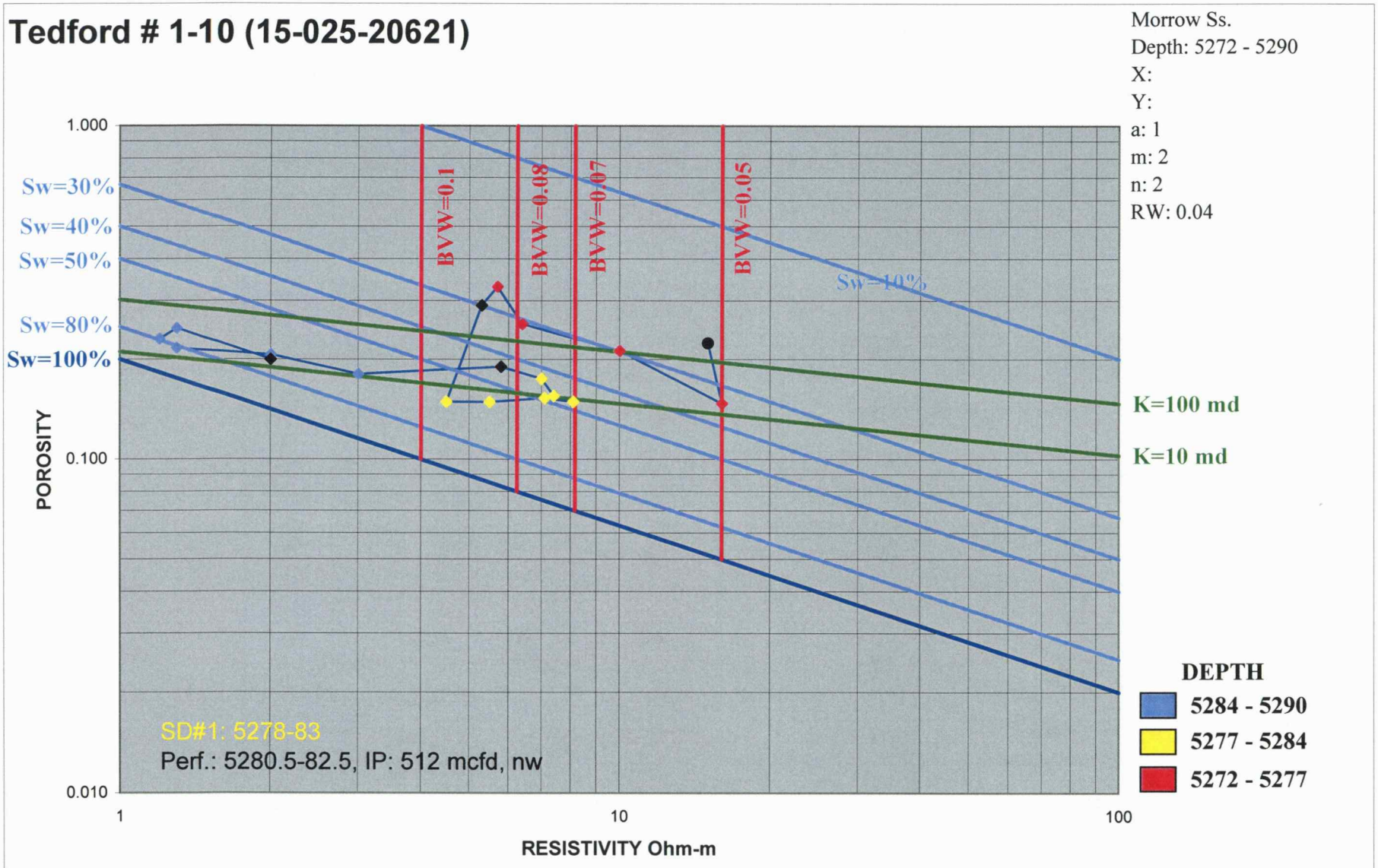

Figure A 19a

Tedford # 1-10 (15-025-20621)

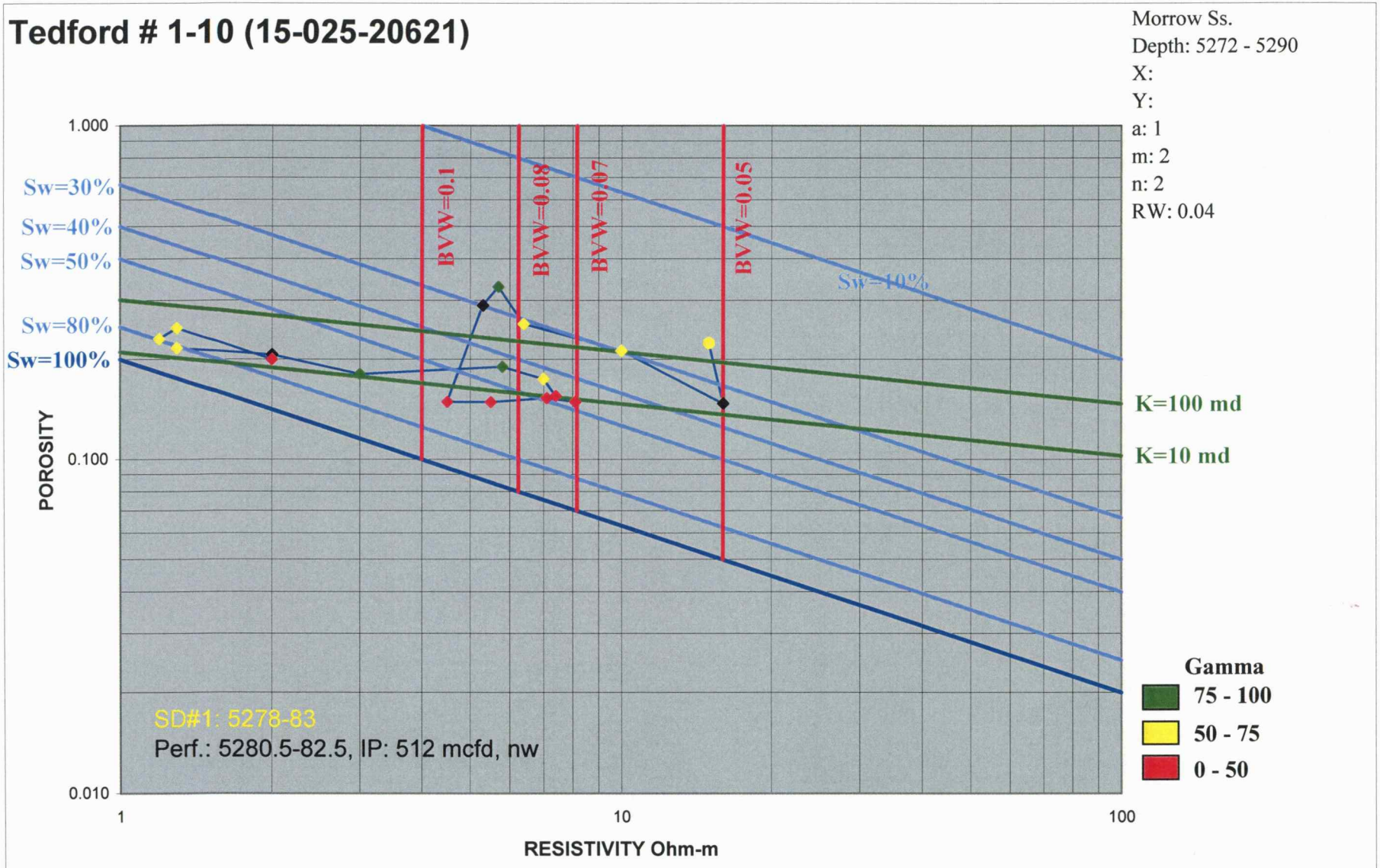

Figure A 19b

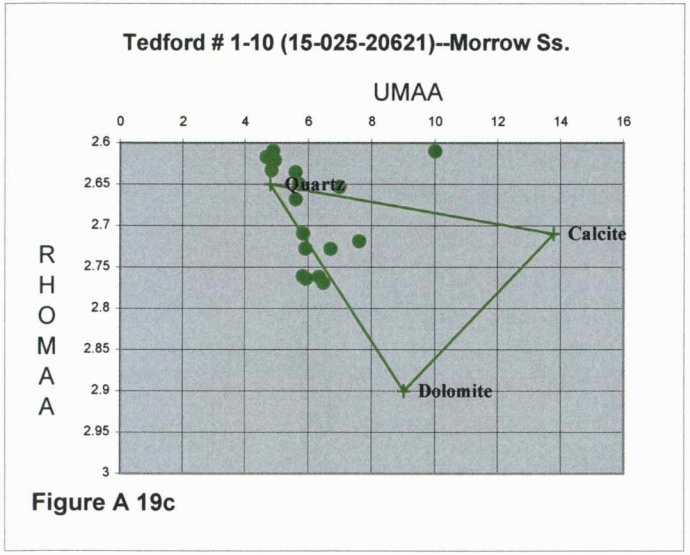

Figure A 19c

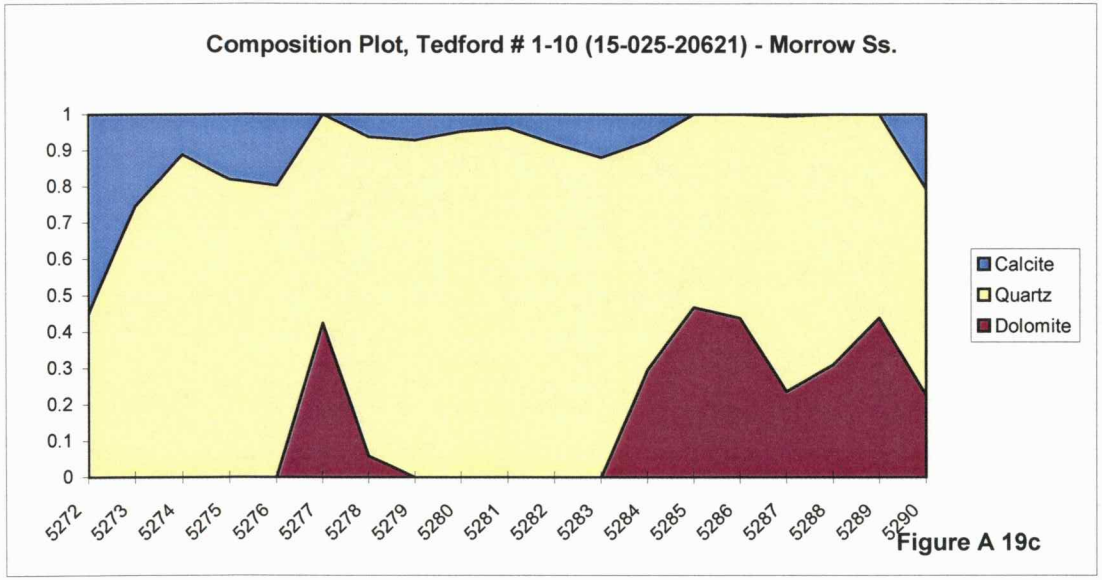

Figure A 19c

Tedford #2-10 (15-025-20669)

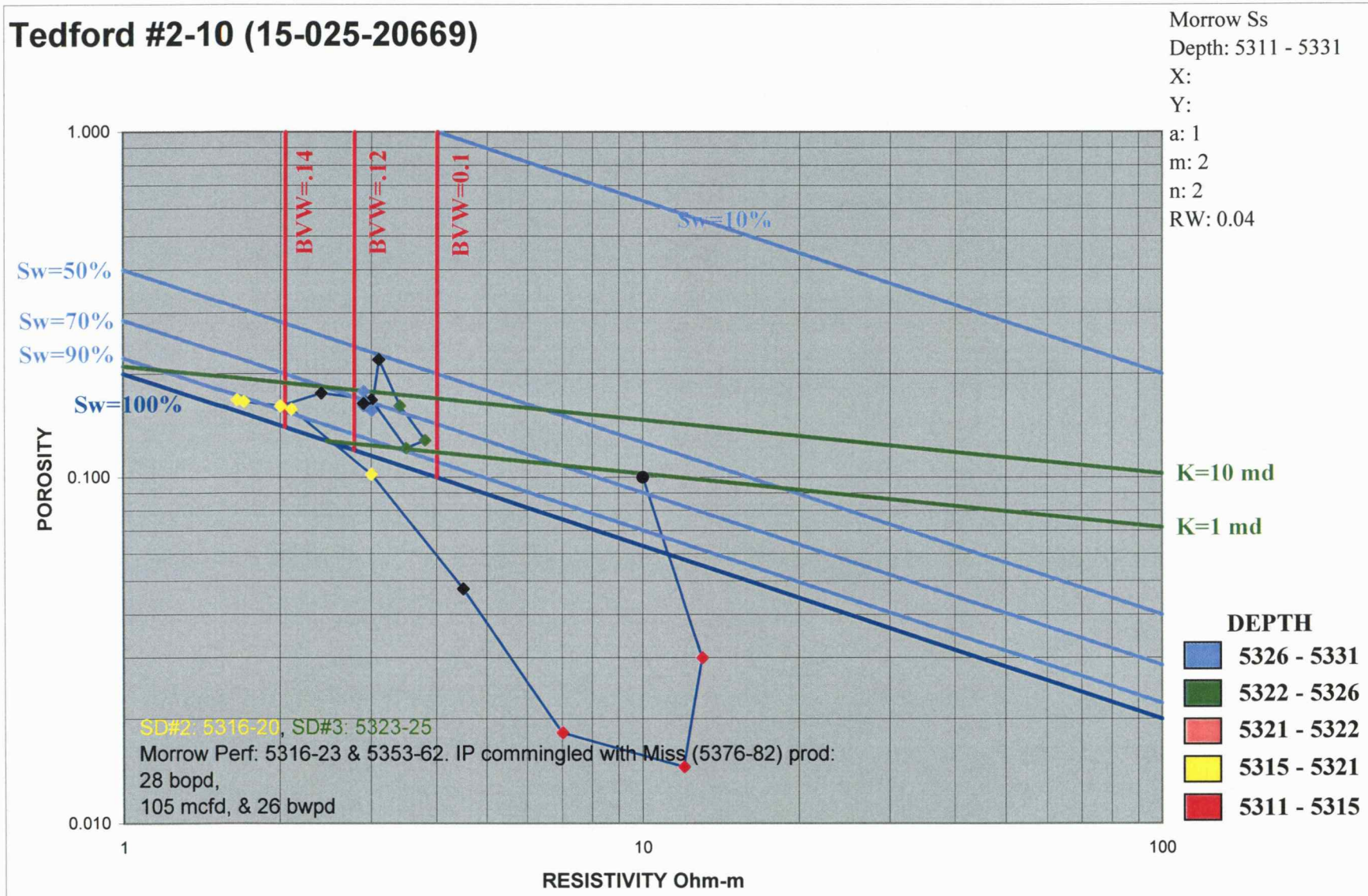

Figure A 20a

Tedford #2-10 (15-025-20669)

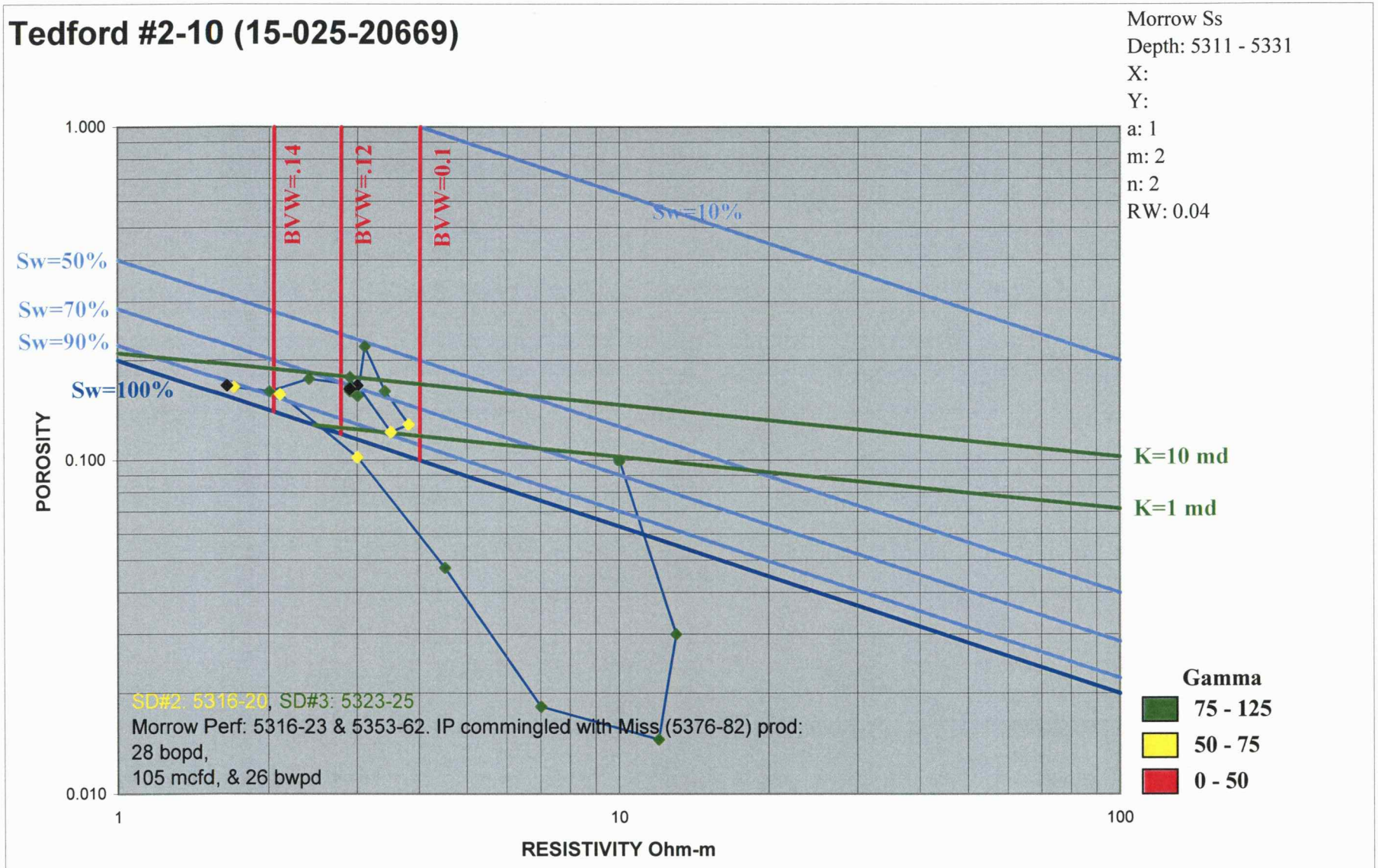

Figure A 20b

Tedford # 2-10 Murfin (15-025-20686)

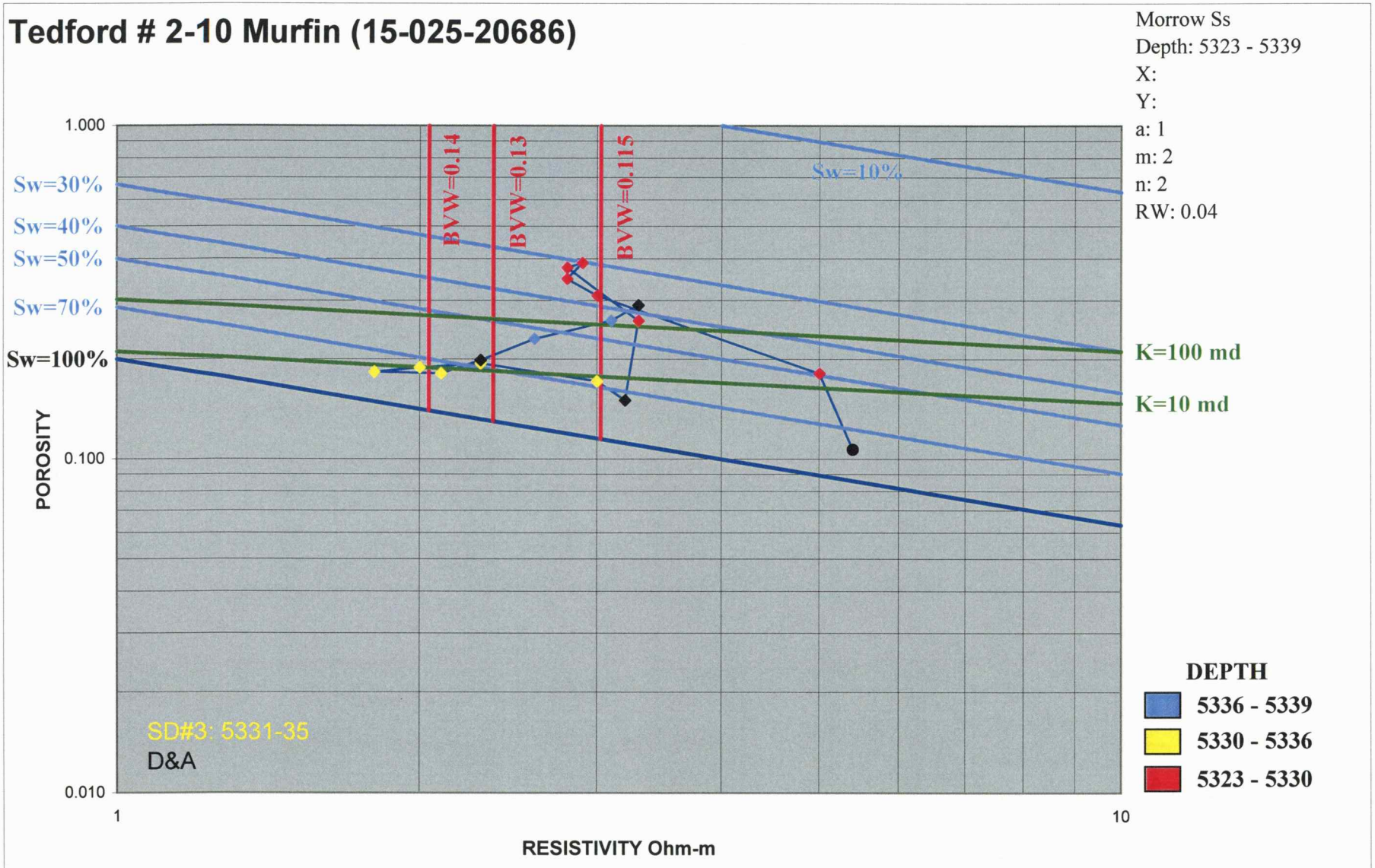

Figure A 21a

Tedford # 2-10 Murfin (15-025-20686)

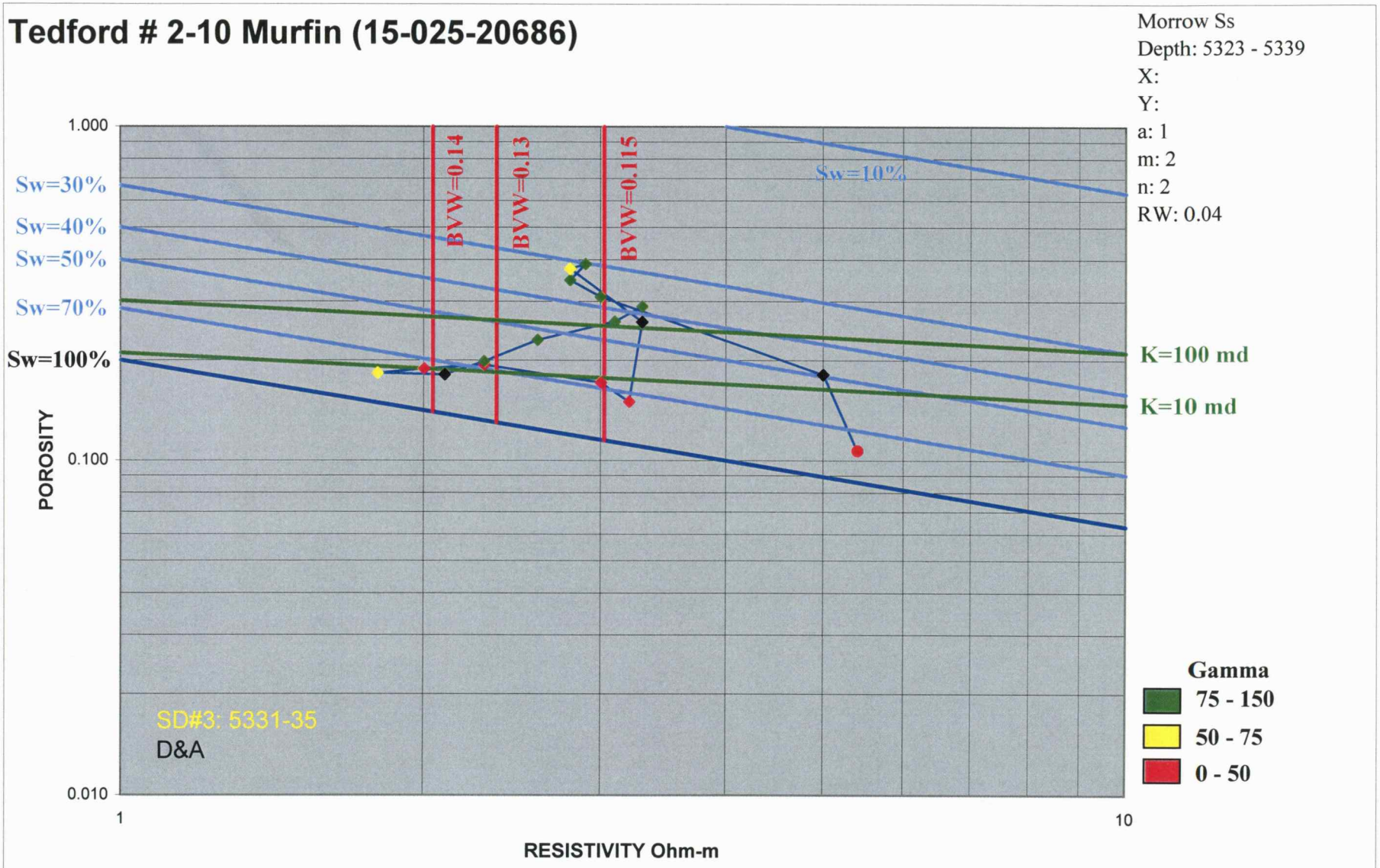

Figure A 21b

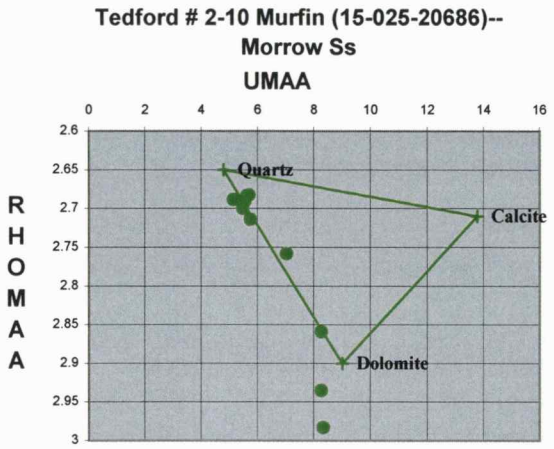

Figure A 21c

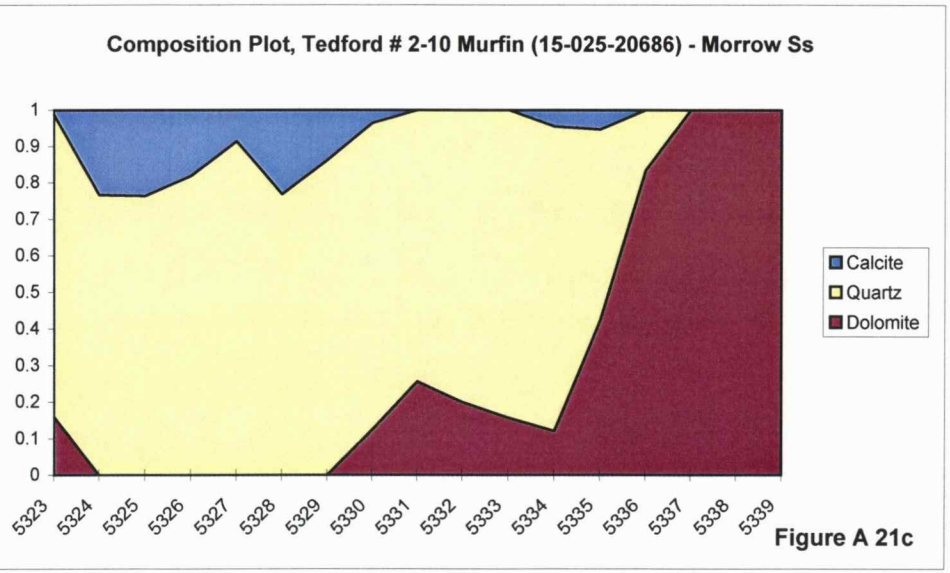

Figure A 21c

Tedford # 3-10 (15-025-20788)

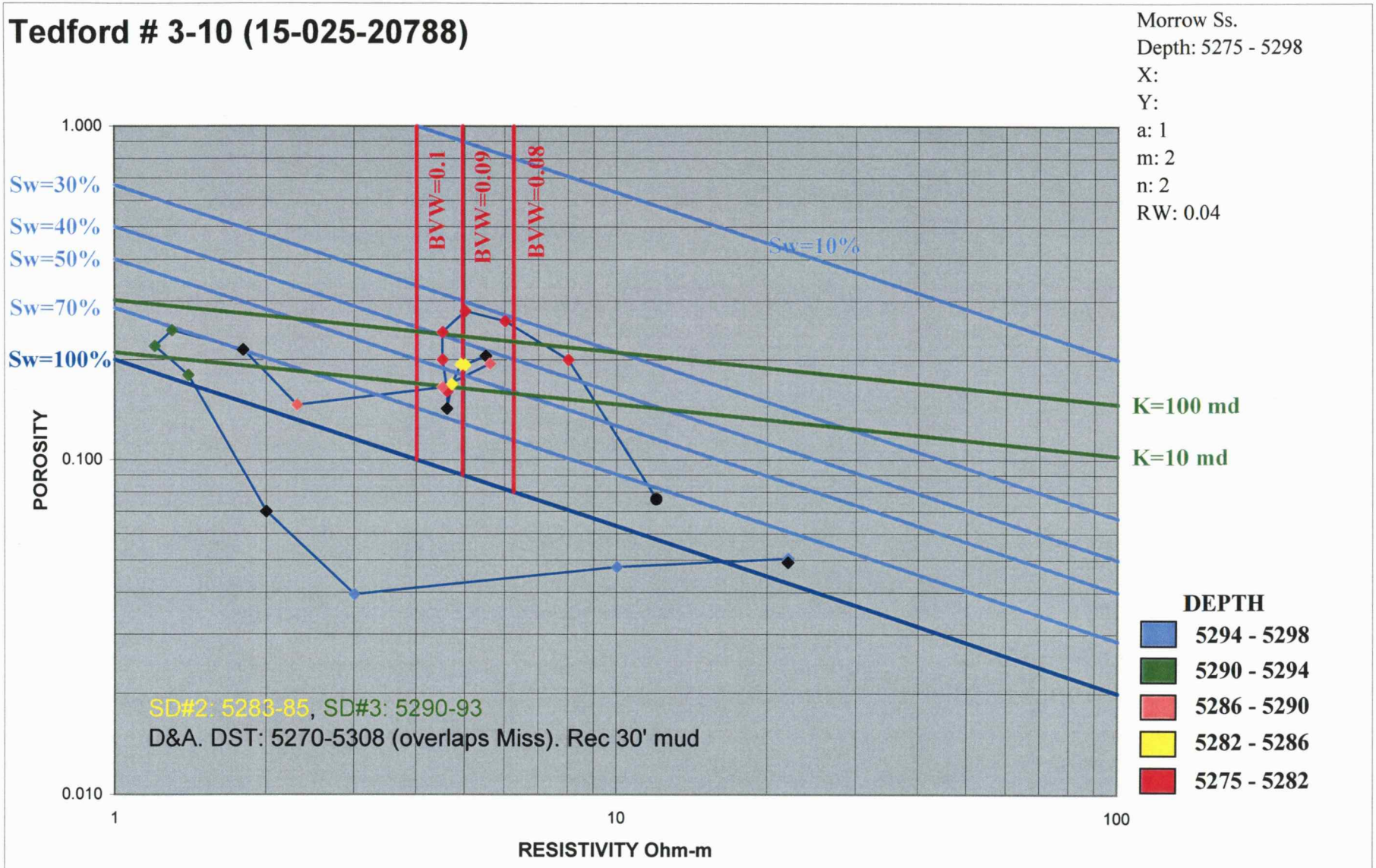

Figure A 22a

Tedford # 3-10 (15-025-20788)

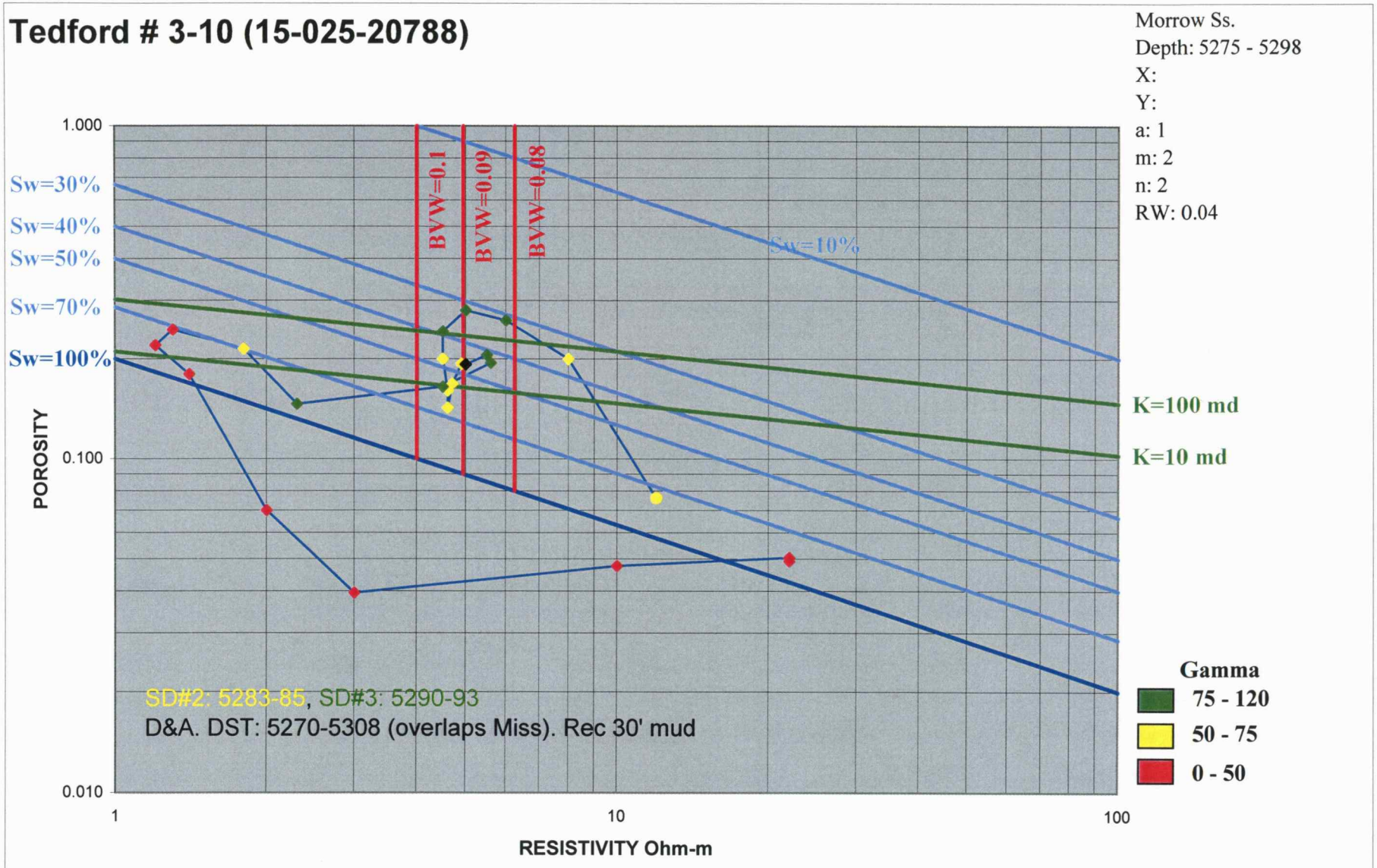

Figure A 22b

Tedford # 4-10 (15-025-20720)

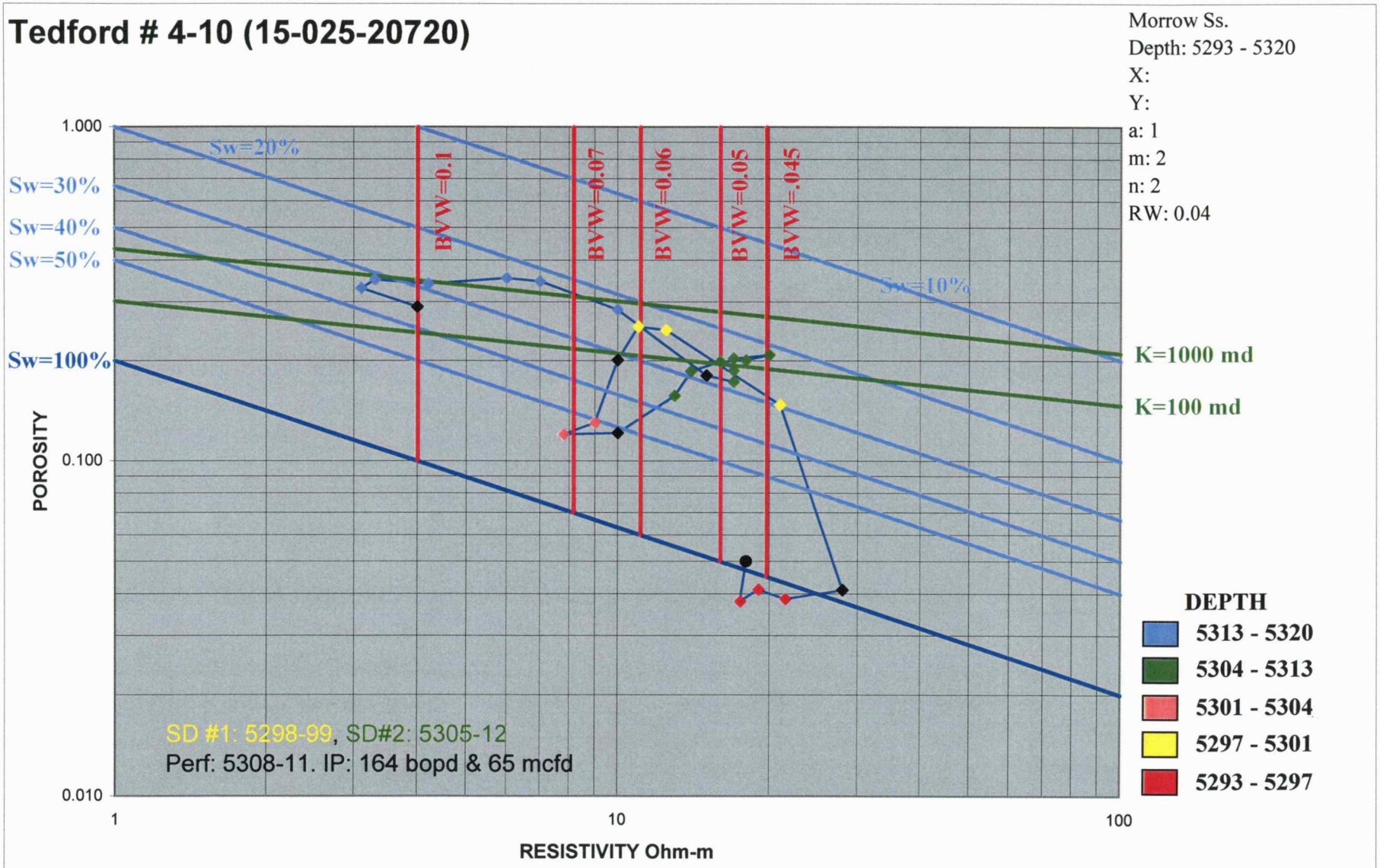

Figure A 23a

Tedford # 4-10 (15-025-20720)

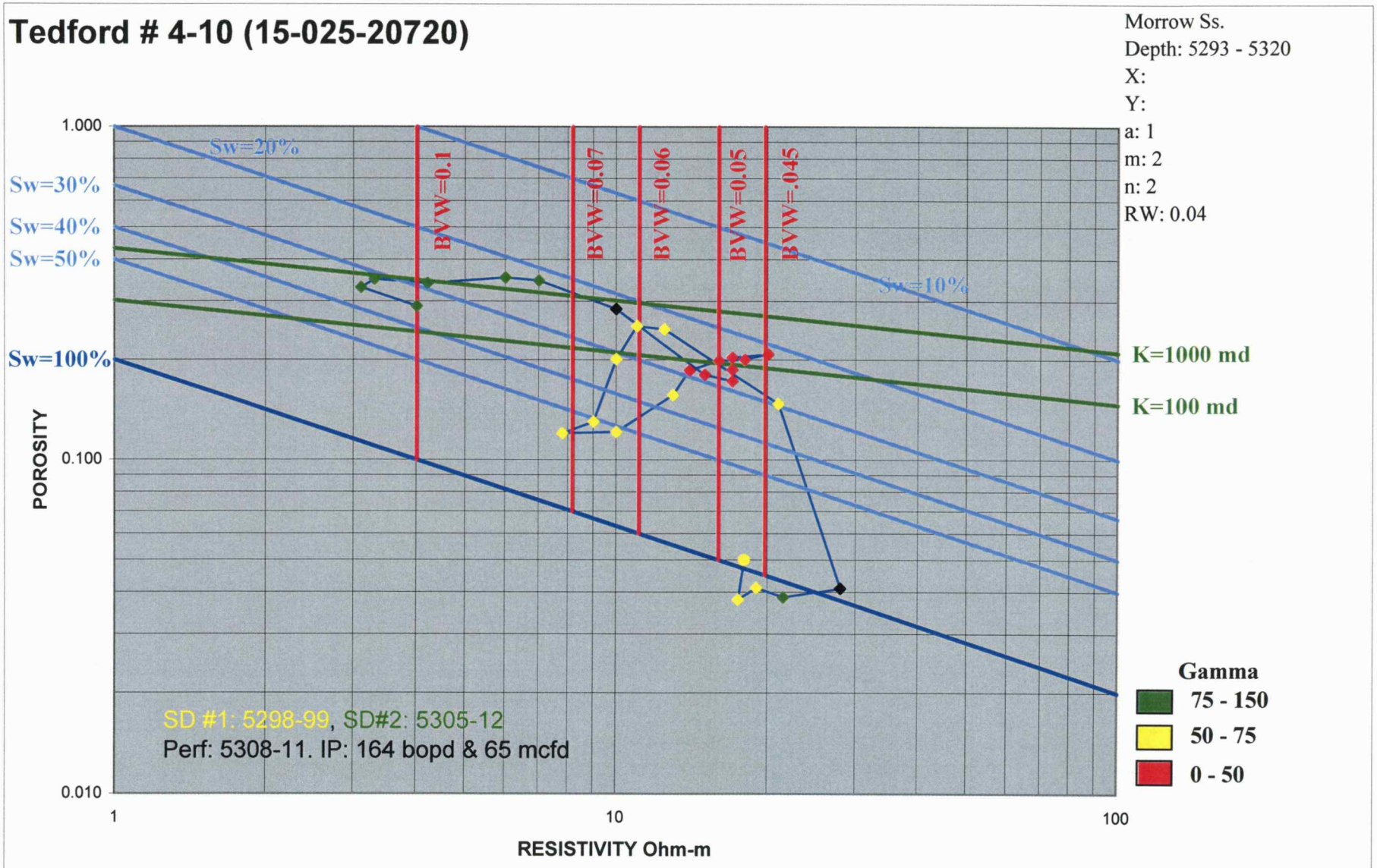

Figure A 23b

Tedford # B1-10 (15-025-20905)

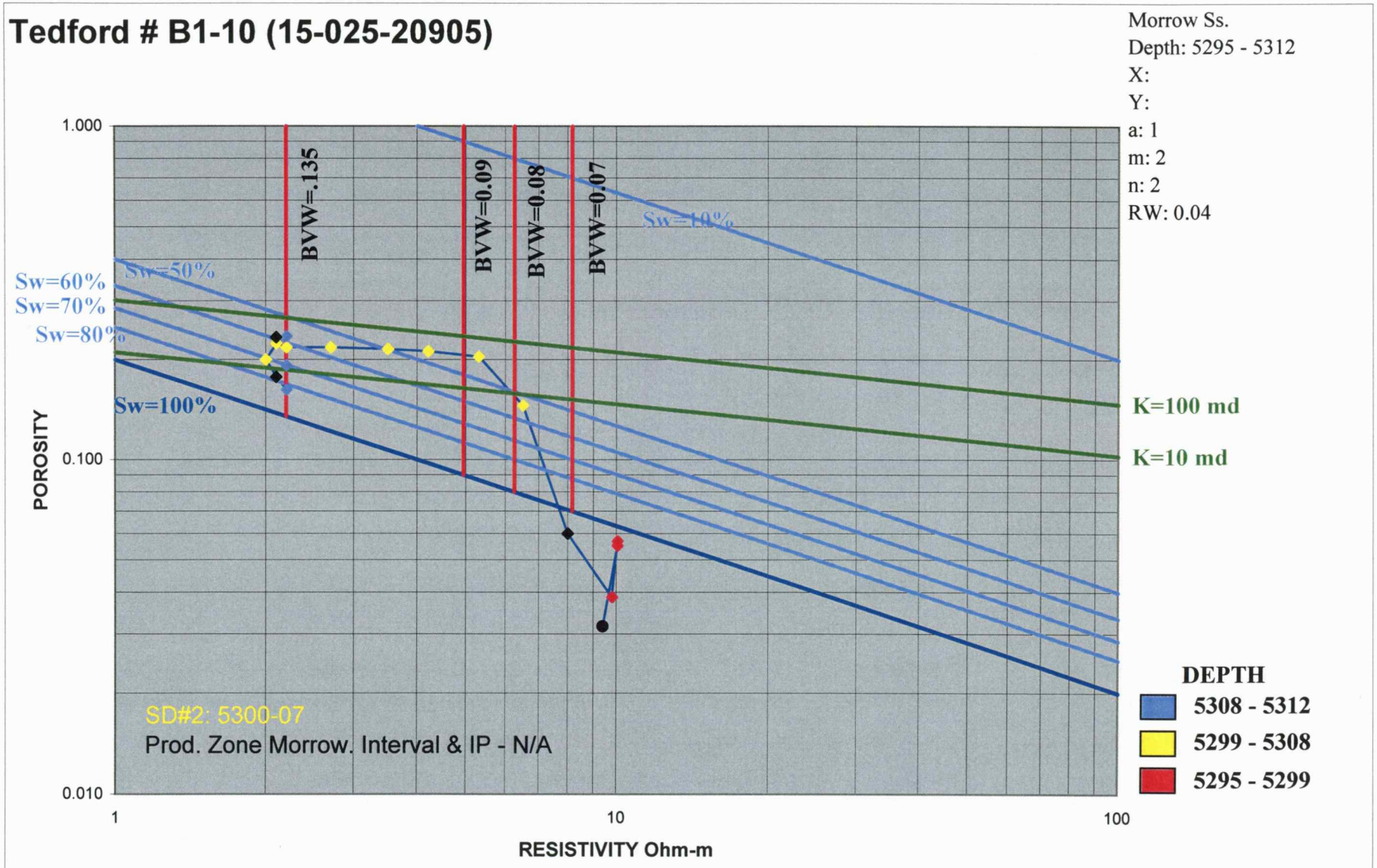

Figure A 24a

Tedford # B1-10 (15-025-20905)

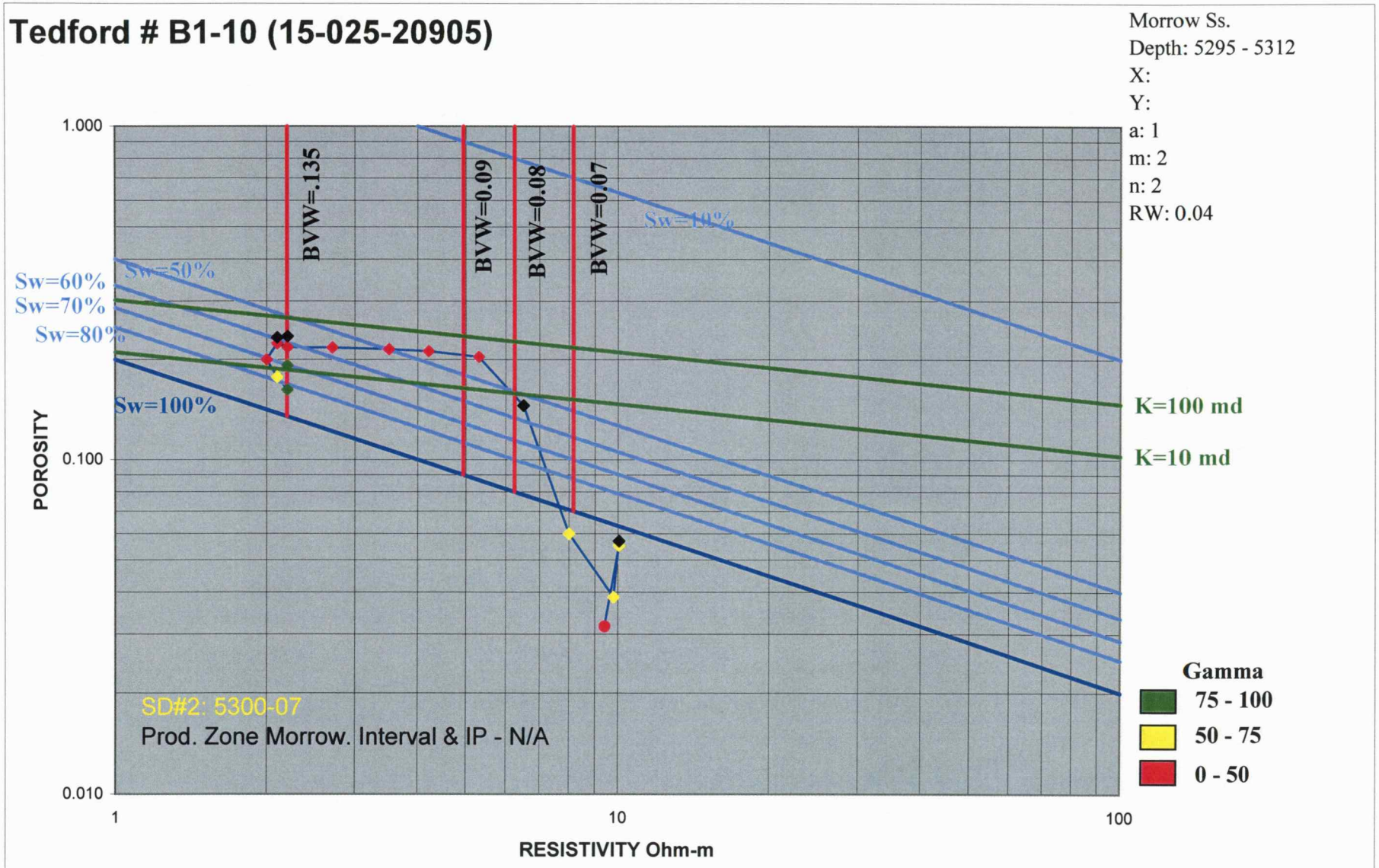

Figure A 24b

Appendix - B

Table B1

Well: **Tedford B1-10 (15-025-20905)**

	from, ft	to, ft	thickness, ft
DST range	5296	5319	23
Pay SD#1			
Pay SD#2	5300	5307	7
Pay SD#3			
Morrow pay			7

entered data
read from correlations
read from Horner plot
calculation

Reservoir gas properties:

Sp gr. =	0.73		gas specific gravity (avg from 3 samples)
Tpc =	386	R	pseudocritical temp
Ppc =	660	psia	pseudocritical pressure

DST analysis - Gas using SPE Monograph method:

Pi =	766	psi	
m =	23	psi/cycle	
Qg =	40.9	Mcfd	
Pwf =	86	psi	(related to Qg - end of second flow)
P I hr =			

Transmissibility:

Kh/mu = 162.6*Qg*Bg/m

Bg = Psc*Tr*1000*Z/(p*Tsc*5.614) gas formation volume factor

Psc =	14.65	psi	pr at standard conditions
Tr =	578	R	Res temp = 118 F
Tsc =	520	R	Std temp in R
p = (Pi+Pw	426	psi	avg of static and flowing pressure
Tpr =	1.50		pseudo reduced temp
Ppr =	0.67		pseudo reduced pressure
Z =	0.932		compressibility factor at p and Tr
Bg =	6.35	RB\Mcf	
Kh/mu =	1834.898	md-ft\cp	

Permeability:

h =	7	ft	pay	
Mol wt of a	29	lb/lb mole		
Mol wt of g	21.17	lb/lb mole		
mu @ 1 ati	0.0111	cp	(@ res temp)	
Vis ratio =	1	cp	atTpr and I	approx outside range
gas vis (mu	0.0111	cp		
K =	2.9	md		

DST analysis - Gas using Low pressure gas method:

Mg =	48000	psi^2/cycle
Qg =	40.9	Mcfd

Transmissibility:

Kh/mu = 1637*Qg*Tr*Z/Mg

Kh/mu =	751.4057	md-ft/cp
K =	1.2	md

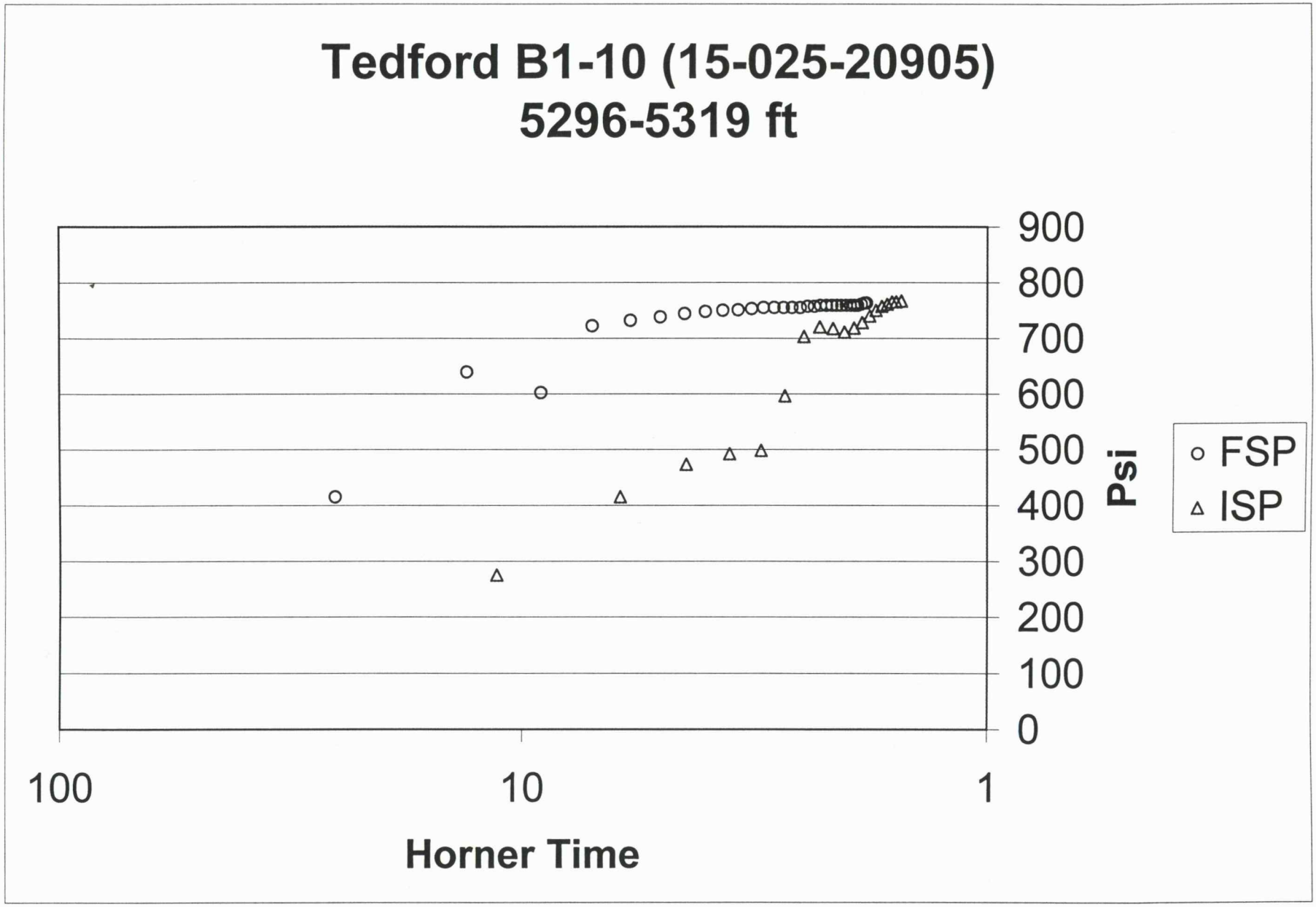
Tedford B1-10 (15-025-20905)
5296-5319 ft
900
800
700
600
500
400
300
200
100
0
Psi
FSP
ISP
100
10
1
Horner Time

Figure B 1A

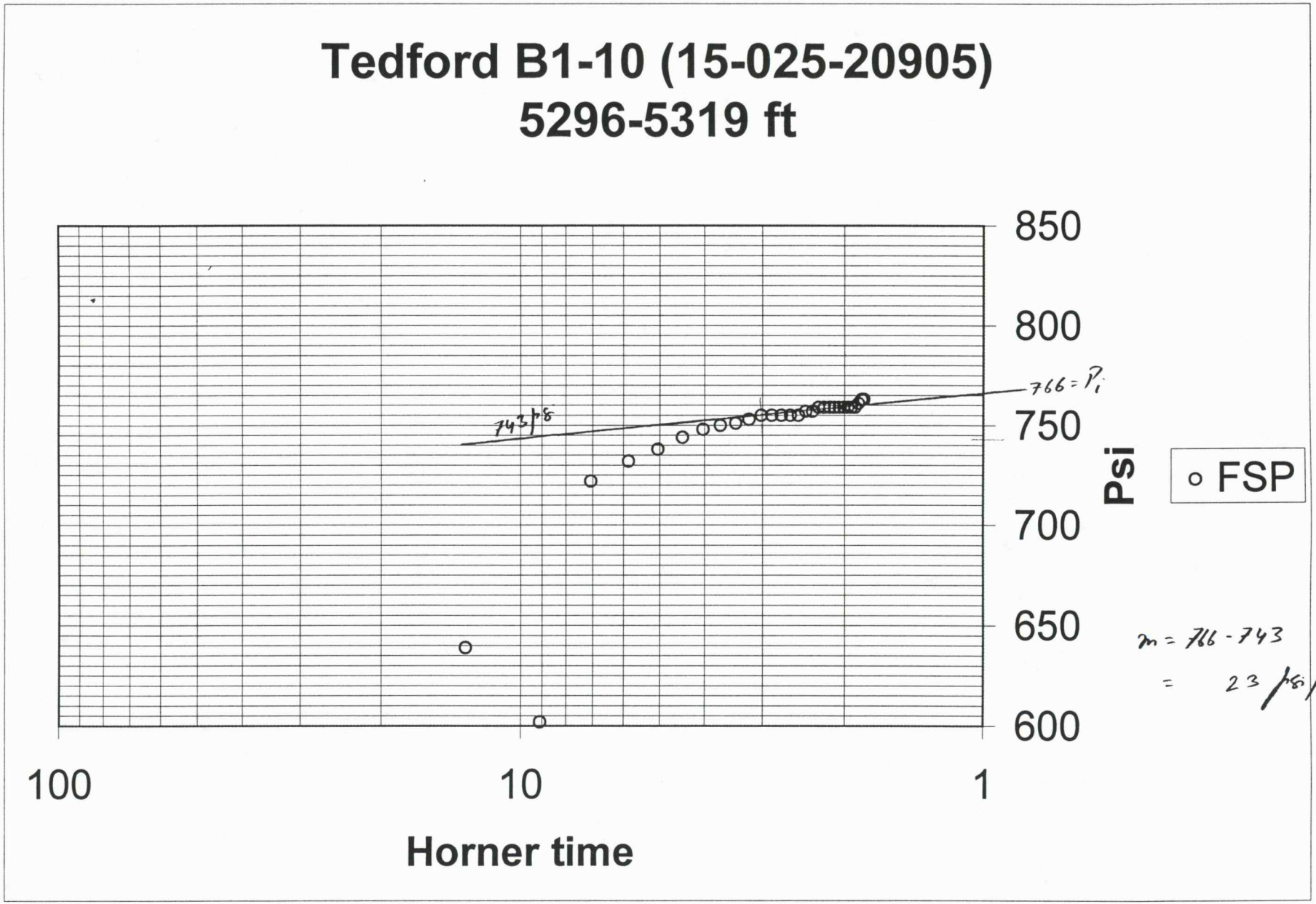
Tedford B1-10 (15-025-20905)
5296-5319 ft
850
800
750
700
650
600
Psi
FSP
766 = Pi
743 psi
m = 766 - 743
= 23 psi/cycle.
100
10
1
Horner time

Figure B 1B

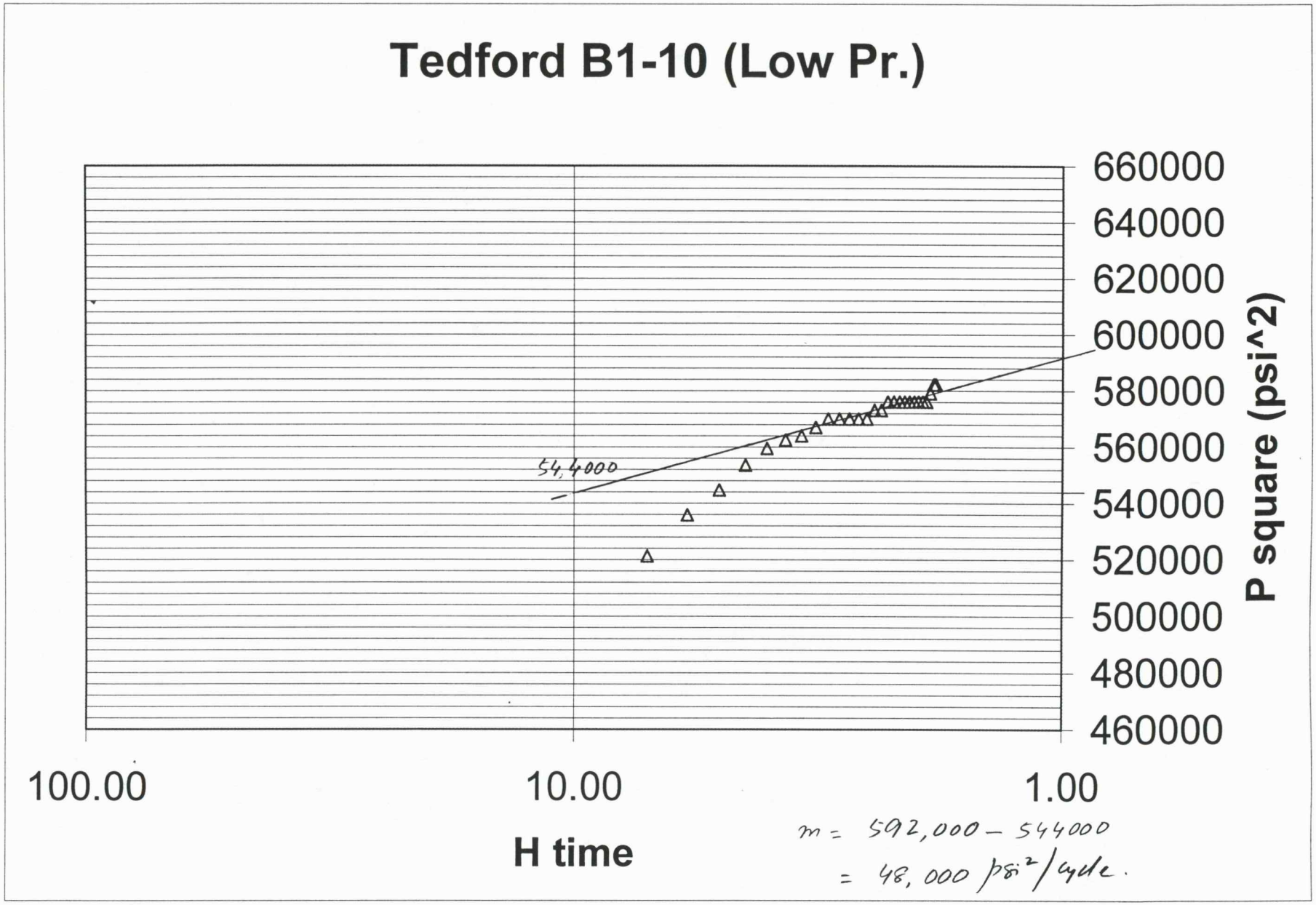
Tedford B1-10 (Low Pr.)
660000
640000
620000
600000
580000
560000
540000
520000
500000
480000
460000
P square (psi^2)
54,4000
100.00
10.00
1.00
H time
m = 592,000 − 544000
= 48,000 psi²/cycle.

Figure B 1C

Table B 2

Well:	Patton #2-3 (15-025-20685)		
	from, ft	to, ft	thickness, ft
DST range	5283	5315	32
Pay SD#1			
Pay SD#2	5293	5300	7
Pay SD#3	5301	5304	3
Morrow pay			10

entered data
read from correlations
read from Horner plot
calculation

Reservoir gas properties:

Sp gr. =	0.73		gas specific gravity (avg from 3 samples)
Tpc =	386	R	pseudocritical temp
Ppc =	660	psia	pseudocritical pressure

DST analysis - Gas using SPE Monograph method:

Pi =	1510.5	psi	
m =	44.5	psi/cycle	
Qg =	1048	Mcfd	
Pwf =	1038.5	psi	(related to Qg - end of second flow)
P I hr =			

Transmissibility:

Kh/mu = 162.6*Qg*Bg/m

Bg = Psc*Tr*1000*Z/(p*Tsc*5.614) gas formation volume factor

Psc =	14.65	psi	pr at standard conditions
Tr =	589	R	Res temp = 129 F
Tsc =	520	R	Std temp
p = (Pi+Pw	1274.5	psi	avg of static and flowing pressure
Tpr =	1.53		pseudo reduced temp
Ppr =	1.95		pseudo reduced pressure
Z =	0.84		compressibility factor at p and Tr
Bg =	1.95	RB\Mcf	
Kh/mu =	7459.993	md-ft\cp	

Permeability:

h =	10	ft	pay
Mol wt of a	29	lb/lb mole	
Mol wt of g	21.17	lb/lb mole	
mu @ 1 atı	0.0111	cp	(@ temp 129 F)
Vis ratio =	1.25	cp	at corresponding Tpr and Ppr
gas vis (mu	0.0139	cp	
K =	10.4	md	

DST analysis - Gas using High pressure gas method:

Pi =	1510.5	psi	
m =	44.5	psi/cycle	
Qg =	1048	Mcfd	
Pwf =	1038.5	psi	(related to Qg - end of second flow)
P I hr =			

Transmissibility:

Kh/mu = 818.5*Qg*Tr*Z/(P1avg*m)

HT - Horner time

P (@ HT =	1510.5		
P (@ HT =	1466		
P1avg =	1488.25	psi	avg pr of Horner straight line
Kh/mu =	6408.238179	md-ft/cp	
K =	8.9	md	

DST analysis - Gas using Low pressure gas method:

Mg =	152500	psi^2/cycle
Qg =	1048	Mcfd

Transmissibility:

Kh/mu = 1637*Qg*Tr*Z/Mg

Kh/mu =	5565.891	md-ft/cp
K =	7.7	md

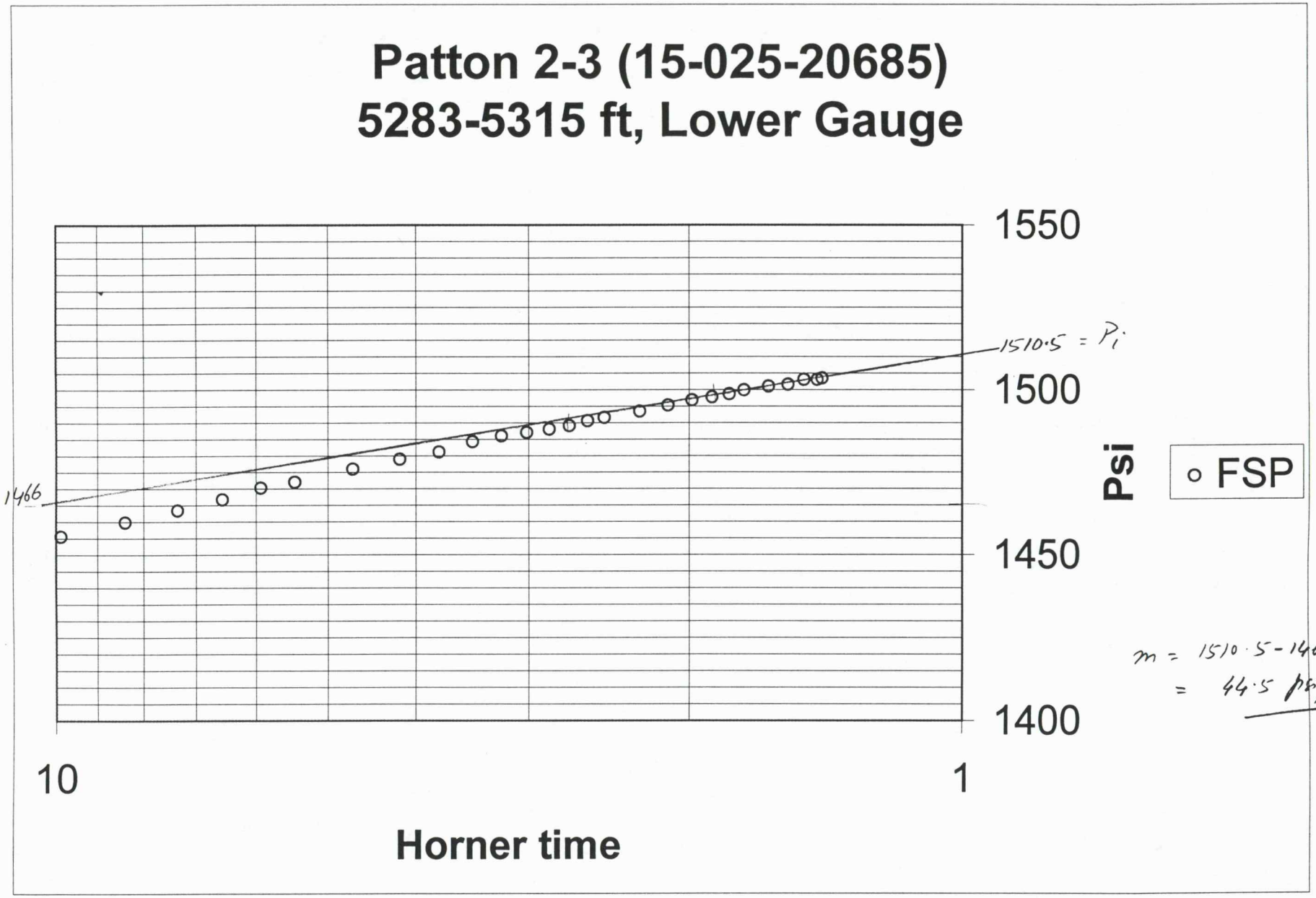
Patton 2-3 (15-025-20685)
5283-5315 ft, Lower Gauge
1550
1500
1450
1400
Psi
FSP
1510.5 = Pi
1466
10
1
Horner time
m = 1510.5 - 1466
= 44.5 psi/cycle.

Figure B 2A

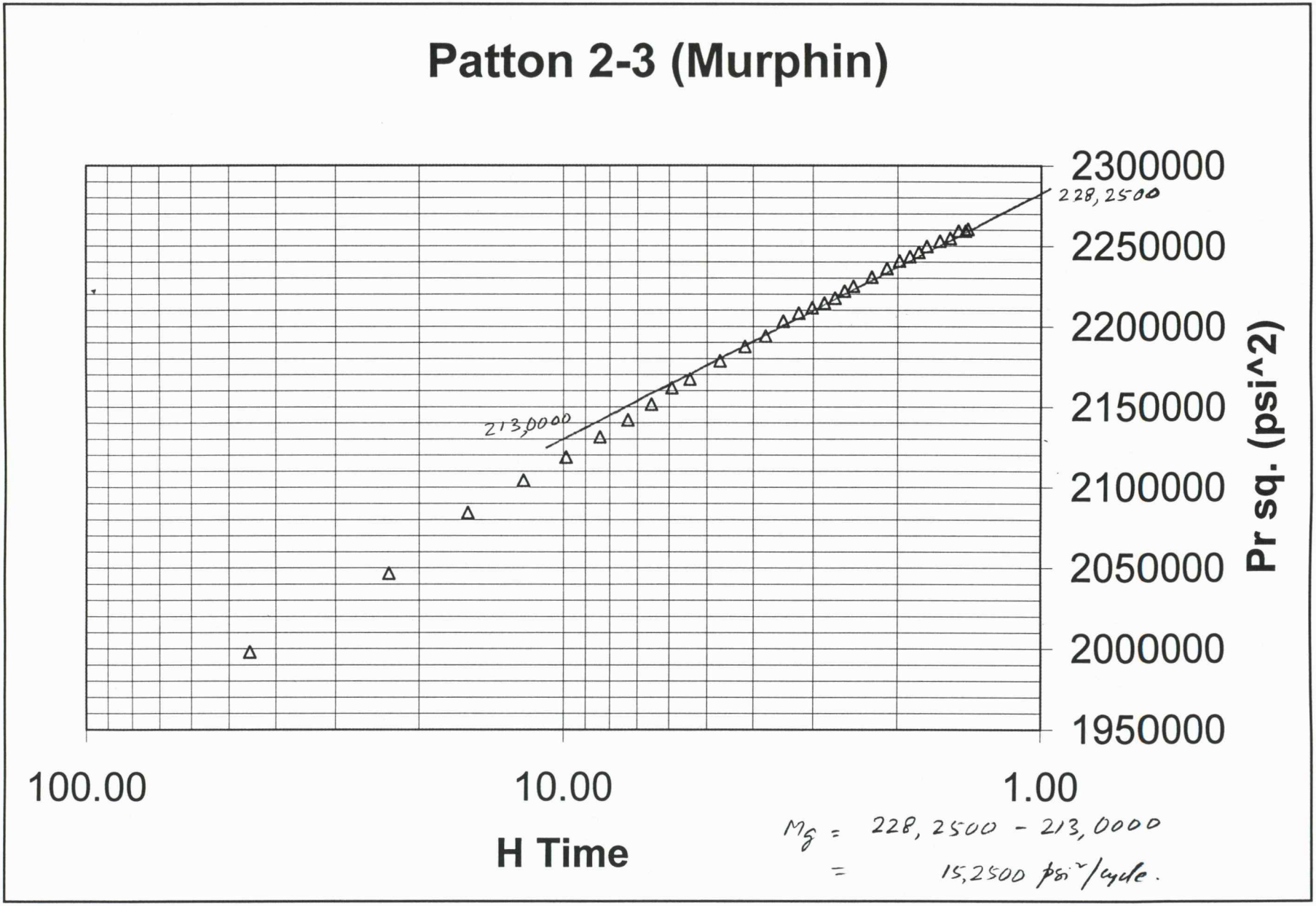
Patton 2-3 (Murphin)
2300000
2250000
2200000
2150000
2100000
2050000
2000000
1950000
Pr sq. (psi^2)
228,2500
213,0000
100.00
10.00
1.00
H Time
Mg = 228,2500 - 213,0000
= 15,2500 psi^2/cycle.

Figure B 2B

Table B3

	entered data
	read from correlations
	read from Horner plot
	calculation

Well: **Tedford 4-10 (15-025-20720)**

	from, ft	to, ft	thickness, ft
DST range	5294	5330	36
Pay SD#1	5298	5299	1
Pay SD#2	5305	5312	7
Pay SD#3			
Morrow pay			8

Reservoir gas properties:

Sp gr. =	0.73		gas specific gravity (avg from 3 samples)
Tpc =	386	R	pseudocritical temp
Ppc =	660	psia	pseudocritical pressure

DST analysis - Gas using SPE Monograph method:

Pi =	1518	psi	
m =	33	psi/cycle	
Qg =	22.9	Mcfd	
Pwf =	711	psi	(related to Qg - end of second flow)
P I hr =			

Transmissibility:

Kh/mu = 162.6*Qg*Bg/m

Bg = Psc*Tr*1000*Z/(p*Tsc*5.614) gas formation volume factor

Psc =	14.65	psi	pr at standard conditions
Tr =	574	R	Res temp = 114 F
Tsc =	520	R	Std temp
p = (Pi+Pw	1114.5	psi	avg of static and flowing pressure
Tpr =	1.49		pseudo reduced temp
Ppr =	1.71		pseudo reduced pressure
Z =	0.84		compressibility factor at p and Tr
Bg =	2.17	RB\Mcf	
Kh/mu =	244.9712	md-ft\cp	

Permeability:

h =	8	ft	pay
Mol wt of a	29	lb/lb mole	
Mol wt of g	21.17	lb/lb mole	
mu @ 1 at	0.0111	cp	(@ temp 114 F)
Vis ratio =	1.25	cp	at corresponding Tpr and Ppr
gas vis (mu	0.0139	cp	
K =	0.4	md	

DST analysis - Gas using High pressure gas method:

Pi =	1518	psi	
m =	33	psi/cycle	
Qg =	22.9	Mcfd	
Pwf =	711	psi	(related to Qg - end of second flow)
P I hr =			

Transmissibility:

Kh/mu = 818.5*Qg*Tr*Z/(P1avg*m)

HT - Horner time

P (@ HT =	1518		
P (@ HT =	1485		
P1avg =	1501.5	psi	avg pr of Horner straight line
Kh/mu =	182.3921	md-ft/cp	
K =	0.3	md	

DST analysis - Gas using Low pressure gas method:

Mg =	85000	psi^2/cycle
Qg =	22.9	Mcfd

Transmissibility:

Kh/mu = 1637*Qg*Tr*Z/Mg

Kh/mu =	212.6456	md-ft/cp
K =	0.4	md

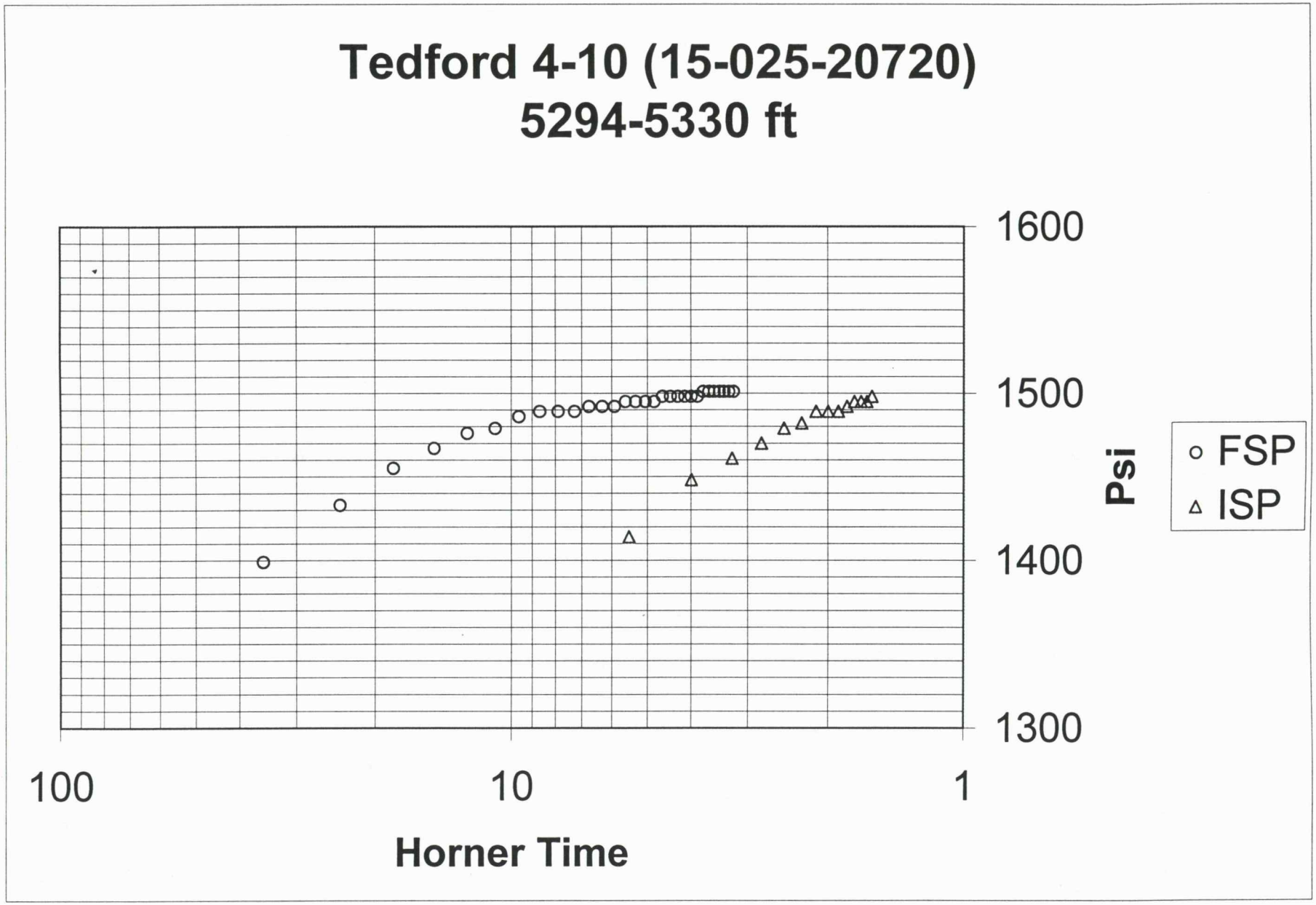
Tedford 4-10 (15-025-20720)
5294-5330 ft
1600
1500
1400
1300
Psi
FSP
ISP
100
10
1
Horner Time

Figure B 3A

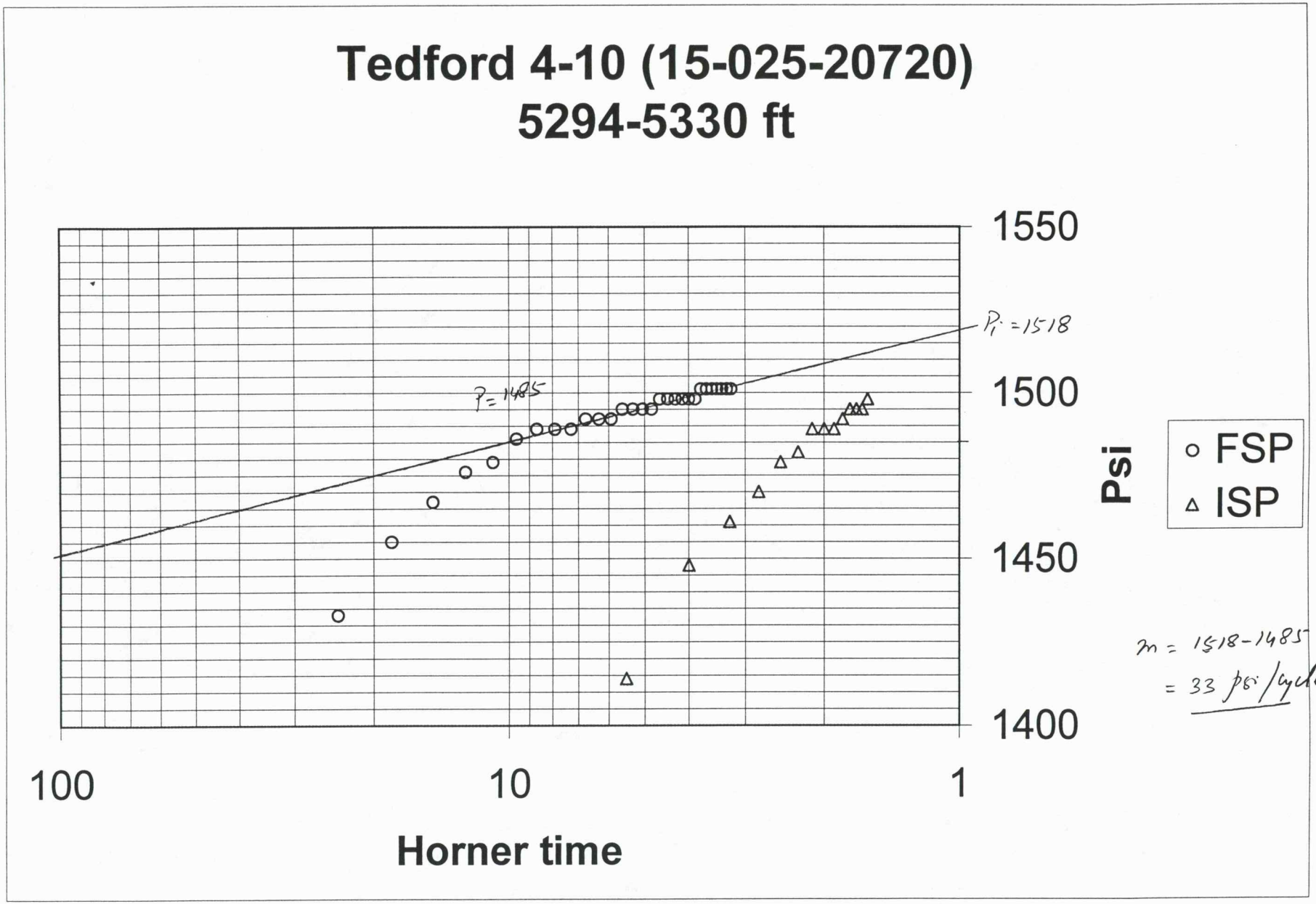
Tedford 4-10 (15-025-20720)
5294-5330 ft
1550
1500
1450
1400
Psi
FSP
ISP
P_i = 1518
P = 1485
m = 1518-1485
= 33 psi/cycle
100
10
1
Horner time

Figure B 3B

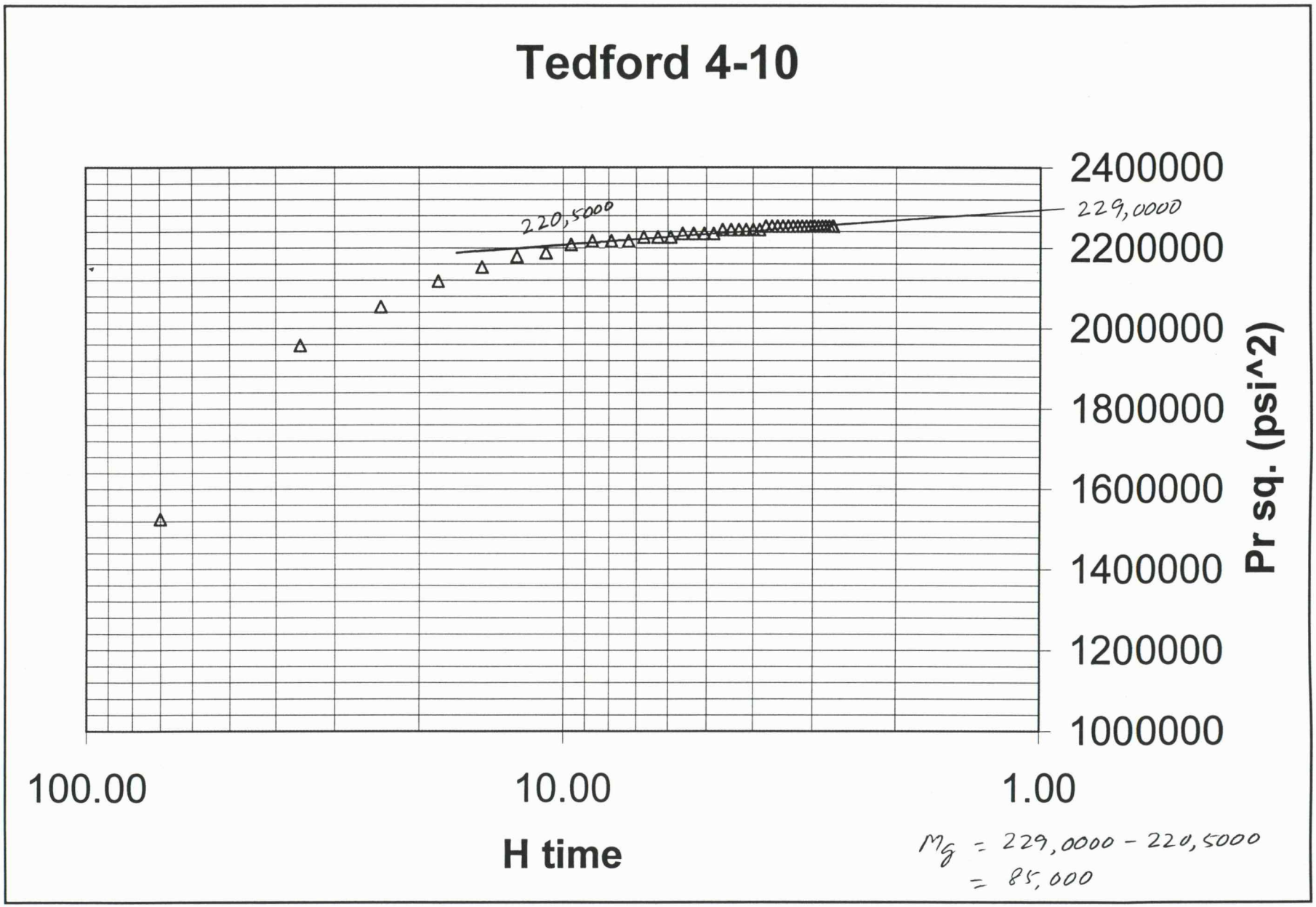
Tedford 4-10
2400000
2200000
2000000
1800000
1600000
1400000
1200000
1000000
Pr sq. (psi^2)
220,5000
229,0000
100.00
10.00
1.00
H time
M_g = 229,0000 - 220,5000
= 85,000

Figure B 3C

Table B 4

Well:	Tedford 1-10 (15-025-20621)		
	from, ft	to, ft	thickness, ft
DST range	5272	5302	30
Pay SD#1	5278	5283	5
Pay SD#2			
Pay SD#3			
Morrow pay			5

entered data
read from correlations
read from Horner plot
calculation

Reservoir gas properties:

Sp gr. =	0.73		gas specific gravity (avg from 3 samples)
Tpc =	386	R	pseudocritical temp
Ppc =	660	psia	pseudocritical pressure

DST analysis - Gas using SPE Monograph method:

Pi =	1637	psi	
m =	18	psi/cycle	
Qg =	1458	Mcfd	
Pwf =	257	psi	(related to Qg - end of second flow)
P I hr =			

Transmissibility:

Kh/mu = 162.6*Qg*Bg/m

Bg = Psc*Tr*1000*Z/(p*Tsc*5.614) gas formation volume factor

Psc =	14.65	psi	pr at standard conditions
Tr =	590	R	Res temp = 130 F
Tsc =	520	R	Std temp in R
p = (Pi+Pw	947	psi	avg of static and flowing pressure
Tpr =	1.53		pseudo reduced temp
Ppr =	1.46		pseudo reduced pressure
Z =	0.875		compressibility factor at p and Tr
Bg =	2.74	RB\Mcf	
Kh/mu =	36031.1	md-ft\cp	

Permeability:

h =	5	ft	pay
Mol wt of a	29	lb/lb mole	
Mol wt of g	21.17	lb/lb mole	
mu @ 1 at	0.0111	cp	(@ 130F)
Vis ratio =	1.2	cp	at corresponding Tpr and Ppr
gas vis (mı	0.0133	cp	
K =	96.0	md	

DST analysis - Gas using High pressure gas method:

Pi =	1637	psi	
m =	18	psi/cycle	
Qg =	1458	Mcfd	
Pwf =	257	psi	(related to Qg - end of second flow)
P I hr =			

Transmissibility:

Kh/mu = 818.5*Qg*Tr*Z/(P1avg*m)

HT - Horner time

P (@ HT =	1637		
P (@ HT =	1619		
P1avg =	1628	psi	avg pr of Horner straight line
Kh/mu =	21023.71	md-ft/cp	
K =	56.0	md	

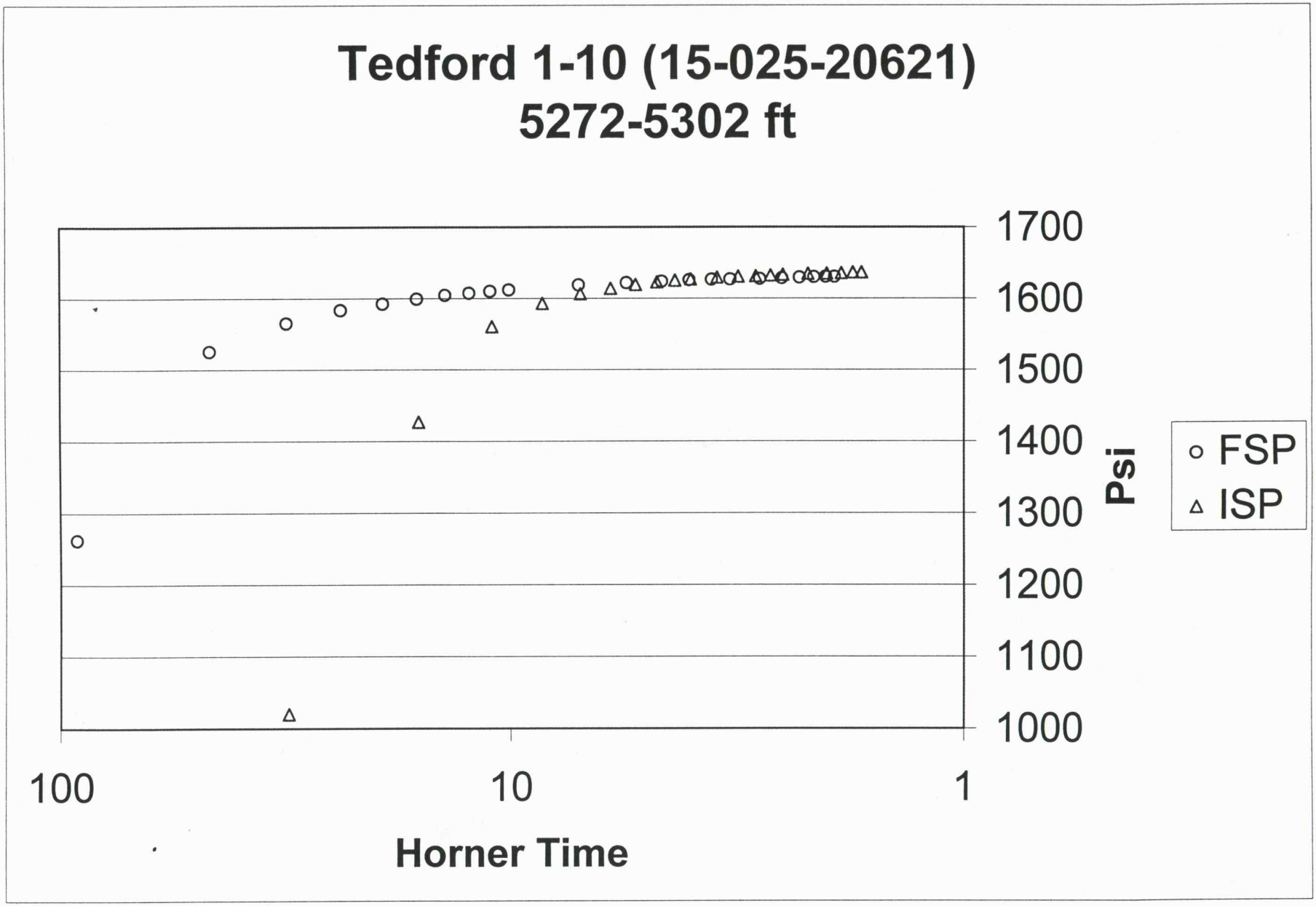
Tedford 1-10 (15-025-20621)
5272-5302 ft
1700
1600
1500
1400
1300
1200
1100
1000
Psi
FSP
ISP
100
10
1
Horner Time

Figure B 4A

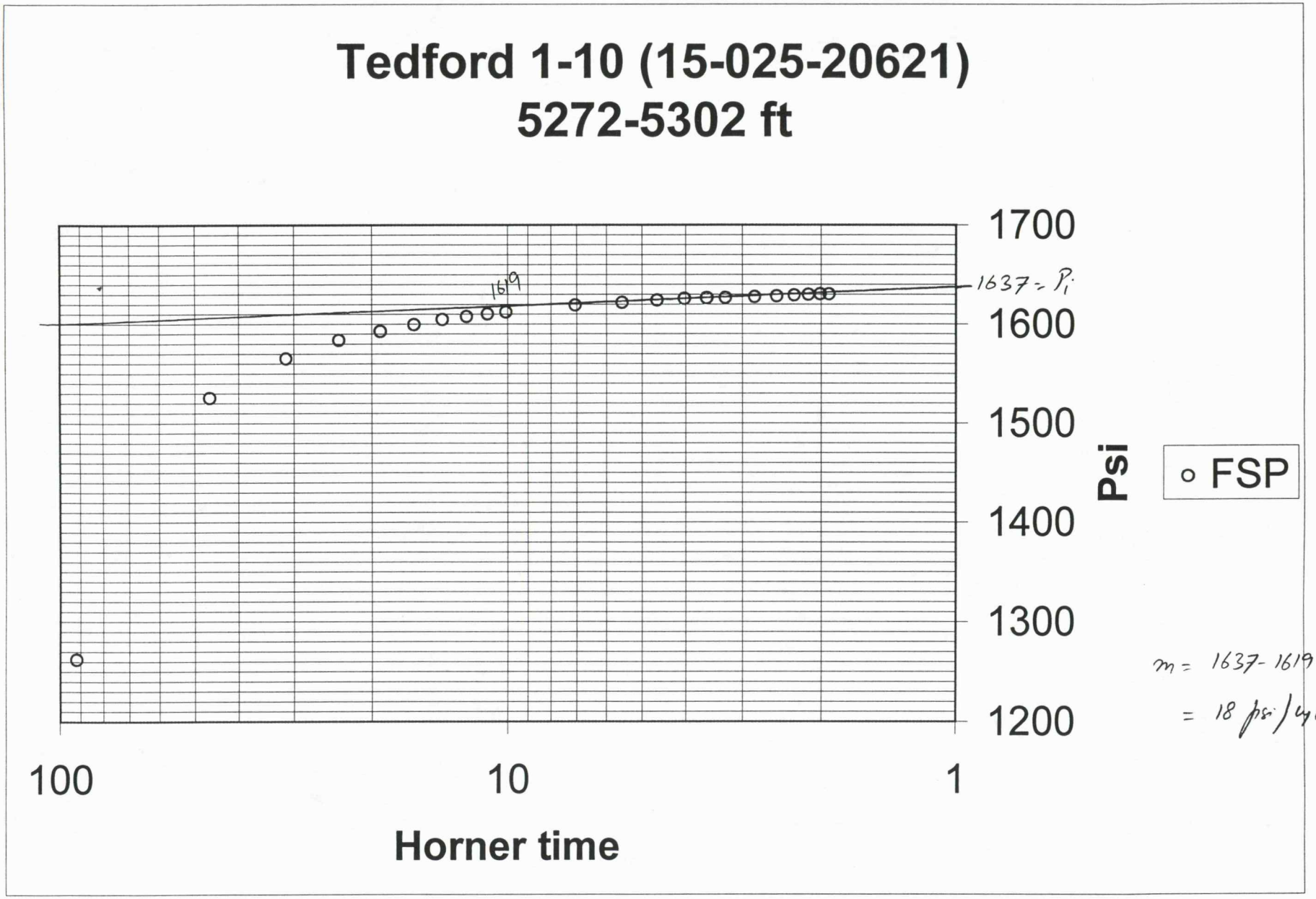
Tedford 1-10 (15-025-20621)
5272-5302 ft
1700
1600
1500
1400
1300
1200
Psi
1619
1637 = Pi
FSP
m = 1637 - 1619
= 18 psi/cycle.
100
10
1
Horner time

Figure B 4B

Table B 5a

As Gas well

Well: **Goeller 1-4 (15-025-20858)**

	from, ft	to, ft	thickness, ft
DST range	5300	5335	35
Pay SD#1			
Pay SD#2	5316	5322	6
Pay SD#3			
Morrow pay			6

entered data
read from correlations
read from Horner plot
calculation

Reservoir gas properties:

Sp gr. =	0.73		gas specific gravity (avg from 3 samples)
Tpc =	386	R	pseudocritical temp
Ppc =	660	psia	pseudocritical pressure

DST analysis - Gas using SPE Monograph method:

Pi =	800	psi	
m =	31.5	psi/cycle	
Qg =	163	Mcfd	
Pwf =	289	psi	(related to Qg - end of second flow)
P I hr =			

Transmissibility:

Kh/mu = 162.6*Qg*Bg/m

Bg = Psc*Tr*1000*Z/(p*Tsc*5.614) gas formation volume factor

Psc =	14.65	psi	pr at standard conditions
Tr =	576	R	Res temp = 116 F
Tsc =	520	R	Std temp in R
p = (Pi+Pw	544.5	psi	avg of static and flowing pressure
Tpr =	1.49		pseudo reduced temp
Ppr =	0.85		pseudo reduced pressure
Z =	0.92		compressibility factor at p and Tr
Bg =	4.88	RB\Mcf	

Kh/mu = 4109.338 md-ft\cp

Permeability:

h = 6 ft pay

Mol wt of a	29	lb/lb mole	
Mol wt of g	21.17	lb/lb mole	
mu @ 1 atı	0.0111	cp	(@ res temp)
Vis ratio =	1	cp	at Tpr and appox outside range
gas vis (mu	0.0111	cp	

K = 7.6 md

DST analysis - Gas using Low pressure gas method:

Mg =	50000	psi^2/cycle
Qg =	163	Mcfd

Transmissibility:

Kh/mu = 1637*Qg*Tr*Z/Mg

Kh/mu = 2827.98167 md-ft/cp

K = 5.2 md

Table B 5b

As oil well

Well: **Goeller 1-4 (15-025-20858)**

	from, ft	to, ft	thickness, ft
DST range	5300	5335	35
Pay SD#1			
Pay SD#2	5316	5322	6
Pay SD#3			
Morrow pay			6

entered data
read from correlations
read from Horner plot
calculation

Reservoir gas properties:

Sp gr., Rog	0.73		gas specific gravity (avg from 3 samples)
Tpc =	386	R	pseudocritical temp
Ppc =	660	psia	pseudocritical pressure

DST analysis - Oil:

Pi =	800	psi	
m =	31.5	psi/cycle	
Qo =	62.16	bbl/d	
Qg =	163	Mcf/d	(doubtful if the well produced 16300 Mcf/d)
Pwf =	289	psi	(related to Qo - end of second flow)
P I hr =			

Transmissibility:

Kh/Muo = 162.6*Qo*Bo/m

GOR, Rs =	2622.3	scf/bbl
API stock t	46	
Sp gr oil, R	0.80	
Res temp =	116	F

Bo = 0.972+0.000147*(Rs*(Rog/Roo)^0.5+1.: GOR outside range of correlation chart

Bo @ bubb 2.52 bbl/STB oil formation volume factor

Kh/Muo = 809.3725 md-ft\cp

Permeability:

h = 6 ft pay

Muo, 1 atm	1.3	cp		
Muo, gas s	0.2	cp	approx.	GOR outside range of correlation chart

K = 27.0 md

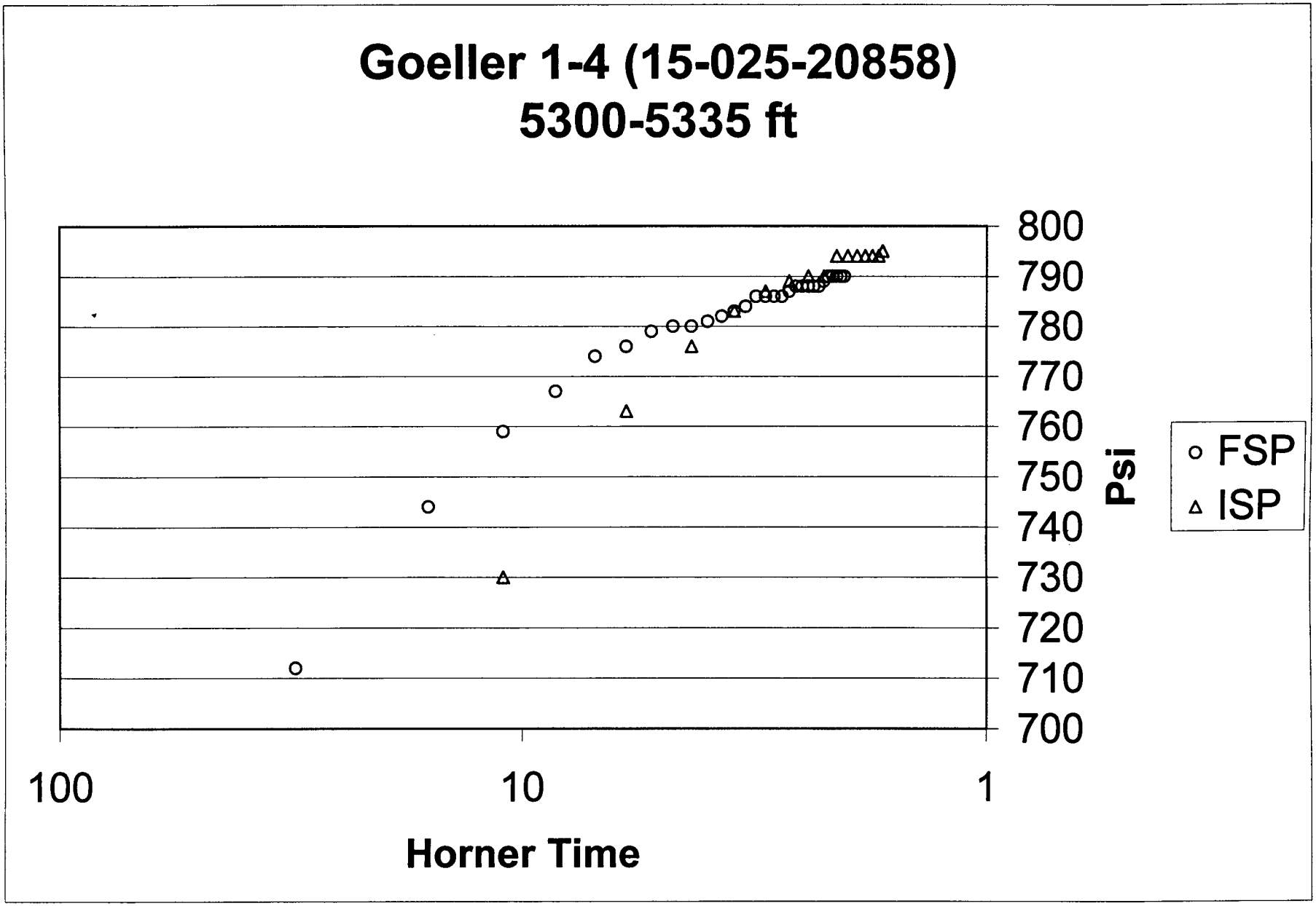
Goeller 1-4 (15-025-20858)
5300-5335 ft
800
790
780
770
760
750
740
730
720
710
700
Psi
FSP
ISP
100
10
1
Horner Time

Figure B 5A

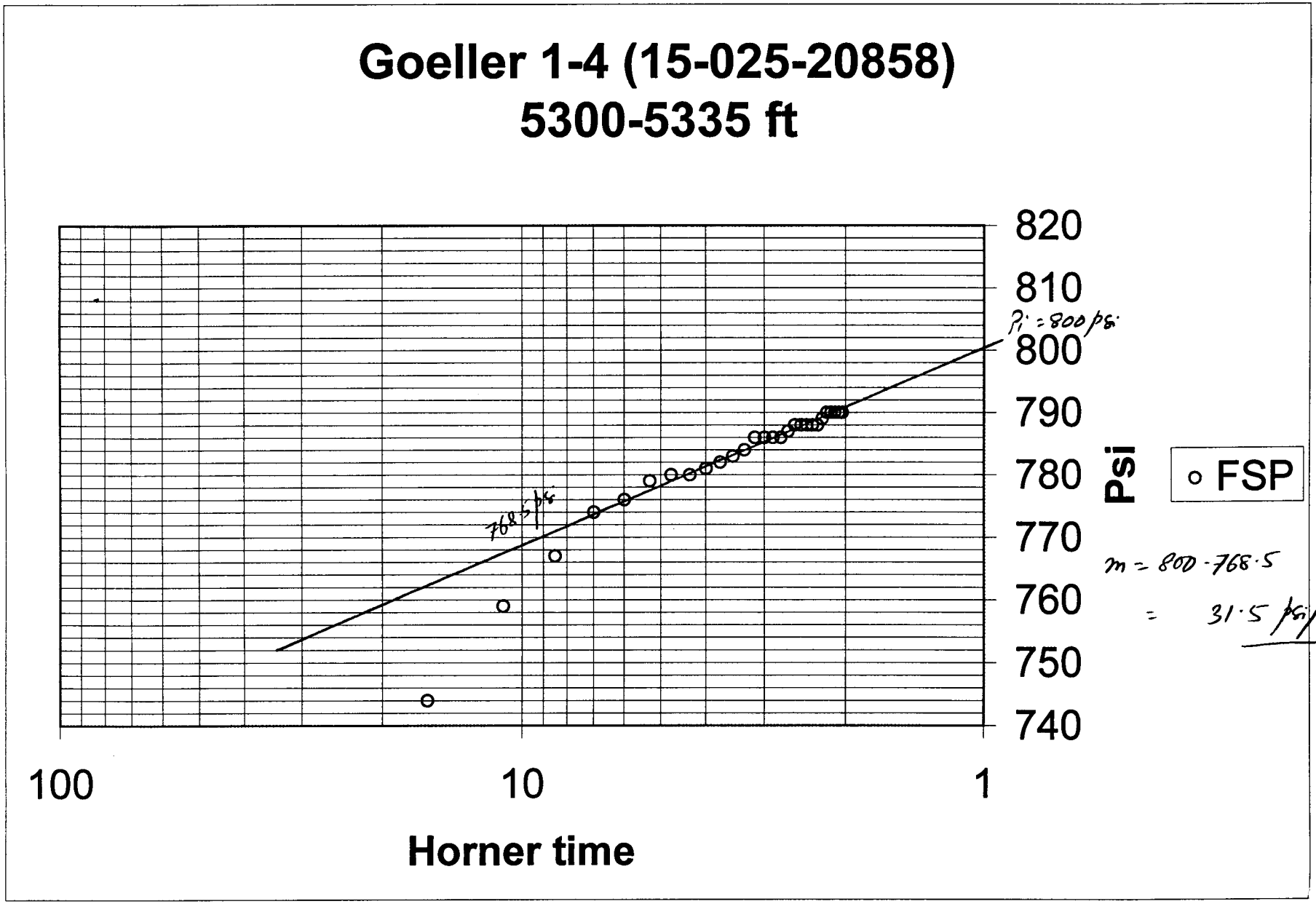
Goeller 1-4 (15-025-20858)
5300-5335 ft
820
810
800
790
780
770
760
750
740
Psi
FSP
Pi = 800 psi
768.5 psi
m = 800 - 768.5
= 31.5 psi/cycle
100
10
1
Horner time

Figure B 5B

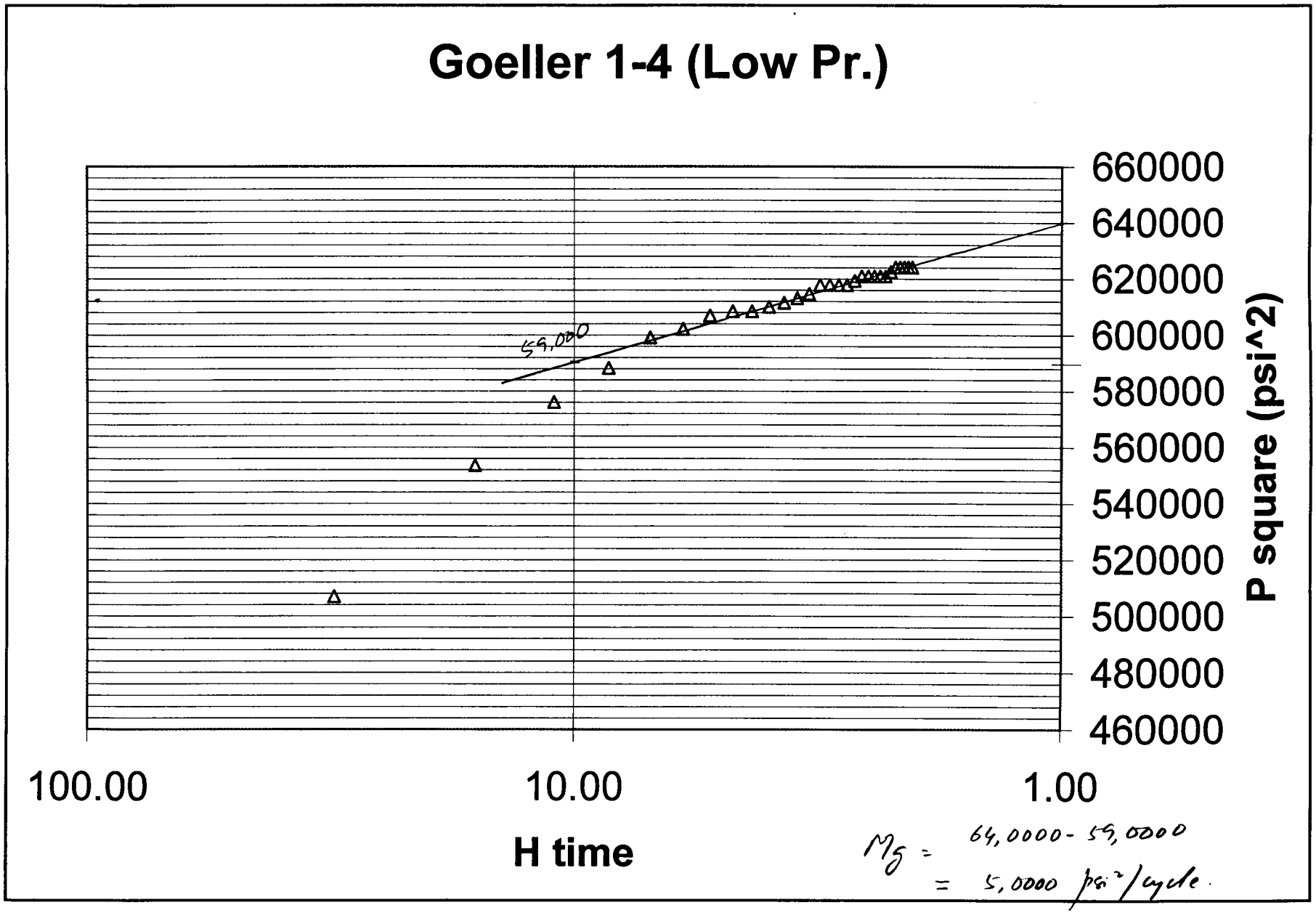
Goeller 1-4 (Low Pr.)
660000
640000
620000
600000
580000
560000
540000
520000
500000
480000
460000
P square (psi^2)
59,000
100.00
10.00
1.00
H time
Mg = 64,0000 - 59,0000
= 5,0000 psi²/cycle.

Figure B 5C

Table B 6

Well: **Norton 1-4 (15-025-20890)**

	from, ft	to, ft	thickness, ft
DST range	5292	5316	24
Pay SD#1			
Pay SD#2	5289	5294	5
Pay SD#3			
Morrow pay			5

entered data
read from correlations
read from Horner plot
calculation

Reservoir gas properties:

Sp gr. =	0.73		gas specific gravity (avg from 3 samples)
Tpc =	386	R	pseudocritical temp
Ppc =	660	psia	pseudocritical pressure

DST analysis - Gas using SPE Monograph method:

Pi =	886	psi	
m =	104	psi/cycle	
Qg =	227	Mcfd	
Pwf =	137	psi	(related to Qg - end of second flow)
P I hr =			

Transmissibility:

Kh/mu = 162.6*Qg*Bg/m

Bg = Psc*Tr*1000*Z/(p*Tsc*5.614) gas formation volume factor

Psc =	14.65	psi	pr at standard conditions
Tr =	578	R	Res temp = 118 F
Tsc =	520	R	Std temp in R
p = (Pi+Pw	511.5	psi	avg of static and flowing pressure
Tpr =	1.50		pseudo reduced temp
Ppr =	0.80		pseudo reduced pressure
Z =	0.92		compressibility factor at p and Tr
Bg =	5.22	RB\Mcf	

Kh/mu = 1851.591 md-ft\cp

Permeability:

h = 5 ft pay

Mol wt of a	29	lb/lb mole	
Mol wt of g	21.17	lb/lb mole	
mu @ 1 at	0.0111	cp	(@ res temp)
Vis ratio =	1	cp	atTpr and I approx outside range
gas vis (mu	0.0111	cp	

K = 4.1 md

DST analysis - Gas using Low pressure gas method:

Mg =	166000	psi^2/cycle
Qg =	227	Mcfd

Transmissibility:

Kh/mu = 1637*Qg*Tr*Z/Mg

Kh/mu = 1190.37 md-ft/cp

K = 2.6 md

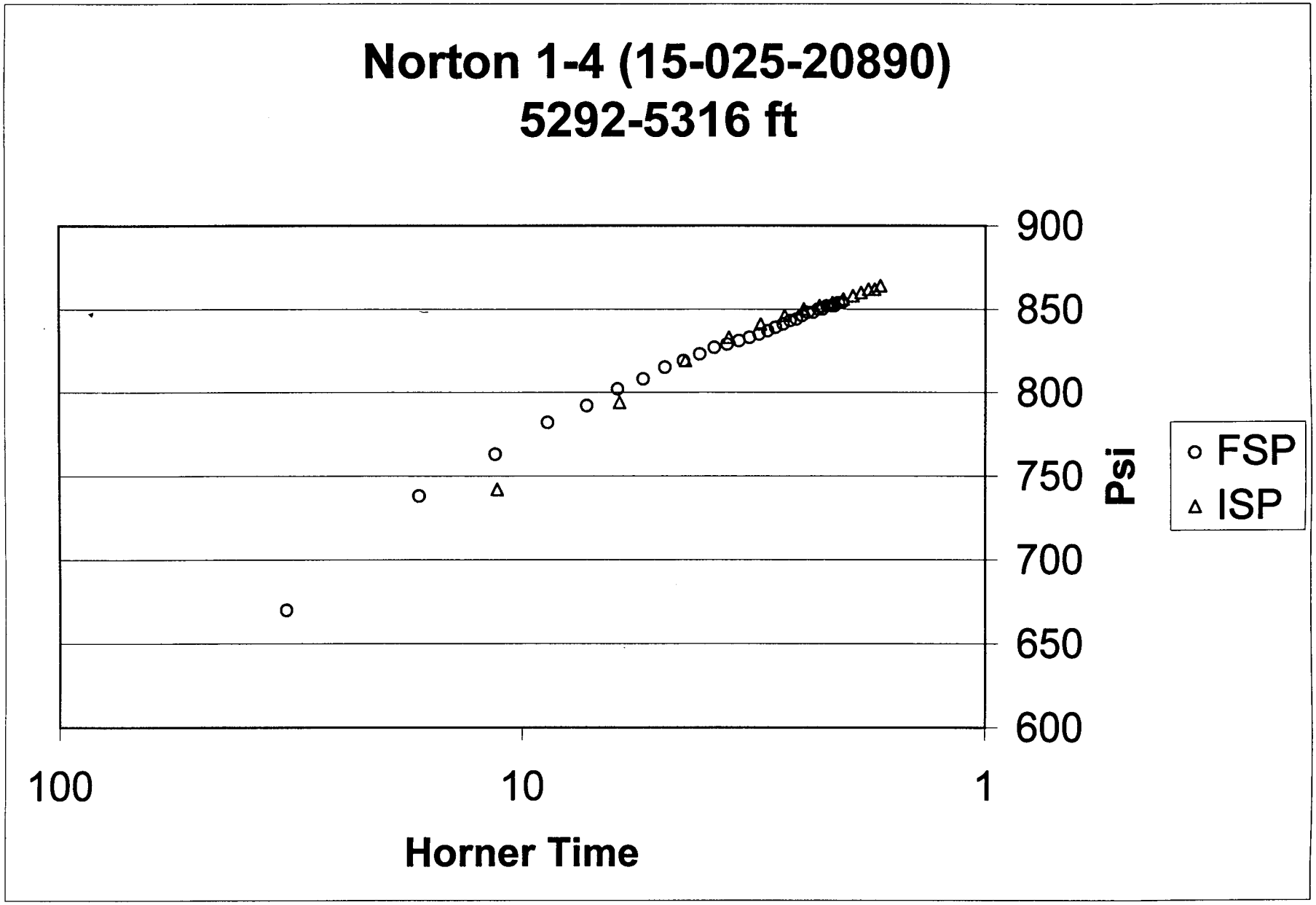
Norton 1-4 (15-025-20890)
5292-5316 ft
900
850
800
750
700
650
600
Psi
FSP
ISP
100
10
1
Horner Time

Figure B 6A

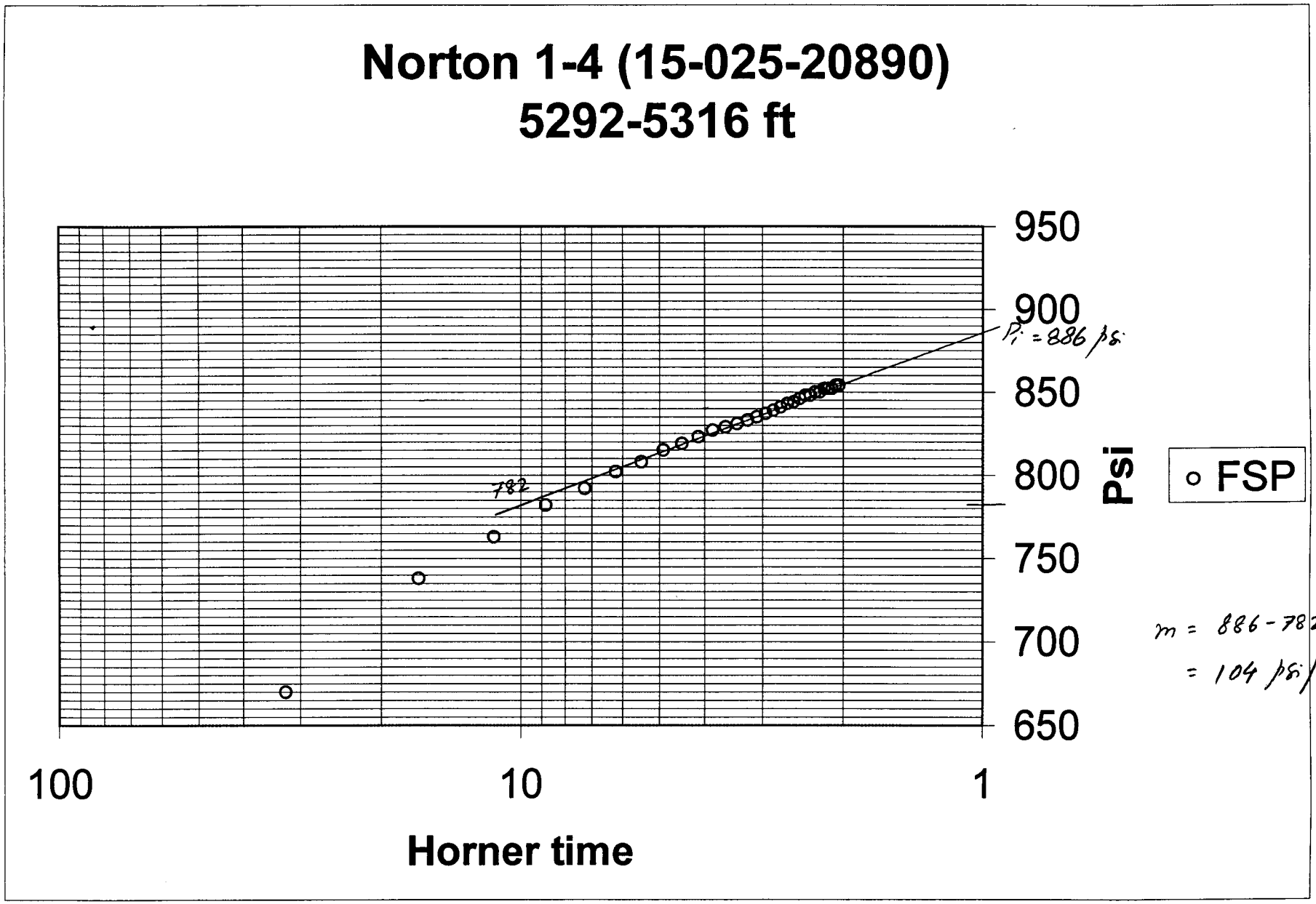
Norton 1-4 (15-025-20890)
5292-5316 ft
950
900
850
800
750
700
650
Psi
Pi = 886 psi
782
FSP
m = 886 - 782
= 104 psi/cycle.
100
10
1
Horner time

Figure B 6B

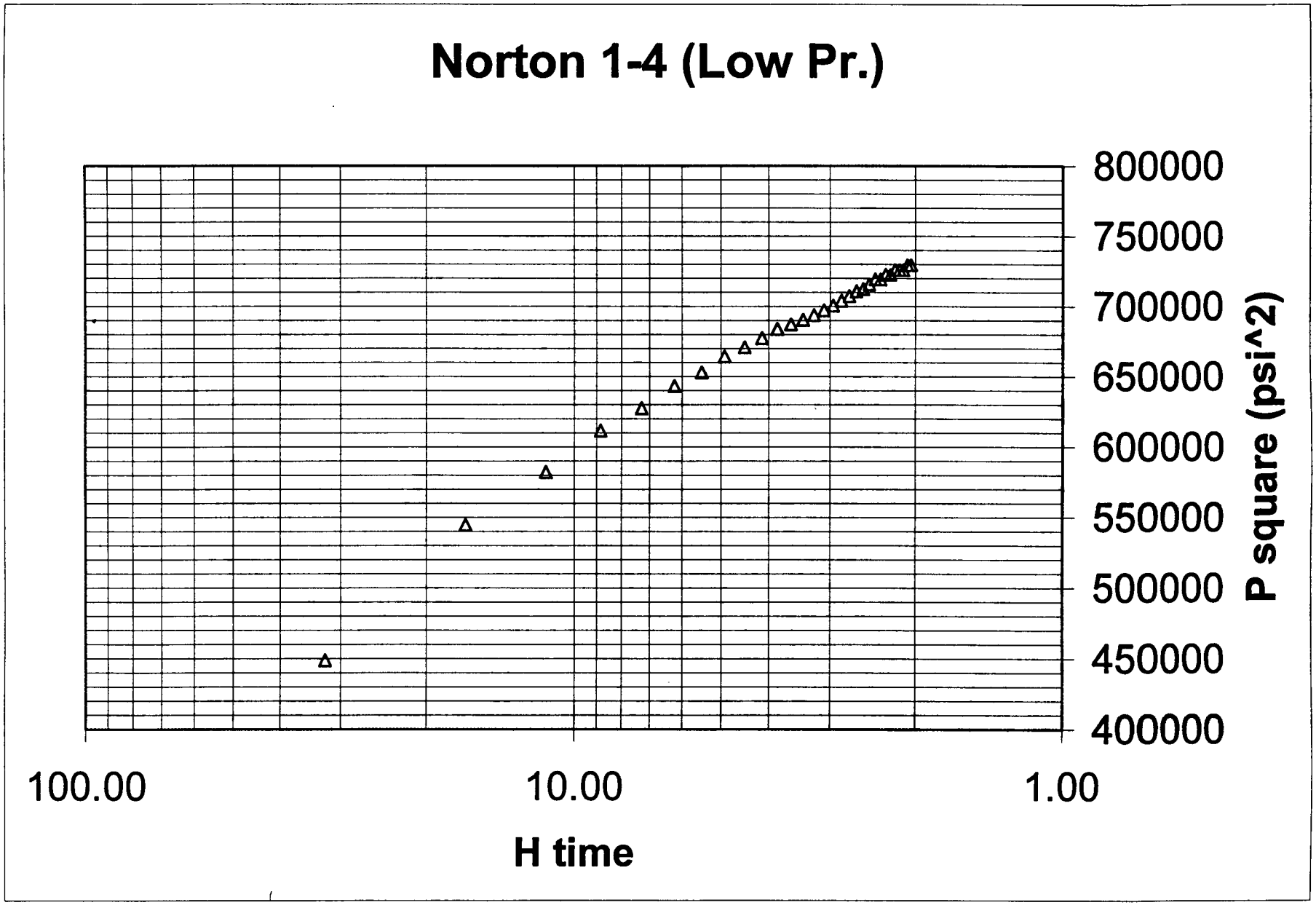
Norton 1-4 (Low Pr.)
800000
750000
700000
650000
600000
550000
500000
450000
400000
P square (psi^2)
100.00
10.00
1.00
H time

Figure B 6C

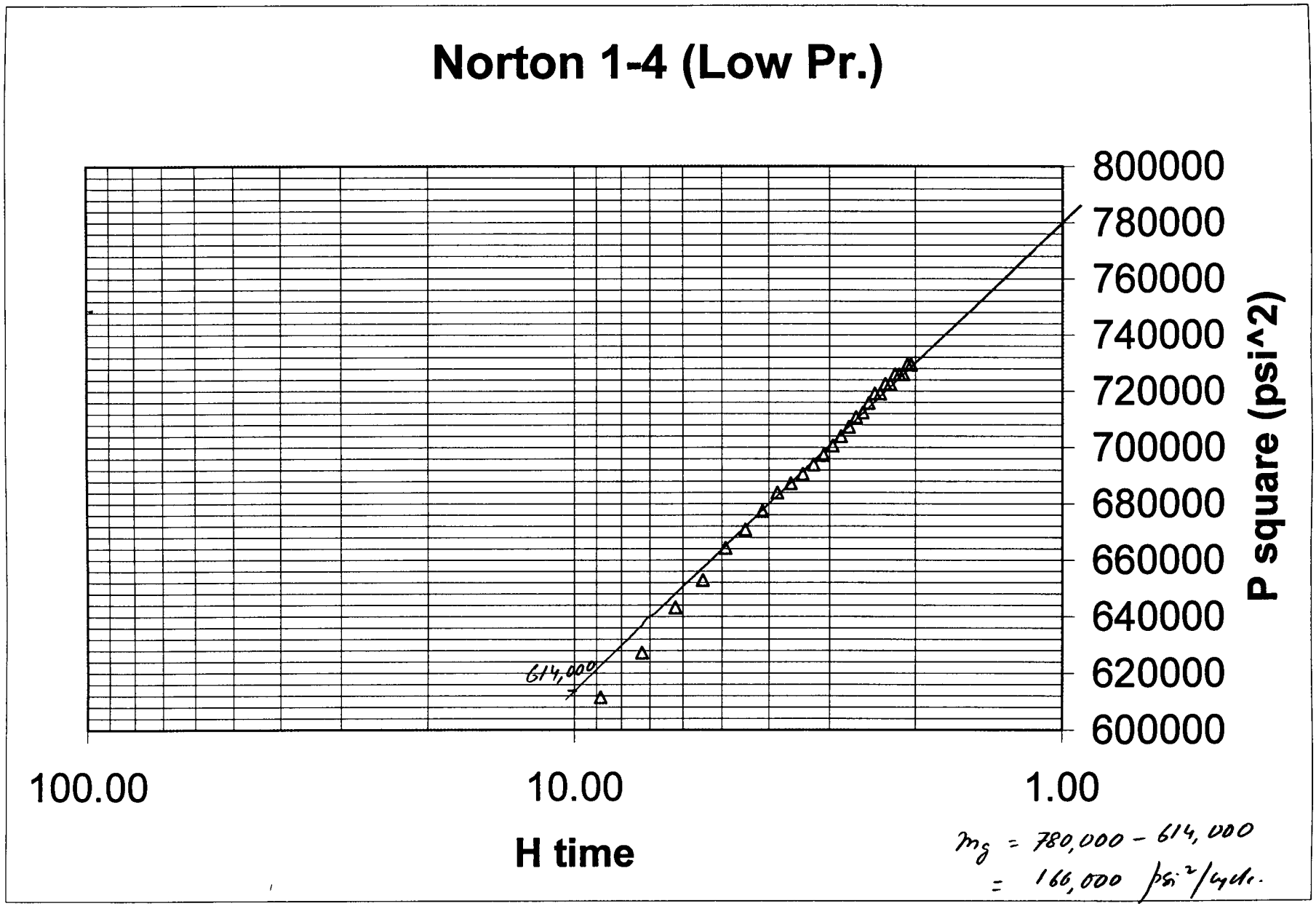
Norton 1-4 (Low Pr.)
800000
780000
760000
740000
720000
700000
680000
660000
640000
620000
600000
P square (psi^2)
614,000
100.00
10.00
1.00
H time
m_g = 780,000 − 614,000
= 166,000 psi²/cycle

Figure B 6D

Appendix - C

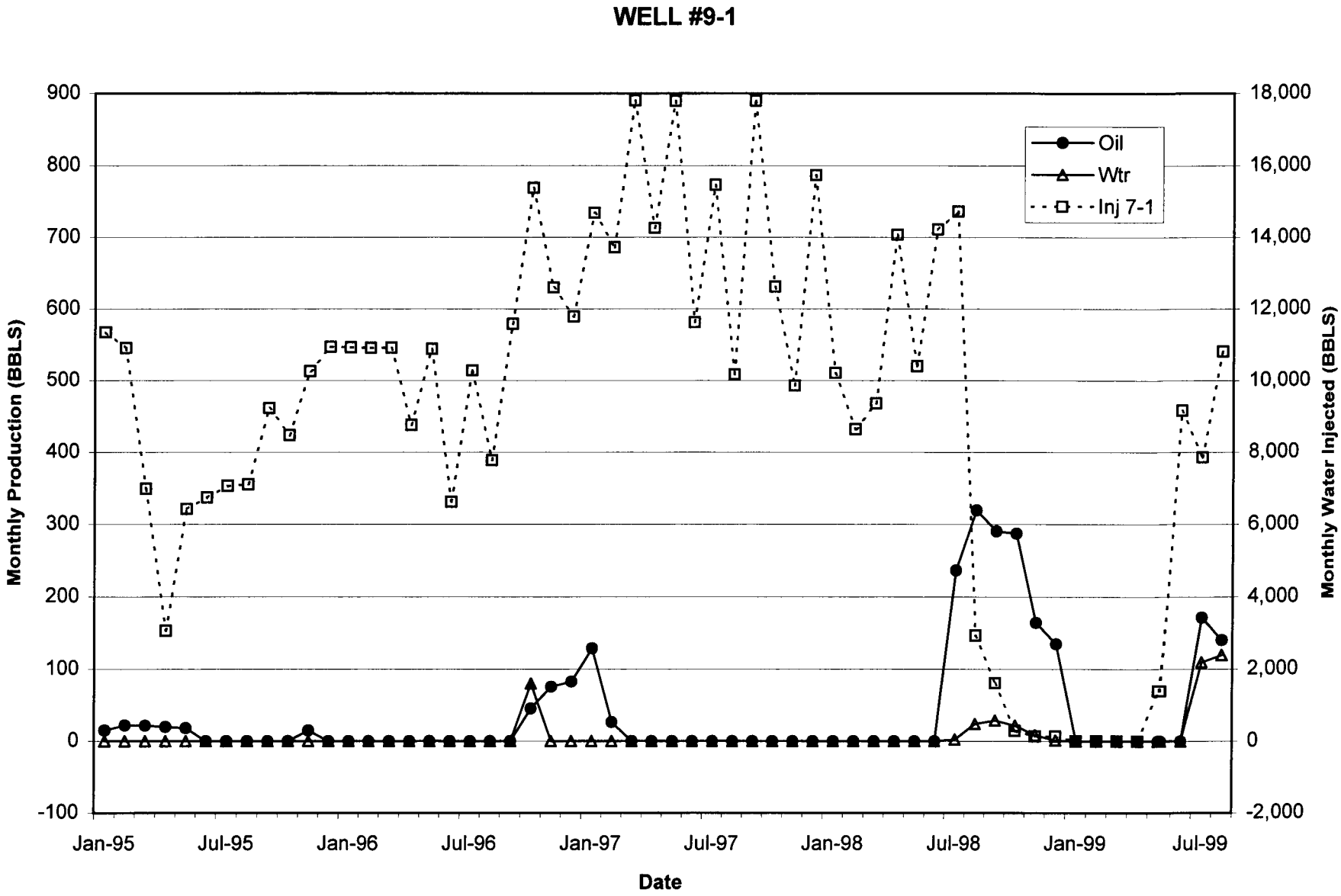
WELL #9-1
Monthly Production (BBLS)
Monthly Water Injected (BBLS)
Date
Oil
Wtr
Inj 7-1
900
800
700
600
500
400
300
200
100
0
-100
18,000
16,000
14,000
12,000
10,000
8,000
6,000
4,000
2,000
0
-2,000
Jan-95
Jul-95
Jan-96
Jul-96
Jan-97
Jul-97
Jan-98
Jul-98
Jan-99
Jul-99

Figure C1

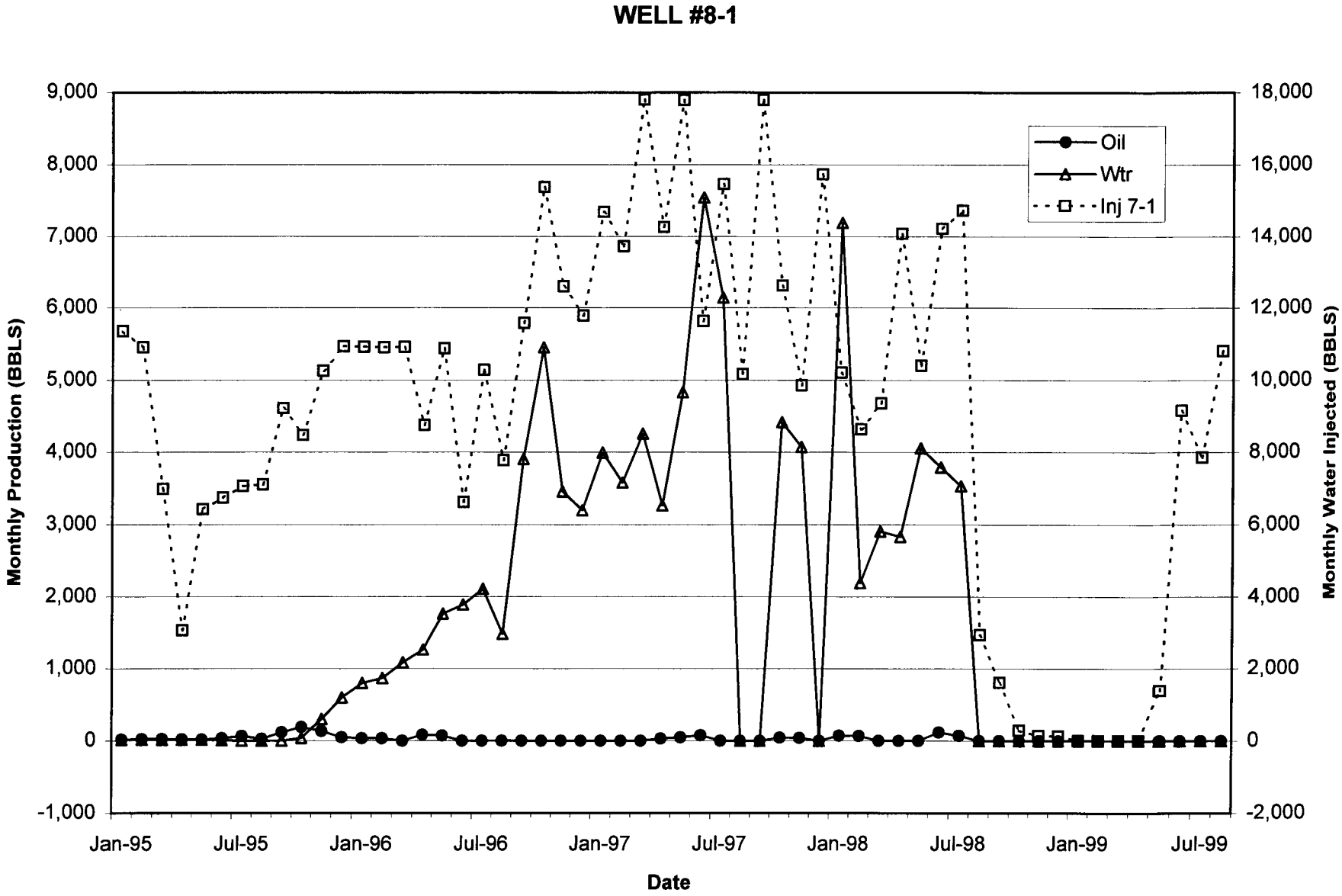
WELL #8-1
Monthly Production (BBLS)
Monthly Water Injected (BBLS)
Date
Oil
Wtr
Inj 7-1
9,000
8,000
7,000
6,000
5,000
4,000
3,000
2,000
1,000
0
-1,000
18,000
16,000
14,000
12,000
10,000
8,000
6,000
4,000
2,000
0
-2,000
Jan-95
Jul-95
Jan-96
Jul-96
Jan-97
Jul-97
Jan-98
Jul-98
Jan-99
Jul-99

Figure C2

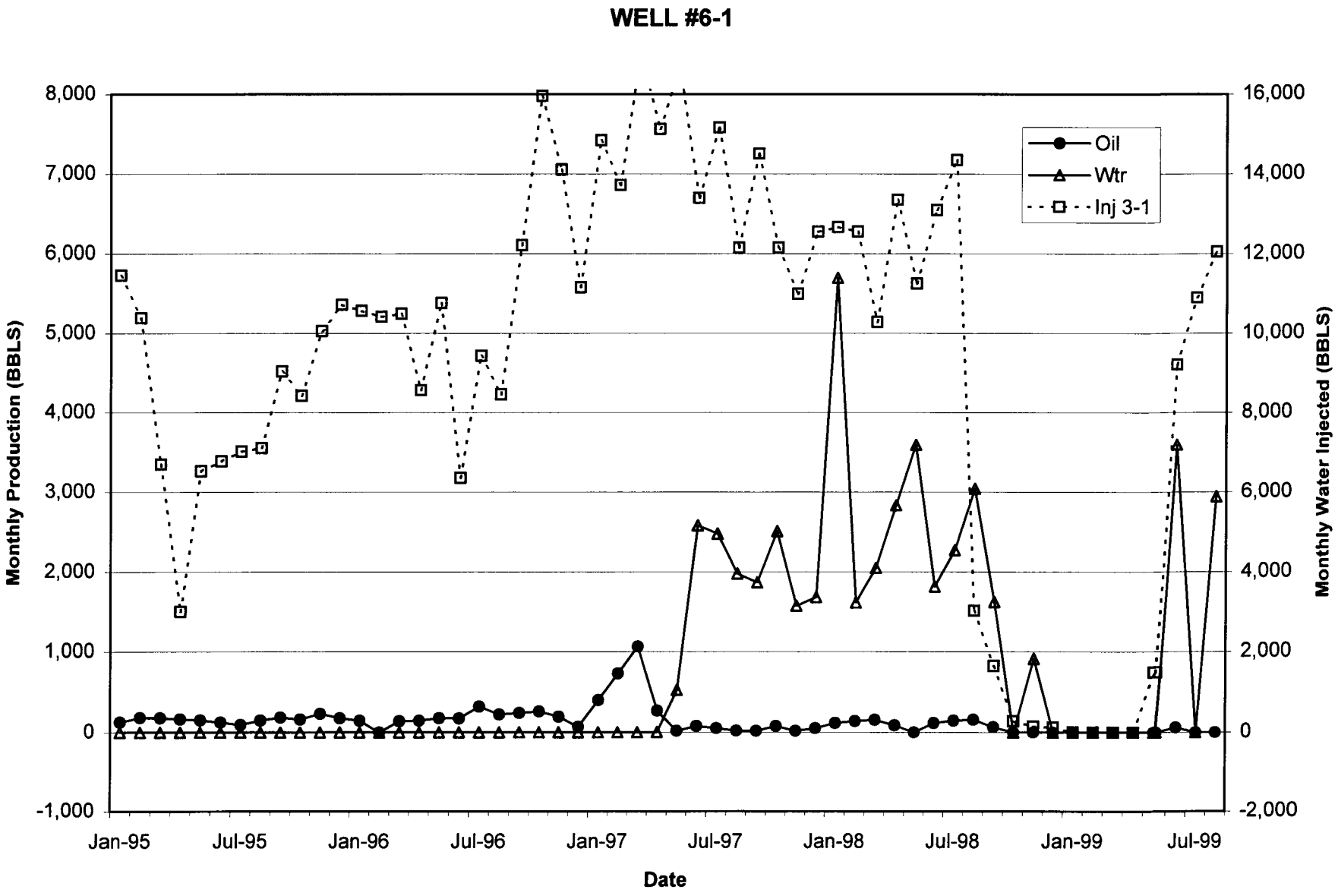
WELL #6-1
Oil
Wtr
Inj 3-1
Monthly Production (BBLS)
Monthly Water Injected (BBLS)
Date
8,000
7,000
6,000
5,000
4,000
3,000
2,000
1,000
0
-1,000
16,000
14,000
12,000
10,000
8,000
6,000
4,000
2,000
0
-2,000
Jan-95
Jul-95
Jan-96
Jul-96
Jan-97
Jul-97
Jan-98
Jul-98
Jan-99
Jul-99

Figure C3

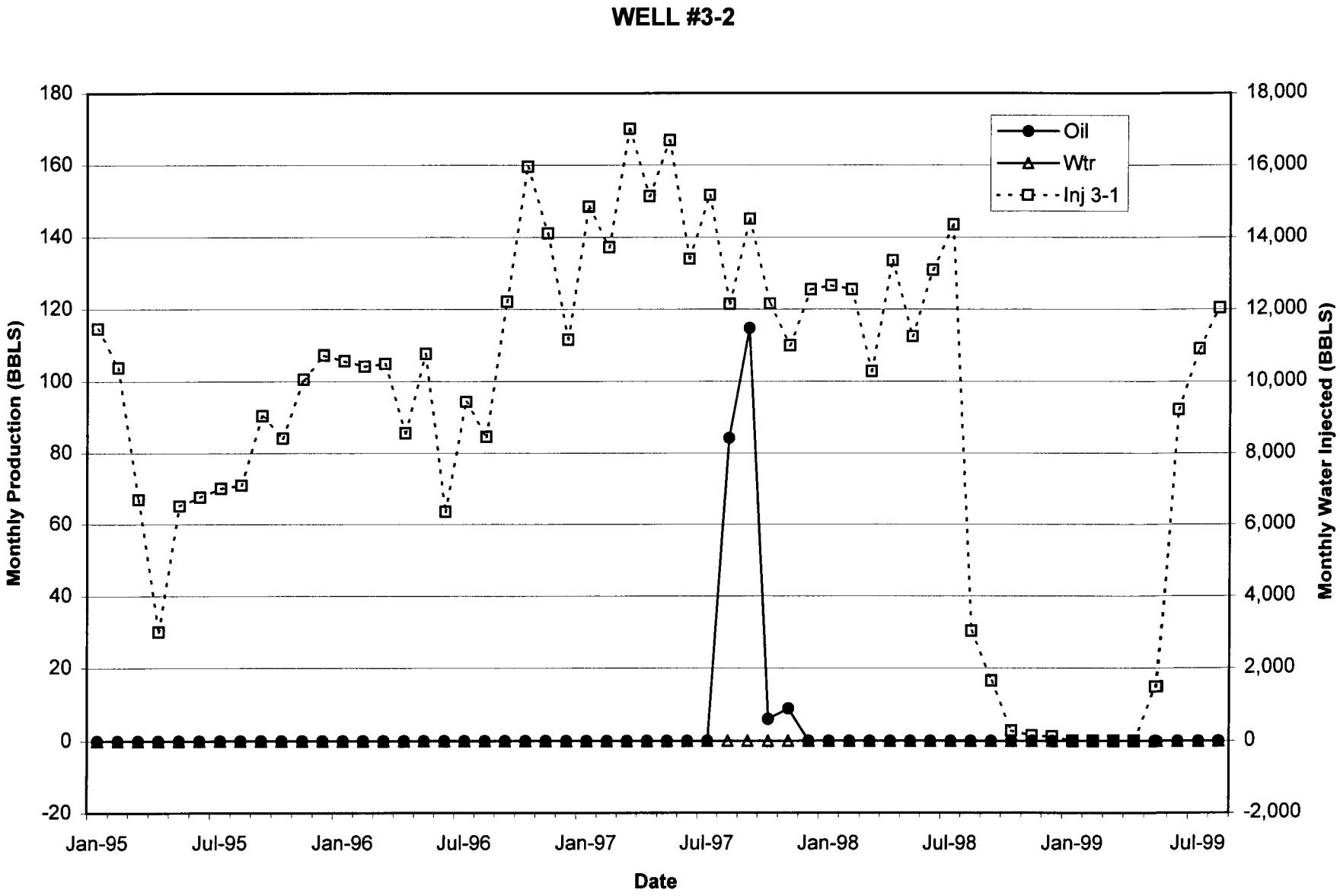
WELL #3-2
Monthly Production (BBLS)
Monthly Water Injected (BBLS)
Date
Oil
Wtr
Inj 3-1
180
160
140
120
100
80
60
40
20
0
-20
18,000
16,000
14,000
12,000
10,000
8,000
6,000
4,000
2,000
0
-2,000
Jan-95
Jul-95
Jan-96
Jul-96
Jan-97
Jul-97
Jan-98
Jul-98
Jan-99
Jul-99

Figure C4

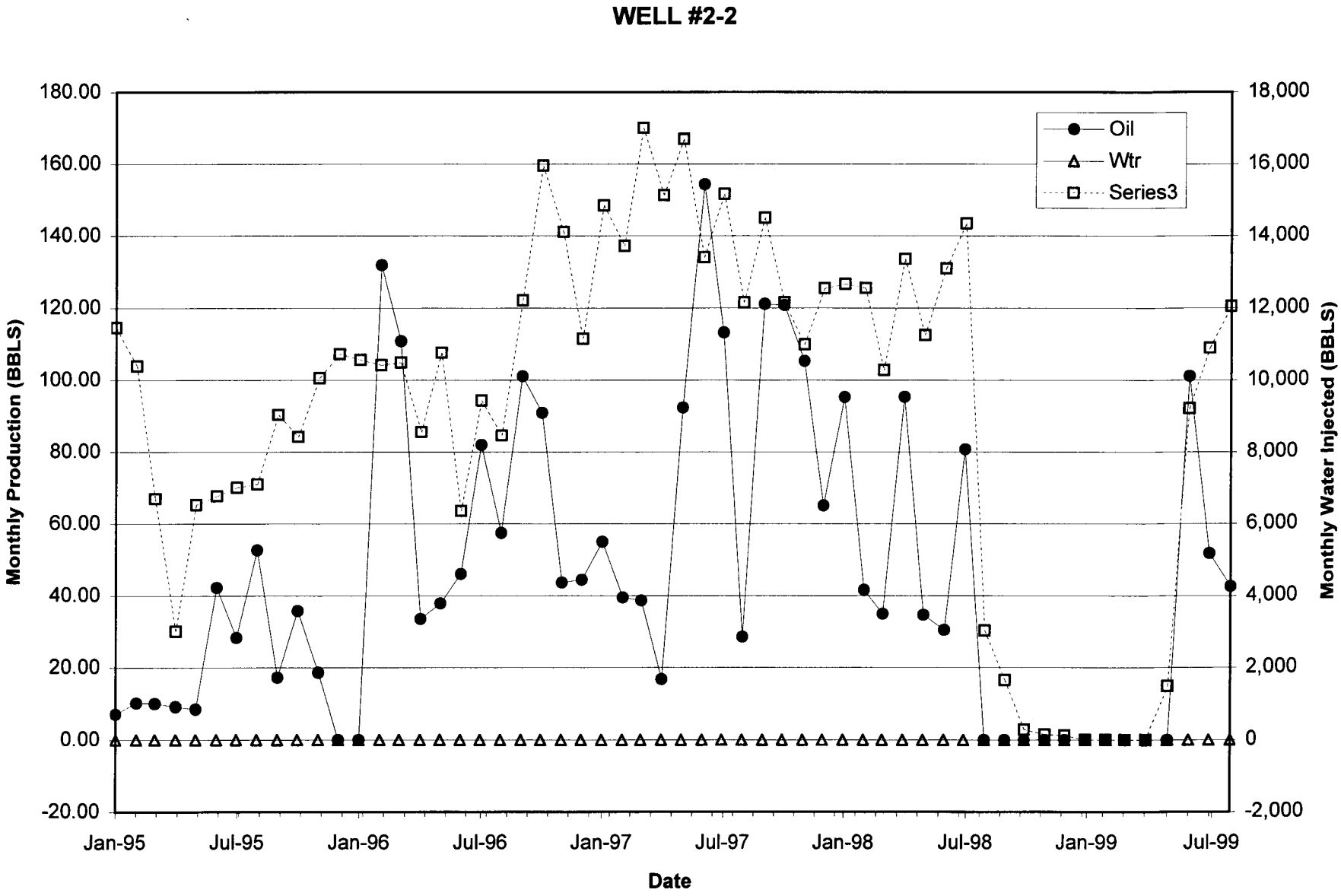
WELL #2-2
Monthly Production (BBLS)
Monthly Water Injected (BBLS)
Date
Oil
Wtr
Series3
180.00
160.00
140.00
120.00
100.00
80.00
60.00
40.00
20.00
0.00
-20.00
18,000
16,000
14,000
12,000
10,000
8,000
6,000
4,000
2,000
0
-2,000
Jan-95
Jul-95
Jan-96
Jul-96
Jan-97
Jul-97
Jan-98
Jul-98
Jan-99
Jul-99

Figure C5

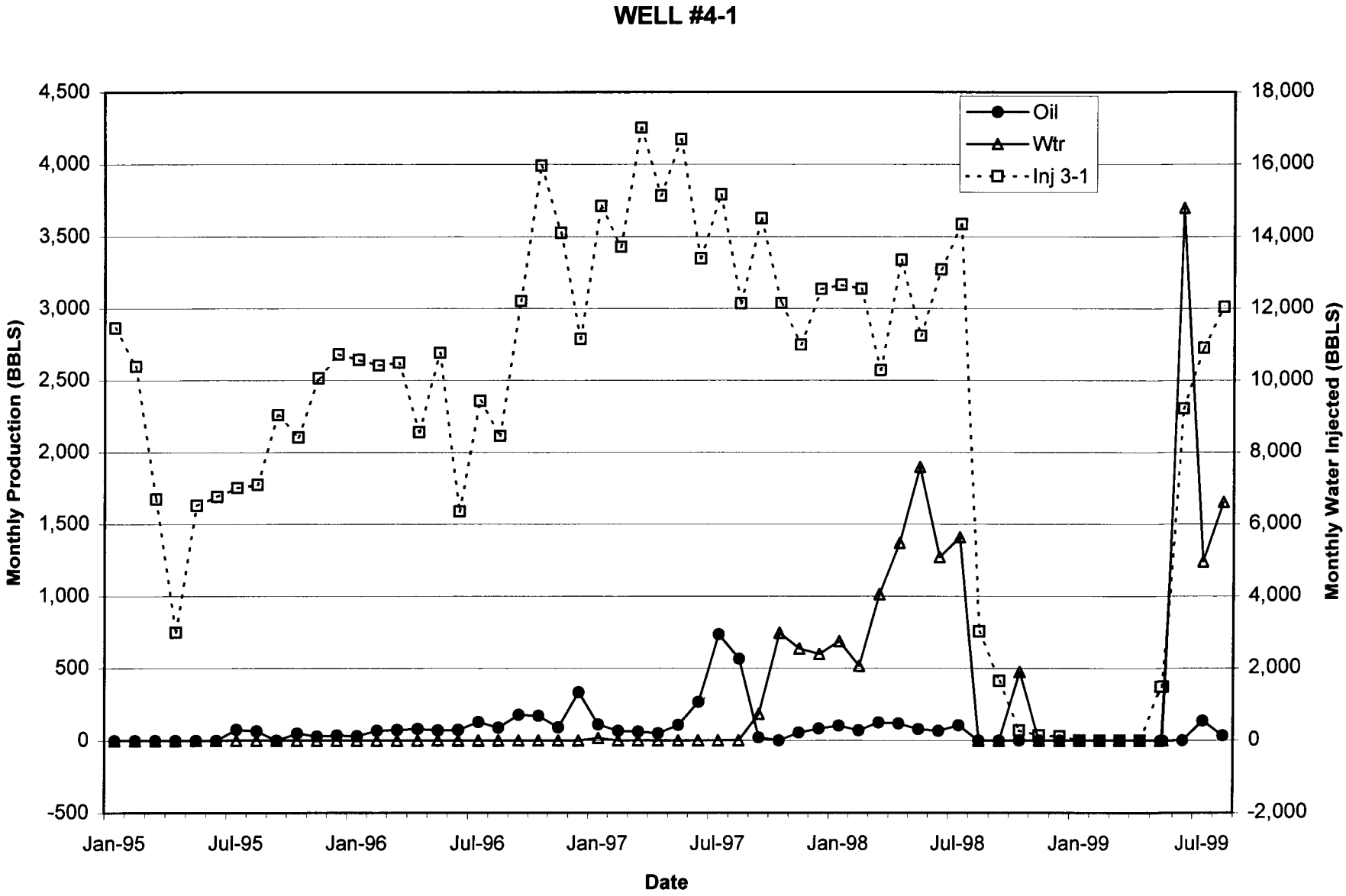
WELL #4-1
Oil
Wtr
Inj 3-1
Monthly Production (BBLS)
Monthly Water Injected (BBLS)
Date
4,500
4,000
3,500
3,000
2,500
2,000
1,500
1,000
500
0
-500
18,000
16,000
14,000
12,000
10,000
8,000
6,000
4,000
2,000
0
-2,000
Jan-95
Jul-95
Jan-96
Jul-96
Jan-97
Jul-97
Jan-98
Jul-98
Jan-99
Jul-99

Figure C6

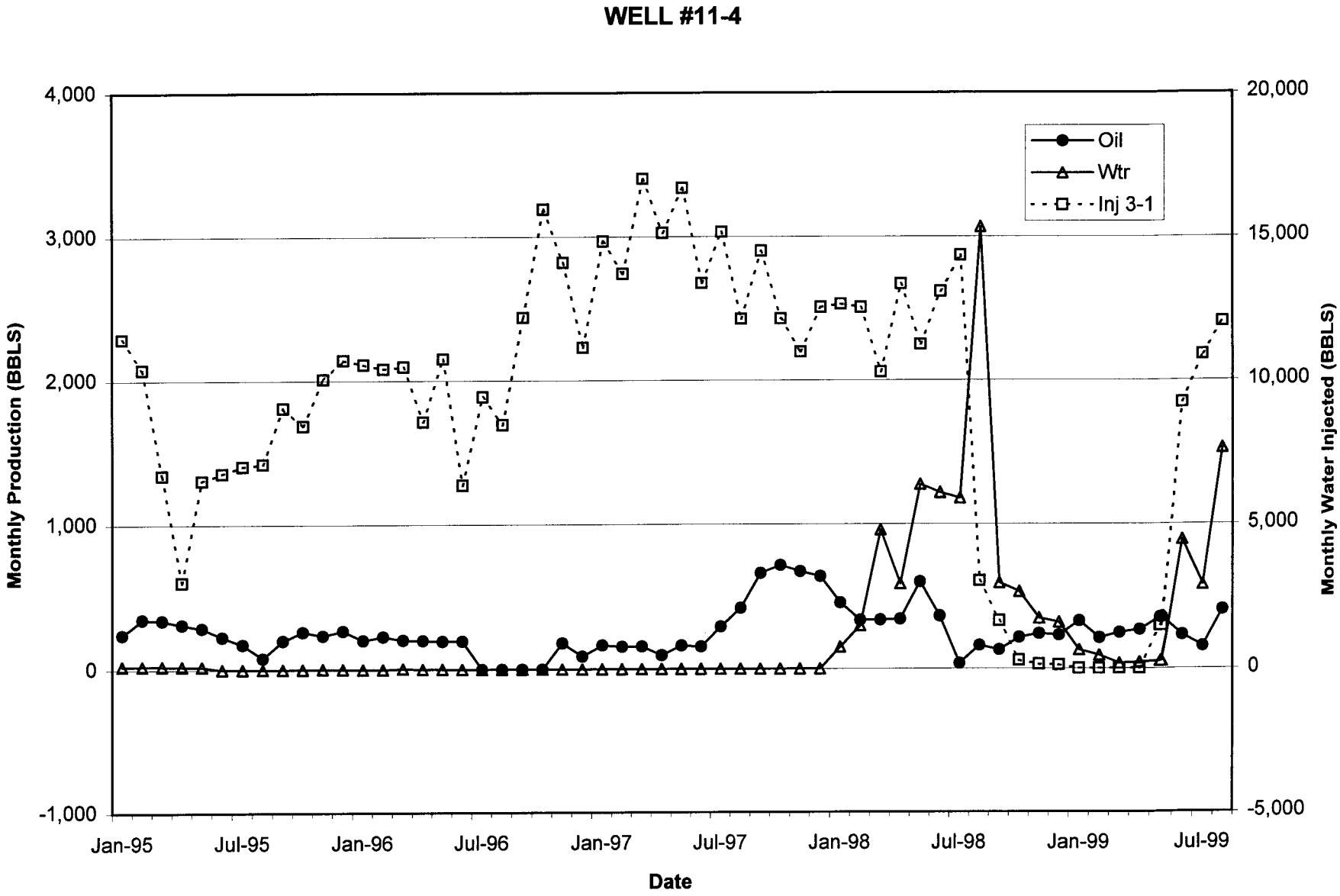
WELL #11-4
Monthly Production (BBLS)
Monthly Water Injected (BBLS)
Date
Oil
Wtr
Inj 3-1
4,000
3,000
2,000
1,000
0
-1,000
20,000
15,000
10,000
5,000
0
-5,000
Jan-95
Jul-95
Jan-96
Jul-96
Jan-97
Jul-97
Jan-98
Jul-98
Jan-99
Jul-99

Figure C7

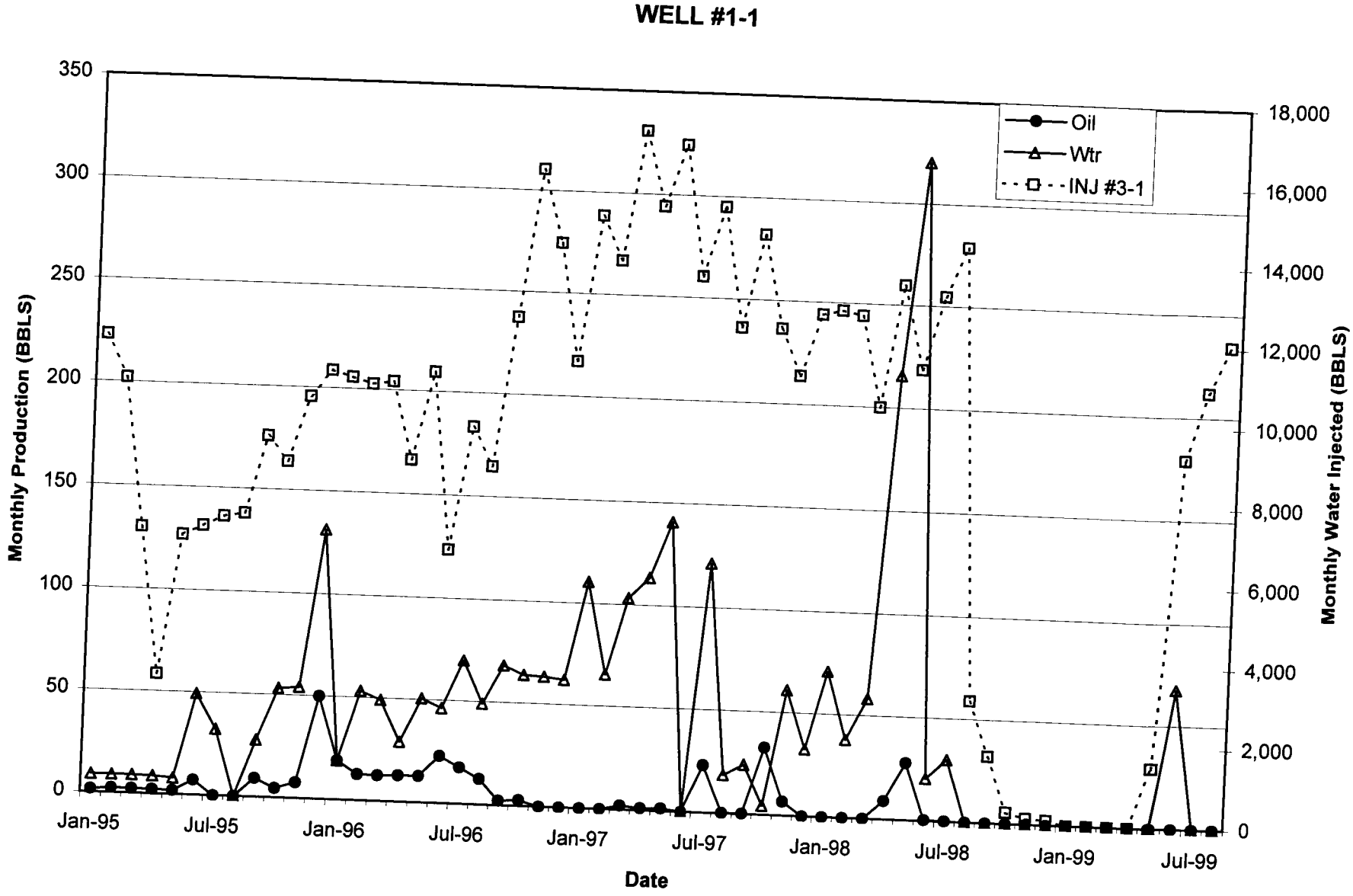
WELL #1-1
Monthly Production (BBLS)
Monthly Water Injected (BBLS)
Date
Oil
Wtr
INJ #3-1
350
300
250
200
150
100
50
0
18,000
16,000
14,000
12,000
10,000
8,000
6,000
4,000
2,000
0
Jan-95
Jul-95
Jan-96
Jul-96
Jan-97
Jul-97
Jan-98
Jul-98
Jan-99
Jul-99

Figure C8

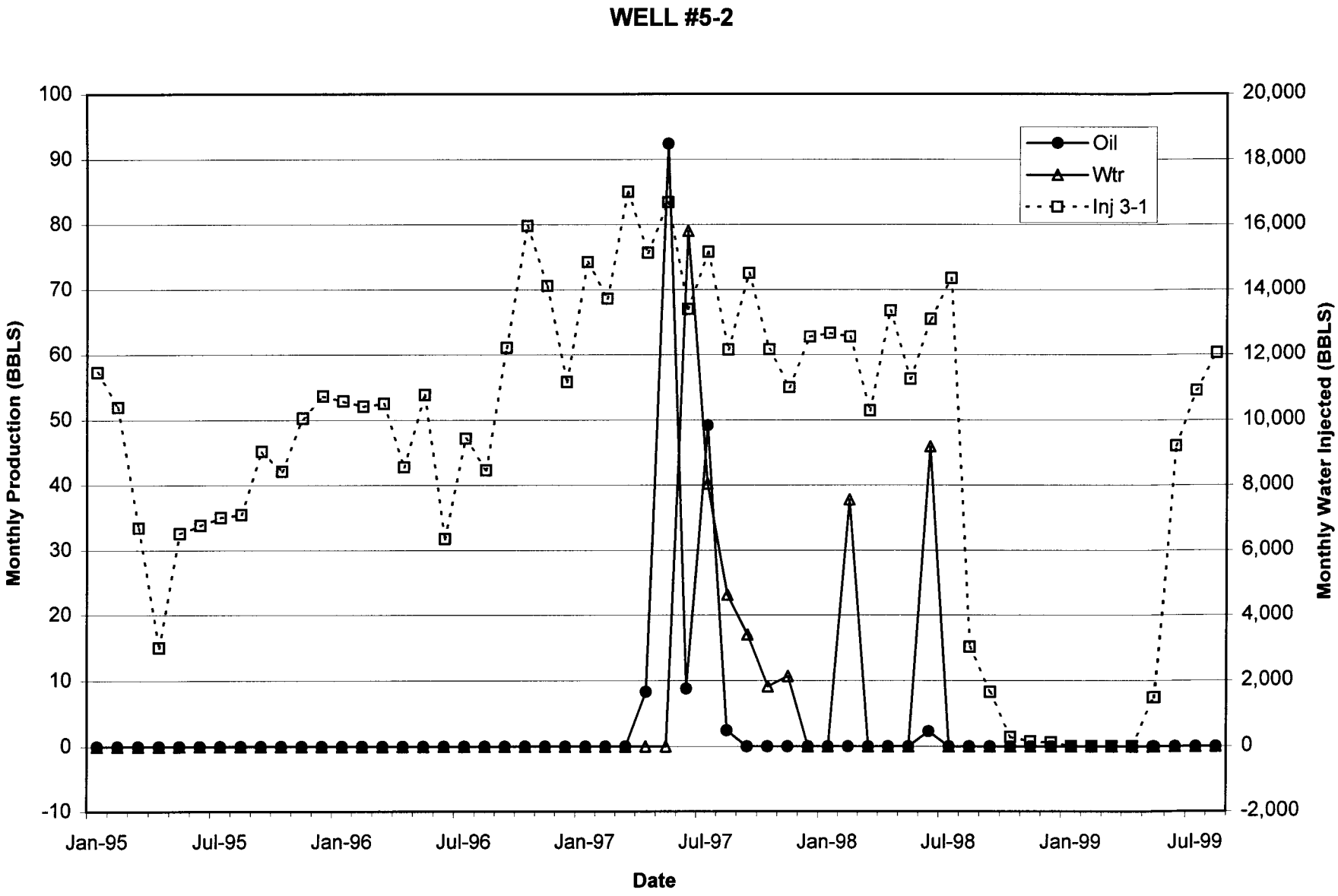
WELL #5-2
Monthly Production (BBLS)
Monthly Water Injected (BBLS)
Date
Oil
Wtr
Inj 3-1
100
90
80
70
60
50
40
30
20
10
0
-10
20,000
18,000
16,000
14,000
12,000
10,000
8,000
6,000
4,000
2,000
0
-2,000
Jan-95
Jul-95
Jan-96
Jul-96
Jan-97
Jul-97
Jan-98
Jul-98
Jan-99
Jul-99

Figure C9

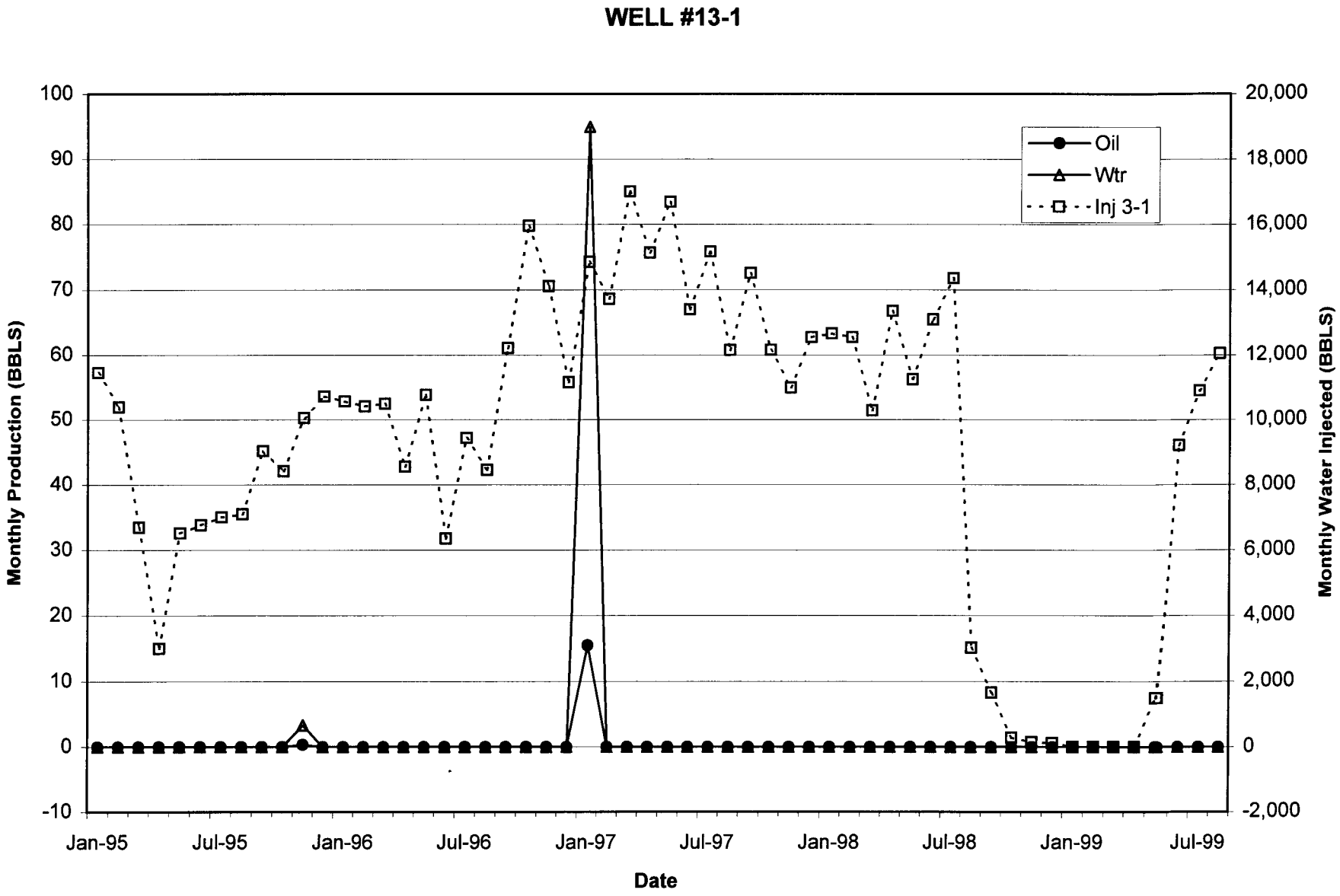
WELL #13-1
Monthly Production (BBLS)
Monthly Water Injected (BBLS)
Date
Oil
Wtr
Inj 3-1
100
90
80
70
60
50
40
30
20
10
0
-10
20,000
18,000
16,000
14,000
12,000
10,000
8,000
6,000
4,000
2,000
0
-2,000
Jan-95
Jul-95
Jan-96
Jul-96
Jan-97
Jul-97
Jan-98
Jul-98
Jan-99
Jul-99

Figure C10

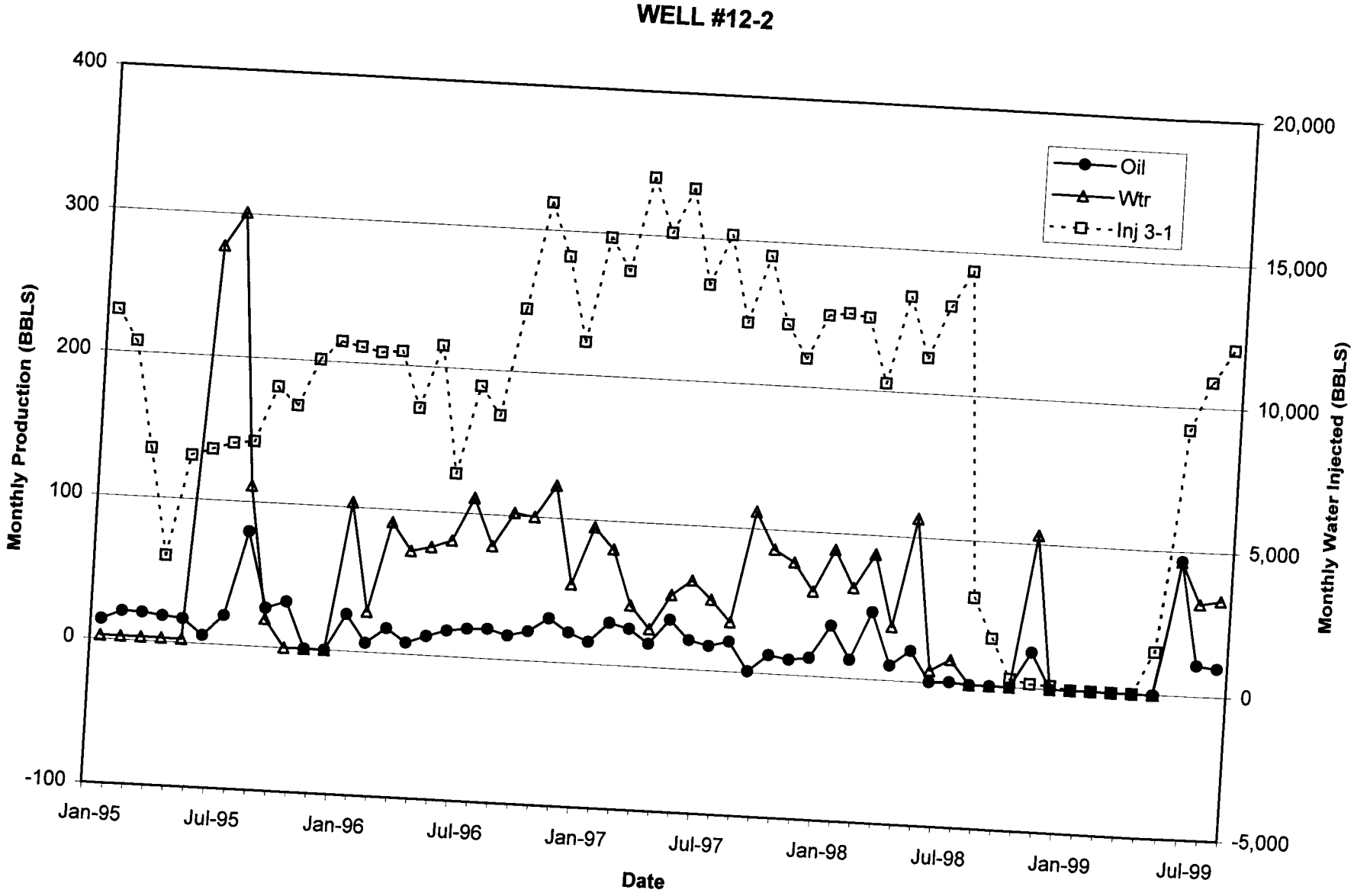
WELL #12-2
Monthly Production (BBLS)
Monthly Water Injected (BBLS)
Date
Oil
Wtr
Inj 3-1
400
300
200
100
0
-100
20,000
15,000
10,000
5,000
0
-5,000
Jan-95
Jul-95
Jan-96
Jul-96
Jan-97
Jul-97
Jan-98
Jul-98
Jan-99
Jul-99

Figure C11